A FLOOD FREQUENCY DERIVATION TECHNIQUE BASED ON KINEMATIC WAVE APPROACH

THESIS

A FLOOD FREQUENCY DERIVATION TECHNIQUE BASED ON KINEMATIC WAVE APPROACH

Submitted by

Luis Guillermo Cadavid

Department of Civil Engineering

In partial fulfillment of the requirements

for the Degree of Master of Scie

Colorado State University

Fort Collins, Colorado

Spring 1987

COLORADO STATE UNIVERSITY

Spring 1987

WE HEREBY RECOMMEND THAT THE THESIS PREPARED UNDER OUR SUPERVISION BY LUIS GUILLERMO CADAVID

ENTITLED A FLOOD FREQUENCY DERIVATION TECHNIQUE BASED ON KINEMATIC WAVE APPROACH

BE ACCEPTED AS FULFILLING IN PART REQUIREMENTS FOR THE DEGREE OF MASTER OF SCIENCE

Committee on Graduate Work

Adviser

Department Head

ABSTRACT

A FLOOD FREQUENCY DERIVATION TECHNIQUE
BASED ON KINEMATIC WAVE APPROACH

The present study deals with the derivation of a methodology to obtain a flood frequency distribution, for small ungaged watersheds, where the overland flow phase is considered to be an important timing component. In the hydrological literature, this technique comprises three components: a rainfall infiltration model, an effective rainfall-runoff model and the probabilistic component.

The study begins with a review of the Geomorphological Instantaneous Unit Hydrograph (GIUH), in order to establish its applicability to the aforementioned type of watersheds.

Some effective rainfall-runoff models currently used in the practice of hydrology, like the GIUH and models based on Kinematic Wave approach, lack the required features or do not consider all possible responses within the watershed. Therefore, a new model is developed and calibrated, based on Kinematic Wave approach, for a first order stream with two symmetrical lateral planes. The model is conformed by analytical and approximate solutions, the latter improved via regression analysis.

The formulated model is used along with a statistical distribution for the effective rainfall intensity and effective duration, in order to derive the flood frequency distribution technique through the probabilistic component. The structure of the equations considered in the different components imposes a numerical

algorithm to compute the flood frequency distribution curve for a given watershed.

The derived technique is proved for hypothetical and real watershed configurations, showing its capability to forecast flood frequency curves for ungaged watersheds and to account for the influence of parameters on the physics of flood formation. Actual watersheds are conceived as first order streams with two symmetrical planes.

Luis Guillermo Cadavid
Department of Civil Engineering
Colorado State University
Fort Collins, CO 80523
Spring 1987

ACKNOWLEDGMENTS

Grateful appreciation is extended to my former advisor and now my co-advisor, Dr. H. W. Shen, for his constant support and sponsorship throughout this study. To my actual advisor, Dr. J. Obeysekera, for his constant guidance and interest in the development of the present study. Special gratitude is also extended to the members of my committee, Dr. J. D. Salas and Dr. S. A. Schumm, for their cooperation.

To my wife, Olga, for her constant support, encouragement and dedication in the achievement of this study. Special acknowledgments for her work on the drawing and part of the typing.

To Mrs. Lesley Noone, from the Intensive English Program at Colorado State University, for her amiability and patience in checking the writing of the final report.

Sincere gratitude to the staff of Technical Typing in the Engineering Research Center of Colorado State University.

Finally, thanks to my family for their encouragement during my studies. Special appreciation is extended to my friends Jorge, Ana and Pablo Restrepo, for their constant friendship, care and company during the development of my graduate studies at Colorado State University.

This study was funded through Contract No. DAAG29-83-K-0160 by the United States Army Research Office.

To my Wife, Olga

To my Mother, Ruth

To my Father, Hernando

TABLE OF CONTENTS

Chapter		Page
1	INTRODUCTION	1
	1.1 General	1
	1.2 Objective	3
	1.3 Review of Related Literature	4
	1.4 Scope of the Study	7
2	THE GIUH AND THE KINEMATIC WAVE APPROACH	9
	2.1 Introduction	9
	2.2 The GIUH	9
	2.3 Computation of the IUH Using the Kinematic Wave Model	14
	2.4 Contrived Watersheds	16
	2.5 Experiments and Results	19
	2.6 Conclusions	27
3	KINEMATIC ROUTING	29
	3.1 Introduction	29
	3.2 Flow Equations and the Kinematic Wave	30
	3.3 Solution to Kinematic Flow Equations for Overland Flow by the Method of Characteristics	33
	3.4 Solution to Kinematic Flow Equations for Channel Flow by the Method of Characteristic	46
	3.5 Some Exact Solutions for the Peak Variables in A First Order Channel	50
	3.5.1 Case 1: Concentration on Plane and Concentration on Channel	50
	3.5.2 Case 3: No Concentration on Plane and Concentration on the Stream	53
	3.6 Approximate Kinematic Routing	56
	3.6.1 Routing and Rising Limb	59
	3.6.2 Routing the Plateau	61
	3.6.3 Routing the Receding Limb	63
	3.7 Computation of the Total Hydrograph using Approximate Kinematic Routing	64
	3.8 Application of the Approximate Kinematic Routing Method	65
	3.8.1 Case 1: Concentration on Plane and Concentration on Channel	66
	3.8.2 Case 2: Concentration on Plane and No Concentration on Channel	69
	3.8.3 Case 3: No Concentration on Plane and Concentration on Channel	72
	3.8.4 Case 4: No Concentration on Plane and No Concentration on Channel	77

Chapter

		Page
	3.8.5 Preliminary Analysis of Results for the Approximate Kinematic Routing	77
	3.9 Improvement of the Equations to Compute Peak Variables	85
	3.10 Summarized Procedure for Computing the Peak Variables	102
	3.11 Final Remarks on the Effective Rainfall-Runoff Model	104
4	FLOOD FREQUENCY DERIVATION	106
	4.1 Introduction	106
	4.2 Rainfall-Infiltration Component	106
	4.3 Probabilistic Component	116
	4.4 Description of the Algorithm to Compute the Flood Frequency Distribution Curve	132
	4.5 Computation of the Flood Frequency Distribution Curve for Hypothetical Configurations	140
	4.6 Sensitivity Analysis for the Flood Frequency Derivation	140
	4.7 Application of the Flood Frequency Derivation Technique to Actual Watersheds	156
	4.8 Discussion Regarding the Flood Frequency Derivation Technique	165
5	SUMMARY, CONCLUSIONS AND RECOMMENDATIONS	170
	5.1 Summary	170
	5.2 Conclusions	171
	5.3 Recommendations for Future Investigations	174
	BIBLIOGRAPHY	176
	Appendix A - HYDRAULIC ROUTING MODEL	178
	A.1 Introduction	178
	A.2 General Description of the Model	179
	A.3 The Hydrologic Component	183
	A.4 The Geomorphic Component	184
	A.5 The Hydraulic Component	188
	A.6 Solution to Kinematic flow Equations for Overland Flow by the Method of Characteristics	190
	A.7 Solution of the Kinematic Flow Equations for Channel Flow with no Upstream Tributaries (First Order Streams)	199
	A.8 Solution of the Flow Equations for Channel Flow with Upstream Tributaries (Second or Higher Order Channels	200
	A.9 Summary of Assumptions and Limitations for the Model	205
	Appendix B - FLOOD FREQUENCY DERIVATION USER MANUAL FOR THE COMPUTER PROGRAM	207
	B.1 Introduction	207
	B.2 Input Data File Description	207

Chapter

		Page
B.3	Program Capacity	209
B.4	Output Description	209
B.5	Program Source Code	209

LIST OF TABLES

Table		Page
2.1	Contrived watersheds geomorphological parameters.....	19
2.2	KIUH and GIUH comparison for the contrived watersheds.....	23
2.3	Estimated values for the peak flow velocity for the contrived watersheds.....	27
3.1	Cases in the analytical integration for channel flow..	47
3.2	Comparison of results for Cases 1 and 3.....	81
3.3	Comparison of results for Cases 2 and 4.....	82
3.4	Typical holding times for Cases 2 and 4.....	86
3.5	Configurations to improve peak variables for Cases 2 and 4.....	87
3.6	Typical time values for Case 2. ($t^* > t_e > t_c$).....	88
3.7	Typical time values for Case 4 ($t_c > t_e > 0$ and $t_p < t_e + t_s''$).....	89
3.8	Simulated and approximate peak variable values for Case 2.....	90
3.9	Simulated and approximate peak variable values for Case 4.....	91
3.10	Properties for the regression models for Cases 2 and 4.....	99
4.1	Equivalent notation for computation of $F_{Q_m}(Q)$.....	128

LIST OF FIGURES

Figure		Page
2.1	Rising and recession limb IUHs obtained using the kinematic wave model. Watershed #2. i_e = 6.0 in/hr..	15
2.2	Incremental IUH procedure (Valdes et al., 1979).....	17
2.3	Incremental IUHs for Watershed #2.....	18
2.4	KIUH and GIUH for Watershed #2, i_e = 0.6 in/hr.....	20
2.5	KIUH and GIUH for Watershed #3, i_e = 0.6 in/hr.....	21
2.6	KIUH and GIUH for Watershed #4, i_e = 6 in/hr.....	22
2.7	Sensitivity analysis on R_B for the GIUH for Watershed #2.....	24
2.8	Sensitivity analysis on R_A for the GIUH for Watershed #2.....	25
2.9	Sensitivity analysis on V for the GIUH for Watershed #2.....	26
3.1	Limiting characteristic line.....	36
3.2	Water depth profile evolution for $t \geq t_e$ and $t_e \geq t_c$.....	40
3.3	Typical discharge hydrograph for the plane when $t_e \geq t_c$.....	42
3.4	Water depth profile evolution for $t \geq t_e$ and $t_e < t_c$..	43
3.5	Typical discharge hydrograph for the plane when $t_e < t_c$.....	45
3.6	Typical discharge hydrographs for a first order stream with symmetrical planes.....	48

Figure		Page
3.7	x-t plane for concentration on plane and concentration on channel	51
3.8	x-t plane for no concentration on plane and concentration on channel	54
3.9	Procedure and notation for the approximate kinematic routing	58
3.10	Case 1	67
3.11	Case 1. I = 1 in/hr, t_e = 70 min	70
3.12	Case 2	71
3.13	Case 2 - I = 1 in/hr, t_e = 50 min	73
3.14	Case 3	74
3.15	Case 3 - I = 10 in/hr, t_e = 12 min	76
3.16	Case 4	78
3.17	Case 4 - I = 1 in/hr, t_e = 40 min	79
3.18	Forecasted time to peak for Case 2	92
3.19	Forecasted time to peak for Case 4	93
3.20	Forecasted peak discharge for Case 2	95
3.21	Forecasted peak discharge for Case 4	96
3.22	Forecasted discharge for Case 2 using the regression model	100
3.23	Forecasted discharge for Case 4 using the regression model	101
4.1	Rainfall-infiltration process (Diaz-Granados et al. (1983))	111
4.2	Integration regions for the flood frequency computation	119
4.3	Integration regions for Configuration 1 and Q = 600 cfs	121
4.4	Integration regions for Configuration 2 and Q = 100 cfs	122

Figure		Page
4.5	Integration regions for Configuration 3 and Q = 600 cfs	123
4.6	Integration regions for Configuration 4 and Q = 600 cfs	124
4.7	Integration regions for Configuration 5 and Q = 600 cfs	125
4.8	Flood frequency distribution curve for Configuration 1	141
4.9	Flood frequency distribution curve for Configuration 2	142
4.10	Flood frequency distribution curve for Configuration 3	143
4.11	Flood frequency distribution curve for Configuration 4	144
4.12	Flood frequency distribution curve for Configuration 5	145
4.13	Sensitivity of the flood frequency distribution curve to changes in the plane width	148
4.14	Sensitivity of the flood frequency distribution curve to changes in the plane slope	149
4.15	Sensitivity of the flood frequency distribution curve to changes in the channel length	150
4.16	Sensitivity of the flood frequency distribution curve to changes in the channel slope	151
4.17	Sensitivity of the flood frequency distribution curve to changes in the mean rainfall intensity	152
4.18	Sensitivity of the flood frequency distribution curve to changes in the mean rainfall duration	153
4.19	Sensitivity of the flood frequency distribution curve to changes in the hydraulic conductivity	154
4.20	Sensitivity of the flood frequency distribution curve to changes in the sorptivity	155
4.21	Ralston Creek Watershed near Iowa City, Iowa	158
4.22	Flood frequency curves for Ralston Creek	162

Figure		Page
4.23	Santa Anita Creek Watershed near Sierra Madre, California	163
4.24	Flood frequency curves for Santa Anita Creek	166
A.1	Map and model representation for a given watershed	180
A.2	Piecewise integration of characteristic lines arising in the x axis	195
A.3	Piecewise integration of characteristic lines arising in the t (or t_o) axis	197
A.4	Rectangular network in the x-t plane	202

Chapter 1

INTRODUCTION

1.1 General

One of the more common tasks found in hydraulic engineering design is the selection of flood events. Generally, the person in charge of the design faces one of two problems: 1) selection of the flood event when annual flood or partial duration series do exist, and 2) determination of a flood value when no historical flood records are available.

In the first kind of approach, the historical data is fitted to a given probability distribution, and the design annual flood is selected by specifying a value for the exceedence probability or return period.

In the second line of design, the first step is given by a rainfall frequency analysis. This allows the assignation of exceedence probabilities or return periods to different values of rainfall intensity and duration. The design chosen values are passed through an infiltration model, producing in this way the effective quantities to be imposed over the watershed. Up to this point, two alternate ways can be followed. In the first, the design engineer picks up a synthetic unit hydrograph and obtain the peak discharge. The second way requires the use of watershed routing models. In either of the latter methodologies, the rainfall return period is assigned to the peak discharge.

For ungaged watersheds, it is also suitable to follow a statistical approach in which the parameters describing a certain flood distribution are derived for the problem watershed via regional analysis.

Since 1972, beginning with the now classical work by Eagleson, a set of works has appeared in the hydrological literature, which in a wide sense can be referred to as derivation of flood frequency distributions. Although the name given to the new methodology is ambiguous, since it can encompass the other approaches already described, it is clarified when the effective rainfall-runoff model is defined.

The method has three components: a rainfall-infiltration component, an effective rainfall-runoff component and a probabilistic component. In the first element, a joint distribution for the total rainfall intensity and duration is proposed, as well as a model for the infiltration process, producing the corresponding probability for null runoff and the joint distribution for the effective intensity and duration. The second model provides a set of equations or algorithms for the computation of the peak variables, peak discharge and time to peak. The transformation of the joint distribution for the effective intensity and duration into the cumulative distribution function for the peak discharge is accomplished via the probabilistic component, integrating the former over certain regions defined by the effective rainfall-runoff model, and adding the probability of null runoff. In the last step, the flood frequency distribution curve is obtained by performing some operations over the cumulative distribution function for the peak discharge.

As stated above, the type of rainfall-runoff model qualifies the derivation of the flood frequency curve. Some authors have used physically based models, while others have included geomorphological approaches.

Obviously, as other methodologies do, the derivation of flood frequency distribution has advantages and disadvantages. In the first category, advantages such as its ability to incorporate climatic, soil, geomorphological and dynamical parameters, and to provide some light into the problem, can be enumerated. In the second, disadvantages like the requirement of invertibility of the functions defining the infiltration model, the development and implementation of numerical algorithms and the consumption of computer time are counted.

1.2 Objectives

The objective of the present study is the derivation of a physically based flood frequency technique for small ungaged watersheds, where the overland flow phase is an important component. Within this main objective, the derivation of an effective rainfall-runoff model for a first order stream with two symmetrical planes is also posed. The constraint in the order of the channel is necessary, given the actual state of the art, in order to preserve the physical quality of the model. This means that for the flood frequency technique application, actual watersheds are conceived as the simple catchment geometry described above.

Some effective rainfall-runoff models suggested in the literature, in regard to flood frequency derivation, lack certain features, like ability to predict peak discharge in small watersheds or complete forecast of the peak discharge given the effective

intensity-duration space. This consideration forces the formulation of an alternate effective rainfall-runoff model upon the basis of physical considerations. The new model has to account for all variables describing the catchment area and the channel, as well as their dynamic properties.

One of the effective rainfall-runoff models frequently used in the literature is the Geomorphological Instant Unit Hydrograph (GIUH). This study also intends a review of such model in regard to its applicability to small watersheds, where the overland flow phase is an important component.

Summarizing, three are the main objectives for the present study: 1) a review of the GIUH approach in regard to its applicability to small watersheds, 2) formulation of a physically based effective rainfall-runoff model, and 3) derivation of a physically based flood frequency distribution for a first order stream.

1.3 Review of Related Literature

The classical work, setting up the methodology for derivation of flood frequency distributions, was published by Eagleson in 1972. More than the results themselves, Eagleson's greatest contribution puts together the elements conforming the methodology. In the rainfall-infiltration component, Eagleson considers the total rainfall intensity and total duration as independent exponentially distributed. Other features pertaining this stage are the consideration of a point rainfall-areal rainfall relationship and the description of the infiltration process through the ϕ index method (Viessman et al., 1977).

In the effective rainfall-runoff component Eagleson develops an algorithm to forecast the peak discharge in a first order stream, using the kinematic wave approach. However, this algorithm does not encompass all possible runoff cases in the catchment area, for example, concentration on the channel given no concentration on the overland flow planes. Besides, its reduction of the decision tree for peak direct streamflow depends on certain values assumed for slope and roughness in the planes and in the stream, as well as on the rainfall intensity.

After deriving the annual flood frequency curve, Eagleson compares it with observations from natural watersheds and obtain a good agreement.

It is important to emphasize in the fact that Eagleson's approach is physical, due to the inclusion of kinematic wave approach, for which, based on work by other authors, he points out important practical advantages as well as the tendency to overestimate peak floods.

The next important step in flood frequency derivation is given by Hebson and Wood (1982). In the rainfall-infiltration model they follow Eagleson works (1972, 1978). In the effective rainfall-runoff model the convolution equation is used, where the unit instantaneous response is assumed to be the Geomorphological Instantaneous Unit Hydrograph (GIUH), formulated back in 1979 by Rodriguez-Iturbe and Valdes (1979). The application of Hebson and Wood's development to two actual watersheds shows good agreement.

In 1983, Diaz-Granados et al. (1983) go a step further in the derivation of flood frequency distributions by considering in the infiltration model a ponding time equation, that is the Philip's

equation. This fact generates a joint probability distribution function for the effective rainfall intensity and duration different from that used in the previous works. In fact, the invertibility condition required in the derived distribution technique (Freeman, 1963), is solved by means of regression analysis performed on dimensionless variables.

In the effective rainfall-runoff component of the flood frequency derivation, Diaz-Granados et al. use the GIUH, in the sense that they take the expressions for the peak discharge and time to peak obtained by Rodriguez-Iturbe and Valdes (1979), assign these values to the triangular instantaneous unit hydrograph developed by Henderson (1963), and obtain an expression for the peak discharge in any watershed as a function of the effective rainfall and geomorphological variables. Once the development is complete, they perform some sensitivity analysis for the variables included in the flood frequency derivation on a hypothetical watershed. The analysis is completed by application to actual watersheds, reporting good results.

In regard to the Geomorphological Instantaneous Unit Hydrograph (GIUH), two works are considered as integral part of the present study. In the first, Rodriguez-Iturbe and Valdes (1979) present the analytical derivation of the GIUH along with the synthesis of the peak discharge and time to peak. In the second, Valdes et al. (1979) summarize the application of the GIUH to real world watersheds.

The review of literature herein presented, related to the derivation of flood frequency distributions, yields two important conclusions: 1) the applicability of the method to actual watersheds and 2) the capability to provide some light into the internal structure of flood frequency distributions, related to variables

describing basin morphology, infiltration behavior and runoff response. These two features make the method an important tool to be applied to ungaged watersheds.

As a last point, it is valuable to provide some references regarding the kinematic wave theory widely used in the present study. Eagleson (1970 and 1972) gives an excellent base for the theoretical development. In the development and applicability of the method to more complex cases, Garbrecht (1984) and Koch (1985) are strongly recommended.

1.4 Scope of the Study

Due to the fact that a straight forward method to the flood frequency derivation could be the adoption of the Geomorphological Instantaneous Unit Hydrograph as the effective rainfall-runoff component, a review of its applicability to small watersheds, where overland flow is an important timing component, is first intended.

The derivation itself of the flood frequency distribution is performed following the steps already outlined for this methodology. Some components are taken from other authors; others are developed as an integral part of this study. Special attention is given to the sensitivity analysis and to the application of the derived flood frequency distribution to two small watersheds.

As the reader will notice, some values regarding the plane and channel dynamics are held constant along the present study. Such values are roughness and the coefficients describing the hydraulic radius cross-sectional area relationship for the channel, $R = aA^b$. Particularly, $a = 0.25$ and $b = 0.35$ are recommended by Koch (1985), based on Garbrecht's findings (1984), who obtained such values after

analysis of several stable channel relationships presented in the literature.

The value of the roughness conditions the coefficient for the depth-discharge relationship in the plane and for the area-discharge in the plane. However, the variation on these coefficients is taken into account through variation of slopes. Besides, when needed, calibrations are performed on dimensionless variables, and the obtained expressions account for all variables representing the process under consideration.

During the development of the present study a kinematic wave computer model was used for the simulation of the rainfall-runoff process in different watersheds. To the best of the author's knowledge, the model is traced back to Simons, Li and Eggert (1976). Spronk (1978) enhanced it substantially and it was modified later by Garbrecht (1984). Furthermore, Koch (1985) did some fine-tuning of the computer code as did the author of the present work. Appendix A presents a description of the model in its theoretical basis, which is completely based on Garbrecht (1984), and it is presented for the sake of completeness.

Chapter 2

THE GIUH AND THE KINEMATIC WAVE APPROACH

2.1 Introduction

Since 1979 the Geomorphological Instantaneous Unit Hydrograph GIUH has been a tool widely used in hydrology to forecast peak discharge and to develop physically based flood frequency distribution curves (Hebson and Wood, 1982; Diaz-Granados et al., 1983).

This chapter is intended to review the applicability of the GIUH to small watersheds where the overland flow is an important timing component. The revision of the method is made on its own basis, that is, comparing the GIUH with the Instantaneous Unit Hydrograph obtained via detailed simulations. These simulations were performed using the kinematic wave model described in Appendix A, and follows the methodology presented by the GIUH's authors (Rodriguez-Iturbe and Valdes, 1979; Valdes et al., 1979).

The basic data required to perform the analysis were obtained from three contrived watersheds (Koch, 1985), all these being third order catchment areas. This order agrees with the GIUH derivation (Rodriguez-Iturbe and Valdes, 1979).

2.2 The GIUH

This section summarizes the basic considerations and expressions used to obtain the GIUH for a third order watershed (Rodriguez-Iturbe and Valdes, 1979).

The derivation of the GIUH is based on the determination of the probability that a rainfall drop chosen at random reaches the watershed outlet at time t. In other words, the GIUH is given by the probability distribution function of the arrival time of rainfall drops to the catchment outlet. The main hypotheses taken into account for the GIUH derivation are: 1) the watershed behaves following the laws of stream numbers, stream lengths and stream areas; 2) the transition probabilities from one state or order to another follow a Markov process, i.e., those probabilities depend only on the actual state; 3) the holding time or the time a drop spends in a given state or order is exponentially distributed and; 4) the dynamic of the drop as it travels along channels is well described by the peak flow velocity, which supposedly remains constant for a given rainfall event within the watershed.

The channel ordering scheme defined by Strahler (1957) is selected. Sources are defined as the points farthest upstream in a channel network, and the outlet is the point farthest downstream. The point at which two channels combine to form one is called junction. It is assumed that multiple junctions do not occur. The ordering scheme proceeds as follows: channels that originate at a source are first order channels; when two channels of order ω join, a channel order $\omega + 1$ is created, and when two channels of different order join, the channel immediately downstream of the junction retains the higher order of the two joining channels. The highest channel order (Ω) in a channel network is also the network order.

The process begins with the probability that the drops start they travel at a given state ω, where ω varies from 1 to Ω, and Ω denotes

the watershed order. These probabilities are designated as $\theta_{\omega}(o)$ and they can be estimated following

$$\theta_1(o) = \frac{R_B^2}{R_A^2} \tag{2.1}$$

$$\theta_2(o) = \frac{R_B}{R_A} - \frac{R_B\,(R_B^2 + 2R_B - 2)}{R_A^2\,(2R_B - 1)} \tag{2.2}$$

$$\theta_3(o) = 1 - \frac{R_B}{R_A} - \frac{1}{R_A^2}\left[\frac{R_B\,(R_B^2 - 3R_B + 2)}{2R_B - 1}\right] \tag{2.3}$$

Subject to $R_B < R_A$.

R_B and R_A represent respectively bifurcation and area ratios, and according to the corresponding laws are defined as

$$R_B = N_{\omega}/N_{\omega+1} \tag{2.4}$$

$$R_A = \bar{A}_{\omega+1}/\bar{A}_{\omega} \tag{2.5}$$

where N_{ω} stands for the number of streams of order ω and $\bar{A}_{\omega}$ for the mean area for the basins of order ω.

The process continues with the computation of the transition probabilities p_{ij} for a drop going from state i to state j; where $j > i$, using the equations

$$p_{12} = \frac{R_B^2 + 2R_B + 2}{2R_B\,(R_B - 1)} \tag{2.6}$$

$$p_{13} = \frac{R_B^2 - 3R_B + 2}{2R_B (R_B - 1)} \tag{2.7}$$

$$p_{23} = 1 \tag{2.8}$$

Finally, the GIUH is computed for a third order watershed as:

$$GIUH(t) = \theta_1(o)\, \phi'_{15} + \theta_2(o)\, \phi'_{25} + \theta_3(o)\, \phi'_{35} \tag{2.9}$$

$$\begin{aligned} \phi'_{15} = &- A_1\lambda_1 \exp(-\lambda_1 t) - A_2\lambda_2 \exp(-\lambda_2 t) \\ &- A_3\lambda_3^* t \exp(-\lambda_3^* t) + A_3 \exp(-\lambda_3^* t) \\ &- A_4\lambda_3^* \exp(-\lambda_3^* t) \end{aligned} \tag{2.10}$$

$$A_1 = (\lambda_3^*)^2 (\lambda_1 p_{13} - \lambda_2)/[(\lambda_2 - \lambda_1)(\lambda_3^* - \lambda_1)^2] \tag{2.11}$$

$$A_2 = (\lambda_3^*)^2 \lambda_1 p_{12}/[(\lambda_2 - \lambda_1)(\lambda_3^* - \lambda_2)^2] \tag{2.12}$$

$$A_3 = \lambda_3^* (\lambda_1\lambda_2 - \lambda_1\lambda_3^* p_{13})/[(\lambda_1 - \lambda_3^*)(\lambda_3^* - \lambda_2)] \tag{2.13}$$

$$\begin{aligned} A_4 = \{&(\lambda_3^*)^3 \lambda_1 p_{13} (\lambda_3^* - \lambda_1)(\lambda_2 - \lambda_3^*) - [3(\lambda_3^*)^2 \\ &- 2\lambda_2\lambda_3^* - 2\lambda_1\lambda_3^* + \lambda_1\lambda_2][\lambda_1\lambda_2 (\lambda_3^*)^2 \\ &- \lambda_1 (\lambda_3^*)^3 p_{13}]\}/[(\lambda_3^*)^2 (\lambda_1 - \lambda_3^*)^2 (\lambda_2 - \lambda_3^*)^2] \end{aligned} \tag{2.14}$$

$$\phi'_{25} = \lambda_2(\lambda_3^*)^2/(\lambda_3^* - \lambda_2)^2 \exp(-\lambda_2 t) - \lambda_2(\lambda_3^*)/(\lambda_3^* - \lambda_2)t$$

$$\exp(-\lambda_3^* t) + \lambda_2\lambda_3^*/(\lambda_3^* - \lambda_2) \exp(-\lambda_3^* t)$$

$$- \lambda_2\lambda_3^* (2\lambda_3^* - \lambda_2)/(\lambda_2 - \lambda_3^*)^2 \exp(-\lambda_3^* t) \quad (2.15)$$

$$\phi'_{35} = (\lambda_3^*)^2 t \exp(-\lambda_3^* t) \quad (2.16)$$

$$\lambda_3^* = 2\lambda_3 \quad (2.17)$$

where λ_ω represents the inverse of the mean holding time for the state ω and is computed, according to the stream length ratio R_L as

$$\lambda_1 = \lambda_3 R_L^2 \quad (2.18)$$

$$\lambda_2 = \lambda_3 R_L \quad (2.19)$$

$$\lambda_3 = V/\bar{L}_3 \quad (2.20)$$

In Equation (2.20) V stands for the peak flow velocity and $\bar{L}_3$ is the mean channel length for basins of order three. The length ratio R_L is defined according to

$$R_L = \bar{L}_{\omega+1}/\bar{L}_\omega \quad (2.21)$$

2.3 Computation of the IUH using the Kinematic Wave Model

The procedure herein presented to obtain the IUH follows that described by Valdes et al. (1979) and is the same by which the GIUH's authors performed its calibration and test.

When an effective rainfall intensity i_e of duration t_e, uniform in time and space, is imposed over the watershed, such that t_e is greater than its time of concentration, the discharge hydrograph Q(t) is composed of the rising limb, a horizontal line showing the steady state, and the recession limb.

Two IUHs can be obtained performing the following operations:

$$h_1(t) = \frac{1}{i_e} \frac{dQ_{ri}(t)}{dt} \tag{2.22}$$

$$h_2(t) = \frac{1}{i_e} \frac{dQ_{re}(t)}{dt} \tag{2.23}$$

The former corresponds to the rising limb and the latter to the recession limb. Due to the fact that the kinematic wave model is not a liner representation of the rainfall runoff process within the watershed, $h_1(t)$ and $h_2(t)$ are quite different, as shown in Figure 2.1, for one of the watersheds used in this section and described in Section 2.4.

In order to overcome the aforementioned problem, the procedure called incremental IUH, described by Valdes et al. (1979) was used. It begins by imposing over the watershed an effective rainfall intensity i_e. Once the watershed has reached the steady state, i.e., for a time t_{e1} greater than the time of concentration, the rainfall intensity is increased an amount Δi_e. The new intensity value ends at

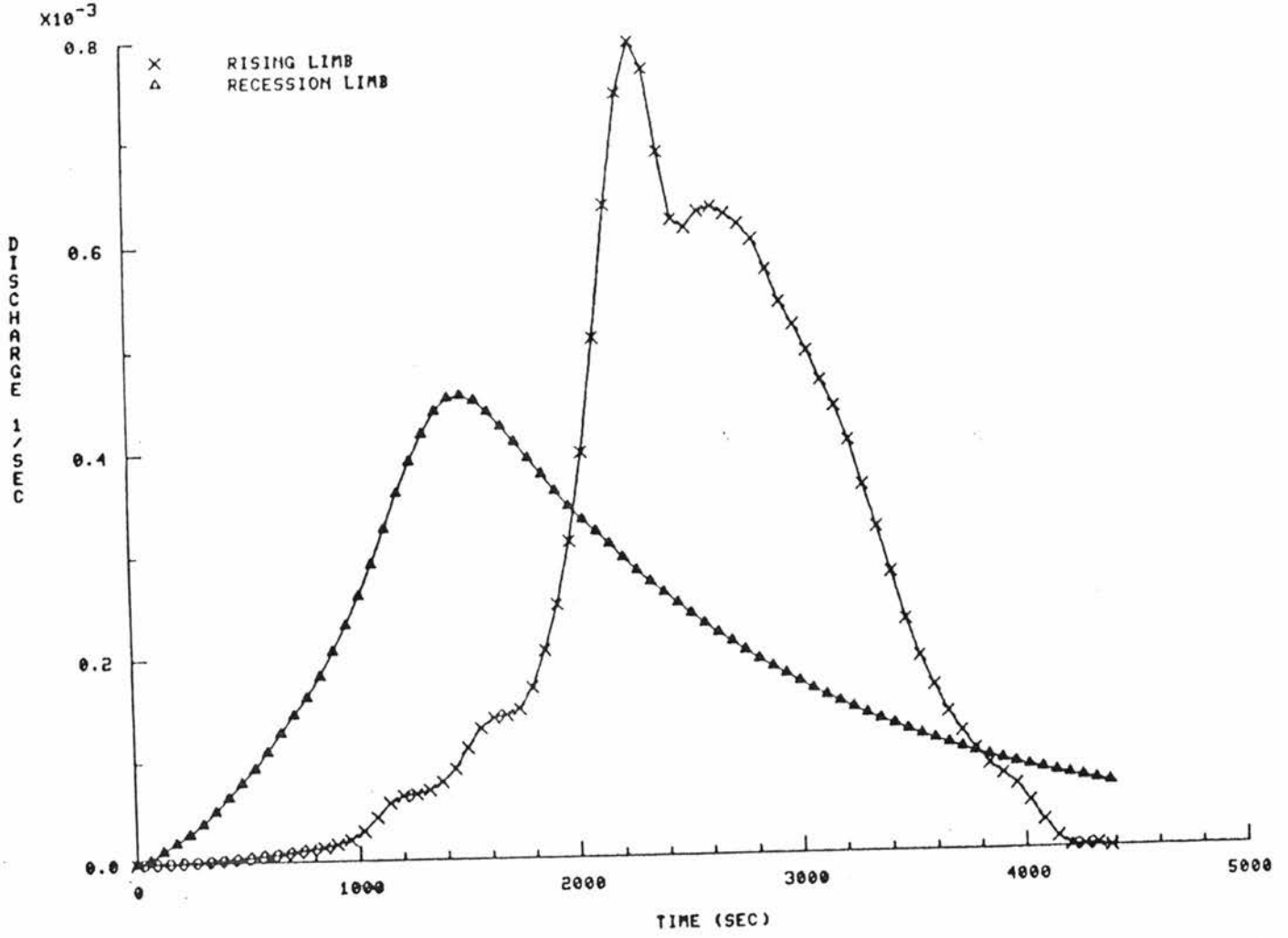

Figure 2.1. Rising and recession limb IUHs obtained using the kinematic wave model. Watershed #2. i_e = 6.0 in/hr.

a time t_{el} lesser than t_e. The value used for Δi_e was 10 percent of i_e, as recommended by Valdes et al. (1979). Figure 2.2 depicts the incremental IUH procedure.

When Equations (2.22) and (2.23), changing i_e by Δi_e, are applied to the upper rising and recession limbs depicted in Figure 2.2, two new IUH are obtained. An example of these are presented in Figure 2.3 for Watershed #2. Due to the fact that a small increase in the effective rainfall intensity does not induce a substantial change in the flow velocity, the two new IUH are practically the same. As the same results were obtained for the other two watersheds, the IUH resulting from the rising limb was adopted as the definitive Kinematic Instantaneous Unit Hydrograph, hereafter referred to as KIUH.

The simulations performed to obtain the KIUH were done with the full watershed area catching rainfall and the same area contributing with runoff to the streams in order to impose on the KIUH the significance of the overland flow component.

2.4 Contrived Watersheds

As mentioned earlier, three watersheds were used during the described analysis. Although they are contrived, they resemble in most of their parameters values commonly encountered in natural catchment areas (Koch, 1985).

The main parameters for each watershed related to the present analysis are listed in Table 2.1. The value given for the time of concentration is valid for a rainfall intensity of 6.0 in/hr and no infiltration. The same values were applied to all experiments, and consequently Δi_e took the value of 0.6 in/hr.

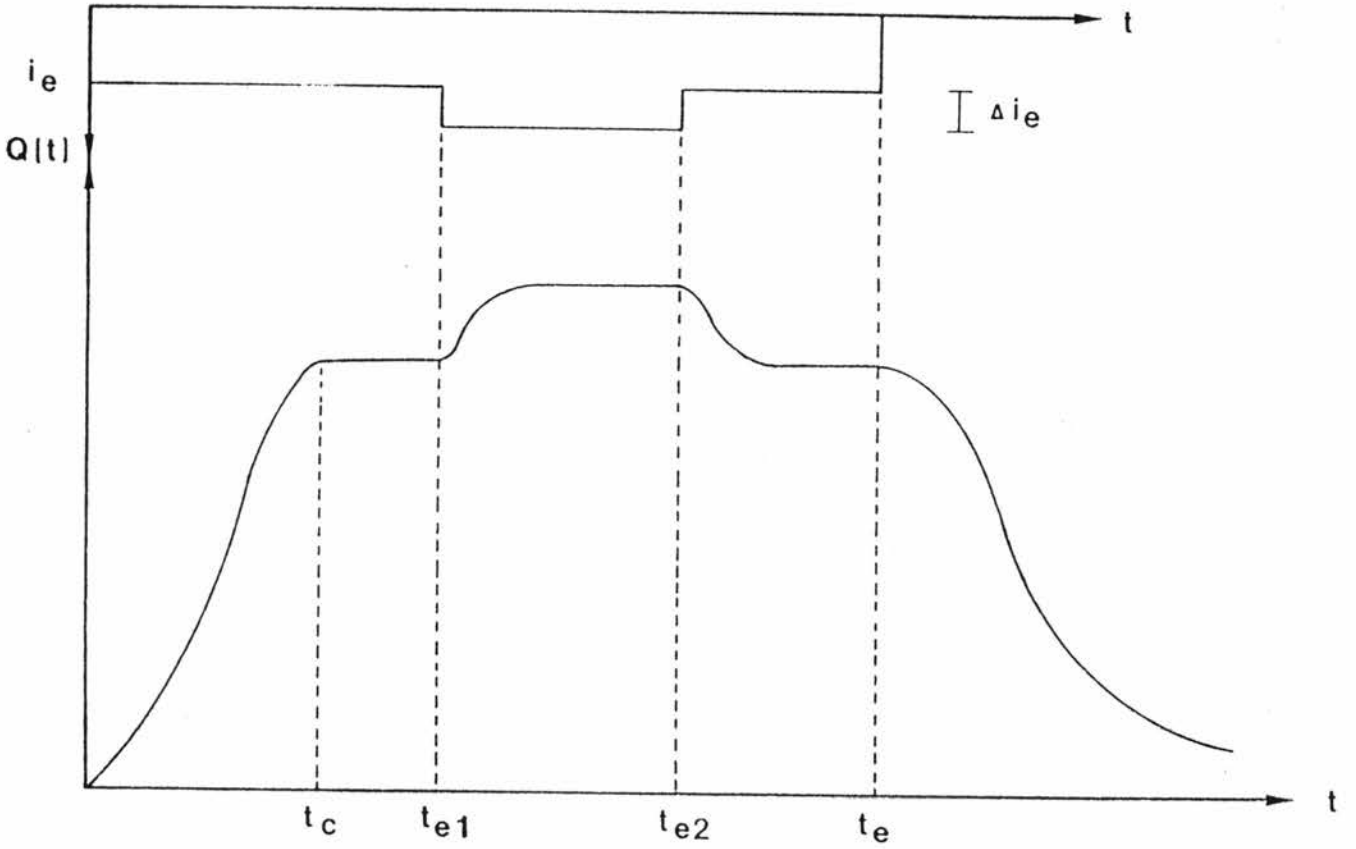

Figure 2.2. Incremental IUH procedure (Valdés et al., 1979).

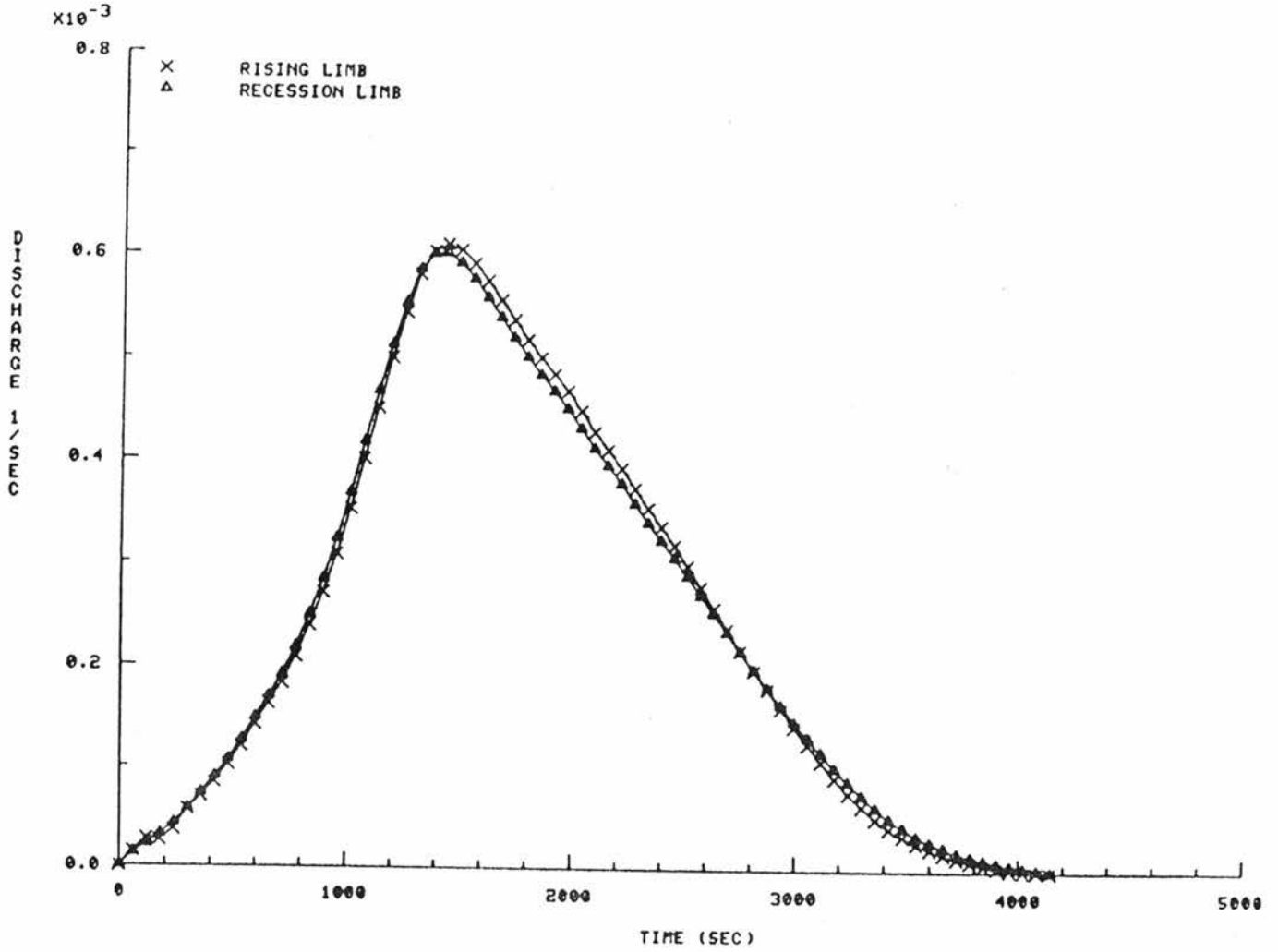

Figure 2.3. Incremental IUHs for Watershed #2.

Table 2.1. Contrived watersheds geomorphological parameters.

Watershed #	2	3	4
Area (mi^2)	3.0	3.0	3.0
Order	3	3	3
Bifurcation Ratio	2.77	3.00	3.13
Length Ratio	1.49	1.22	1.76
Area Ratio	3.62	3.91	4.29
Concentration time (min)	75	74	57

Up to this point it is necessary to estimate the peak flow velocity V in order to compute the GIUH for the three contrived watersheds. Following Valdes et al. (1979), this velocity is assumed constant through the whole watershed, and for experimental purposes they recommend to take it as that corresponding to the first steady state when the incremental intensity rainfall pattern is simulated for each watershed. Assuming this guideline, values of 8.05 and 14.10 ft/sec were obtained, the former for watersheds 2 and 3 and the latter for watershed 4.

2.5 Experiments and Results

The first experiment performed was the computation and comparison of the KIUH and the GIUH. Figures 2.4, 2.5 and 2.6 present graphical results for the three contrived watersheds, and Table 2.2 summarizes some important numerical results.

In Table 2.2 K stands for kinematic results and G denotes values related to the GIUH. The comparison of results is made in terms of percent difference, defined as

$$\Delta\ (\%) = \frac{(\text{Value})_K - (\text{Value})_G}{(\text{Value})_K} \times 100 \qquad (2.24)$$

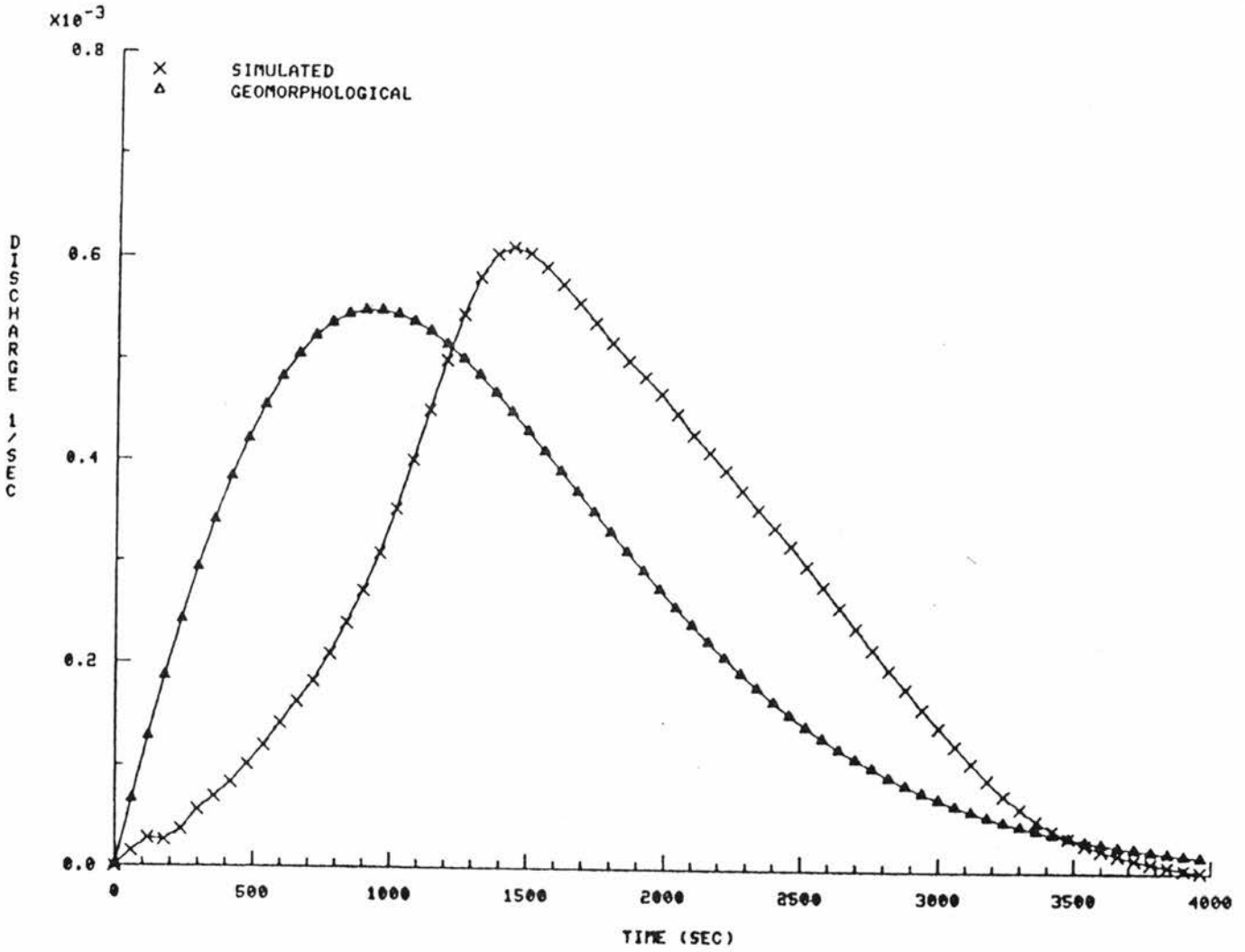

Figure 2.4. KIUH and GIUH for Watershed #2, i_e = 0.6 in/hr.

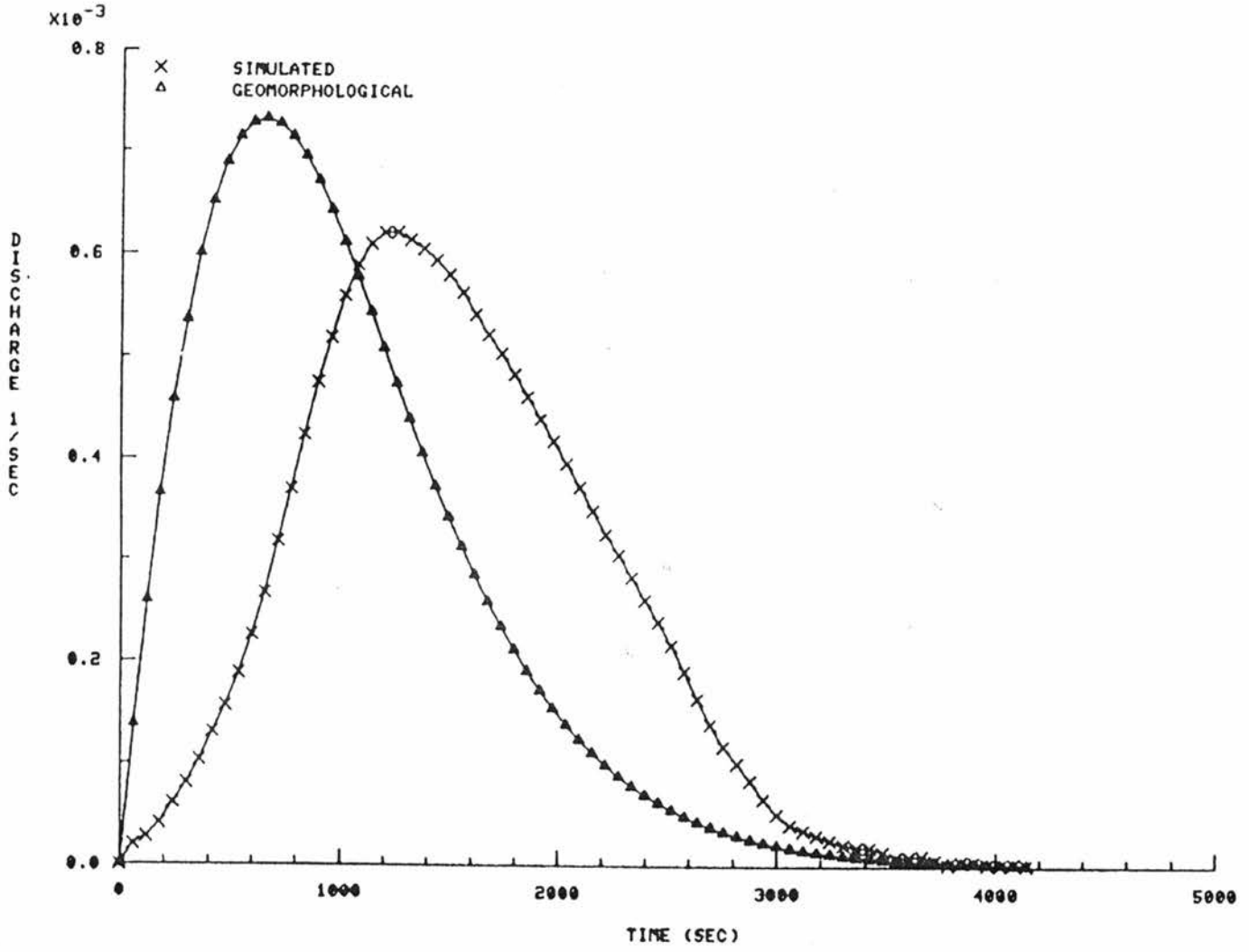

Figure 2.5. KIUH and GIUH for Watershed #3, i_e = 0.6 in/hr.

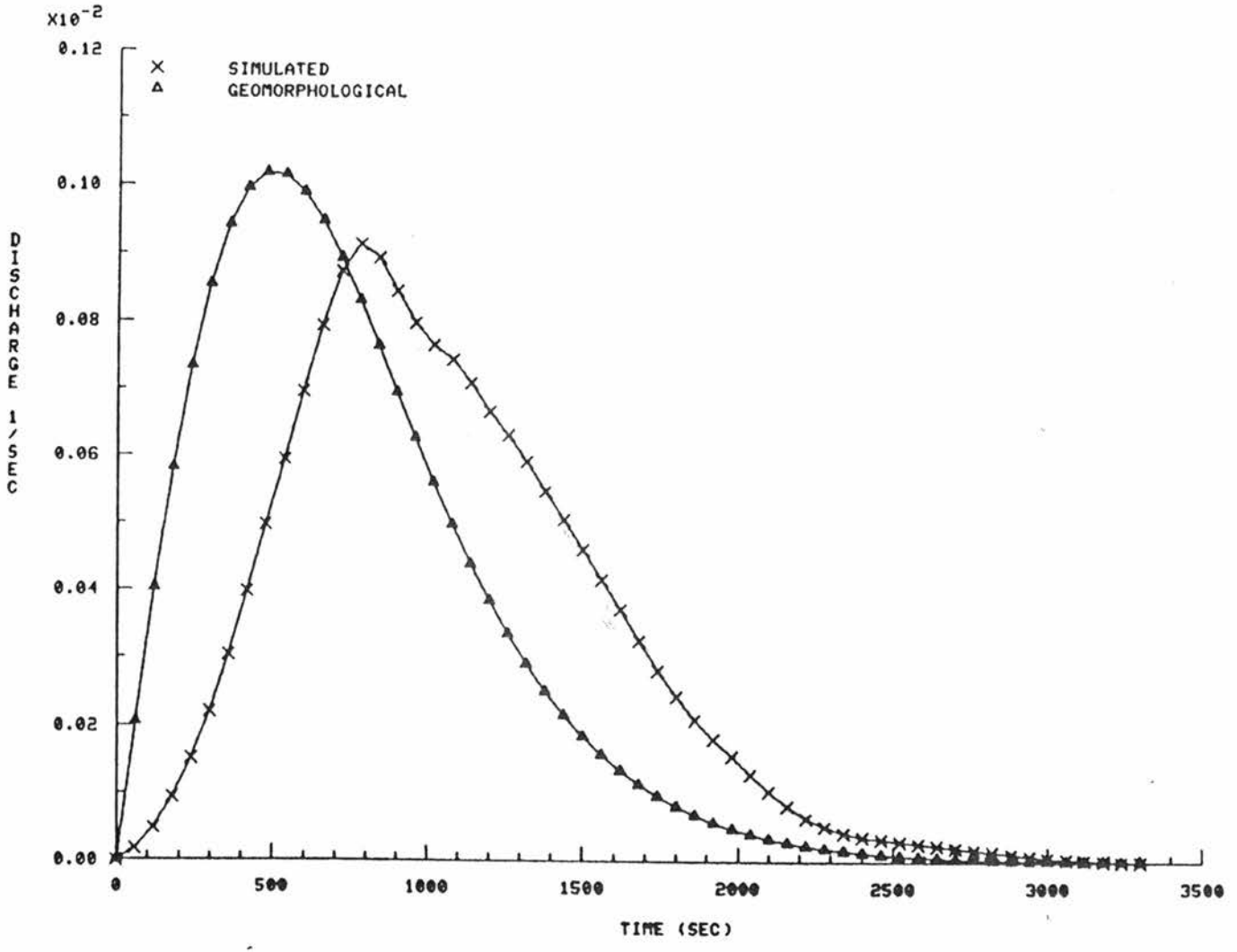

Figure 2.6. KIUH and GIUH for Watershed #4, i_e = 6 in/hr.

Table 2.2. KIUH and GIUH comparison for the contrived watersheds.

Watershed #	2	3	4
$(q_p)_K$ (1/sec)	0.6098×10^{-3}	0.6205×10^{-3}	0.9124×10^{-3}
$(q_p)_G$ (1/sec)	0.5475×10^{-3}	0.7316×10^{-3}	0.1017×10^{-2}
Δq_p (%)	10.2%	-17.9%	-11.5%
$(t_p)_K$ (min)	24	20	13
$(t_p)_G$ (min)	15	11	6
Δt_p (%)	37.5%	45%	38.5%

As can be observed from the graphical and numerical results, there is no agreement between the KIUH and the GIUH.

Up to this point, one can suspect that the poor agreement obtained is due to a bad estimation in the geomorphological ratios or in the dynamical velocity. Figures 2.7 through 2.9 summarize graphically a sensitivity analysis performed for Watershed #2, in order to guess the values of the aforementioned parameters which generate a good fitting. The necessary conclusion is that no agreement is reached at all.

Another attempt to obtain a more adequate estimated value for the peak flow velocity is made through the expression obtained after calibration for the GIUH peak variables (Rodriguez-Iturbe and Valdes, 1979). When q_p, peak discharge, is given in 1/sec, t_p, time to peak, in seconds, V in ft/sec and L_3 in ft, the equations are:

$$q_p = 0.3639 \, R_L^{0.43} \, \frac{V}{L_3} \tag{2.25}$$

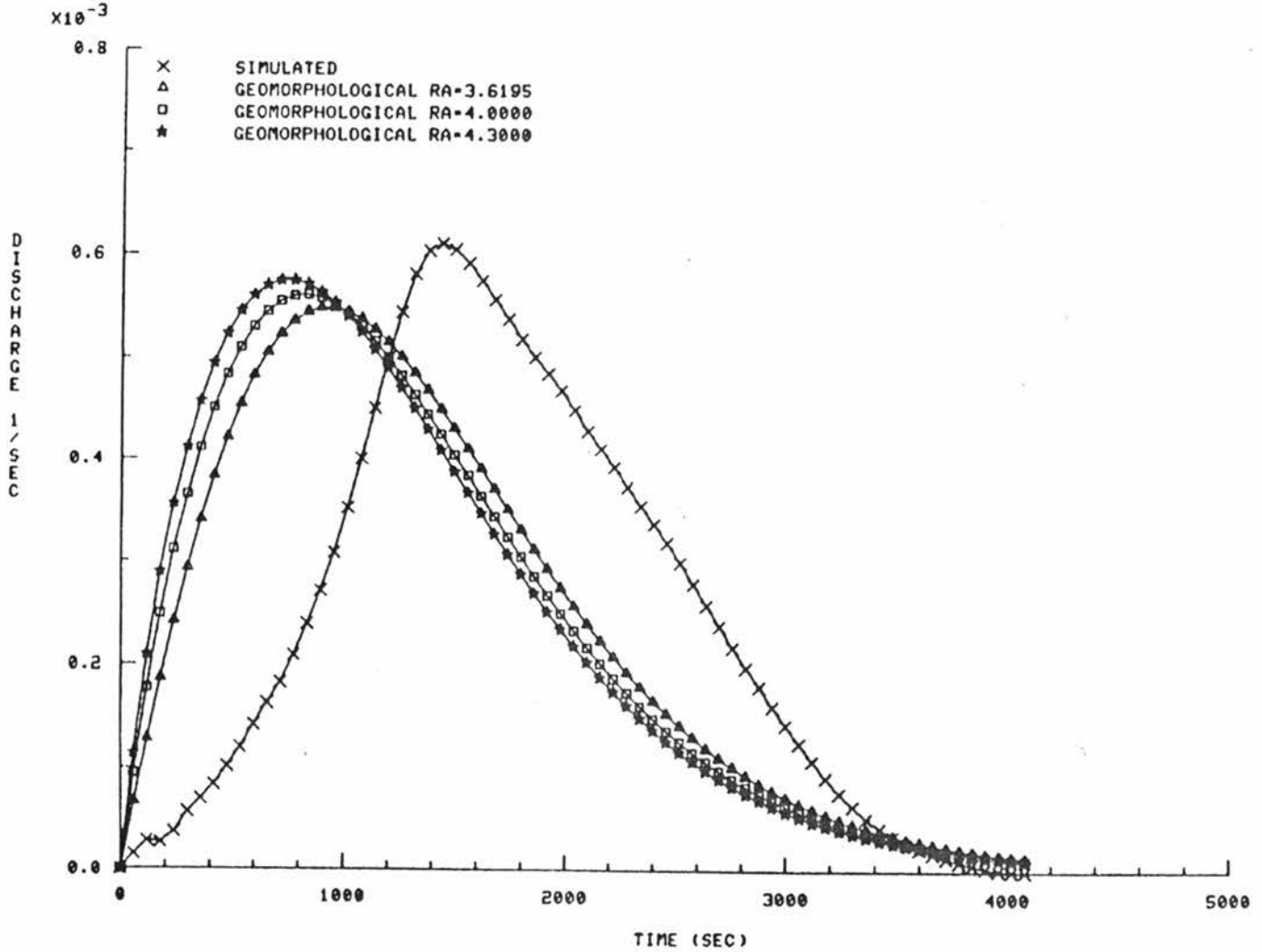

Figure 2.8. Sensitivity analysis on R_A for the GIUH for Watershed #2.

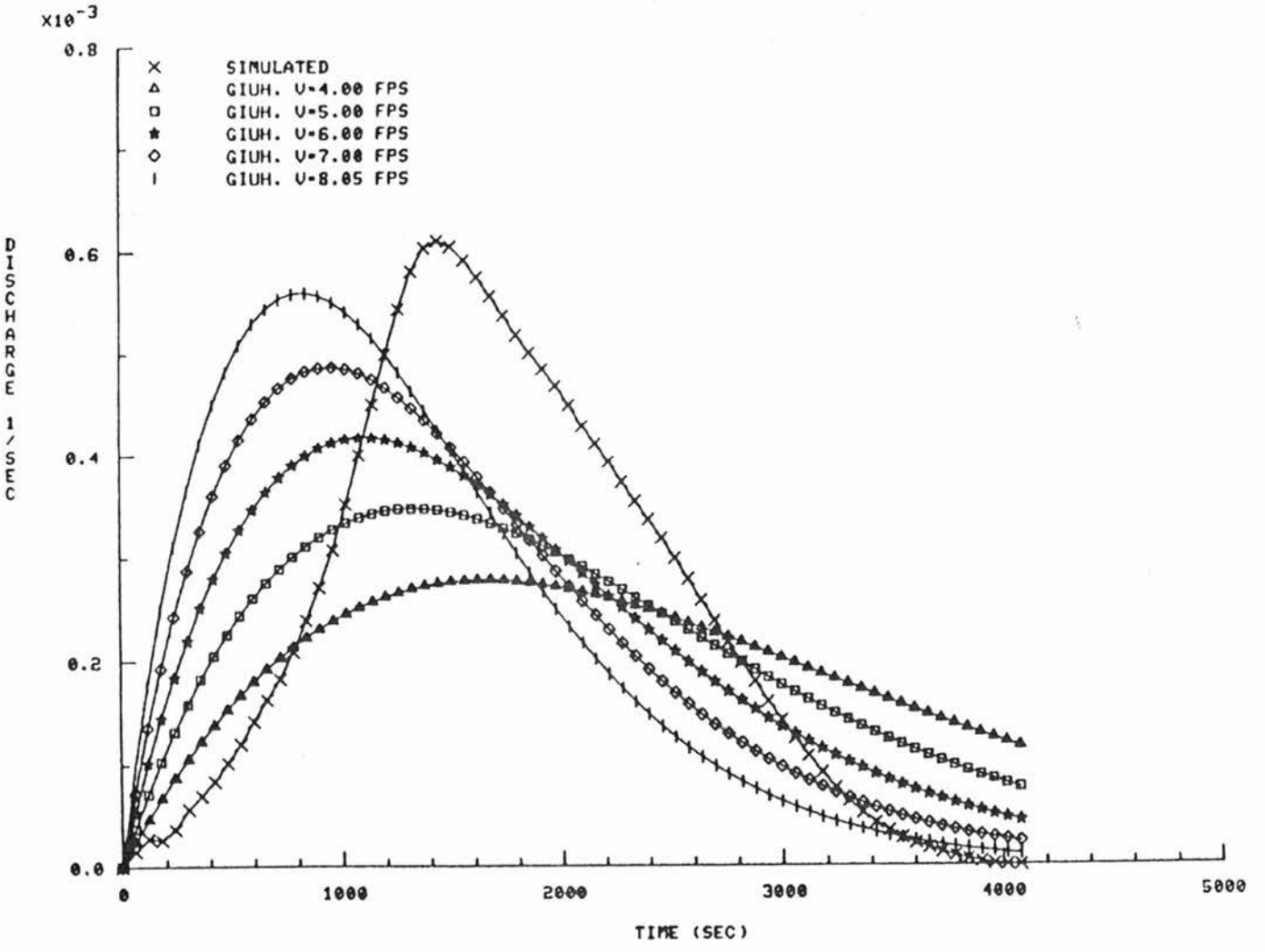

Figure 2.9. Sensitivity analysis on V for the GIUH for Watershed #2.

$$t_p = 1.5840 \frac{1}{R_L^{0.38}} \left(\frac{R_B}{R_A}\right)^{0.55} \frac{L_3}{V} \qquad (2.26)$$

As one obtains $(q_p)_K$ and $(t_p)_K$ via kinematic wave simulation along with the incremental IUH procedure, two values of V can be estimated from the above equations, denoted respectively V_q and V_t.

Table 2.3 summarizes the values of V_q and V_t for Watersheds 2, 3 and 4.

The results obtained for the peak flow velocity lead to the conclusion that it is impossible to obtain a unique velocity allowing the joint estimation of q_p and t_p.

Table 2.3. Estimated values for the peak flow velocity for the contrived watersheds.

Watershed	2	3	4
$(q_p)_K$ (1/sec)	0.6098×10^{-3}	0.6205×10^{-3}	0.9124×10^{-3}
$(t_p)_K$ (sec)	1440	1200	780
$L\Omega$ (ft)	6239	4032	6633
R_L	1.49	1.22	1.76
R_A	3.62	3.91	4.29
R_B	2.77	3.00	3.13
V_q (fps)	8.81	6.32	13.05
V_t (fps)	5.09	4.27	9.14
V (fps)	8.05	8.05	14.10

2.6 Conclusions

The most important conclusion, yielded by the comparison of the Geomorphological Instantaneous Unit Hydrograph GIUH and the Kinematic

Instantaneous Unit Hydrograph KIUH, performed on three contrived watersheds, is given by the inadequacy of the former to describe the response for small watersheds where overland flow is considered to be an important timing component.

This conclusion is based on the experiments performed. The KIUH, derived via simulation, considers overland flow, while the GIUH incorporates the catchment areas for each order just as initial states with no holding time within them.

The overland flow effect is observed in the behavior of the peak flow and time to peak. The peak flow for the KIUH tends to be less than the GIUH peak flow for two of the three analyzed examples, indicating that the latter enables a lesser holding time than the former. Furthermore, the time to peak shows the same behavior.

Another concern is the ability of the geomorphological ratios to describe the watershed shape and arrangement. In small watershed, sample variations in these parameters are larger and more important than in medium or large watersheds, and their variations are not included in the GIUH.

The conclusions herein presented do not pretend to disqualify the GIUH as a tool useful for hydrological forecast and synthesis in medium or large watersheds, where overland flow plays no significant role, cases for which the authors have proved its applicability. They are directed toward the applicability of the GIUH to small watersheds where overland flow is considered to be an important timing component.

In regard to this, the inclusion of an extra state, given by the holding time in the planes as suggested by Gupta et al. (1980), can yield better results, providing the required timing or storage component.

Chapter 3

KINEMATIC ROUTING

3.1 Introduction

As stated previously, the scope of this work encompasses the derivation of flood frequency distributions for small watersheds, where the overland flow is an important timing component. In order to achieve this, an effective rainfall-runoff model has to be derived where such a component is included and plays an important role.

The effective rainfall-runoff model is derived for a catchment area formed by two symmetrical planes and a first order stream, i.e., no upstream tributaries to the channel are considered.

The tool used to obtain the aforementioned model is the kinematic wave theory. First, for the sake of completeness, the analytical solution for the discharge hydrograph in the plane is presented, based on Eagleson (1970) and Garbrecht (1984). After investigation regarding the analytical solution for the channel, some significant results are obtained. These can be considered as an extension of Eagleson's work (1972).

An approximate kinematic routing model is developed and used, together with theoretical results, in order to forecast the peak discharge and time to peak for any rainfall event and for any first order catchment. In the last stage, some equations used in the forecasting model are improved via regression analysis performed on dynamic watershed variables.

3.2 Flow Equations and the Kinematic Wave

The differential equations of motion for one-dimensional, incompressible, free surface flow in a channel can be written as:

$$\frac{\partial A}{\partial t} + \frac{\partial Q}{\partial x} = q \tag{3.1}$$

$$\frac{\partial Q}{\partial t} + \frac{\partial}{\partial x}\left(\frac{Q^2}{A}\right) + gA\frac{\partial y}{\partial x} = gA\,(S_o - S_f) \tag{3.2}$$

where Q represents the discharge through the cross-sectional area A in a given time t, q represents the lateral inflow per unit length in x direction, y is the average depth of flow in the section, S_o stands for the channel slope, S_f for the friction slope and g denotes the gravity constant. The above equations represent a gradually varied unsteady flow and other assumptions inherent to them are: uniform distribution of velocities through the section, hydrostatic pressure distribution along the vertical, small channel slope and no momentum exchange due to lateral inflow. The solution for these two equations must yield the flow properties Q and A as a function of position x and time t.

The kinematic wave approximation considers that the inertia and pressure terms in the equations of motion are negligible compared to the gravity and friction terms, so that the following set of equations is obtained:

$$\frac{\partial A}{\partial t} + \frac{\partial Q}{\partial x} = q \tag{3.3}$$

$$S_o = S_f \tag{3.4}$$

Equation (3.4) can be expressed as a uniform flow resistance formula. In the present work, the Manning's equation according to the English system of units is selected, and is given by:

$$Q = \frac{1.486}{n_c} AR^{2/3} S_c^{1/2} \tag{3.5}$$

where n_c is the Manning's roughness coefficient, S_c is the channel bed slope and R is the hydraulic radius. By definition, R = A/P, in which P stands for the wetted perimeter and can be expressed as a function of the area. Thus, the cross-sectional shape is described by means of

$$R = aA^b \tag{3.6}$$

where a and b are determined either empirically or assuming a regular well-defined geometrical shape.

Plugging Equation (3.6) into Equation (3.5) yields the following result

$$Q = \alpha_c A^{\beta c} \tag{3.7}$$

$$\alpha_c = \frac{1.486}{n_c} a^{2/3} S_c^{1/2} \tag{3.8}$$

$$\beta c = 1 + \frac{2b}{3} \tag{3.9}$$

Notice that Equation (3.7) enables the consideration of other flow resistance formulas different from Manning's equation.

The kinematic wave equation is obtained by multiplying Equation (3.3) by $\partial Q/\partial A$, yielding

$$\frac{\partial Q}{\partial t} + \frac{\partial Q}{\partial A}\left(\frac{\partial Q}{\partial x} - q\right) = 0 \tag{3.10}$$

The term $\partial Q/\partial A$ is known as kinematic wave celerity (also referred to as the Kleitz-Seddon celerity) and represents the local travel velocity for the incremental unit width discharge $\partial Q/\partial x - q$:

$$\frac{\partial Q}{\partial A} = \alpha_c \beta c A^{\beta c - 1} = \beta c \frac{Q}{A} = \beta c V \tag{3.11}$$

where V stands for the mean velocity of flow.

The equations of motion considering kinematic wave approximation for the overland flow are obtained by analogy with Equations (3.3) and (3.4), taking into account that such a flow is similar to that in a wide channel. Therefore, the flow properties are expressed per unit width:

$$\frac{\partial y}{\partial t} + \frac{\partial q}{\partial x} = i_e \tag{3.12}$$

$$q = \alpha_p y^{\beta p} \tag{3.13}$$

where y represents the flow depth, q the discharge per unit width and i_e the effective precipitation intensity. The coefficients α_p and βp for the plane are also obtained using Manning's equation, but

considering that the plane behaves like a very wide channel, i.e., R≈y. Under these conditions

$$\alpha_p = \frac{1.486}{n_p} S_p^{1/2} \tag{3.14}$$

$$\beta p = 5/3 \tag{3.15}$$

where n_p and S_p stands for the plane roughness and plane slope, respectively.

3.3 Solution to Kinematic Flow Equations for Overland Flow by the Method of Characteristics

In the following paragraphs, Equations (3.12) and (3.13) are solved using the method of characteristics. Then, that solution is applied to the case of overland flow produced by a constant effective rainfall intensity. For the solution when variable rainfall intensity is considered see Appendix A.

The essence of the method of characteristics, when applied to the equations of motion, is to find a space-time locus (x = x(t)) along which a discontinuity of the partial derivatives of the flow properties, unit width discharge and flow depth, exists. This locus defines the path of wave propagation along which an observer moving with it can describe the process in terms of an ordinary differential equation.

Considering the definition of a total differential, the following two equations can be written

$$\frac{\partial q}{\partial x} dx + \frac{\partial q}{\partial t} dt = dq \tag{3.16}$$

$$\frac{\partial y}{\partial x} dx + \frac{\partial y}{\partial t} dt = dy \tag{3.17}$$

Equations (3.12), (3.13), (3.16) and (3.17) comprise a system of equations where the partial derivatives are considered as unknowns. If this system is expressed in matrix notation, the discontinuity is given, in first place, by vanishing the determinant of the coefficient matrix, and secondly, by applying the same condition to the four determinants obtained replacing the columns in the matrix coefficient by the independent term vector. The first condition, after some term manipulations, gives rise to the equation

$$\frac{dx}{dt} = \alpha_p \beta p y^{\beta p-1} \tag{3.18}$$

The second condition implies the equations

$$\frac{dq}{dx} = i_e \tag{3.19}$$

$$\frac{dy}{dt} = i_e \tag{3.20}$$

$$\frac{dq}{dt} = (i_e)\ \alpha_p \beta p y^{\beta p-1} \tag{3.21}$$

Equation (3.18) defines the characteristic lines in space time coordinates and it simply states that the discontinuity or perturbation travels along those lines with a velocity equal to the previous defined celerity (Equation (3.11)).

Equations (3.19) through (3.21) are valid only along the characteristic lines. An important physical observation obtained from those equations is that the discharge, the depth, the mean flow

velocity and the celerity remain constant along the characteristic lines, under the absence of effective rainfall intensity.

Calling W the width of the plane, the following initial and boundary conditions, respectively, can be posed

$$y = 0,\ 0 \leq x \leq W,\ t = 0 \tag{3.22}$$

$$y = 0,\ x = 0,\ t \geq 0. \tag{3.23}$$

Besides, the effective rainfall pattern is completely defined by the intensity i_e and duration t_e. Then, integration of Equation (3.20) between zero and any time t gives

$$y = i_e t \tag{3.24}$$

Taking this result to Equation (3.18) and integrating between an initial point $(x_o,\ t_o)$ and another generic (x,t), the equation describing the characteristic path is

$$x - x_o = \alpha_p\ i_e^{\beta p-1}(t - t_o)^{\beta p} \tag{3.25}$$

An important result, shown in Figure 3.1, is obtained by making $x_o = 0$ and $t_o = 0$. The resulting line is called the limiting characteristic and is described by:

$$x_w = \alpha_p\ i_e^{\beta p-1}\ t_w^{\beta p} \tag{3.26}$$

where x_w and t_w denote the coordinates of a point on the limiting characteristic.

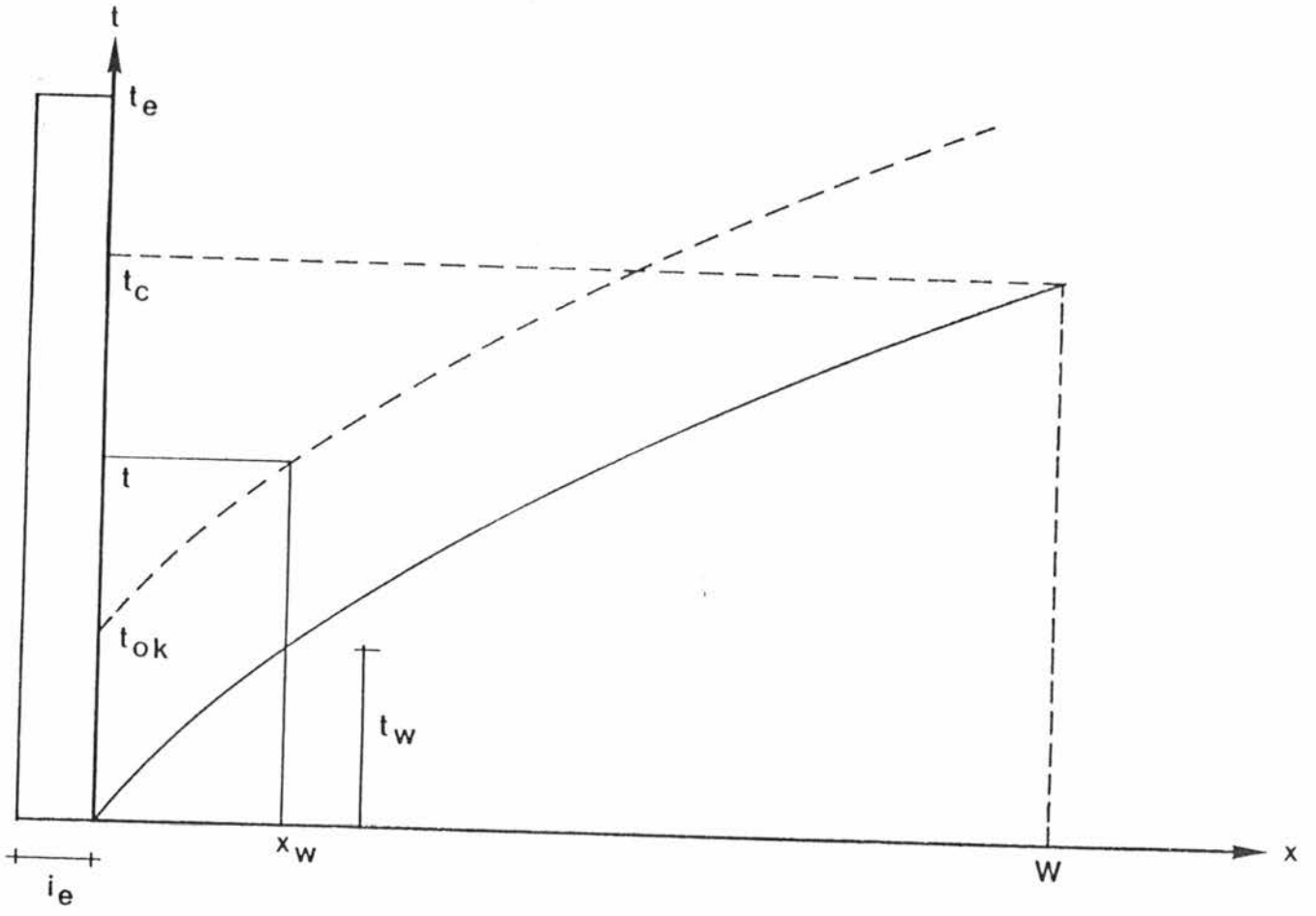

Figure 3.1. Limiting characteristic line.

In Figure 3.1 the effective rainfall pattern is shown at the left. However, the same pattern holds true for all values of x.

Now, let the effective duration tend to infinity, such that the plane attains concentration, which means that the hydrograph at the plane outlet (x=W) reaches a steady state, and beyond a certain time, called time of concentration, no increase in the discharge takes place. The depth, for all characteristic arising at the x-axis, is governed by Equation (3.24). Notice that all these characteristic lines are located below the limiting characteristic.

The characteristic lines arising at the t-axis, at a time t_{ok} and $x_o = 0$, are governed by the two following equations, obtained after integration of Equations (3.20) and (3.18).

$$y = i_e(t - t_{ok}) \tag{3.27}$$

$$x = \alpha_p \, i_e^{\beta p-1}(t - t_{ok})^{\beta p} \tag{3.28}$$

Applying Equation (3.28) to any value of x, $0 \leq x \leq W$, say x_w one obtains

$$t - t_{ok} = \left[\frac{x_w \, i_e^{1-\beta p}}{\alpha_p}\right]^{1/\beta p} \tag{3.29}$$

Now, going back to Equation (3.26), one realizes that the right hand term of Equation (3.29) is t_w.

$$t - t_{ok} = t_w \tag{3.30}$$

For a given location x_w, t_w will not change, thus $t - t_{ok}$ and the depth remain constant above the limiting characteristic. Such value of the depth is computed by means of

$$y = i_e t_w \tag{3.31}$$

On the other hand, the value of t_w is obtained, for a given location x_w, using Equation (3.26). Particularly, for $x = W$, the limiting characteristic time value is computed as:

$$t_c = \left(\frac{W\ i_e^{1-\beta p}}{\alpha_p} \right)^{1/\beta p} \tag{3.32}$$

which defines the point beyond of which discharge is constant at the plane outlet and so it represents the time of concentration for the plane.

Now, let the effective rainfall duration take a finite value greater than the time of concentration for the plane. The final objective is given by the determination of the discharge hydrograph at the plane outlet, i.e., for x=W.

Up to this point, the depth hydrograph at the plane outlet is described by Equation (3.24) for $0 \leq t \leq t_c$ and by

$$y = i_e t_c \tag{3.33}$$

for $t \leq t_c \leq t_e$, where t_e stands for the effective rainfall duration. After the excess rainfall stops, Equations (3.19), (3.20) and (3.21) have to be equated to zero. As it has been stated, this means that

discharge, depth and celerity remain constant along characteristic lines.

Figure 3.2 depicts the evolution of the water surface profile for times greater than t_e. The equation for the steady state profile ($t = t_e$) is obtained by making $t = t_w$ in Equation (3.24) and replacing it in (3.26), yielding the following result

$$y = \left[\frac{x_w \; i_e}{\alpha_p}\right]^{1/\beta p} \tag{3.34}$$

One can now pick up a point on the profile at time $t = t_e$, and knowing that the future of the depth lies on a common characteristic, use the propagation celerity C to locate the point in space at any time $t > t_e$. From Figure 3.2 and Equation (3.18) integrated for y constant the following is obtained

$$x - x_w = \alpha_p \; y^{\beta p-1}(t - t_e) \tag{3.35}$$

Notice that the right hand side term in Equation (3.35) can be interpreted as $C \; \Delta t$. Obtaining x_w in Equation (3.34) and taking it to (3.35), after some term manipulation yields

$$x = \alpha_p \; y^{\beta p-1} \left[\frac{y}{i_e} + \beta p(t - t_e)\right] \tag{3.36}$$

This last equation defines the characteristic lines after the effective rainfall ends.

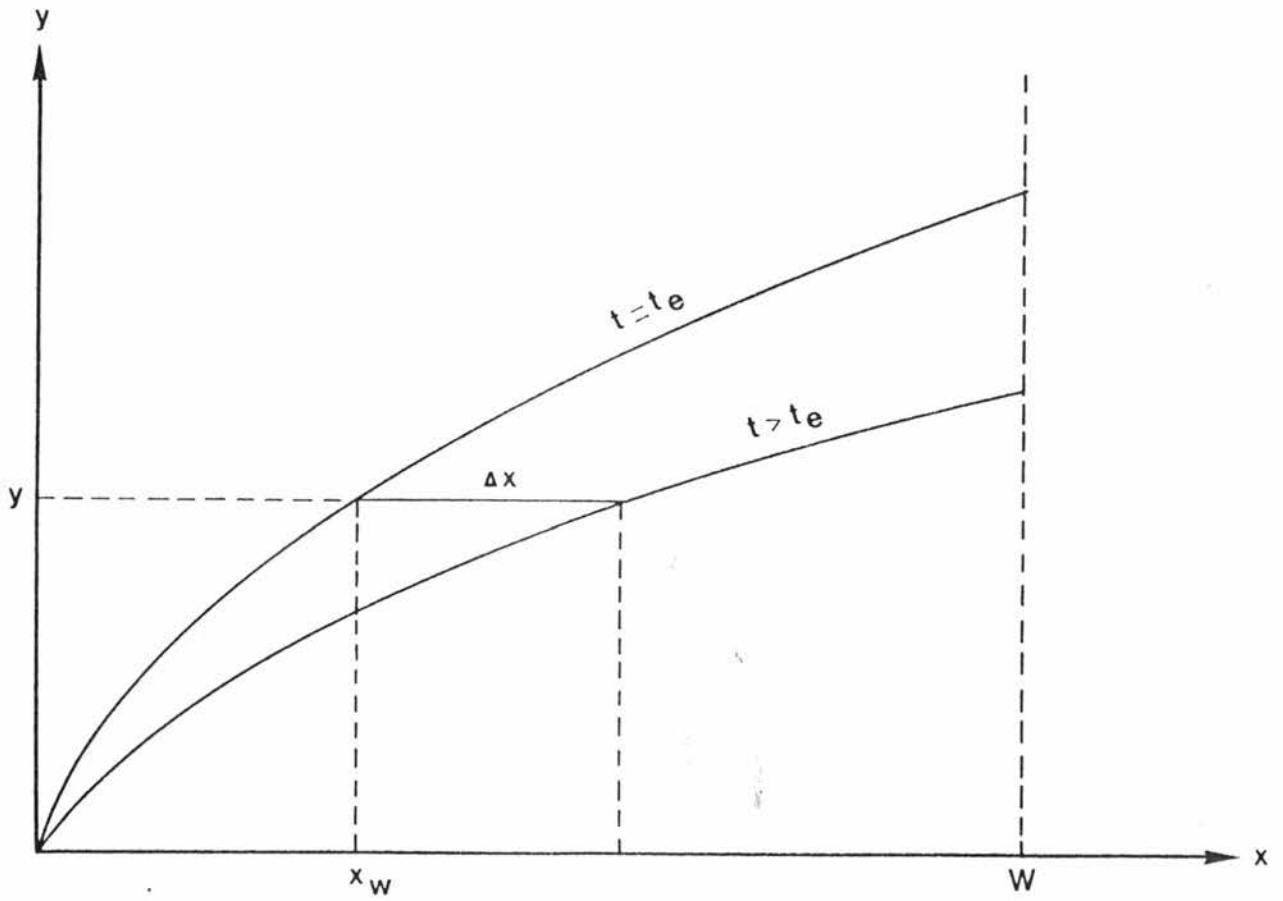

Figure 3.2. Water depth profile evolution for $t \geq t_e$ and $t_e \geq t_c$.

At this point, it is possible to summarize the computation of the discharge hydrograph at the plane outlet when concentration is attained ($t_e \geq t_c$) as follows:

$$y = i_e t, \quad 0 \leq t < t_c \tag{3.37}$$

$$y = i_e t_c, \quad t_c \leq t \leq t_e \tag{3.38}$$

$$W = \alpha_p \, y^{\beta p - 1} \left[\frac{y}{i_e} + \beta p (t - t_e) \right], \quad t_e < t < \infty \tag{3.39}$$

$$q = \alpha_p \, y^{\beta p} \tag{3.40}$$

$$t_c = \left(\frac{W \, i_e^{1-\beta p}}{\alpha_p} \right)^{1/\beta p} \tag{3.41}$$

Notice that the computation of y from Equation (3.39) for a specific value of t requires the use of a numerical algorithm, since such a equation cannot be reduced to a closed solution for y.

Figure 3.3 presents the typical shape for the plane outlet hydrograph when concentration is attained.

Now, the case when the excess rainfall ceases before the initial perturbation has reached the catchment outlet is considered. Figure 3.4 describes the evolution of the water surface profile for times equal or greater than the effective duration t_e.

The maximum profile (ABC) takes place at $t = t_e$. For a time $t > t_e$ point B will move to B_1 and the new profile will be AB_1C. At a time t_p the profile will not be a broken line anymore, when point B reaches point C. Taking into account that the depth for $0 \leq t \leq t_e$ is

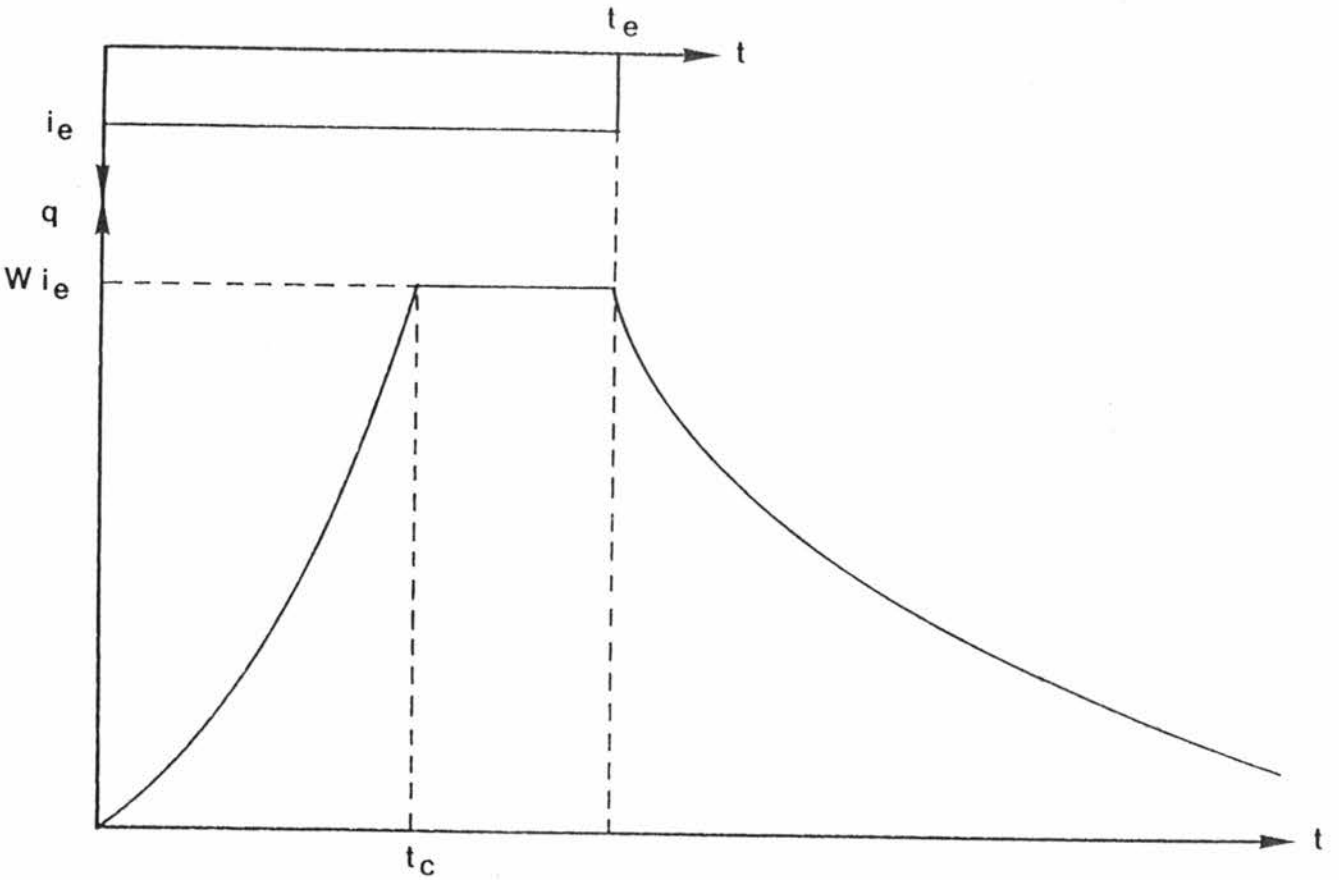

Figure 3.3. Typical discharge hydrograph for the plane when $t_e \geq t_c$.

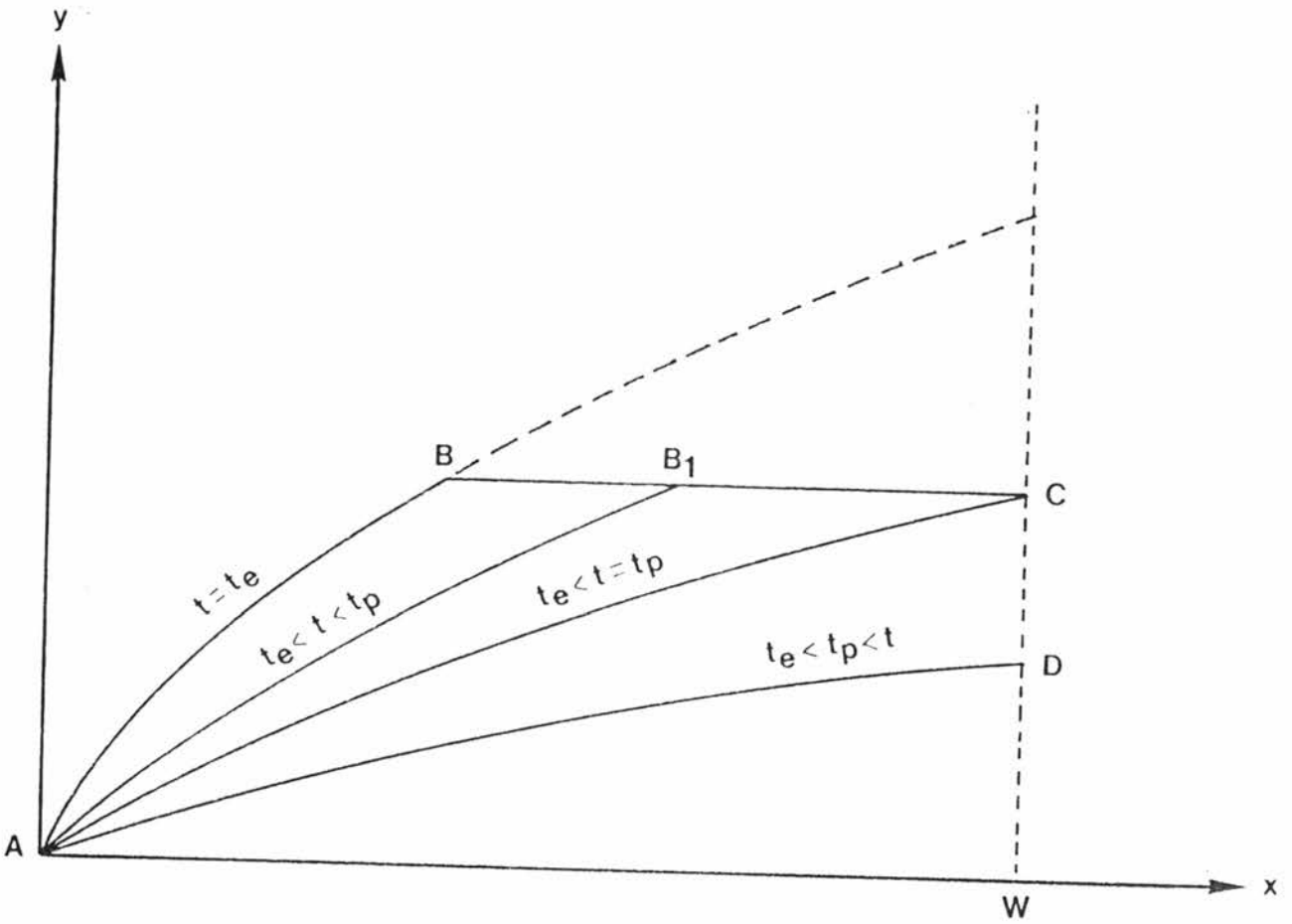

Figure 3.4. Water depth profile evolution for $t \geq t_e$ and $t_e < t_c$.

given by Equation (3.24), and that the depth for $t = t_e$ is $i_e t_e$, the time t_p is computed as:

$$t_p = \frac{\beta p - 1}{\beta p} t_e + \frac{W}{\alpha_p \beta p (i_e t_e)^{\beta p - 1}} \tag{3.42}$$

For $t > t_p$ the procedure for obtaining the depth is the same as that presented for the case of concentration on the plane. Hence, the computation of the discharge hydrograph at the plane outlet for an effective rainfall lasting less than the time of concentration is summarized via the following set of equations:

$$y = i_e t \quad , \quad 0 \leq t < t_e \tag{3.43}$$

$$y = i_e t_e \quad , \quad t_e \leq t \leq t_p \tag{3.44}$$

$$W = \alpha_p \, y^{\beta p - 1} \left[\frac{y}{i_e} + \beta p (t - t_e) \right] \quad , \quad t_p < t \tag{3.45}$$

$$q = \alpha_p \, y^{\beta p} \tag{3.46}$$

$$t_p = \frac{\beta p - 1}{\beta p} t_e + \frac{W}{\alpha_p \beta p (i_e t_e)^{\beta p - 1}} \tag{3.47}$$

Again the solution of Equation (3.45) for y requires an appropriate numerical method.

Figure 3.5 depicts the plane hydrograph for $t_e < t_c$.

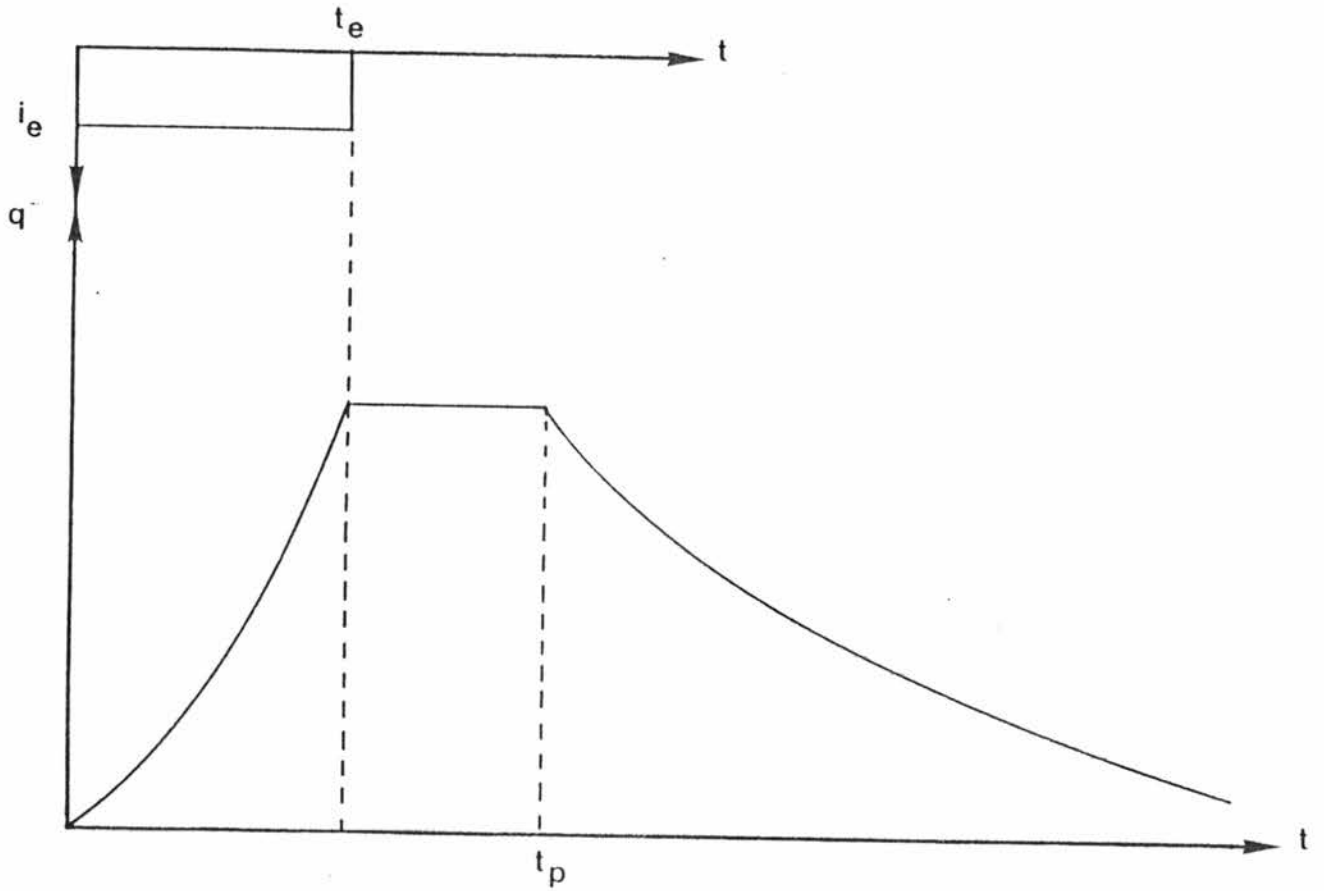

Figure 3.5. Typical discharge hydrograph for the plane when $t_e < t_c$.

3.4 Solution to Kinematic Flow Equations for Channel Flow by the Method of Characteristic

Following a procedure similar to that outlined in Section 3.3 and beginning with Equations (3.3) and (3.7), the expressions governing the flow in a channel along characteristic lines are obtained as:

$$\frac{dx}{dt} = \alpha_c \beta c \, A^{\beta c - 1} \tag{3.48}$$

$$\frac{dQ}{dx} = q \tag{3.49}$$

$$\frac{dA}{dt} = q \tag{3.50}$$

$$\frac{dQ}{dt} = q \, \alpha_c \beta c \, A^{\beta c - 1} \tag{3.51}$$

where q stands for the total lateral inflow, i.e., the addition of the left and right plane hydrographs.

The objective in this case would be the integration of the above equations when q is derived from those results obtained in the previous section. The initial and boundary conditions are

$$A = 0 \, , \quad 0 \leq x \leq L_c \, , \; t = 0 \tag{3.52}$$

$$A = 0 \, , \; x = 0 \, , \; t \geq 0 \tag{3.53}$$

where L_c represents the channel length.

Following a hierarchical approach to the solution, the first case to be considered would be a first order stream with equal lateral planes. This means that there would be no upstream inflow and that

the lateral inflow hydrograph could be computed as two times the hydrograph produced by one plane.

Table 3.1 presents all possible combinations of cases to be considered by the analytical integration of the characteristic equations, in order to describe completely the discharge hydrograph in the channel. Figure 3.6 depicts the four possible hydrographs. Table 3.1 has been elaborated on the basis of concentration on the planes and concentration on the channel. The concept of concentration on the plane has been stated in Section 3.3. Concentration on the channel means that under a constant input to the channel, during a certain time interval, the discharge hydrograph at the downstream end reaches a steady state.

Table 3.1. Cases in the analytical integration for channel flow.

	Plane	Channel
Case 1	Concentration	Concentration
Case 2	Concentration	No concentration
Case 3	No concentration	Concentration
Case 4	No concentration	No concentration

It must be pointed out that Case 1 implies concentration in the whole catchment area.

Although the problem is considered well posed, it is not possible to obtain the analytical solution for the first order channel discharge hydrograph. In first place, this is due to the fact that the plane hydrograph can not be expressed analytically in a complete fashion; the solution for its receding limb requires the use of some numerical scheme, so that a set of numerical values is obtained. On

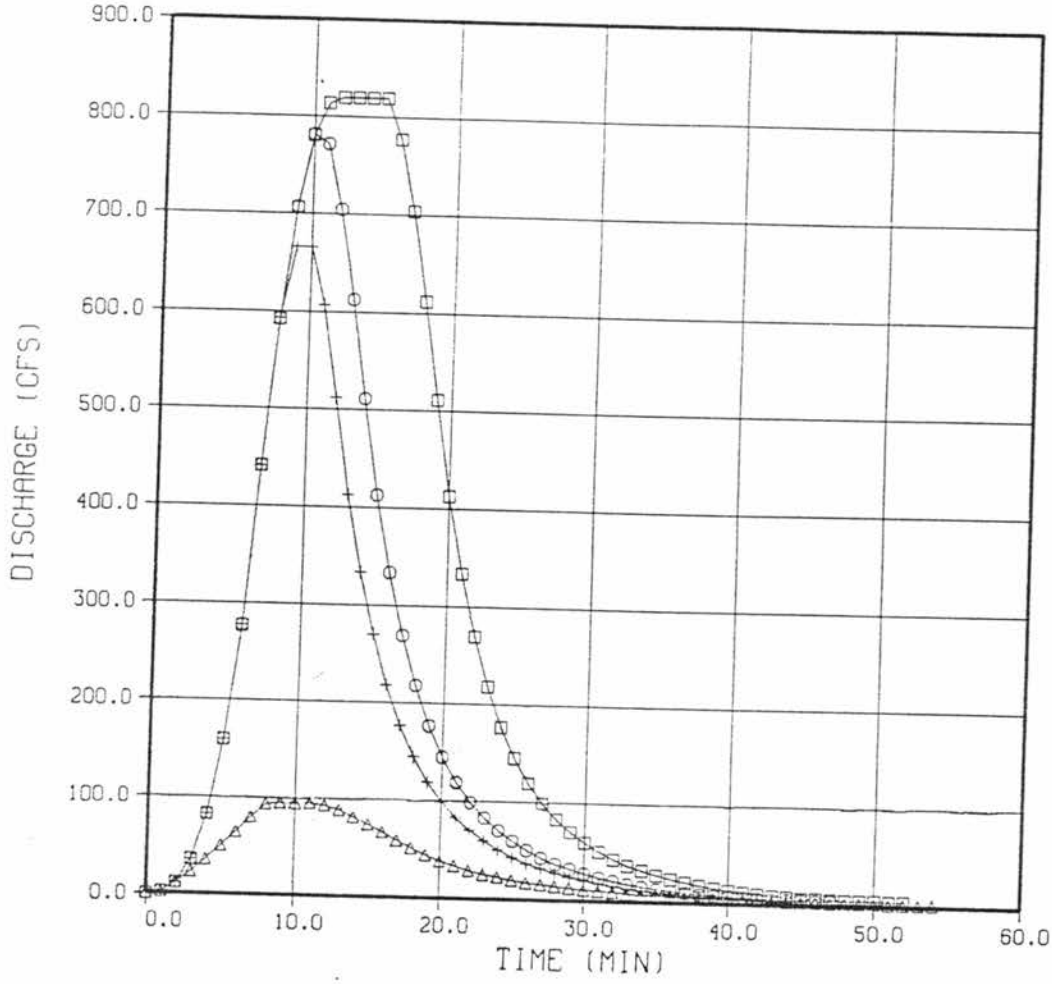

Figure 3.6. Typical discharge hydrographs for a first order stream with symmetrical planes.

the other hand, an analytical integration can be intended for the receding limb and the plateau, but the presence of some integrals with no closed solution makes this second attempt impossible.

Obviously, when the first order channel is considered along with two different planes, the solution becomes more complicated. The input inflow, once the two lateral hydrographs are added, could be like a step function, a double-peak hydrograph, or even a simple plane hydrograph.

Continuing with the hierarchical approach, one can go further into second or higher order channels. However, in addition to the aforementioned restrictions, a third one appears, given by the an upstream boundary condition. As there is upstream tributary inflow, condition (3.53) is no longer valid and a finite difference scheme is required.

Summarizing, this section shows that it is impossible to obtain a complete analytical solution for the channel discharge hydrograph, even in the simpler case, the first order stream with two symmetrical planes. However, the reasoning here exposed does not inhibit an analytical solution for the first order channel, in some cases, for the peak discharge and time to peak, and an approximate solution for the others, as will be shown in the following sections.

Some values regarding the plane and channel dynamics are held constant. Such values are roughness and the coefficients describing the hydraulic radius cross-sectional area relationship for the channel, $R = aA^b$. Particularly, $a = 0.25$ and $b = 0.35$ are recommended by Koch (1985), based on Garbrecht's findings (1984). This last author obtain such values after analysis of several stable channel relationships presented in the literature.

3.5 Some Exact Solutions for the Peak Variables in a First Order Channel

The cases when concentration on the stream is attained are suitable of exact solution for the time to peak and peak discharge in the discharge hydrograph. These cases encompass the two possible responses on the plane, concentration and no concentration.

3.5.1 Case 1: Concentration on Plane and Concentration on Channel

Figure 3.7 presents an scheme of the plane x - t, used to obtain the analytical solution when concentration are present on both elements, plane and channel. The catchment unit herein considered is a first order unit, composed by two symmetrical planes of width W and a channel of length L_c. Therefore, the uniformly distributed input along the channel is given by two times the plane hydrograph, and since there is concentration on the planes, this hydrograph is given by Equations (3.37) through (3.41). Although the input is shown on the t axis, it is the same along the full channel length. Obviously, there is no upstream tributaries and the conditions given in (3.52) and (3.53) are valid.

Here, the concept of concentration on the channel can be presented more clearly. The rising limb in the plane's hydrograph lasts from zero to t_c. The characteristic line starting at $x = 0$ and $t = t_c$ will arrive a the channel downstream end at a time $t_c + t_s$. The channel outflow hydrograph will then increase from zero to a given value during the interval zero to $t_c + t_s$. Any characteristic line starting at $x = 0$ and times greater than t_c, and arriving downstream before the rainfall ends, will produce the same discharge as that starting at t_c, since both of them are submitted to the same

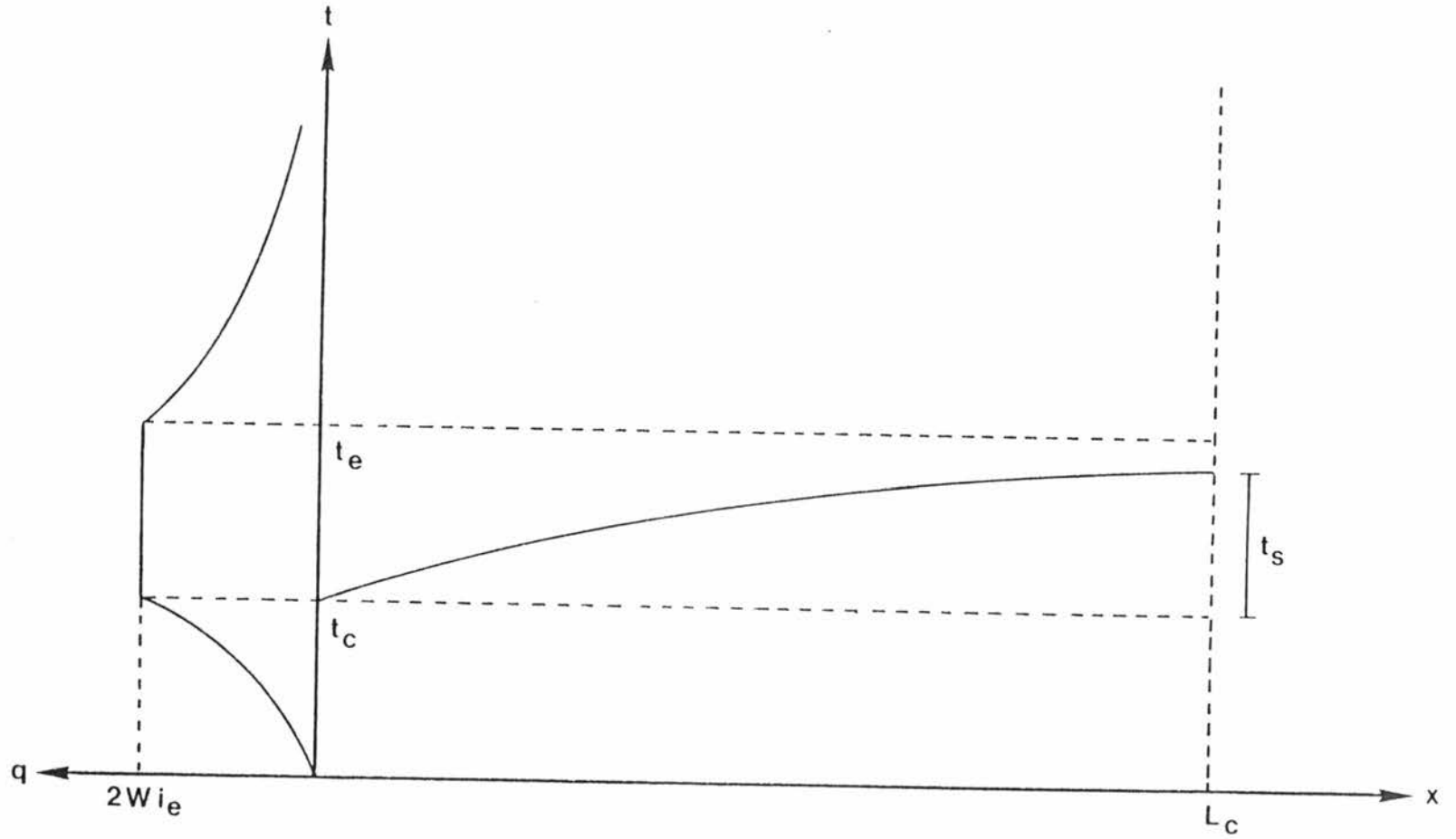

Figure 3.7. x-t plane for concentration on plane and concentration on channel.

accreation of inflow. Then, after $t_c + t_s$ the discharge at the downstream end of the channel becomes constant, and that time represents the total time of concentration for the whole watershed. Calling such a time t^*

$$t^* = t_c + t_s \tag{3.54}$$

The objective is to describe the characteristic starting at t_c in order to obtain t_s and the maximum discharge. For this case t^* will also represent the time to peak

As the channel has two symmetrical planes, Equation (3.50), for the time interval t_c to t_e, together with Equations (3.38), (3.40) and (3.41), evaluated for the same interval, yields

$$\frac{dA}{dt} = 2Wi_e \tag{3.55}$$

Integration of Equation (3.55) between t_c and a time t less than t_e gives

$$A = 2Wi_e(t - t_c) \tag{3.56}$$

Taking this result to Equation (3.48) and integrating it between the same limits, the desired characteristic equation is

$$x = \alpha_c(2Wi_e)^{\beta c-1}(t - t_c) \tag{3.57}$$

Evaluating this last equation for $x = L_c$ and $t = t_s$, t_s is given by

$$t_s = \left[\frac{L_c}{\alpha_c(2Wi_e)^{\beta c-1}}\right]^{1/\beta c} \tag{3.58}$$

Combining Equations (3.41), (3.54) and (3.58) the concentration time for the whole catchment area is obtained as

$$t^* = \left[\frac{W\ i_e^{1-\beta p}}{\alpha_p}\right]^{1/\beta p} + \left[\frac{L_c}{\alpha_c (2Wi_e)^{\beta c-1}}\right]^{1/\beta c} \qquad (3.59)$$

The time to peak, denoted by t_m, can be obtained also by using Equation (3.59).

$$t_m = t^* \qquad (3.60)$$

The maximum discharge Q_m is computed by plugging Equation (3.59) into (3.56) and applying Equation (3.7)

$$Q_m = 2L_c\ W\ i_e \qquad (3.61)$$

This is an expected result, since concentration in the whole watershed means a continuity condition between the effective rainfall and the discharge at the catchment outlet, with no change in the storage.

Equations (3.60) and (3.61) are applicable for computing the peak variables given that the following condition is met

$$t_e \geq t^* \qquad (3.62)$$

3.5.2 Case 3: No Concentration on Plane and Concentration on the Stream

Figure 3.8 presents the scheme of the plane x - t, used to obtain the analytical solution when concentration is present on the stream, but not on the plane. Again, the catchment has two symmetrical planes of width W and a channel of length L_c. The uniformly distributed input along the channel is given by two times the input hydrograph,

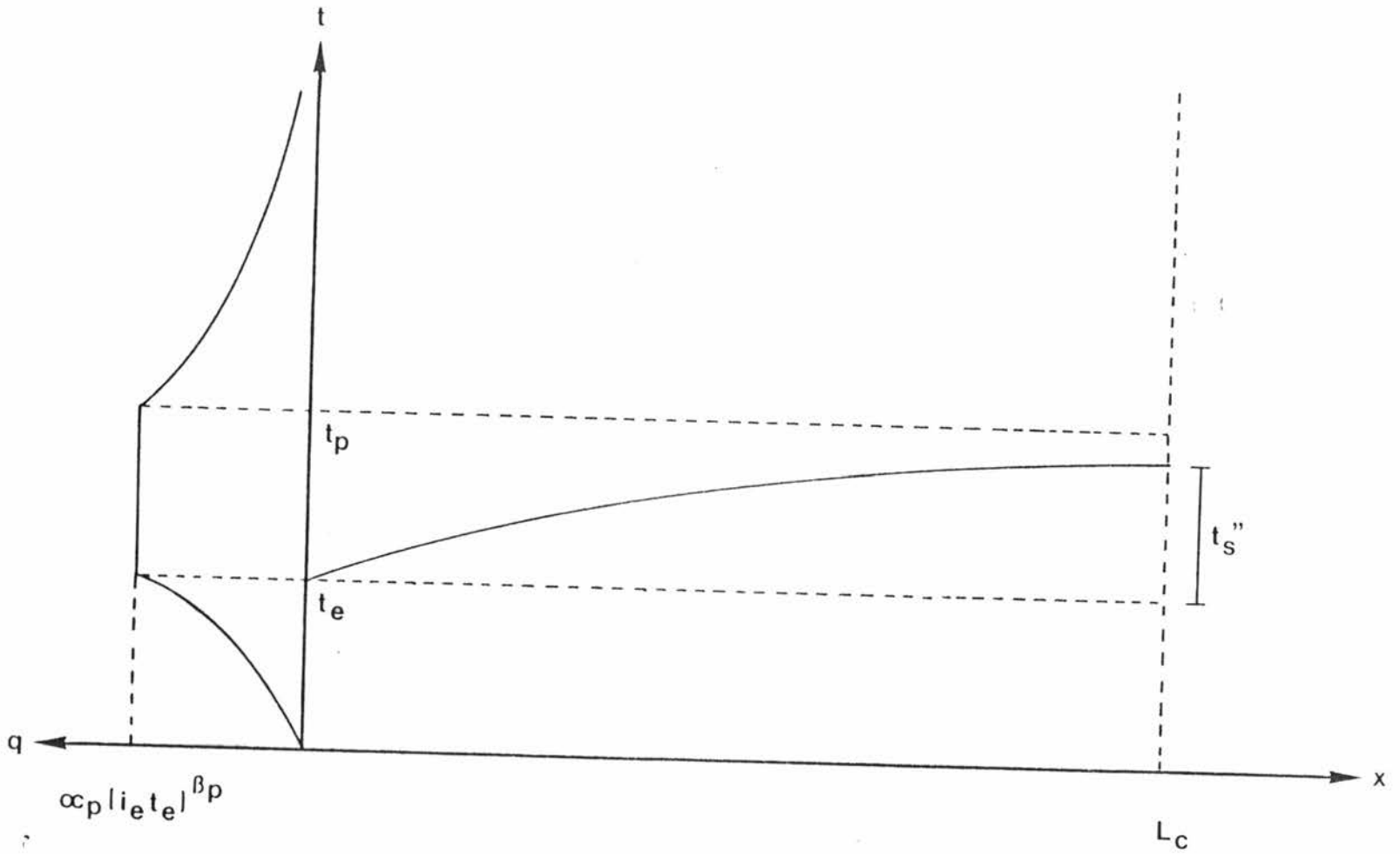

Figure 3.8. x-t plane for no concentration on plane and concentration on channel.

given by equations (3.43) and (3.47). As there is no upstream tributaries, the conditions given in (3.52) and (3.53) are still applicable.

The behavior of the channel hydrograph is similar to that described in Section 3.5.1. Hence, after the time $t_e + t_s''$ the discharge in the channel outlet behaves as a plateau. The objective is then to describe the characteristic line starting at t_e and arriving at the downstream end at the time $t_e + t_s''$. Equation (3.50), considering the aggregated discharge for both planes in the time interval t_e to $t_e + t_s''$, given by Equations (3.44) and (3.46), becomes

$$\frac{dA}{dt} = 2\alpha_p (i_e t_e)^{\beta p} \tag{3.63}$$

Following the same procedure as that presented for Case 1, the results obtained are:

$$t_s'' = \left\{ \frac{L_c}{\alpha_c [2\alpha_p (i_e t_e)^{\beta p}]^{\beta c - 1}} \right\}^{1/\beta c} \tag{3.64}$$

$$t_m = t_e + t_s'' \tag{3.65}$$

$$Q_m = 2L_c \alpha_p (i_e t_e)^{\beta p} \tag{3.66}$$

where t_m and Q_m stands for the time to peak and peak discharge, respectively.

Equations (3.64) through (3.66) are applicable for computing the peak variables in a first order channel with symmetrical planes given that the following condition is attained

$$t_e + t''_s \leq t_p \tag{3.67}$$

where t_p is computed using Equation (3.47).

3.6 Approximate Kinematic Routing

Figure 3.7 and Figure 3.8 show clearly the reason for which it is not possible to obtain analytical solutions for the peak variables for Cases 2 and 4. In both cases, as there is not concentration on the channel, the characteristic line responsible for the peak discharge cannot be located exactly. For example, for Case 2, it could start before, at or after t_c and it would arrive before, at or after t_e. The analytical solution would require the integration of the characteristic lines for the complete x - t plane, a task considered impossible as was stated earlier. A similar reasoning is applicable to Case 4.

This section is intended to solve the foregoing gap by developing, based on physical considerations, approximate relationships to compute the peak variables for Cases 2 and 4.

The approximate relationships herein obtained are based on two properties observed in the kinematic wave approach. The first is given by the fact that no attenuation of the hydrograph takes place as it travels along the channel. Only deformation occurs in the hydrograph, formed by increased steepness of the rising limb and flattening of the receding limb. This means that under the presence

of lateral inflow, the discharge will always increase in the downstream direction, and when there is no lateral inflow entering the channel, any discharge will remain constant as it travels along the channel.

The second property, related to some values used in the present study, is given by the weak dependence of the wave celerity on the discharge. This enables the possibility of translating a given discharge in the channel, without considering an accreation of the flow contributing to the wave celerity.

As in the preceding cases, the runoff area under consideration comprises two lateral symmetrical planes with no upstream inflow, i.e., a first order stream. The approximate sketch is formed by the stream with the plane hydrographs, Q_p, as point inputs in the upstream and downstream ends of the channel. The upper plane hydrograph is translated to the downstream end, using the approximate kinematic routing and the hydrograph denoted by Q_L is obtained. The addition of Q_p and Q_L in a time proper manner produces Q, the total discharge hydrograph.

Figure 3.9 presents the sketch for the approximate kinematic routing, as well as some variables used during the development.

The total plane hydrograph Q_p is computed as

$$Q_p = L_c \, q \tag{3.68}$$

where q is computed using Equations (3.37) to (3.41) or Equations (3.443) to (3.47) depending on whether there is concentration on the plane or not.

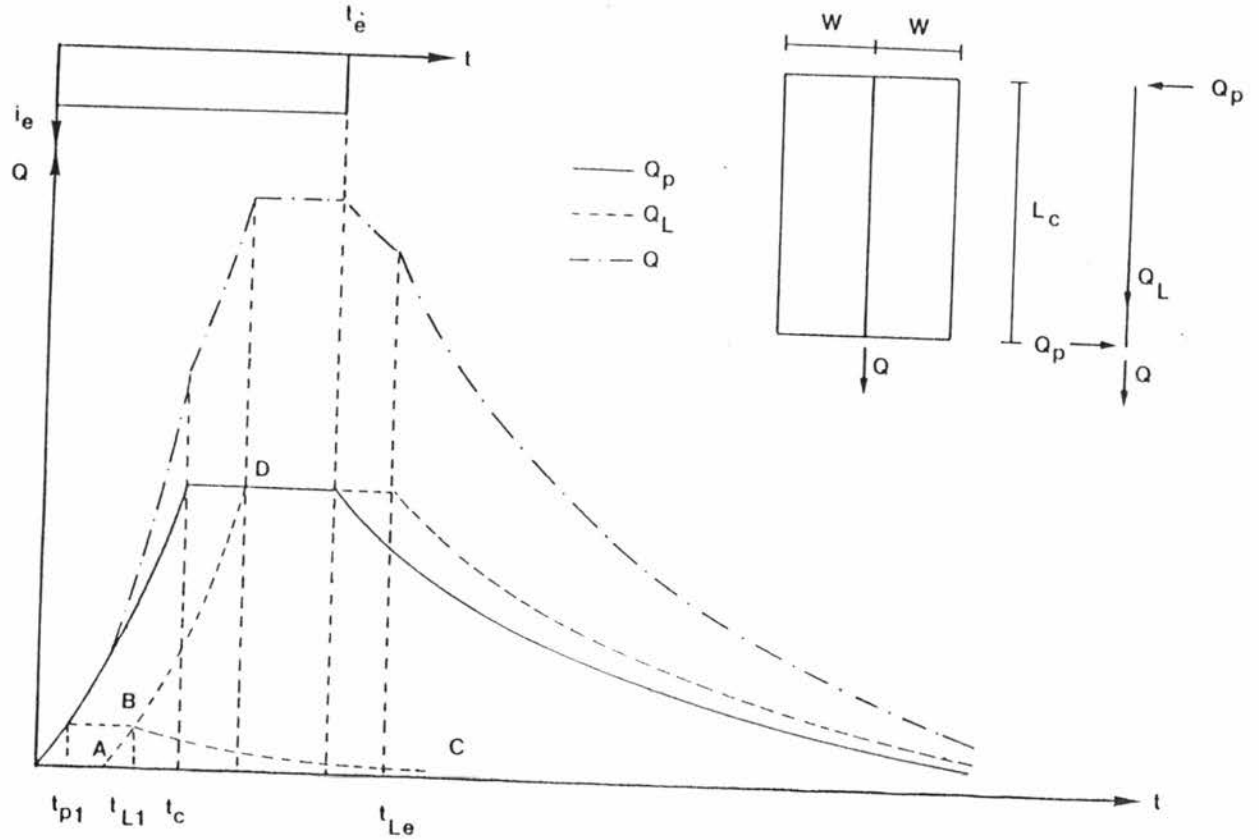

Figure 3.9. Procedure and notation for the approximate kinematic routing.

Equation (3.48) defines the characteristic paths for the channel, while Equation (3.7) defines the area-discharge relationship. Replacing A in Equation (3.48) in terms of Q by means of Equation (3.7), the former becomes

$$\frac{dx}{dt} = \alpha_c \beta c \left[\frac{Q}{\alpha_c}\right]^{1-1/\beta c} \tag{3.69}$$

If Q is considered constant while the wave travels along the channel, calling t the time at which the discharge Q enters the channel in the upstream end and t_L the time at which the wave arrives downstream, the following result is yielded after integration of Equation (3.69)

$$L_c = \alpha_c \beta c \left[\frac{Q}{\alpha_c}\right]^{1-1/\beta c} (t_L - t) \tag{3.70}$$

Now, as Q is the discharge in the channel, at this point it is necessary to analyze the behavior of Equation (3.70) when the different values of Q given by the conditions in the plane are used. Remember that the objective is to route Q_p from the upstream end to the downstream end of the channel.

3.6.1 Routing the Rising Limb

No matter which case is under analysis, the rising limb for the hydrograph entering the upstream end is given by

$$Q_p = L_c \alpha_p (i_e t)^{\beta p} \tag{3.71}$$

Making $Q = Q_p$ and taking Equation (3.71) to (3.70),

$$L_c = \alpha_c \beta c \left[\frac{L_c \alpha_p (i_e t)^{\beta p}}{\alpha_c} \right]^{1-1/\beta c} (t_L - t) \qquad (3.72)$$

This equation may be used in two different ways: 1) given a value of t, time at which a given discharge enters the channel upstream end, Equation (3.72) yields the time t_L at which such discharge arrives downstream; 2) if t_L is specified in advance, Equation (3.72) gives the time t at which a given discharge was produced upstream.

As will be seen later, the second way is the more adequate for computational purposes, but requires a numerical algorithm in order to solve for t.

However, the first way of using Equation (3.72) enables the formulation of some limitations for the approximate kinematic routing. If t_L is obtained as a function of t

$$t_L = \frac{L_c}{\alpha_c \beta c} \left[\frac{\alpha_c}{\alpha_p L_c i_e^{\beta p}} \right]^{1-1/\beta p} t^{\beta p(1/\beta c - 1)} + t \qquad (3.73)$$

one realizes that due to the values of βp and βc used in this study ($\beta p = 5/3$, $\beta c = 1.233$) two sentences can be done

$$\lim_{t \to 0} t_L = \infty \qquad (3.74)$$

$$\lim_{t \to \infty} t_L = \infty \qquad (3.75)$$

which allows one to conclude that for some value of t there is a maximum for t_L, denoted t_{L1}, below of which the approach is no longer

valid (Figure 3.9). Making $dt_L/dt = 0$ and solving, the limiting value of t, denoted t_{pl}, is given by

$$t_{pl} = \left\{ \frac{\alpha_c \beta c^2}{L_c \beta p(\beta c-1)} \left[\frac{L_c \alpha_p i_e^{\beta p}}{\alpha_c} \right]^{1-1/\beta c} \right\}^{\beta c/[\beta p(1-\beta c)-\beta c]} \tag{3.76}$$

Consequently, the value of t_{L1} can be calculated as

$$t_{L1} = \frac{L_c}{\alpha_c \beta c} \left[\frac{\alpha_c}{\alpha_p L_c i_e^{\beta p}} \right]^{1-1/\beta p} t_{pl}^{\beta p(1/\beta c-1)} + t_{pl} \tag{3.77}$$

It must be pointed out that the variables denoted at t_{pl} and t_{L1} do not have any physical meaning. They just mark a boundary for the applicability of the approximate kinematic routing, to be analyzed further.

Therefore, as shown in Figure 3.9, the routed rising limb would be given by curve CBD. Obviously, the branch BC does not present any physical meaning. Therefore, it is proposed to approach this part by the straight line AB. The validity of this assumption will be verified later.

3.6.2 Routing the Plateau

Whether there is concentration on the planes or not, the time duration of the plateau is known. Denoting by D_p such duration, for concentration on planes it is given by

$$D_p = t_e - t_c \tag{3.78}$$

and for the case of no concentration

$$D_p = t_p - t_e \tag{3.79}$$

The first point on the plateau, corresponding to the t_c or t_e, whichever is the case, must be routed following the procedure described in the previous section, i.e., Equation (3.72). The corresponding discharge will have a travel time given by the difference between the downstream arrival time and the upstream entering time. This means, that for the two cases aforementioned, the travel time is given by

$$t_{T_c} = t_{L_c} - t_c \tag{3.80}$$

$$t_{T_e} = t_{L_e} - t_e \tag{3.81}$$

where t_T with the subindex c or e stands for the travel time with concentration or no concentration respectively; similarly for t_L, but denoting the downstream arrival time.

As the discharge remains constant in the plateau, all points will have the same travel time, and neither shortening nor elongation of the plateau length will take place. In other words, for routing the plateau, one calculates the travel time for the first point or maximum discharge in the upstream hydrograph and then translates it. The same length of the plateau, beginning at this last point, appears at the downstream hydrograph.

3.6.3 Routing the Receding Limb

The last point in the plateau or the first point in the recession curve has been already solved as explained above. The recession limb is routed by solving simultaneously the following set of equations

$$t_L = \frac{L_c}{\alpha_c \beta c} \left(\frac{\alpha_c}{Q}\right)^{1-1/\beta p} + t \tag{3.82}$$

$$\alpha_p y^{\beta p+1} \left[\frac{y}{i_e} + \beta p(t - t_e)\right] - W = 0 \tag{3.83}$$

$$Q_L = L_c \alpha_p y^{\beta p} \tag{3.84}$$

$$Q_L = Q \tag{3.85}$$

The first equation, obtained from (3.70), gives the downstream time. The second one includes the depth at the plane outlet at a time t, necessary to calculate the discharge by means of Equations (3.84) and (3.85). Equation (3.85) is the condition of no attenuation.

There are five unknowns in the four equations: t, t_L, Q, Q_L and y. In order to solve the system, one has to specify one of them. Again, as in the routing of the rising limb, one can specify t or t_L, and, as it will be stated further, the more adequate is t_L. Anyway, no matter which time one specifies, a numerical scheme is needed to solve the system and obtain at last, Q_L and t or t_L.

3.7 Computation of the Total Hydrograph using Approximate Kinematic Routing

Up to this point, two hydrographs are known. The first one is the hydrograph entering the upstream or the downstream end of the channel, denoted by Q_p. The second is the hydrograph produced when Q_p, entering the upstream end, is routed to the channel outlet, producing the hydrograph denoted by Q_L. The addition to Q_p and Q_L in a timely proper manner yields the total hydrograph Q, or

$$Q(t) = Q_p(t) + Q_L(t) \tag{3.86}$$

Although one is able to compute the discharge and timing for the individual hydrographs, due to the following facts it is difficult to obtain an analytical closed expression for the total hydrograph:

1. The hydrograph at the plane outlet can only be expressed in an analytical closed manner for the rising limb and for the plateau, but not for the recession limb, where some numerical scheme must be used to solve the equations.
2. The routed hydrograph can not be computed in a straight forward manner. Especially the routing of the recession limb requires the solution of a set of equations, which can only be obtained using some numerical algorithm.

The aforementioned limitations require a procedure for computation which begins by calculating the plane hydrograph for a time increment uniform along the simulation horizon. Obviously, the points where the hydrograph is not continuous do not agree with such criteria. Then, the discontinuity points in the hydrograph arriving downstream are computed and the whole hydrograph is calculated using

the same time step and the proper expressions for each part. In this case, the values for the time are specified in such a way that they agree with those times in the upstream hydrograph. Finally, the hydrograph ordinates with the same time values are added, yielding the total hydrograph at the channel outlet.

3.8 Application of the Approximate Kinematic Routing Method

In this numeral, the approximate kinematic routing is applied to a small watershed formed by two symmetrical planes and one channel, with the following characteristic values:

Plane width:	$W = 658$ ft
Plane roughness:	$n_p = 0.30$
Plane slope:	$S_p = 0.096$
Channel length:	$L_c = 1861$ ft
Channel roughness:	$n_c = 0.04$
Channel slope:	$S_c = 0.026$

The applications were performed for rainfall intensities of 1.0, 5.0 and 10.0 in/hr. The rainfall durations were selected in an arbitrary way, in order to show how this parameter gives rise to the same four cases described in Table 3.1. The objective of this section is to compute, for each case, the discharge hydrograph for the whole catchment area using the approximate kinematic routing, to compare this hydrograph with that obtained via detailed kinematic simulation (Appendix A) and to formulate approximate expressions to compute the peak discharge and time to peak for each case. Whenever is possible, the approximate expressions are compared with the analytical solutions

derived in Section 3.5. The tool for the approximate kinematic routing was a FORTRAN computer program.

3.8.1 Case 1: Concentration on Plane and Concentration on Channel

For this case, the rainfall effective duration t_e produces concentration in the planes, in the channel and in the whole watershed. The following times are defined in Figure 3.10 and the expressions for their computation are given in Equations (3.90) through (3.94).

t_c: concentration time for the planes

t_{pl}: minimum upstream time generating downstream discharge

t_{Ll}: minimum downstream time

t_{Lc}: initial downstream time for the plateau

t_e: final downstream time for the plateau

From the approximate kinematic point of view, concentration on the stream, which does not require concentration on planes, means that the plateaus for the two hydrographs at the downstream end have a common time interval during which equal discharges take place. Hence, concentration in the planes and in the channel implies concentration in the whole watershed.

The condition for Case 1 is:

$$t_e > t_{Lc} > t_c > t_{Ll} \tag{3.87}$$

The expressions recommended for approximating the peak discharge Q_m and time to peak t_m are:

$$Q_m = 2L_c W i_e \tag{3.88}$$

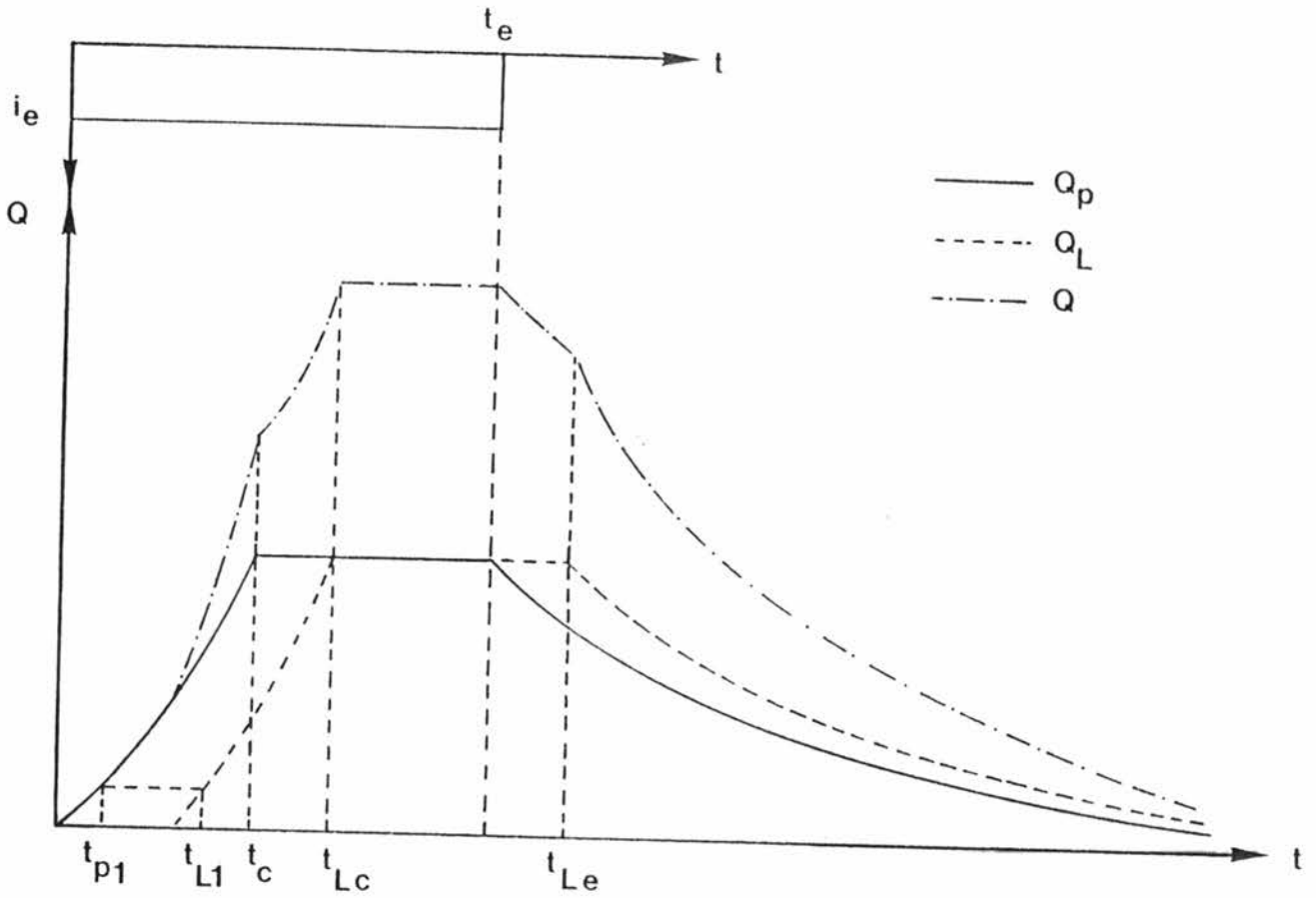

Figure 3.10. Case 1.

$$t_m = t_{Lc} \tag{3.89}$$

$$t_c = \left[\frac{W\, i_e^{1-\beta p}}{\alpha_p}\right]^{1/\beta p} \tag{3.90}$$

$$t_{p1} = \left\{\frac{\alpha_c \beta c^2}{L_c \beta p(\beta c-1)}\left[\frac{L_c \alpha_p i_e^{\beta p}}{\alpha_c}\right]^{\frac{\beta c-1}{\beta c}}\right\}^{\frac{\beta c}{[\beta p(1-\beta c)-\beta c]}} \tag{3.91}$$

$$t_{L1} = \frac{L_c}{\alpha_c \beta c}\left[\frac{\alpha_c}{L_c \alpha_p (i_e t_{p1})^{\beta p}}\right]^{1-1/\beta c} + t_{p1} \tag{3.92}$$

$$t_{Lc} = \frac{L_c}{\alpha_c \beta c}\left[\frac{\alpha_c}{L_c W i_e}\right]^{1-1/\beta c} + \left[\frac{W i_e^{1-\beta p}}{\alpha_p}\right]^{1/\beta p} \tag{3.93}$$

$$t_{Le} = \frac{L_c}{\alpha_c \beta c}\left[\frac{\alpha_c}{L_c W i_e}\right]^{1-1/\beta c} + t_e \tag{3.94}$$

Equation (3.88) for computing the peak discharge agrees completely with Equation (3.61). Equations (3.60) and (3.59) for computing the time to peak can be written in a similar way to Equations (3.89) and (3.93) as

$$t_m = \frac{L_c}{\alpha_c\, \beta c}\left[\frac{\alpha_c \beta c\ ^{\beta c/(\beta c-1)}}{2\, L_c\, W\, i_e}\right]^{1-1/\beta c} + \left[\frac{W\, i_e^{1-\beta p}}{\alpha_p}\right]^{1/\beta p} \tag{3.95}$$

Equations (3.95) and (3.93) are similar in shape. The first term in both of them stands for the holding time in the stream and the second for the concentration time for the planes. However, the holding time

in the stream in Equation (3.95) includes additionally the coefficient $\left[(\beta c/2)^{\beta c/(\beta c-1)}\right]^{1-1/\beta c}$ which evaluated numerically for $\beta c = 1.2333$ yields 1.0818. This means that under the assumption of the channel cross-sectional behaving as the value defined by βc, the first term in Equation (3.93) underestimates the channel holding time by approximately an 8%. Therefore, the applicability of Equations (3.89) and (3.93) depends on the channel holding time-plane concentration time ratio; the smaller the ratio the more applicable the equations.

Figure 3.11 presents the application of Case 1 to the example catchment.

3.8.2 Case 2: Concentration on Plane and No Concentration on Channel

The rainfall duration enables the development of concentration in the planes, but no concentration on the channel nor in the whole watershed, as shown in Figure 3.12. The times are defined as in Case 1 and the expressions for computing them are the same. The condition giving rise to Case 2 is

$$t_{Lc} > t_e > t_c > t_{L1} \tag{3.96}$$

and the approximate expressions for the peak discharge Q_m and the time to peak t_m are

$$Q_m = 2L_c W i_e \tag{3.97}$$

$$t_m = (t_e + t_{Lc})/2 \tag{3.98}$$

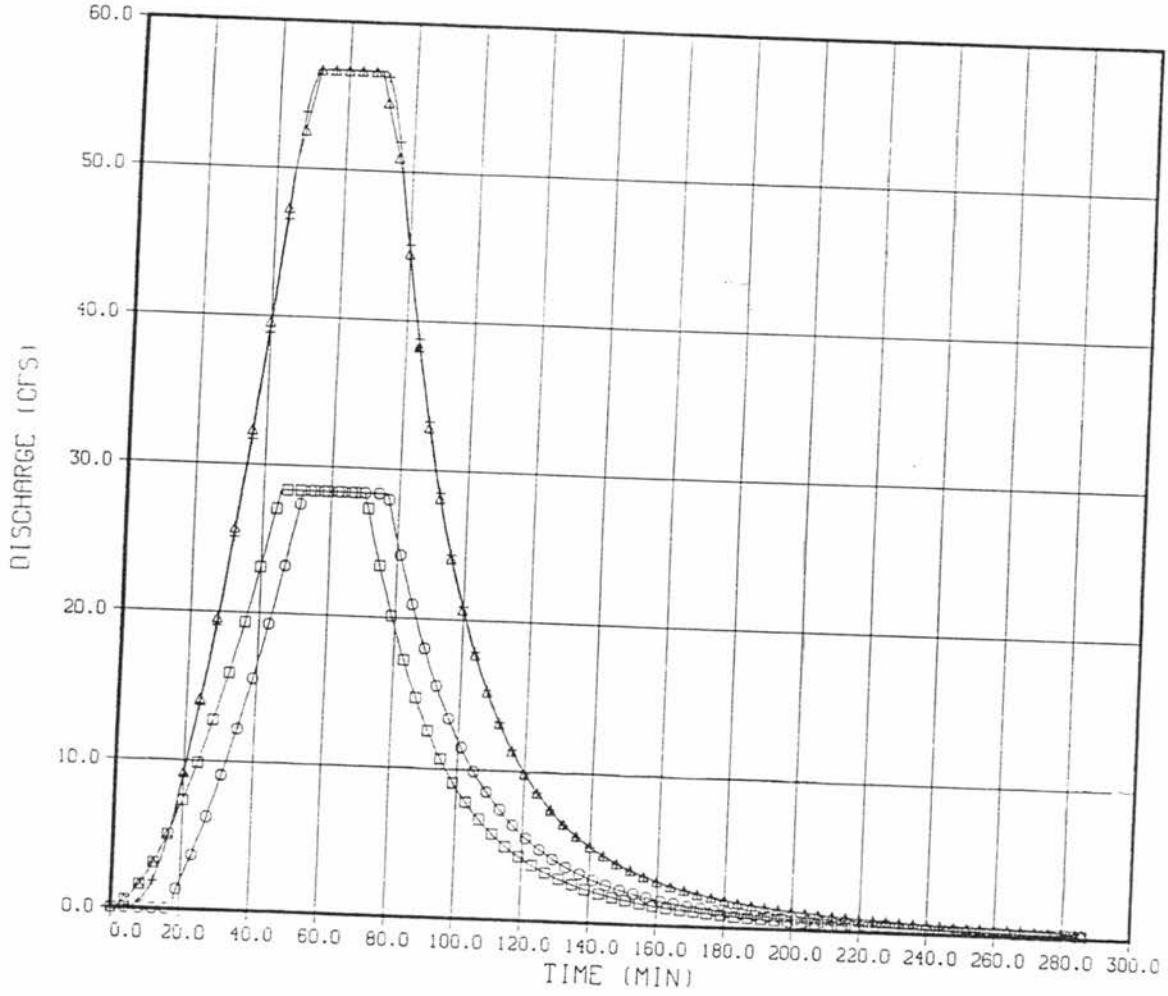

+ : Simulated discharge hydrograph
Δ : Total discharge hydrograph
□ : Upstream discharge hydrograph
o : Downstream discharge hydrograph

Figure 3.11. Case 1. I = 1 in/hr, t_e = 70 min.

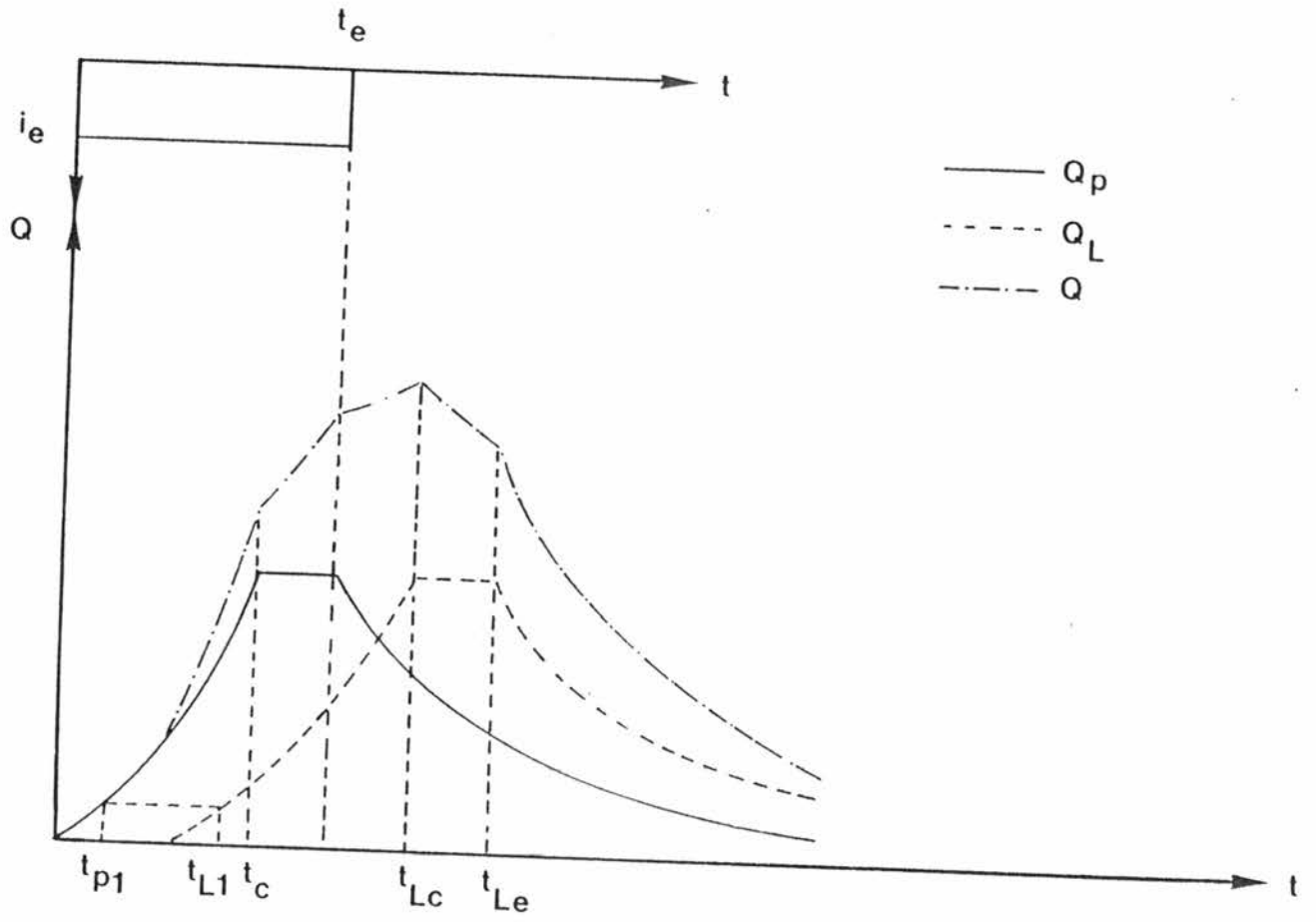

Figure 3.12. Case 2.

Notice that when $t_e = t_{Lc}$, Case 2 becomes Case 1. Figure 3.13 depicts the results for Case 2 when applied to the catchment example.

3.8.3 Case 3: No Concentration on Plane and Concentration on Channel

The rainfall duration for Case 3 is such that it does not generate concentration in the lateral planes, but does in the stream. Hence, no concentration is attained in the whole watershed. Figure 3.14 presents the notation for Case 3. The times are defined as follows, upon the basis that t_e stands for the effective rainfall duration:

t_{p1}: minimum upstream time generating downstream discharge

t_{L1}: minimum downstream time

t_p : final upstream time for the plateau

t_{Le}: initial downstream time for the plateau

t_{Lp}: final downstream time for the plateau

The condition generating Case 3 is

$$t_c > t_e > t_{L1} \quad \text{and} \quad t_p > t_{Le} \tag{3.99}$$

The equations needed to compute the characteristic times are:

$$t_p = \frac{\beta p - 1}{\beta p} t_e + \frac{W}{\alpha_p \beta p (i_e t_e)^{\beta p - 1}} \tag{3.100}$$

$$t_{p1} = \left\{ \frac{\alpha_c \beta c^2}{L_c \beta p (\beta c - 1)} \left[\frac{L_c \alpha_p i_e^{\beta p}}{\alpha_c} \right]^{\frac{\beta c - 1}{\beta c}} \right\}^{\frac{\beta c}{[\beta p (1 - \beta c) - \beta c]}} \tag{3.101}$$

$$t_{L1} = \frac{L_c}{\alpha_c \beta c} \left[\frac{\alpha_c}{L_c \alpha_p (i_e t_{p1})^{\beta p}} \right]^{1 - 1/\beta c} + t_{p1} \tag{3.102}$$

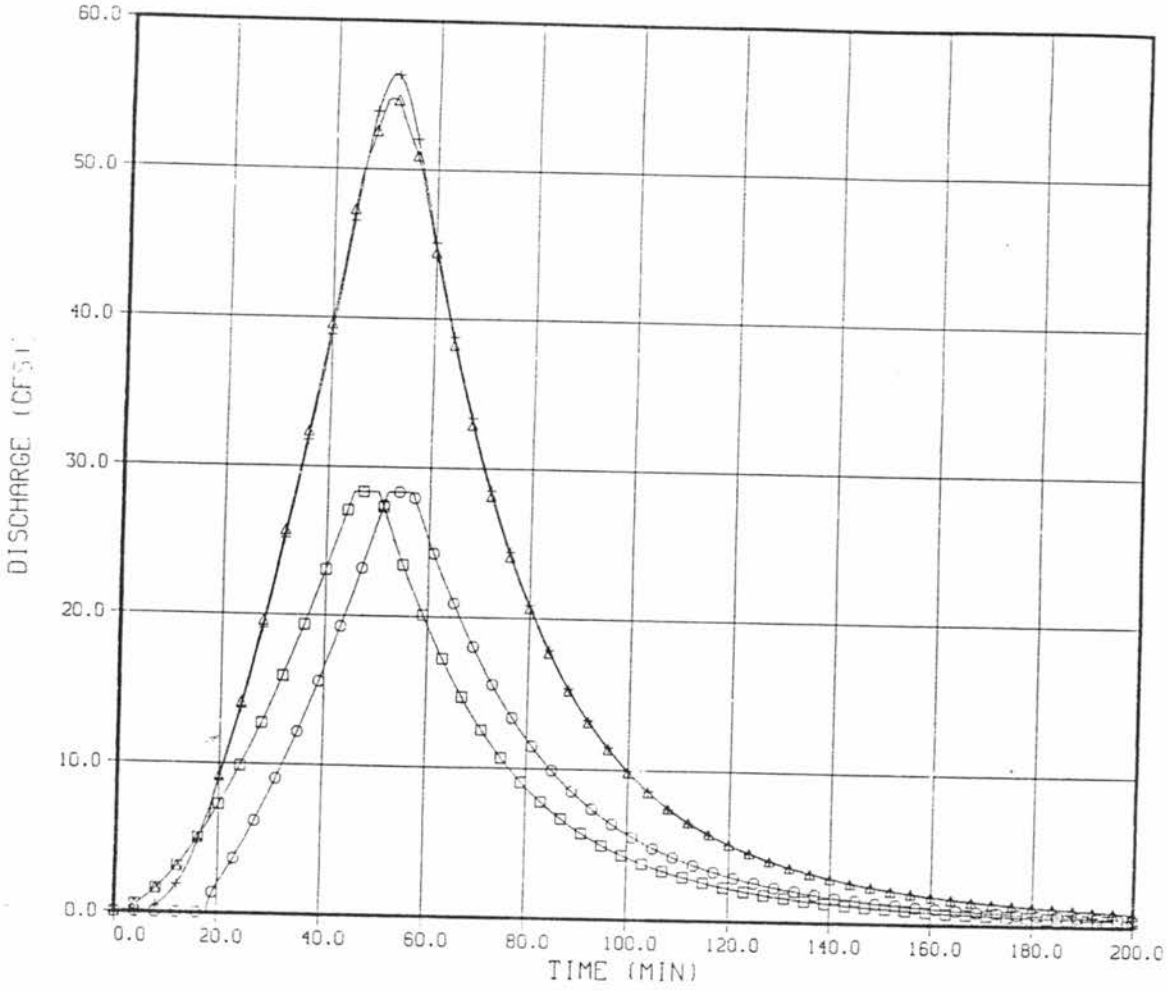

+ : Simulated discharge hydrograph
Δ : Total discharge hydrograph
□ : Upstream discharge hydrograph
o : Downstream discharge hydrograph

Figure 3.13. Case 2 - I = 1 in/hr, t_e = 50 min.

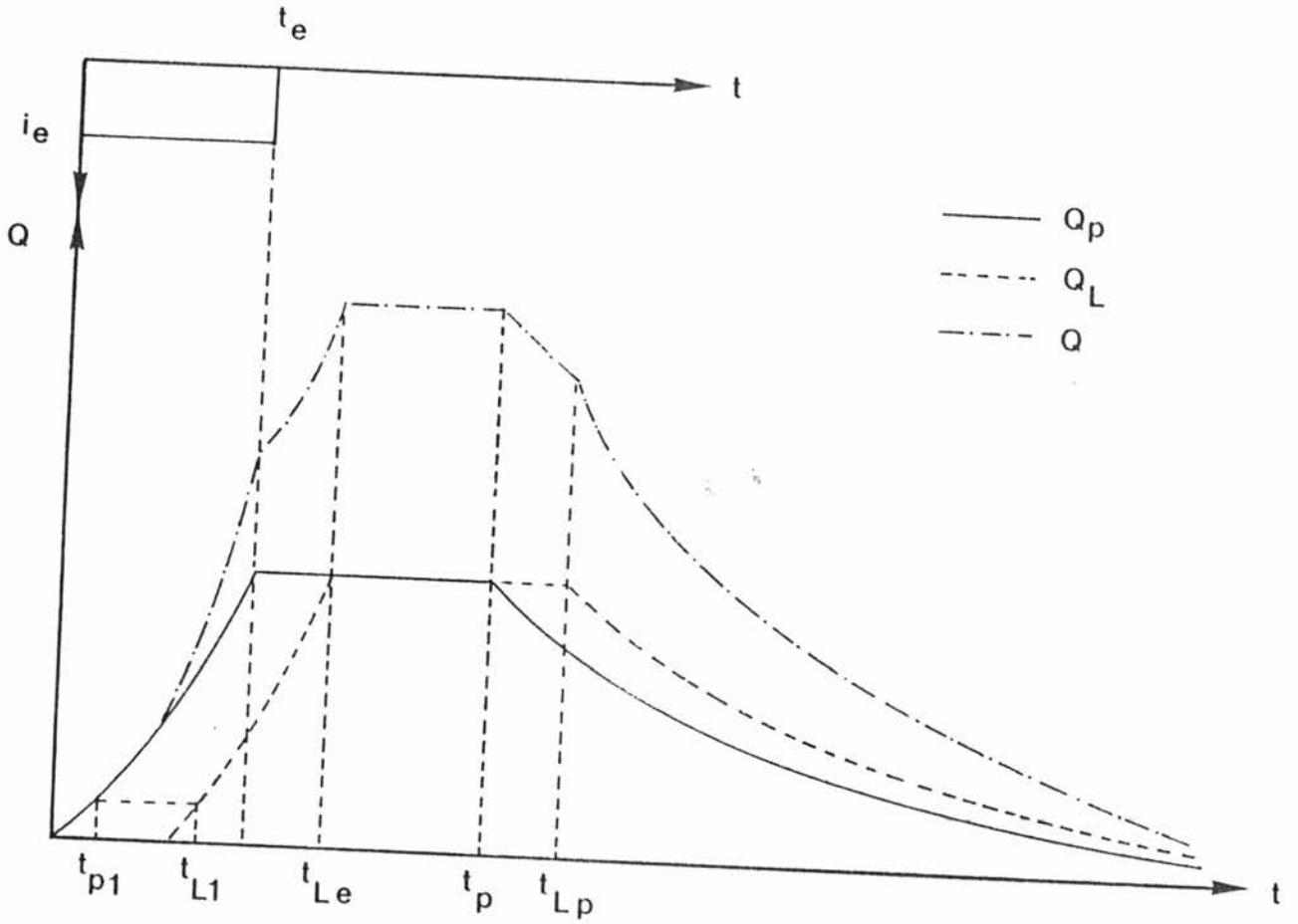

Figure 3.14. Case 3.

$$t_{Le} = \frac{L_c}{\alpha_c \beta c} \left[\frac{\alpha_c}{L_c \alpha_p (i_e t_e)^{\beta p}} \right]^{1-1/\beta c} + t_e \qquad (3.103)$$

$$t_{Lp} = \frac{L_c}{\alpha_c \beta c} \left[\frac{\alpha_c}{L_c \alpha_p (i_e t_e)^{\beta p}} \right]^{1-1/\beta c} + t_p \qquad (3.104)$$

Finally, the recommended approximate expression for the total maximum discharge and its time are:

$$Q_m = 2 L_c \alpha_p (i_e t_e)^{\beta p} \qquad (3.105)$$

$$t_m = t_{Le} \qquad (3.106)$$

Equation (3.105) provides the same result as the analytical result for Case 3. The time to peak, from Equations (3.64) and (3.65), can be rewritten as

$$t_m = \frac{L_c}{\alpha_c \beta c} \left[\frac{\alpha_c \ \beta c^{\beta c/(\beta c-1)}}{2 \ L_c \ \alpha_p (i_e t_e)^{\beta p}} \right]^{1-1/\beta c} + t_e \qquad (3.107)$$

The same analysis as presented for Case 1 is valid for Case 3. The first term in Equation (3.103) or the stream holding time gives an approximate error of 8% and the adequacy of this equation depends again on the relative values of the channel holding time and the effective rainfall duration.

Figure 3.15 presents the application of Case 3 to the example catchment.

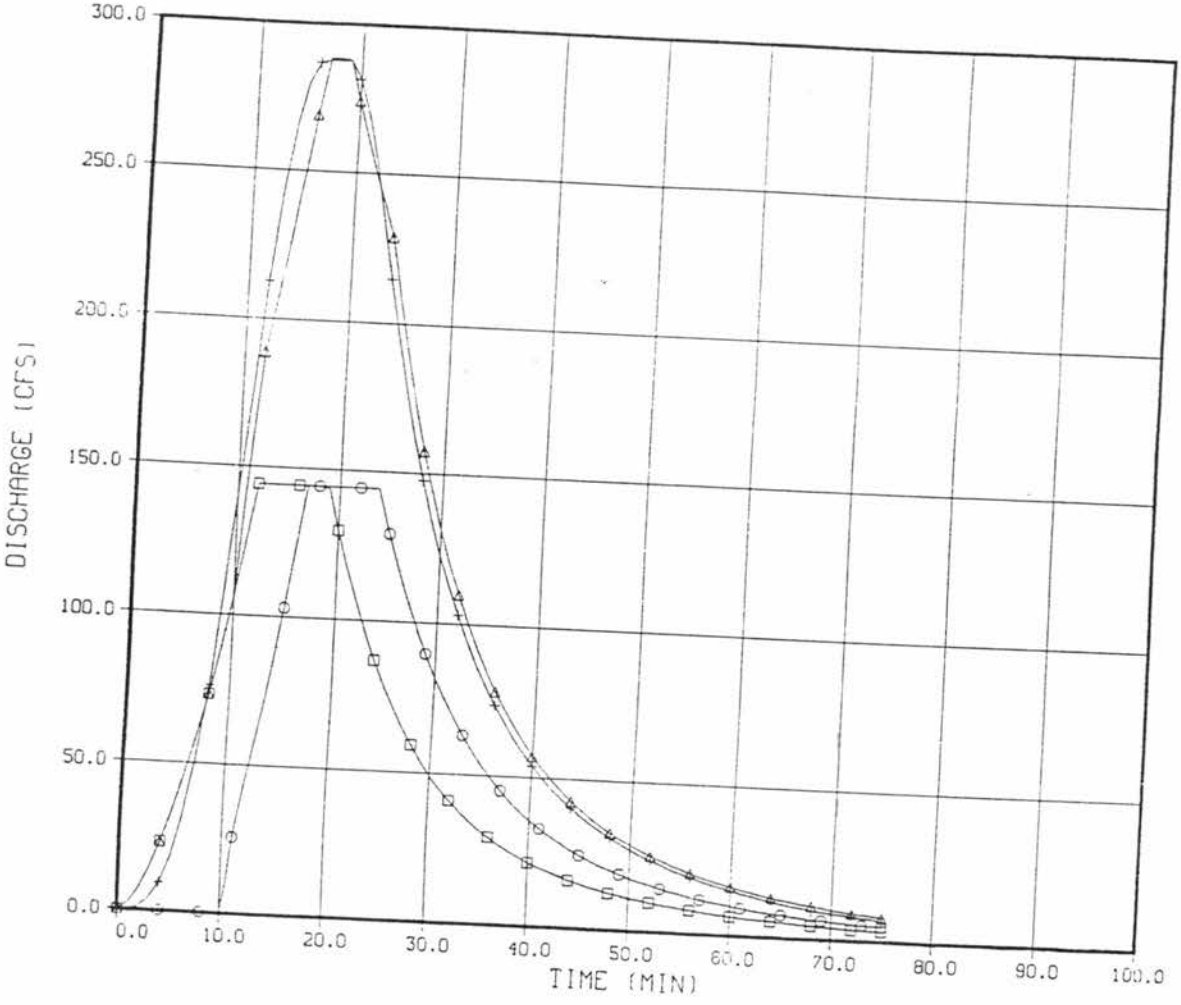

+ : Simulated discharge hydrograph
Δ : Total discharge hydrograph
□ : Upstream discharge hydrograph
o : Downstream discharge hydrograph

Figure 3.15. Case 3 - I = 10 in/hr, t_e = 12 min.

3.8.4 Case 4: No Concentration on Plane and No Concentration on Channel

The last case to be covered is given by a rainfall duration that does not enable concentration in any component of the watershed. The different characteristic times are defined and computed as in Case 3. Using Figure 3.16 as a definition sketch, the conditions giving rise to Case 3 are

$$t_c > t_e > t_{L1} \quad \text{and} \quad t_{Le} > tp \tag{3.108}$$

The equations used to approximate the peak discharge Q_m and its time t_m are

$$Q_m = 2L_c\alpha_p(i_e t_e)^{\beta p} \tag{3.109}$$

$$t_m = (t_p + t_{Le})/2 \tag{3.110}$$

Figure 3.17 presents the application of Case 4 to the example watershed.

3.8.5 Preliminary Analysis of Results for the Approximate Kinematic Routing

The present development has been done under the hypothesis that the kinematic wave approach stands for the simulation of the rainfall-direct runoff process in a first order stream. Hence, the best way to perform a test on the validity of the simplified method is to compare its results with those obtained via detailed simulation, using the hydraulic routing model described in Appendix A.

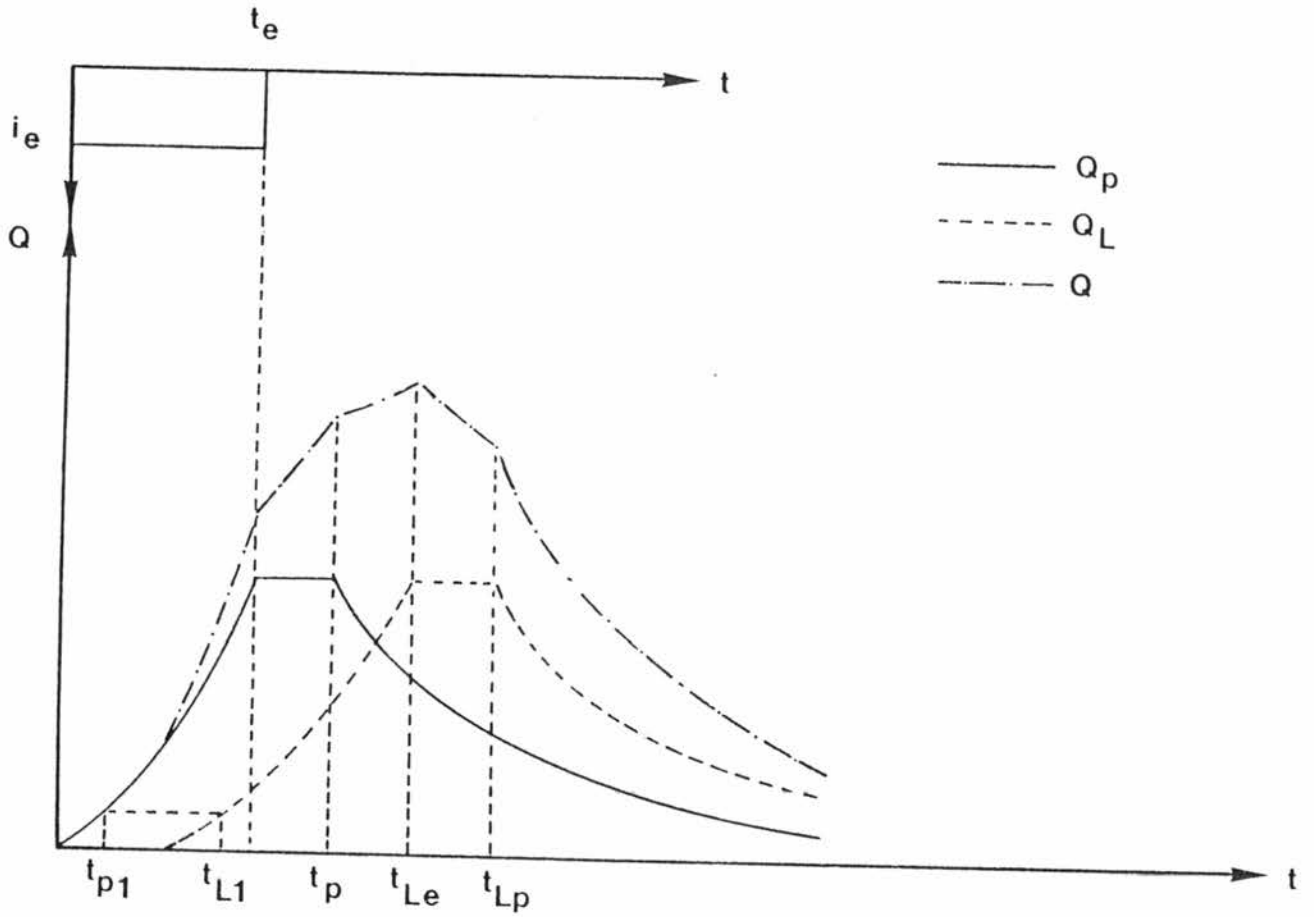

Figure 3.16. Case 4.

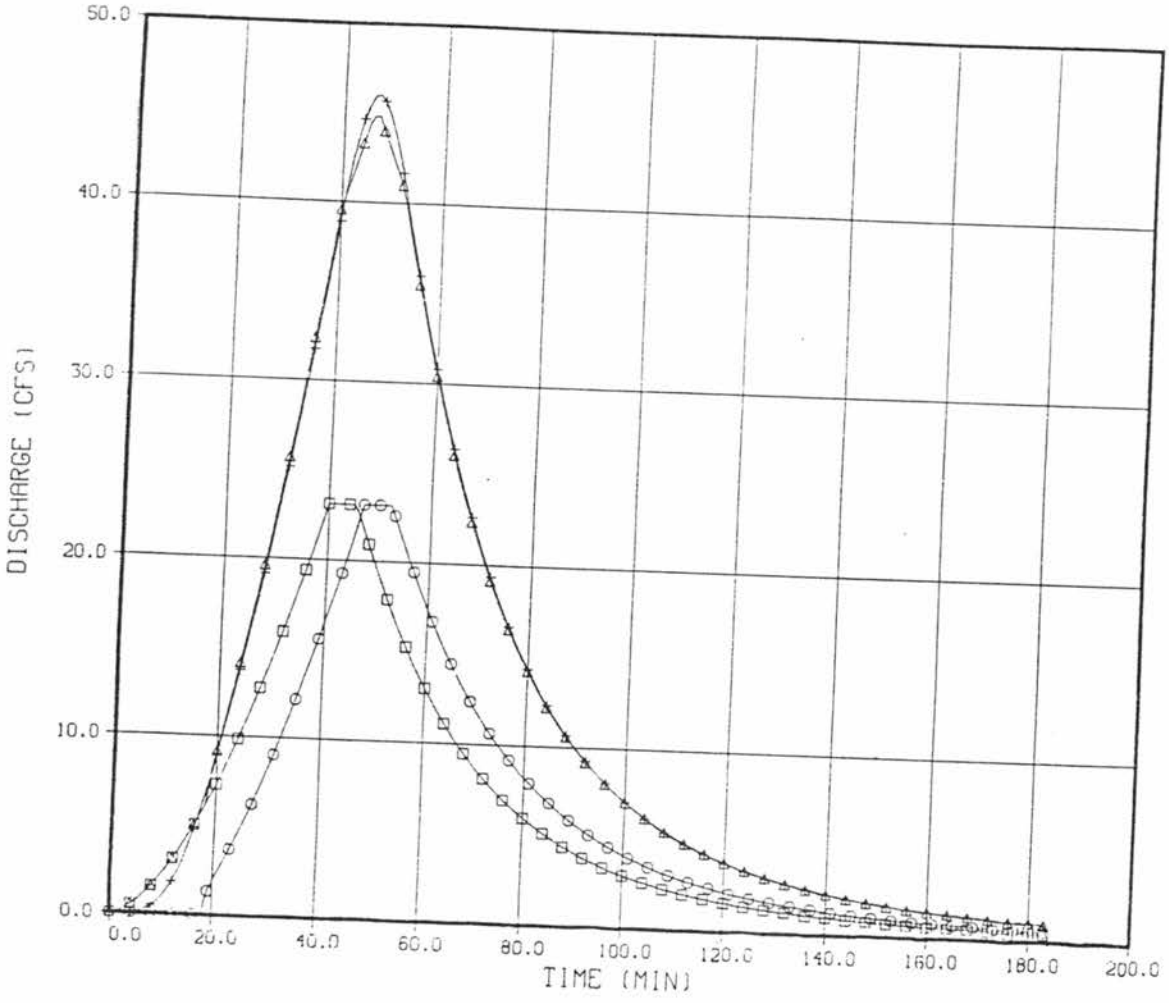

+ : Simulated discharge hydrograph
Δ : Total discharge hydrograph
□ : Upstream discharge hydrograph
o : Downstream discharge hydrograph

Figure 3.17. Case 4 - I = 1 in/hr, t_e = 40 min.

All the experiments were performed for the first order watershed described at the beginning of this section, applying detailed simulation, the simplified kinematic routing and the expressions recommended in each case to approximate the peak parameters. Hence, the comparison is done for the maximum discharge and the time to peak in terms of percent difference $\Delta(\%)$ with respect to the simulated values

$$\Delta(\%) = \frac{(\text{Value}) - (\text{Value})s}{(\text{Value})s} \times 100 \qquad (3.111)$$

where (Value) stands for the estimation via the simplified kinematic routing or via the approximations, for any peak parameter, and (Value)s stands for values obtained using detailed simulation.

First, Table 3.2 presents the comparison of results for those cases where an analytical solution is possible. The comparison is done in terms of the simulated, approximated and analytical results. The results summarized in Table 3.2 allows one to conclude, as it was expected, that the analytical solution does better than any other approach, even the simulation. This is due to the fact that the detailed simulation model described in Appendix A is also an approximation, even for the first order stream, since the lateral planes hydrographs are added and translated into inflow histograms, a step in which some accuracy is lost.

Table 3.3 presents the results for those cases where no analytical exact solution is feasible. They show that, for the selected example, the simplified kinematic routing and the approximate expressions for the peak parameters provide good estimation. For example, for the peak discharge, the maximum percent difference in

Table 3.2. Comparison of results for Cases 1 and 3.

Case	i_e (in/hr)	t_e (min)	SIMULATION Q_m (cfs)	SIMULATION t_m (min)	ANALYTICAL Q_m (cfs)	ANALYTICAL t_m (min)	ANALYTICAL ΔQ_m (%)	ANALYTICAL Δt_m (%)	APPROXIMATION Q_m (cfs)	APPROXIMATION t_m (min)	APPROXIMATION ΔQ_m (%)	APPROXIMATION Δt_m (%)
1	1.0	70	56.7	54	56.7	52	0	-3.7	56.7	52	0	-3.7
3	1.0	25	21.1	34	21.1	34	0	0	21.1	33	0	-3.0
1	5.0	35	283.5	29	283.5	29	0	0	283.5	29	0	0
3	5.0	15	131.9	21	131.7	21	-0.2	0	131.7	20	-0.2	-5.0
1	10.0	25	566.9	23	566.9	23	0	0	566.9	23	0	0
3	10.0	12	287.7	17	288.3	17	0.2	0	288.3	16	0.2	-5.9

Plane width: $W = 658$ ft

Plane roughness: $n_p = 0.30$

Plane slope: $S_p = 0.096$

Channel length: $L_c = 1861$ ft

Channel roughness: $n_c = 0.04$

Channel slope: $S_c = 0.026$

Table 3.3. Comparison of results for Cases 2 and 4.

Case	i_e (in/hr)	t_e (min)	SIMULATION Q_m (cfs)	SIMULATION t_m (min)	SIMPLIFICATION Q_m (cfs)	SIMPLIFICATION t_m (min)	SIMPLIFICATION ΔQ_m (%)	SIMPLIFICATION Δt_m (%)	APPROXIMATION Q_m (cfs)	APPROXIMATION t_m (min)	APPROXIMATION ΔQ_m (%)	APPROXIMATION Δt_m (%)
2	1.0	50	56.4	51	54.8	51	-2.8	0	56.7	51	0.5	0.0
4	1.0	40	46.0	47	44.9	47	-2.4	0	46.2	46	0.4	-2.1
2	5.0	25	269.9	26	249.4	28	-7.6	7.7	283.7	27	5.1	3.9
4	5.0	20	211.8	24	203.6	25	-3.9	4.2	212.8	25	0.5	-3.9
2	10.0	20	550.0	21	510.2	22	-7.2	4.8	567.6	21	3.2	0
4	10.0	15	412.9	18	388.9	19	-5.8	5.6	418.2	19	1.3	-5.8

Plane width: $W = 658$ ft

Plane roughness: $n_p = 0.30$

Plane slope: $S_p = 0.096$

Channel length: $L_c = 1861$ ft

Channel roughness: $n_c = 0.04$

Channel slope: $S_c = 0.026$

absolute value given by the simplified method is 7.6% whereas for the approximation it is around 5.1%. In the same order, for the time to peak, one obtains 9.1% and 5.8%. It is also important to point out that the maximum time difference does not exceed two minutes (2.0 min).

Up to this point of the development, it seems to be that the approximate expressions for peak discharge and time to peak are adequate for estimation in a first order stream. Also, from Figures 3.11, 3.13, 3.15 and 3.17 one concludes that the simplified kinematic routing is able to predict the time distribution of the discharge in a fairly good manner.

In order to make some final judgements about the applicability of the method, two other aspects must be analyzed. The first one is given by the lower boundary established for the effective rainfall intensity, denoted by t_{L1}. On the other hand, the example herein developed presents the feature of small holding times in the channel compared to those for the plane. Besides, the analysis made for the approximation and exact solutions for Case 1 and Case 3 in Sections 3.7.1 and 3.7.3 suggests that the larger the channel (or its holding time) and the shorter the plane (or its holding time) the worse the approximation. The first aspect to be analyzed, the lower boundary t_{L1}, intends to replace it by zero.

The second one, related to both Cases 2 and 4 intends to improve the purposed approximated expressions. However, further analysis is required for Cases 2 and 4; Cases 1 and 3 are completely accepted and described by the analytical solutions. Under the acceptance of the analytical solutions for Cases 1 and 3, the equations describing Cases 2 and 4 can be rewritten as follows:

- Case 2: Concentration on Planes and No Concentration on Channel

$$t^* > t_e > t_c \tag{3.112}$$

$$Q_m = 2\, L_c\, W\, i_e \tag{3.113}$$

$$t_m = (t_e + t^*)/2 \tag{3.114}$$

where t^* is the concentration time for the whole catchment area and is given in Equation (3.59)

- Case 4: No Concentration on Planes and No Concentration on Channel

$$t_c > t_e > 0 \quad \text{and} \quad t_p < t_e + t''_s \tag{3.115}$$

$$Q_m = 2\, L_c\, \alpha_p\, (i_e t_e)^{\beta p} \tag{3.116}$$

$$t_m = (t_p + t_e + t''_s)/2 \tag{3.117}$$

where t''_s is the holding time in the channel when there is concentration on this element, but not on the planes, and is computed using Equation (3.64).

The condition differentiating Cases 3 and 4 is the relationship between t_p and $t_e + t''_s$. When the rainfall intensity is such that t_p is greater than $t_e + t''_s$, Case 3 is attained; when the opposite condition is true, Case 4 appears. For given catchment configuration and given effective rainfall intensity, a function $f(t_e) = t_p - t_e - t''_s$ can be defined as

$$f(t_e) = \frac{W}{\alpha_p \beta p (i_e t_e)^{\beta p - 1}} - \left\{ \frac{L_c}{\alpha_c [2\alpha_p (i_e t_e)^{\beta p}]^{\beta c - 1}} \right\}^{1/\beta c} - \frac{t_e}{\beta p} \qquad (3.118)$$

such that $f(t_e) > 0$ means Case 3 and $f(t_e) < 0$ defines Case 4. Through all the development it was realized that the effective rainfall intensities for Case 4 ($f(t_e) < 0$) are greater than the rainfall intensities for Case 3 ($f(t_e) > 0$); even for some catchment configurations and intensities Case 3 may not be defined. Anyway, as Case 3 has an analytical solution, the lower boundary t_{L1} can be replaced confidently by zero. Under this reformulation of the problem, Table 3.4 presents the holding times for the plane and the channel used as example in this section, applicable to the aspects to be analyzed for Cases 2 and 4.

3.9 Improvement of the Equations to Compute Peak Variables

In the preceding section it was established that some shortcomings for the approximated peak variables may arise when the holding time in the channel is similar or even greater than the holding time in the plane.

In order to solve this problem and since no further analytical solution is possible, the tool used to improve the peak variables for Cases 2 and 4 was regression analysis. To perform this, five different plane-channel configurations were defined, which are expected to represent a wide range of cases. The values defining each configuration are presented in Table 3.5, where θ_p and θ_c represent the inclination angle for the plane and the channel, and except for Configuration 5, they are related via (Garbrecth, 1984)

Table 3.4. Typical holding times for Cases 2 and 4.

Case	i_e (in/hr)	t_e (min)	t_c (min)	t_s (min)	t* (min)	t_c/t_s (-)	t_s'' (min)	t_e/t_s'' (-)
2	1.0	50	45.2	7.2	52.4	6.3	--	--
4	1.0	40	--	--	--	--	7.4	5.4
2	5.0	25	28.6	5.3	33.9	5.4	--	--
4	5.0	20	--	--	--	--	5.6	3.6
2	10.0	20	18.0	4.6	22.6	3.9	--	--
4	10.0	15	--	--	--	--	4.9	3.1

Note: -- means time not applicable for the respective case.

Plane width: $W = 658$ ft Channel length: $L_c = 1861$ ft

Plane roughness: $n_p = 0.30$ Channel roughness: $n_c = 0.04$

Plane slope: $S_p = 0.096$ Channel slope: $S_c = 0.026$

Table 3.5. Configurations to improve peak variables for Cases 2 and 4.

Configuration	W (ft)	S_p (-)	θ_p (°)	L_c (ft)	S_c (-)	θ_c (°)
1	2618	0.176	10	990	0.055	3.2
2	658	0.364	20	1861	0.131	7.5
3	356	0.577	30	4966	0.220	12.4
4	2618	0.577	30	990	0.220	12.4
5	356	0.100	5.7	4966	0.010	0.6

$$S_c = \tan[(S_p/4)^{1.25}] \tag{3.119}$$

In Table 3.5 the roughness for plane and channel were held constant in 0.30 and 0.04 respectively. For each of the configurations, six effective rainfall intensities were used, 0.5, 1.0, 2.0, 4.0, 7.0 and 10.0 in/hr and for each intensity proper effective durations were chosen to generate Cases 2 and 4. Table 3.6 list typical time values for Case 2 and Table 3.7 does for Case 4.

Tables 3.8 and 3.9 present the basic data needed to perform the regression analysis, for Cases 2 and 4 respectively. The data is made up of the peak variables, obtained by simulation and using the approximate expressions defined by Equations (3.112) through (3.117).

The first variable to be analyzed is the time to peak. Figures 3.18 and 3.19 present a graphical comparison of the forecasted and simulated values. Besides, Tables 3.8 and 3.9 show that the maximum percent difference are 10 and 12% for Case 2 and 4 respectively, the maximum absolute differences being two (2) and three (3) minutes. The graphical comparison along with the magnitude of the errors allows one to conclude that the approximation proposed is good enough, and no further improvement is required for the time to peak. Furthermore,

Table 3.6. Typical time values for Case 2. ($t^* > t_e > t_c$)

Configuration	i_e (in/hr)	t_e (min)	t_c (min)	t_s (min)	t^* (min)	t_c/t_s (-)
1	0.5	115	113.9	2.8	116.7	40.7
	1.0	87	86.3	2.4	88.7	36.0
	2.0	66	65.4	2.1	67.5	31.1
	4.0	50	49.6	1.9	51.5	26.1
	7.0	40	39.6	1.7	41.3	23.3
	10.0	35	34.4	1.6	36.0	21.5
2	0.5	42	40.0	4.2	44.2	9.5
	1.0	32	30.3	3.7	34.0	8.2
	2.0	25	23.0	3.3	26.3	7.0
	4.0	18	17.4	2.9	20.3	6.0
	7.0	15	13.9	2.6	16.5	5.3
	10.0	13	12.1	2.4	14.5	5.0
3	0.5	28	24.1	8.6	32.7	2.8
	1.0	22	18.3	7.5	25.8	2.4
	2.0	16	13.8	6.6	20.4	2.1
	4.0	14	10.5	5.8	16.3	1.8
	7.0	10	8.4	5.2	13.6	1.6
	10.0	10	7.3	4.9	12.1	1.5
4	0.5	80	79.8	1.6	81.4	49.9
	1.0	61	60.5	1.4	61.9	43.2
	2.0	46	45.8	1.2	47.0	38.2
	4.0	35	34.7	1.1	35.8	31.5
	7.0	28	27.8	1.0	28.7	27.8
	10.0	--	24.1	0.9	25.0	26.8
5	0.5	50	40.8	29.9	70.7	1.4
	0.5	60	40.8	29.9	70.7	1.4
	1.0	35	30.9	26.3	57.2	1.2
	1.0	45	30.9	26.3	57.2	1.2
	2.0	27	23.4	23.0	46.4	1.0
	2.0	40	23.4	23.0	46.4	1.0
	4.0	20	17.7	20.2	37.9	0.9
	4.0	40	17.7	20.2	37.9	0.9
	7.0	18	14.2	18.2	32.4	0.8
	7.0	28	14.2	18.2	32.4	0.8
	10.0	15	12.3	17.0	29.3	0.7
	10.0	25	12.3	17.0	29.3	0.7

Note: -- means no effective rainfall duration due to narrow range of variation.

Table 3.7. Typical time values for Case 4 ($t_c > t_e > 0$ and $t_p < t_e + t''_s$).

Configuration	i_e (in/hr)	t_e (min)	t_c (min)	t_p (min)	t''_s (min)	t_e/t''_s (-)
1	0.5	112	113.9	113.9	2.8	40.0
	1.0	84	86.3	86.4	2.5	33.6
	2.0	64	65.4	65.4	2.2	29.1
	4.0	48	49.6	49.6	1.9	25.3
	7.0	39	39.6	39.6	1.7	22.9
	10.0	33	34.4	34.4	1.6	20.6
2	0.5	37	40.0	40.1	4.3	8.3
	1.0	27	30.3	30.5	3.9	6.9
	2.0	21	23.0	23.0	3.4	6.2
	4.0	15	17.4	17.5	3.0	5.0
	7.0	12	13.9	14.0	2.7	4.4
	10.0	10	12.1	12.2	2.6	3.8
3	0.5	20	24.1	24.4	9.1	2.2
	1.0	15	18.3	18.5	8.0	1.9
	2.0	9	13.8	14.7	7.5	1.2
	4.0	6	10.5	11.5	6.9	0.9
	7.0	7	8.4	9.1	6.1	1.1
	10.0	5	7.3	7.6	5.5	0.9
4	0.5	79	79.8	79.8	1.6	49.4
	1.0	60	60.5	60.5	1.4	42.9
	2.0	45	45.8	45.8	1.2	37.5
	4.0	34	34.7	34.7	1.1	30.9
	7.0	27	27.8	27.8	1.0	1.0
	10.0	--	24.1	--	--	--
5	0.5	35	40.8	41.1	31.4	1.1
	0.5	30	40.8	42.0	33.0	0.9
	0.5	25	40.8	43.9	34.9	0.7
	0.5	20	40.8	47.3	37.5	0.5
	1.0	25	30.9	31.4	28.1	0.9
	1.0	20	30.9	32.8	30.1	0.7
	1.0	10	30.9	43.3	37.5	0.3
	2.0	20	23.4	23.6	24.2	0.8
	2.0	15	23.4	24.9	26.5	0.6
	2.0	10	23.4	28.8	30.1	0.3
	4.0	10	17.7	19.6	24.2	0.4
	4.0	5	17.7	26.8	30.1	0.2
	7.0	10	14.2	14.7	20.3	0.5
	7.0	5	14.2	19.1	25.2	0.2
	10.0	10	12.3	12.5	18.1	0.6
	10.0	5	12.3	15.5	22.6	0.2

Note: -- means no effective rainfall duration due to narrow range of variation.

Table 3.8. Simulated and approximate peak variable values for Case 2.

Configuration	i_e (in/hr)	t_e (min)	SIMULATION Q_m (cfs)	SIMULATION t_m (min)	APPROXIMATION Q_m (cfs)	APPROXIMATION t_m (min)
1	0.5	115	59.8	116	60.0	116
	1.0	87	119.3	88	120.0	88
	2.0	66	238.7	67	240.0	67
	4.0	50	476.7	51	480.0	51
	7.0	40	832.9	41	839.9	41
	10.0	35	1193.6	36	1199.9	35
2	0.5	42	28.1	43	28.3	43
	1.0	32	56.0	33	56.7	33
	2.0	25	113.0	25	113.4	26
	4.0	18	216.6	18	226.8	19
	7.0	15	389.9	15	396.8	16
	10.0	13	555.2	13	566.9	14
3	0.5	28	39.3	30	40.9	30
	1.0	22	78.8	23	81.8	24
	2.0	16	150.2	17	163.7	18
	4.0	14	316.7	14	327.4	15
	7.0	10	510.3	11	572.9	12
	10.0	10	779.7	10	818.5	11
4	0.5	80	59.7	81	60.0	80
	1.0	61	119.6	62	120.0	61
	2.0	46	239.1	47	240.0	47
	4.0	35	479.4	36	480.0	35
	7.0	28	839.9	29	839.9	27
5	0.5	50	35.5	60	40.9	60
	0.5	60	39.6	65	40.9	65
	1.0	35	63.3	47	81.8	46
	1.0	45	76.4	51	81.8	51
	2.0	27	121.0	37	163.7	37
	2.0	40	159.4	42	163.7	43
	4.0	20	219.7	30	327.4	29
	4.0	32	316.2	34	327.4	35
	7.0	18	404.9	25	572.9	25
	7.0	28	559.0	29	572.9	30
	10.0	15	530.7	23	818.5	22
	10.0	25	794.0	26	818.5	27

Table 3.9. Simulated and approximate peak variable values for Case 4.

Configuration	i_e (in/hr)	t_e (min)	SIMULATION Q_m (cfs)	SIMULATION t_m (min)	APPROXIMATION Q_m (cfs)	APPROXIMATION t_m (min)
1	0.5	112	58.2	115	58.3	114
	1.0	84	114.6	87	114.6	87
	2.0	64	230.9	66	231.3	66
	4.0	48	454.5	50	454.6	50
	7.0	39	810.3	41	817.3	40
	10.0	33	1121.0	35	1121.0	35
2	0.5	37	24.8	41	24.9	41
	1.0	27	46.7	31	46.7	31
	2.0	21	97.1	23	97.6	24
	4.0	15	176.8	17	176.8	18
	7.0	12	309.8	14	309.8	14
	10.0	10	414.3	12	414.3	12
3	0.5	20	28.7	26	30.0	27
	1.0	15	55.6	20	58.9	21
	2.0	9	78.7	15	79.9	16
	4.0	6	127.3	12	129.0	12
	7.0	5	232.9	10	242.0	11
	10.0	5	394.1	9	438.4	9
4	0.5	79	58.8	81	59.0	80
	1.0	60	117.7	61	118.4	61
	2.0	45	231.7	46	232.8	46
	4.0	34	462.4	35	463.3	35
	7.0	27	801.7	28	801.7	28
5	0.5	35	25.2	55	31.7	54
	0.5	30	21.0	54	24.5	53
	0.5	25	16.5	53	18.1	52
	0.5	20	12.1	53	12.5	52
	1.0	25	44.3	44	57.5	42
	1.0	20	33.6	42	39.6	41
	1.0	10	12.4	45	12.5	45
	2.0	20	88.0	35	125.8	34
	2.0	15	61.9	35	77.9	33
	2.0	10	35.8	36	39.6	35
	4.0	10	96.3	29	125.8	27
	4.0	5	36.9	33	39.6	31
	7.0	10	207.1	25	319.8	23
	7.0	5	83.0	28	100.7	25
	10.0	10	333.3	23	579.5	20
	10.0	5	136.9	25	182.5	22

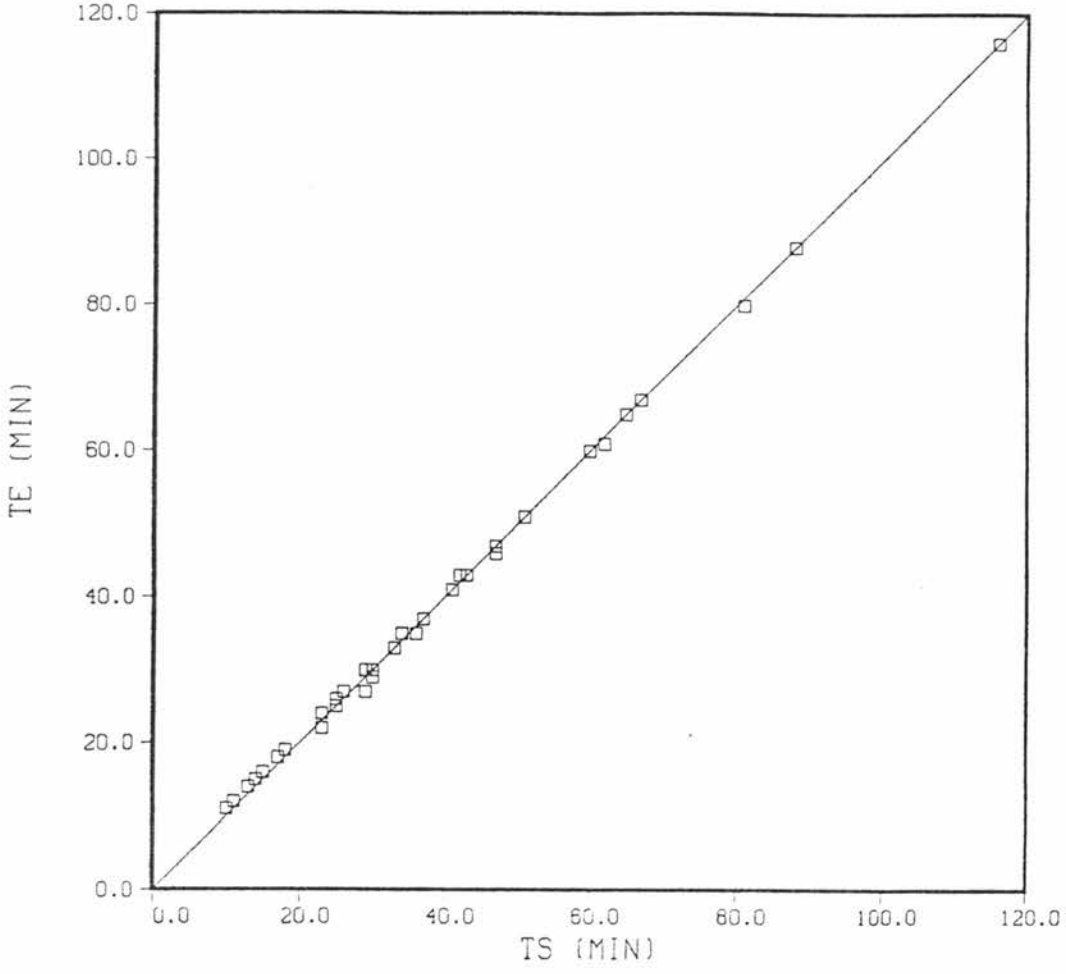

TE : Estimated time to peak
TS : Simulated time to peak

Figure 3.18. Forecasted time to peak for Case 2.

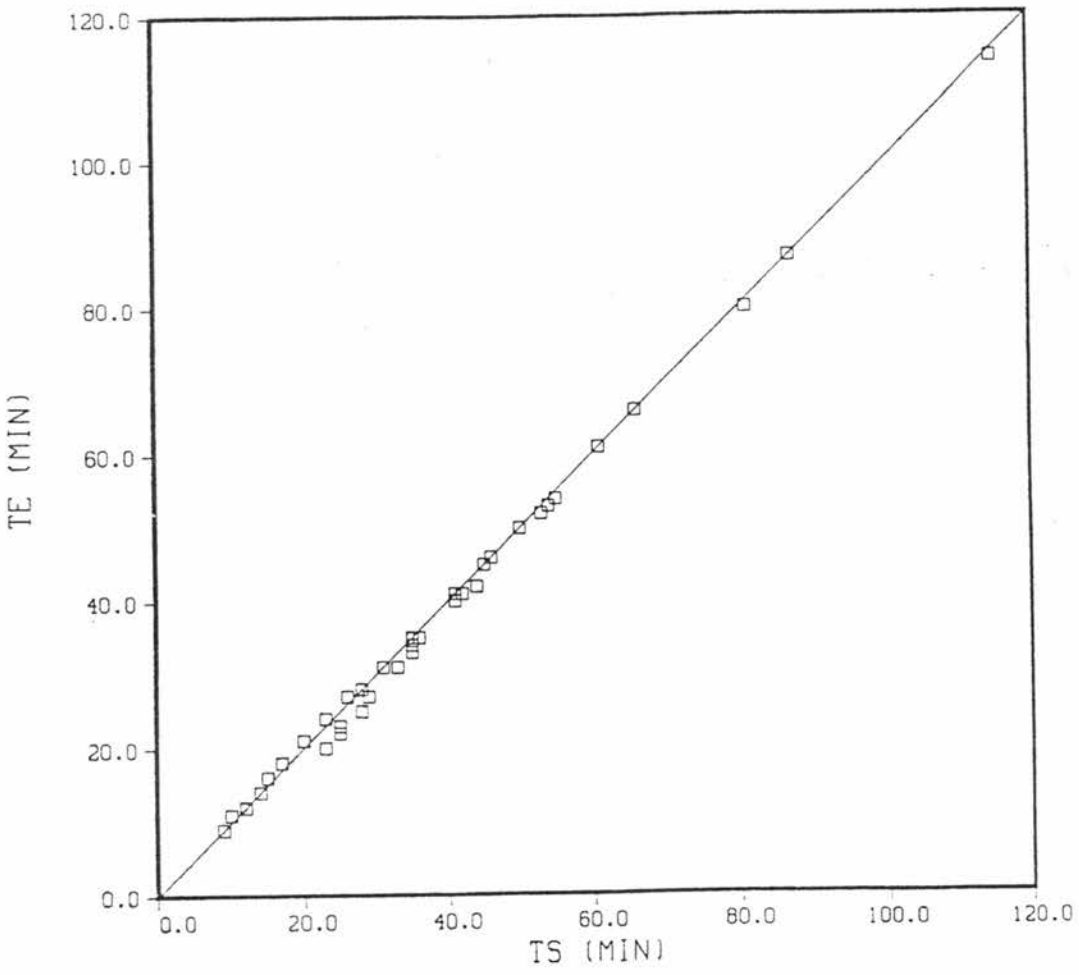

TE : Estimated time to peak
TS : Simulated time to peak

Figure 3.19. Forecasted time to peak for Case 4.

this conclusion is reinforced by the fact that this variable is not required for the derivation of the flood frequency distribution, the main objective of this work.

During the regression analysis performed on the peak discharge, some considerations were made. First, variables with a truly physical link with the problem were selected, and second, those variables were made dimensionless, in such a way that the obtained relationship can be applied to other configurations with a certain confidence. This last consideration solves, at least in part, the problem of the reduced basic data to perform the regression, where it is practically impossible to cover all configurations.

For the sake of illustration, Figures 3.20 and 3.21 present the forecasted peak discharge. The objective of the regression analysis is to bring all points as close as possible to the perfect agreement line.

Equations (3.113) and (3.116) forecast the peak discharge for Cases 2 and 4, but these equations are the same for Cases 1 and 3 respectively. Hence, a good selection for the dependent variables for Cases 2 and 4 is given by the ratio, expressed in percentage, between the true discharge and the forecasted discharge, or

$$\Delta Q = \frac{Q_{ms}}{Q_{ma}} \times 100 \qquad (3.120)$$

where Q_{ms} stands for the peak discharge obtained by simulation and Q_{ma} does for the approximation, i.e. when Equations (3.113) or (3.116) are applied, whichever is the case. In other words, ΔQ represents the

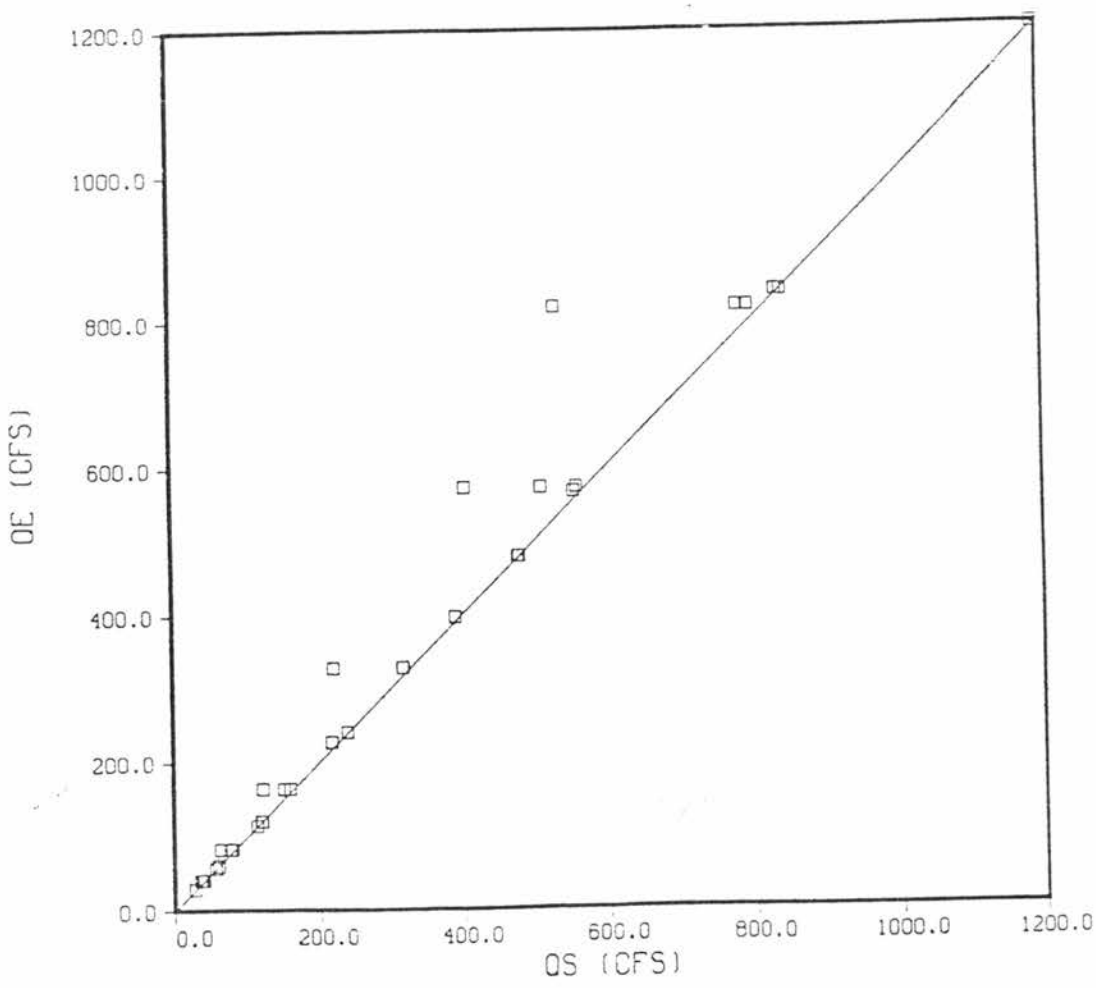

QE : Estimated peak discharge
QS : Simulated peak discharge

Figure 3.20. Forecasted peak discharge for Case 2.

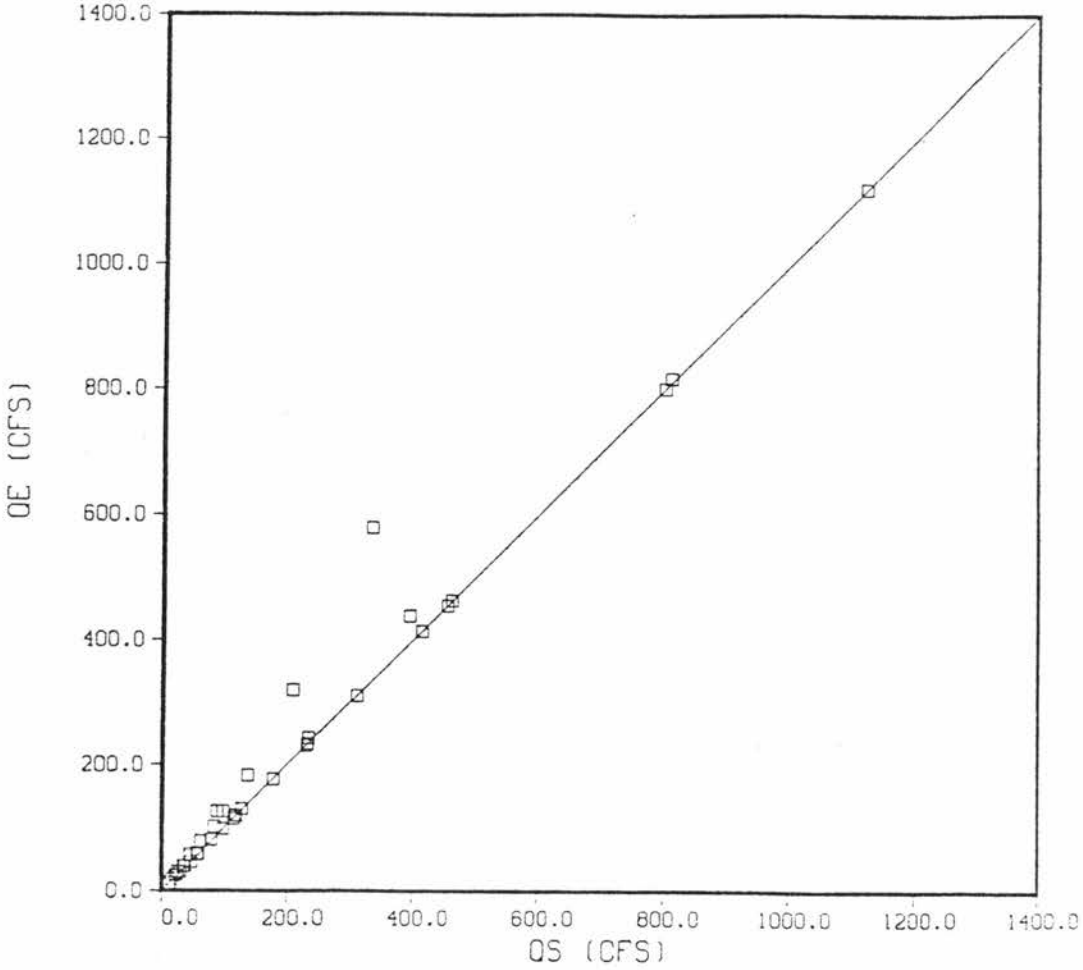

QE : Estimated peak discharge
QS : Simulated peak discharge

Figure 3.21. Forecasted peak discharge for Case 4.

percent of the peak discharge under concentration that appears at the catchment outlet when there is no concentration.

The selection of independent variables can be done by considering that in Case 2 no concentration is attained, since the effective duration t_e is less than the total time of concentration. The first independent variable for Case 2 is proposed to be

$$\Delta t = \frac{t_e}{t^*} \times 100 \tag{3.121}$$

The second variable involves the distance x_R traveled by the characteristic starting at $x = 0$ and $t = t_c$ when $t = t_e$, obtained by integration of Equations (3.38), (3.40), (3.50) and (3.48) as

$$x_R = \alpha_c (W\ i_e)^{\beta c - 1} (t_e - t_c)^{\beta c} \tag{3.122}$$

The dimensionless independent variable is defined as

$$\Delta x = \frac{x_R}{L_c} \times 100 \tag{3.123}$$

The independent variables Δt and Δx represent, in a certain way, the percentage of concentration attained in Case 2 with respect to Case 1.

Following a similar reasoning, the independent dimensionless variables for Case 4 are defined as

$$\Delta t = \frac{t_p}{t_e + t''_s} \times 100 \tag{3.124}$$

$$x_R = \alpha_c [2\ \alpha_p (i_e t_e)^{\beta p}]^{\beta c - 1}\ (t_p - t_e)^{\beta c} \tag{3.125}$$

$$\Delta x = \frac{x_R}{L_c} \times 100 \tag{3.126}$$

Once the variables to be entered in the regression analysis have been defined, a last consideration is taken into account. In order to preserve mathematical continuity between the analytical and approximate equations, any chosen regression model must provide $\Delta Q = 100$ for $\Delta t = 100$ and $\Delta x = 100$. In addition to the inclusion of this point into the regression data set, and since any proposed model will not pass exactly through the forced point, some transformation must be performed on the selected model. Such a transformation can be either the subtraction of the residual for $\Delta Q = 100$ or the division by the estimated value for $\Delta Q = 100$. The transformation yielding the minimum regression standard error and the minimum maximum percent error was chosen in each case.

After performing all the necessary computations and analyzing different kind of models, the model giving the best fitting was defined by the independent variables in the natural logarithm space and the dependent variable in the real space. The model selected for Case 2 is

$$\Delta Q = -129.697 + 49.878\ \text{Ln}\ \Delta t \tag{3.127}$$

Similarly, for Case 4

$$\Delta Q = -118.552 + 47.458\ \text{Ln}\ \Delta t \tag{3.128}$$

At last, Δx was not included in the models, since its contribution to the explained variance of ΔQ was not significant, 1.7% and 0.7% for Cases 2 and 4 respectively.

Table 3.10 summarizes the properties for the models presented in Equations (3.127) and (3.128). For Case 2 ΔQ varied between 100 and 64.8 while Δt varied between 100 and 51.20. The same variation ranges for Case 4 were 100, 57.52 and 100, 44.48.

Table 3.10. Properties for the regression models for Cases 2 and 4.

Property	Case 2	Case 4
Coefficient of determination	0.959	0.951
Standard error (%)	2.04	2.56
Maximum percent error (%)	5.74	7.03

Plugging Equations (3.113), (3.120) and (3.121) in (3.124) the resulting model for Case 2 is

$$Q_m = 0.02 \left[-129.697 + 49.878 \text{ Ln} \left(\frac{100\ t_e}{t^*}\right)\right] L_c\ W\ i_e \qquad (3.129)$$

Doing the same with Equations (3.115), (3.120), (3.124) and (3.128), the equation recommended for Case 4 is

$$Q_m = 0.02 \left[-118.552 + 47.458 \text{ Ln} \left(\frac{100\ t_p}{t_e + t''_s}\right)\right] L_c\ \alpha_p (i_e t_e)^{\beta p} \qquad (3.130)$$

Figures 3.22 and 3.23 present a graphical representation of the behavior of the forecasting models for Cases 2 and 4.

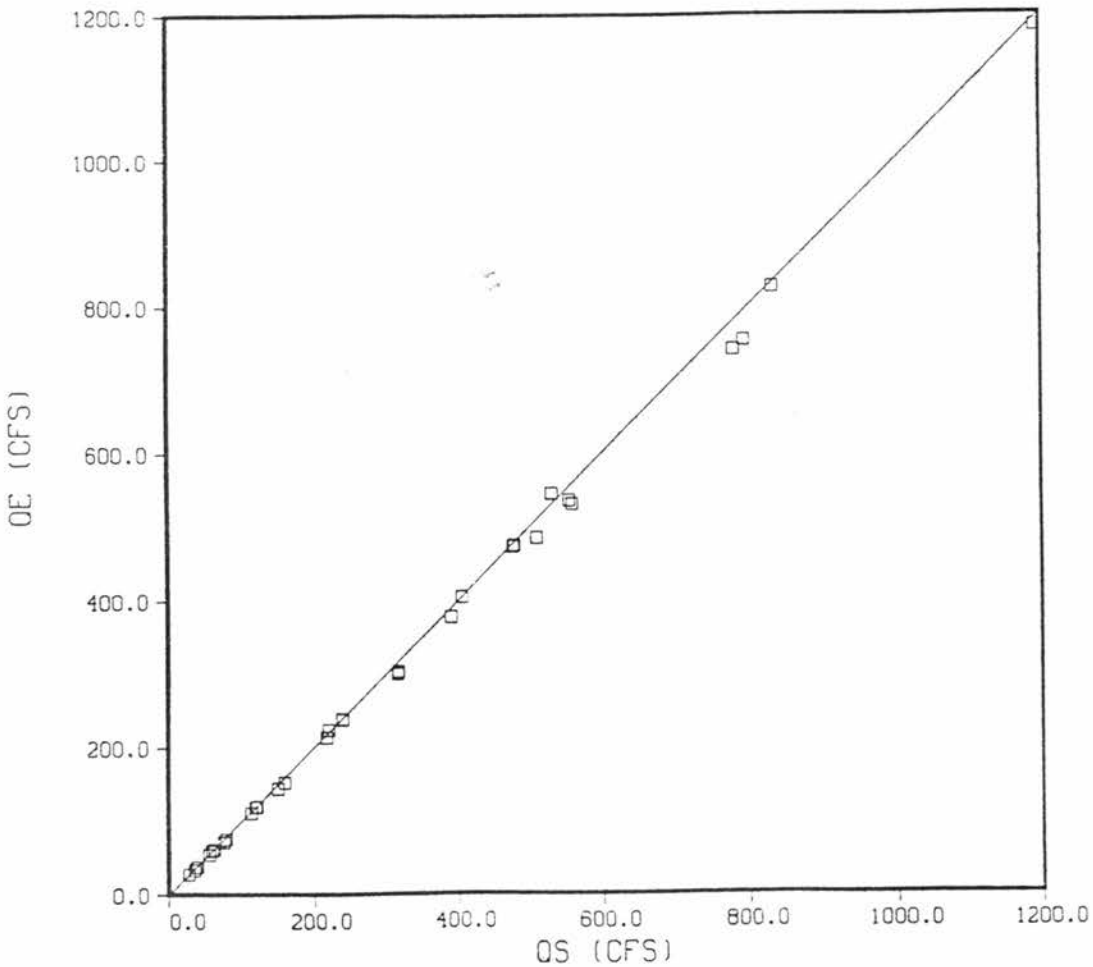

QE : Estimated peak discharge (improved)
QS : Simulated peak discharge

Figure 3.22. Forecasted discharge for Case 2 using the regression model.

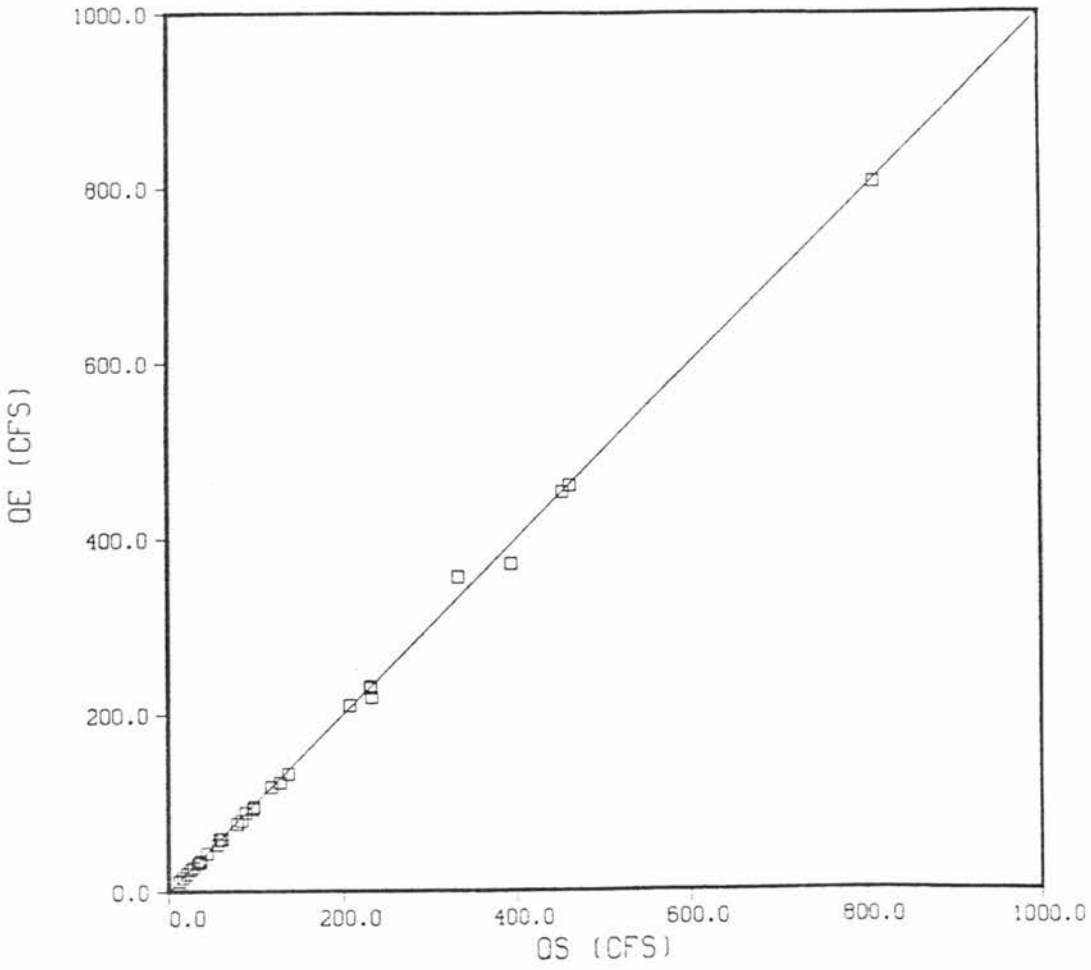

QE : Estimated peak discharge (improved)
QS : Simulated peak discharge

Figure 3.23. Forecasted discharge for Case 4 using the regression model.

3.10 Summarized Procedure for Computing the Peak Variables

This section is intended to present a summary of the equations used to predict the peak discharge and time to peak, when an effective rainfall intensity i_e of duration t_e is imposed over a catchment area formed by a first order stream of length L_c and two symmetrical planes of width W.

1. Step 1: Compute the coefficients and exponents in the area-discharge relationship for the plane and stream.

$$\alpha_p = \frac{1.486}{n_p} S_p^{1/2} \tag{3.131}$$

$$\beta p = 5/3 \tag{3.132}$$

$$\alpha_c = \frac{1.486\ (0.25)^{2/3}}{n_c} S_c^{1/2} \tag{3.133}$$

$$\beta c = 1 + 0.7/3 \tag{3.134}$$

where n stands for roughness and S for slope, and p distinguishes plane's properties from stream's properties.

2. Step 2: Compute the following times

$$t_c = \left[\frac{W\ i_e^{1-\beta p}}{\alpha_p}\right]^{1/\beta p} \tag{3.135}$$

$$t_s = \left[\frac{L_c}{\alpha_c (2\ W\ i_e)^{\beta c - 1}}\right]^{1/\beta c} \tag{3.136}$$

$$t^* = t_c + t_s \tag{3.137}$$

where t_c is the concentration time in the plane, t_s concentration time in the stream given concentration on plane and t^* is the total time of concentration.

3. Step 3: Apply Case 1 when $t_e \geq t^*$ as

$$Q_m = 2\ L_c\ W\ i_e \tag{3.138}$$

$$t_m = t^* \tag{3.139}$$

4. Step 4: Apply Case 2 when $t^* > t_e \geq t_c$ as

$$Q_m = 0.02\left[-129.697 + 49.878\ \text{Ln}\left(\frac{100\ t_e}{t^*}\right)\right] L_c\ W\ i_e \tag{3.140}$$

$$t_m = (t_e + t^*)/2 \tag{3.141}$$

5. Step 5: Compute the following times

$$t_p = \frac{\beta p - 1}{\beta p}\ t_e + \frac{W}{\alpha_p\ \beta p\ (i_e t_e)^{\beta p - 1}} \tag{3.142}$$

$$t_s'' = \left\{\frac{L_c}{\alpha_c[2\ \alpha_p (i_e t_e)^{\beta p}]^{\beta c - 1}}\right\}^{1/\beta c} \tag{3.143}$$

6. Step 6: Apply Case 3 when $t_c > t_e$ and $t_e + t_s'' \leq t_p$ as

$$Q_m = 2\ L_c\ \alpha_p (i_e\ t_e)^{\beta p} \tag{3.144}$$

$$t_m = t_e + t''_s \tag{3.145}$$

7. Step 7: Apply Case 4 when $t_c > t_e$ and $t_e + t''_s > t_p$ as

$$Q_m = 0.02\left[-118.552 + 47.458\ \mathrm{Ln}\left(\frac{100\ t_p}{t_e + t''_s}\right)\right] L_c \alpha_p (i_e t_e)^{\beta p} \tag{3.146}$$

$$t_m = (t_p + t_e + t''_s)/2 \tag{3.147}$$

3.11 Final Remarks on the Effective Rainfall-Runoff Model

As was stated in the introduction for the present chapter, and as the interested reader may verify, the effective-rainfall runoff model herein developed follows closely Eagleson's work (1972), not only in the notation, but in the determination of some characteristic times for the catchment area. However, Eagleson's work lacks some important features: first, the runoff cases considered depend on his decision tree, which was reduced upon the basis of particular values for rainfall intensity and discharge coefficients, and second, the development does not cover all effective-rainfall runoff, for example concentration on channel given no concentration on planes.

It is the believe of the author that the developed effective rainfall-runoff model solves the shortcomings found in Eagleson's study. Through the derivation and calibration of the effective rainfall-runoff model, the variables describing roughness and the hydraulic radius-area relationship for the channel were held constant. The value of the roughness conditions the coefficient for the depth-discharge relationship in the plane and for the area-discharge in the plane. However, the variation on these coefficients was taken into

account through variation of slopes. Besides, the calibrations was performed on dimensionless variables, and the obtained expressions account for all variables representing the process under consideration.

A serious shortcoming can be put on the model due to the fact that regression analysis was employed. However, this fact can make the model more flexible since the same technique may be applied to other configurations, actual or hypothetical, depending on modeler's needs.

At last, the use of the model is recommended since it has been obtained through analytical development combined with regression analysis, the latter performed on dimensionless variables.

Chapter 4

FLOOD FREQUENCY DERIVATION

4.1 Introduction

The objective of this chapter is to put together the different components of the flood frequency derivation technique.

For the rainfall-infiltration component, the results given by Diaz-Granados et al. (1983) are taken.

The effective rainfall-runoff model has been already developed and formally presented in Chapter 3.

Once this elements are put together an algorithm for the computation is developed and translated into a computer FORTRAN code, to be run in the CYBER205. The user manual for this program is presented in Appendix B.

The flood frequency derivation technique is applied to the five configurations used in Chapter 3 (Table 3.5) and a sensitivity analysis is performed. To improve any judgment about the applicability of the method, this is applied to two real world small watersheds.

4.2 Rainfall-Infiltration Component

In Chapter 3 an algorithm was implemented in order to estimate the peak discharge and time to peak for a first order stream with symmetrical lateral planes. The computation is performed as function

of the effective rainfall intensity i_e, the effective duration t_e and the catchment geometry and dynamics.

Unfortunately, in real world watersheds, neither the effective intensity nor the effective duration can be measured. In the best of the cases, a cumulative rainfall depth record along time is obtained. From the total precipitation depth and total duration t_r an average total intensity i_r can be estimated. Now, if marginal or joint probability distribution functions (pdf) are formulated for i_r and t_r, along with an infiltration model, the joint pdf for i_e and t_e can be obtained.

Following Eagleson (1972), it will be supposed, for the present study, that the total rainfall point intensity i_r and the total rainfall duration t_r are independent exponentially distributed as

$$f_{Ir}(i_r) = \beta^* \exp(-\beta^* i_r), \quad i_r \geq 0 \tag{4.1}$$

$$f_{Tr}(t_r) = \delta \exp(-\delta\, t_r), \quad t_r \geq 0 \tag{4.2}$$

where β^* and δ are given as

$$\beta^* = 1/\bar{i}_{rm} \tag{4.3}$$

$$\delta = 1/\bar{t}_{rm} \tag{4.4}$$

In the last two equations $\bar{i}_{rm}$ and $\bar{t}_{rm}$ represent the mean total point rainfall intensity and mean total duration respectively.

Eagleson (1972) propose the following expression in order to account for the difference between point precipitation and areal precipitation:

$$k = 1 - \exp(-1.1\delta^{-1/4})[1 - \exp(-0.01A_c)] \tag{4.5}$$

where δ is given in hours and A_c, the catchment area, in square miles, and k represents the ratio between the areal total depth and point depth precipitation. Furthermore, supposing that the duration for both events, areal and point, area the same, he concludes that the inverse of the mean areal precipitation, β, is related to β^* as

$$\beta = \beta^*/k \tag{4.6}$$

Therefore, the pdf for the total areal rainfall intensity is written as

$$f_{Ir}(i_r) = \beta \exp(-\beta i_r),\ i_r \geq 0 \tag{4.7}$$

and the joint pdf for i_r and t_r in view of their assumed independence, as

$$f_{Ir,Tr}(i_r,t_r) = \beta\delta \exp(-\beta i_r - \delta t_r) \tag{4.8}$$

For a uniform rainfall of intensity i_r and duration t_r, the infiltration process is describe via the set of equations:

$$f = i_r,\ 0 < t \leq t_o \tag{4.9}$$

$$f = \frac{1}{2} St^{-1/2} + K_s, \quad t_o < t \leq t_r \tag{4.10}$$

$$t_o = \frac{S^2}{2(i_r - K_s)^2}, \quad i_r > K_s \tag{4.11}$$

where f is the infiltration capacity rate at any time t, S is the sorptivity, K_s the hydraulic conductivity and t_o is the ponding time, defined as the time at which the upper layer of soil saturates and a film of water forms, being able to generate runoff (Morel-Seytoux, 1981).

Equation (4.10) can be recognized as Philip's equation, with a slight difference, given by the fact that the gravitational infiltration rate has been replaced by K_s, value to which, in several infiltration models, the capacity rate has to tend when the rainfall duration is large (Morel-Seytoux, 1981). This assumption sounds valid and add simplicity to the computations.

The sorptivity S measures the capacity of the soil to absorb water. Based on Koch (1981), for a steady rainfall intensity, S can be computed as

$$S = \left[2K_s(\theta_s - \theta_i)H_c \right]^{1/2} \tag{4.12}$$

where θ_s and θ_i are the soil water content at natural saturation and at the beginning of the rainfall, respectively, both of them dimensionless, and H_c is the capillary drive or suction head.

Equation (4.11), obtained by Eagleson (1978) as an approximation, gives the ponding time as a function of sorptivity, rainfall intensity

and hydraulic conductivity. This last term appears in Equation (4.11) by the same reason as in Equation (4.10).

Equation (4.9) through (4.11) state that when the time is less than the ponding time, the infiltration capacity is greater than the rainfall intensity and no runoff takes place. If i_r is greater than K_s, progressively, the water content of the soil increases up to a value when ponding is reached. After this, part of rainfall infiltrates following Equation (4.10) while the remaining portion produces runoff. Figure 4.1 depicts a schematic representation of the rainfall-infiltration process.

The area denoted d_e in Figure 4.1 represents the effective depth and was approached by Eagleson (1978) as

$$d_e = (i_r - K_s) - S(t_r/2)^{1/2} \tag{4.13}$$

Defining the effective duration t_e as

$$t_e = t_r - t_o \tag{4.14}$$

the mean effective intensity is computed via

$$i_e = d_e/t_e \tag{4.15}$$

With the results presented up to this point, the probability of null runoff, denoted by $P[i_e = 0, t_e = 0]$, can be computed as

$$P[i_e = 0, t_e = 0] = P[i_r \leq K_s] + P[t_r \leq t_o, i_r > K_s] \tag{4.16}$$

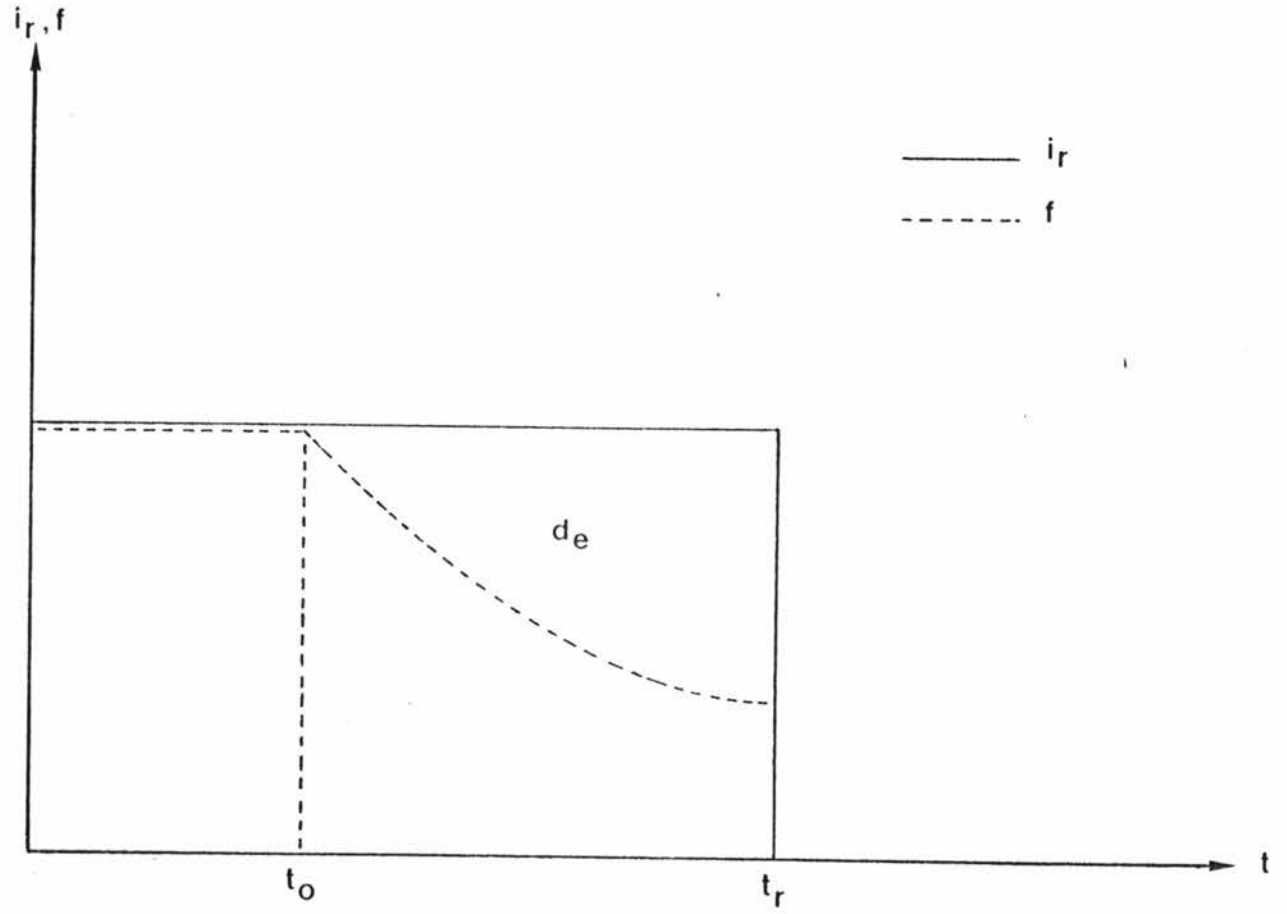

Figure 4.1. Rainfall-infiltration process (Diaz-Granados et al. (1983)).

The first probability can be obtained from Equation (4.7), as the cumulative pdf of i_r evaluated at K_s, yielding the result

$$P[i_r \leq K_s] = 1 - \exp(-\beta K_s) \tag{4.17}$$

To compute the probability of the rainfall duration being less or equal than the ponding time when simultaneously the rainfall intensity is greater than the hydraulic conductivity, the following integration has to be performed

$$P[t_r \leq t_o,\ i_r > K_s] = \beta\delta \int_0^{\infty} \left[\int_{K_s}^{i_{ro}} \exp\left(-\beta i_r - \delta t_r\right) di_r \right] dt_r \tag{4.18}$$

The upper limit in the inner integral, i_{ro}, must be obtained from Equation (4.11) as a function of t_r and it represents the intensity generating a ponding time equal to such duration

$$i_{ro} = \frac{1}{2} S t_r^{-1/2} + K_s \tag{4.19}$$

Note that Equation (4.19) can also be obtained by replacing f and t by i_r and t_r in Equation (4.10). Taking (4.19) to Equation (4,18), solving the inner integral and taking this result along with expression (4.17) to Equation (4.16), the null runoff probability is

$$P\,[i_e = 0,\ t_e = 0] = 1 - \delta \exp(-\beta K_s) \int_0^{\infty} \exp\left[-\delta t_r - \beta S (2t_r)^{-1/2} \right] dt_r \tag{4.20}$$

Equation (4.20) has no closed solution. Although one can solve it numerically for particular values of the parameters, Eagleson

(1972) presents an approximation for this kind of integral. Using his own notation, he proposed

$$a \int_0^{\infty} \exp(-at - bt^{-m})\, dt \approx \exp\left[\frac{-\sigma}{m}\right] \sigma^{(-\sigma+1)}\, \Gamma(\sigma) \tag{4.21}$$

$$\sigma = a\left[\frac{mb}{a}\right]^{1/(m+1)} \tag{4.22}$$

provided σ is of order of unity. The notation $\Gamma(.)$ stands for the Gamma function.

For the present case $a = \delta$, $b = \beta S/(2)^{1/2}$ and $m = 1/2$. Therefore the following results are yielded

$$P\,[i_e = 0, t_e = 0] = 1 - \Gamma(\sigma)\sigma^{-\sigma} \exp(-\beta K_s - 2\sigma) \tag{4.23}$$

$$\sigma = \delta \left[\frac{\beta S}{(2)^{3/2}\delta}\right]^{2/3} \tag{4.24}$$

Using the above results, Diaz-Granados et al. (1983) derive a joint pdf for the effective intensity and effective duration. First, they obtain the marginal distribution for the effective duration and then multiply it by the conditional distribution for i_e given t_e. This is

$$f_{Ie,Te}(i_e, t_e) = f_{Ie/Te}(i_e, t_e)\, f_{Te}(t_e) \tag{4.25}$$

In order to obtain the marginal distribution for t_e the following operation is performed:

$$f_{Te}(t_e) = \frac{d}{dt_e} \left(P[t_e = 0] + P[0 < t_e < t_{e1}]\right) \qquad (4.26)$$

The first term in the derivative is equal to the null runoff probability, since, as Diaz-Granados et al. (1983) stated, t_e is equal to zero if and only if i_e is equal to zero.

The second term between parenthesis in Equation (4.26) is obtained by double integration of (4.8), between t_e and $t_o + t_e$ as functions of i_r along t_e direction, and between K_s and infinite along i_r. Again, an unsolvable integral is found, but a closed approximate solution for (4.26) is finally obtained by letting the term between parenthesis, the cumulative pdf for t_e, tend to one when t_e tends to infinite. The final result, reported by Diaz-Granados et al. (1983), is

$$f_{Te}(t_e) = \delta\ \Gamma(\sigma + 1)\sigma^{-\sigma} \exp(-\beta K_s - 2\sigma - \delta t_e) \qquad (4.27)$$

The evaluation of $f_{Ie/Te}(i_e, t_e)$ requires the invertibility of the function defined by Equations (4.13), (4.14) and (4.15), or

$$i_e = (i_r - K_s)\left(1 + \frac{t_o}{t_e}\right) - \left(\frac{t_o}{2t_e^{\,2}} + \frac{1}{2t_e}\right)^{1/2} \qquad (4.28)$$

The invertibility condition means that i_r has to be obtained as a function of i_e and t_e. This is necessary since

$$f_{Ie/Te}(i_e, t_e) = \frac{d}{di_e} F_{Ie/Te}(i_e, t_e) \qquad (4.29)$$

or

$$f_{Ie/Te}(i_e,\ t_e) = \frac{d}{di_e} P[I_e \leq i_e/\ t_e] \tag{4.30}$$

Now, expressing Equation (4.28) as $I_e = g(I_r)$, since t_e assumes a given value

$$f_{Ie/Te}(i_e,\ t_e) = \frac{d}{di_e} P[g(I_r) \leq i_e/\ t_e] \tag{4.31}$$

Equation (4.31), applying the invertibility condition, gives

$$f_{Ie/Te}(i_e,\ t_e) = \frac{d}{di_e} P[I_r \leq g^{-1}(i_e)\ /\ t_e] \tag{4.32}$$

In the right hand side term of Equation (4.32) one recognizes the cumulative pdf of i_r, evaluated at $g^{-1}(i_e)$ for a given value of t_e. Making the explained replacement and developing the derivative

$$f_{Ie/Te}(i_e,\ t_e) = f_{Ir}(g^{-1}(i_e)) \left| \frac{dg^{-1}(i_e)}{di_e} \right| \tag{4.33}$$

where the absolute value $|.|$ in the last term has been added in order to account for the possibility of $g^{-1}(i_e)$ increasing or decreasing monotonically (Freeman, 1963).

Unfortunately, Equation (4.28) can not be inverted, since t_o is a function of i_r and t_e depends on t_o. In order to solve this problem, Diaz-Granados et al. (1983) approached the above function by performing regression analysis on some dimensionless variables, obtaining for i_r

$$i_r = 1.4434\ S^{k_1}\ t_e^{k_2}\ i_e^{k_3} \tag{4.34}$$

with

$$k_1 = 0.1558 \tag{4.35}$$

$$k_2 = -0.0779 \tag{4.36}$$

$$k_3 = (1 - k_1) \tag{4.37}$$

Finally, the conditional pdf for i_e is computed as

$$f_{Ie/Te}(i_e,\ t_e) = 1.4434\ k_3 \beta \left(\frac{S}{i_e}\right)^{k_1} t_e^{k_2}$$

$$\exp\left(-1.4434\ \beta\ S^{k_1}\ i_e^{k_3}\ t_e^{k_2} \right) \tag{4.38}$$

Plugging Equations (4.27) and (4.38) into (4.25), the joint pdf for i_e and t_e is

$$f_{Ie,Te}(i_e,\ t_e) = 1.4434\ k_3\ \beta\ \delta\ \exp(-\beta K_s - 2\sigma)\ \Gamma(\sigma + 1)$$

$$\sigma^{-\sigma} \left(\frac{S}{i_e}\right)^{k_1} t_e^{k_2} \exp\left(-\delta t_e - 1.4434\ \beta\ S^{k_1} i_e^{k_3} t_e^{k_2} \right) \tag{4.39}$$

4.3 Probabilistic Component

Once the joint pdf for i_e and t_e has been presented, the probabilistic component, already used in part in the previous section,

deals with linking the rainfall-infiltration component and the effective rainfall-runoff model.

The effective rainfall-runoff model was formulated in Chapter 3 and a summary is presented in Section 3.10.

The first objective of the probabilistic component is given by the determination of the cumulative pdf for the peak discharge, $F_{Q_m}(Q)$. Once this computation has been accomplished, the return period for a given value of Q can be computed as (Eagleson, (1972); Diaz-Granados et al. (1983))

$$T_r = \frac{1}{m_\nu [1 - F_{Q_m}(Q)]} \tag{4.40}$$

where T_r stands for the return period. It represents the average number of years elapsed between the occurrence of two events with the same magnitude for Q. The term m_ν in Equation (4.40) denotes the average number of independent rainfall events per year, from which just one is selected to conform the flood annual series. Note that Equation (4.40) does not consider any base flow discharge in the watershed, term considered negligible within the present study (Diaz-Granados et al. (1983)).

As stated above, before any application of Equation (4.40) is intended, it is necessary to set up an algorithm for computing $F_{Q_m}(Q)$.

In the present development, as is the case in most of previous related works, the randomness in the peak discharge is given by the randomness in the rainfall. This means that no probabilistic behavior is assigned to other variables, like soil and morphologic parameters, except for Eagleson's work (1972), where he considered a variable

catchment width depending on rainfall conditions. However, this fine-tuning will not be included in the present work.

By definition, the cumulative pdf for the peak discharge Q_m is

$$F_{Q_m}(Q) = P\,[Q_m(i_e,t_e) \leq Q] \tag{4.41}$$

In words, $F_{Q_m}(Q)$ gives the probability of the random variable Q_m being less or equal than a certain value Q. Equation (4.41) points out that the randomness in Q_m depends on the randomness of i_e and t_e. Hence, in order to determine the above probability, it is necessary to integrate the joint pdf of i_e and t_e over certain regions. Figure 4.2 illustrates the plane i_e - t_e and the regions where the integration has to be performed. The boundaries for those regions depend on the value given to Q. As stated through the development of the effective rainfall-runoff model and summarized en Section 3.10, four cases for computing the discharge are to be considered.

Although the definition of the boundaries depends on the value given to Q, for the sketch presented in Figure 4.2, these are conformed as follows:

- Region 1: from $t_e = t_s + t_c$ to $Q_{m1}(i_e,t_e) = Q$ for t_{e12} to t_{emax}.

- Region 2: from $t_e = t_c$ to $t_e = t_s + t_c$ for t_{e12} to t_{emax} and from $t_e = t_c$ to $Q_{m2}(i_e,t_e) = Q$ for t_{e24} to t_{e12}.

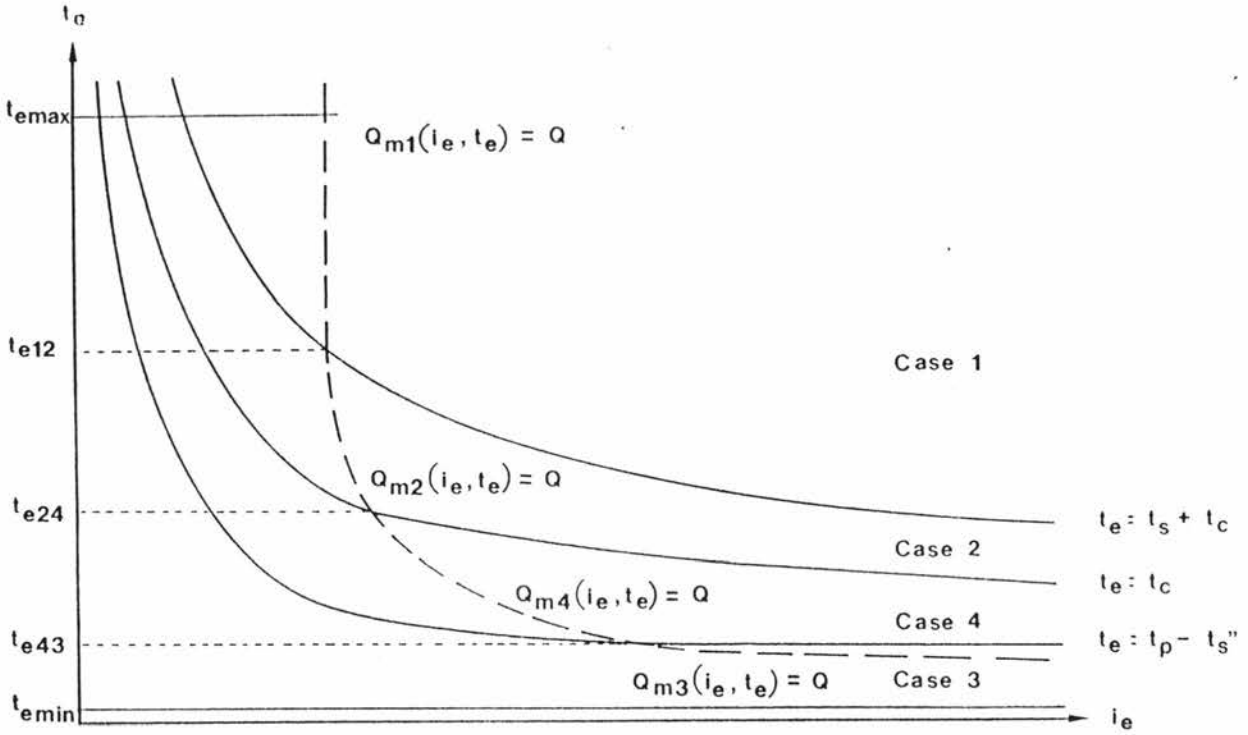

Figure 4.2. Integration regions for the flood frequency computation.

- Region 3: from $t_e = t_p - t_s''$ to $t_e = t_c$ for t_{e24} to t_{emax} and from $t_e = t_p - t_s''$ to $Q_{m4}(i_e,t_e) = Q$ for t_{e43} to t_{e24}.

- Region 4: from $i_e = 0$ to $t_e = t_p - t_s''$ for t_{e43} to t_{emax} and from $i_e = 0$ to $Q_{m3}(i_e,t_e) = Q$ for t_{emin} to t_{e43}.

In the above definition, $Q_{mi}(i_e,t_e) = Q$ stands for the functional relationship used to compute the discharge for Case i, i = 1, .., 4. Similarly, t_{eij} denotes the intersection point of $Q_{mi}(i_e,t_e) = Q$ with the boundaries between two cases. For instance, t_{e24} represents the intersection point of $Q_{m2}(i_e,t_e) = Q$ (or $Q_{m4}(i_e,t_e) = Q$) with the boundary between Cases 2 and 4, $t_e = t_c$. Each region, as defined above, delimits the zone where $Q_{mi}(i_e,t_e) \leq Q$, within the range of application for Case i. Figures 4.3 through 4.7 present integration regions for the five configurations used in Section 3.9 (Table 3.5) and some values of Q.

Based on the aforementioned considerations, the cumulative pdf $F_{Q_m}(Q)$ can be computed as

$$F_{Q_m}(Q) = P[\, i_e = 0,\ t_e = 0] + \sum_{i=1}^{4} \int_{Ri} f_{Ie,Te}(i_e,\ t_e)\, di_e\, dt_e \qquad (4.42)$$

where Ri stands for region i and the null runoff probability has been included properly.

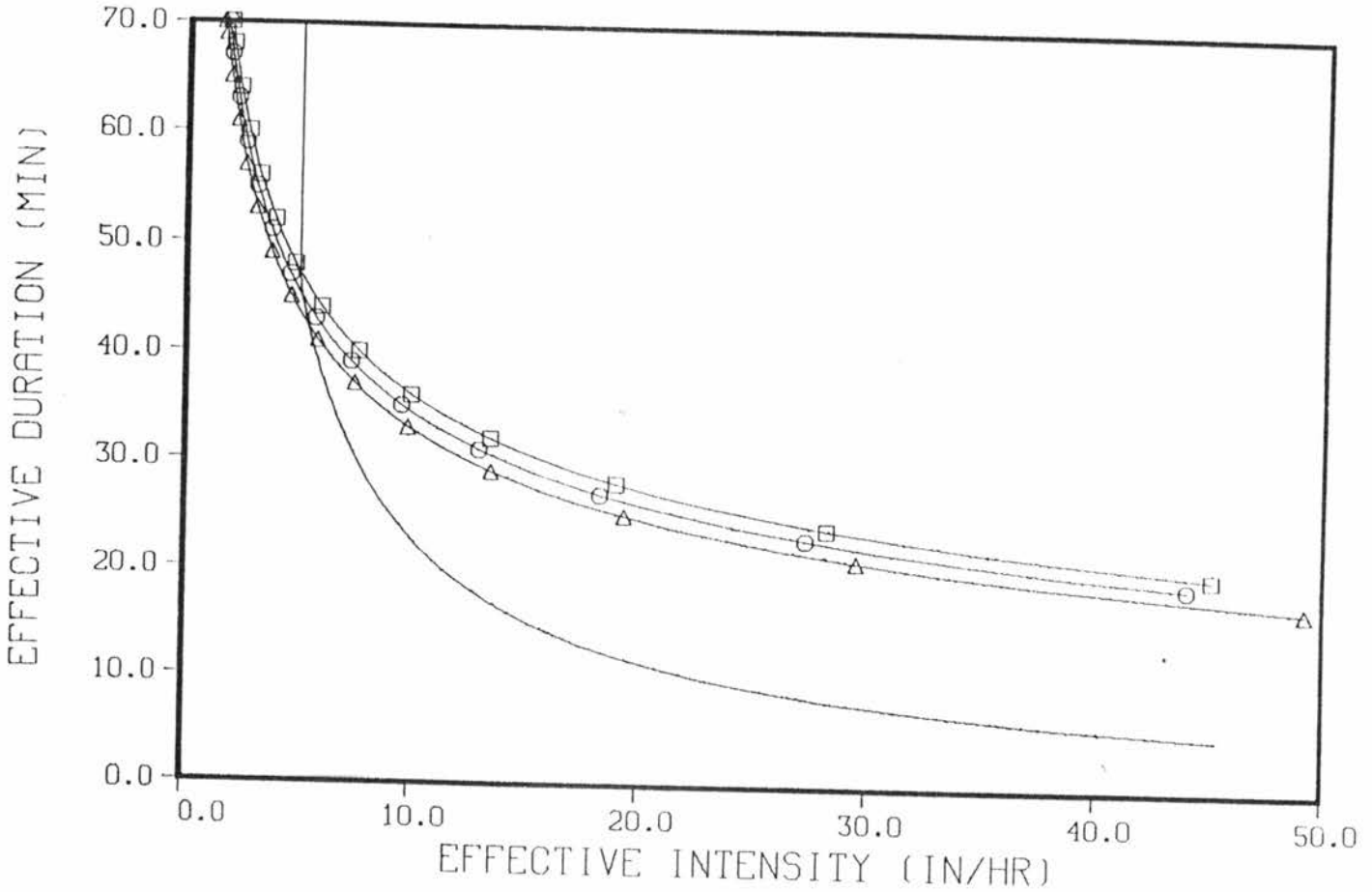

Figure 4.3. Integration regions for Configuration 1 and Q = 600 cfs (see Table 3.5 for configuration definition).

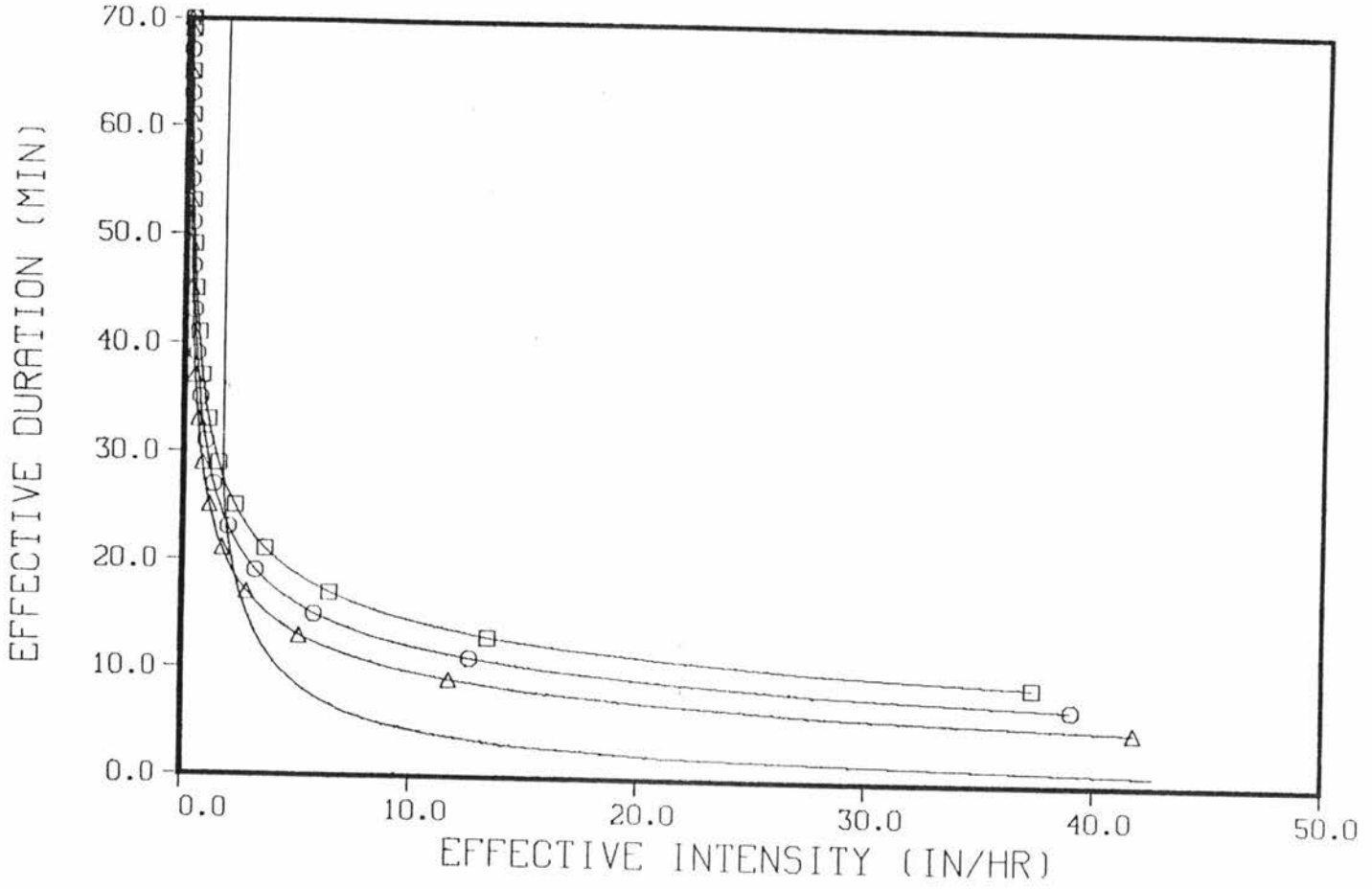

Figure 4.4. Integration regions for Configuration 2 and Q = 100 cfs (see Table 3.5 for configuration definition).

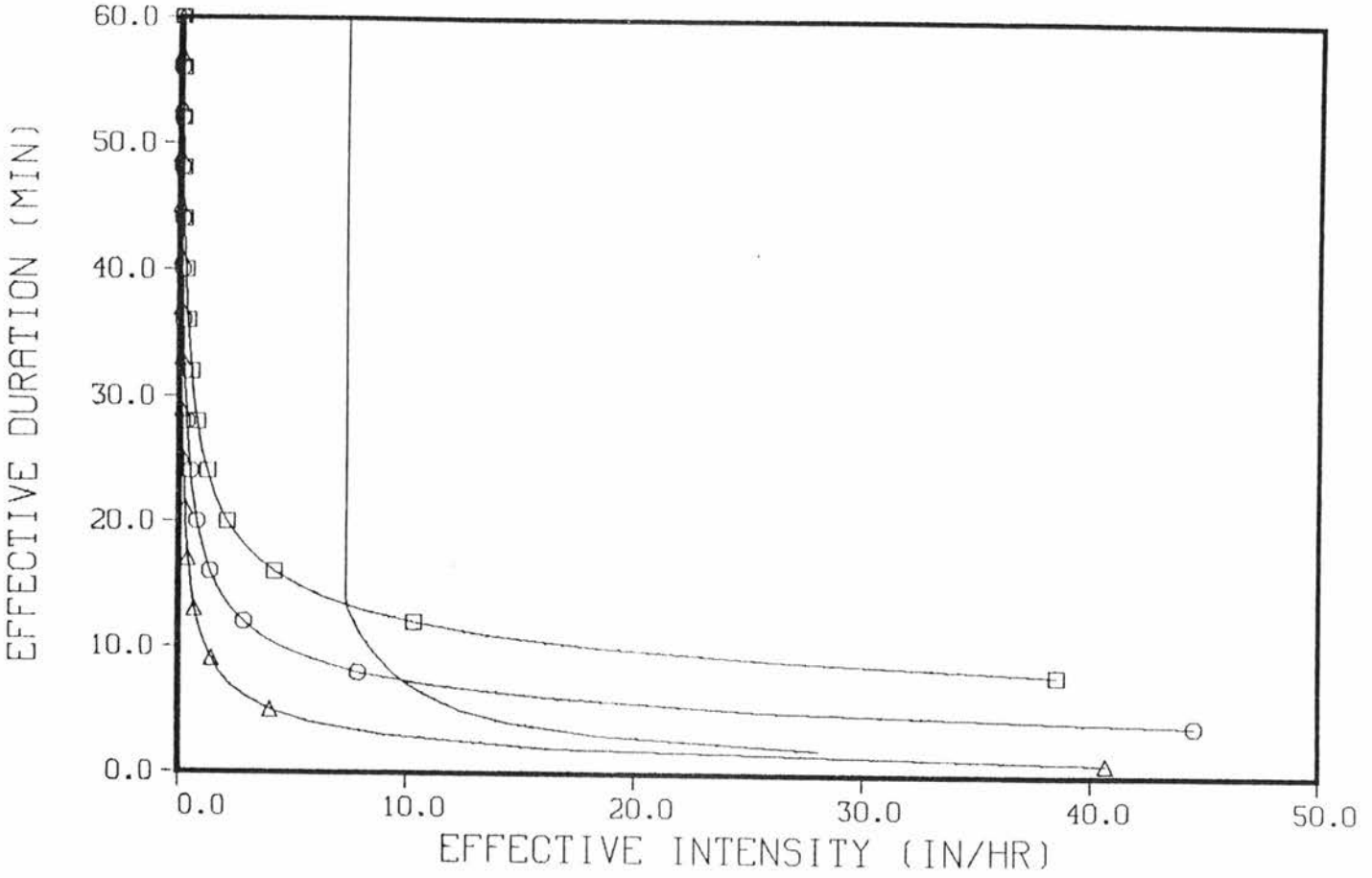

Figure 4.5. Integration regions for Configuration 3 and Q = 600 cfs (see Table 3.5 for configuration definition).

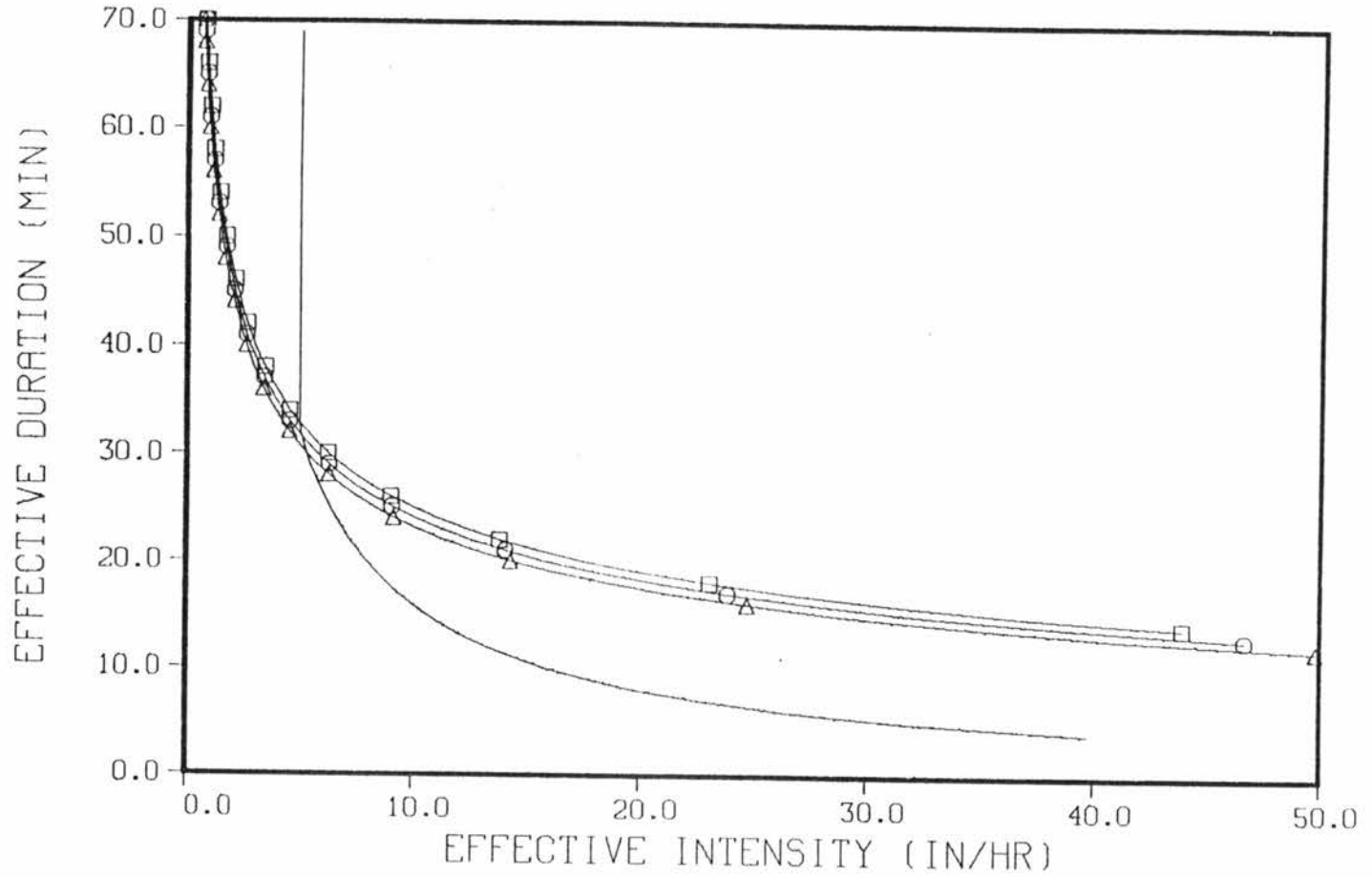

Figure 4.6. Integration regions for Configuration 4 and Q = 600 cfs (see Table 3.5 for configuration definition).

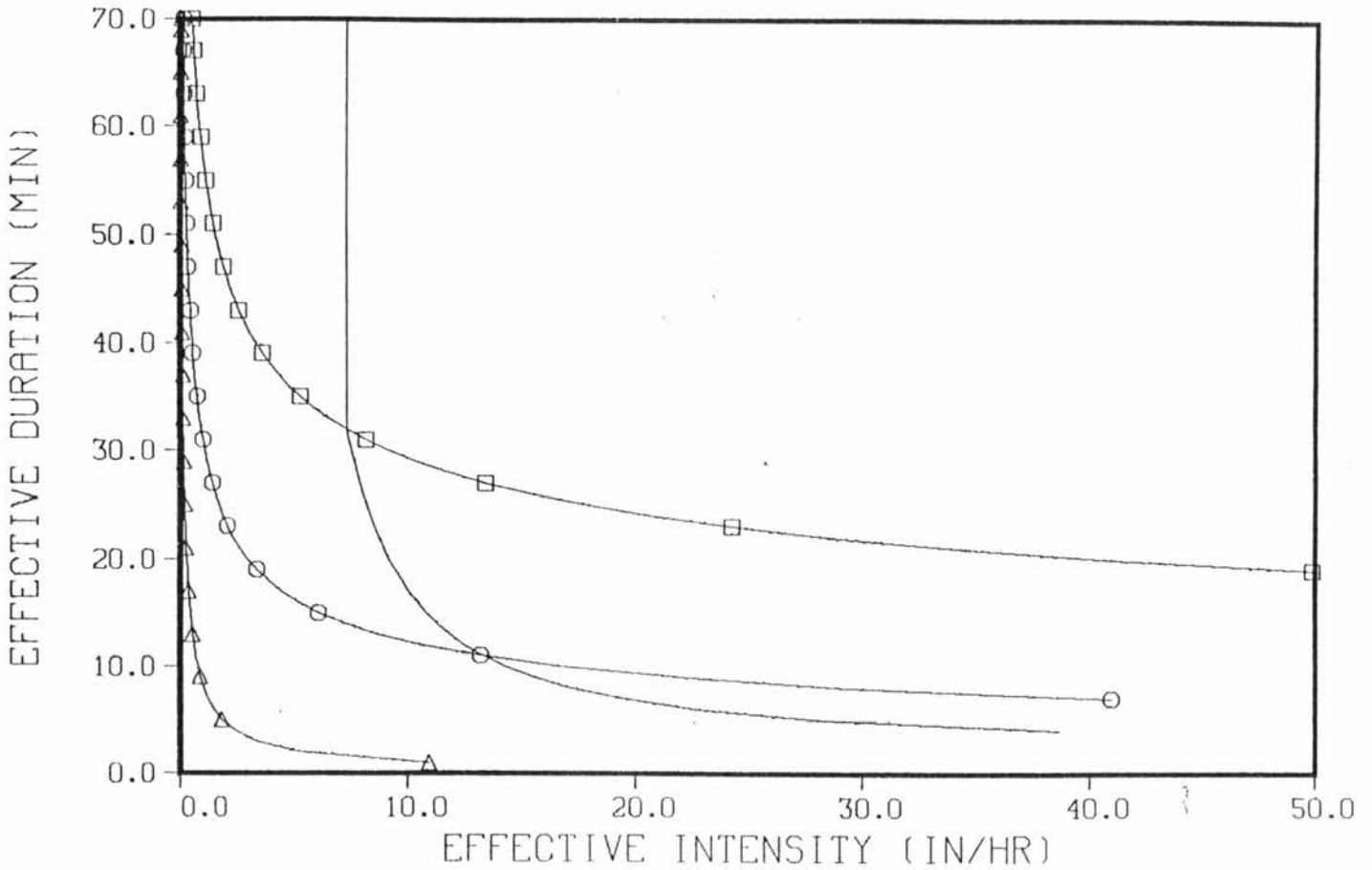

Figure 4.7. Integration regions for Configuration 5 and Q = 600 cfs (see Table 3.5 for configuration definition).

Before any further step is given in regard to the application of Equation (4.42), it is valuable to analyze the integration of $f_{Ie,Te}(i_e, t_e)$, function defined by Equation (4.39). Again, following the work by Diaz-Granados et al. (1983), one realizes that it is possible to integrate Equation (4.39) in the i_e direction. Calling ϕ and ψ respectively

$$\phi = 1.4434\ k_3\ \beta\ \delta\ \exp(-\beta k_s - 2\sigma)\ \Gamma(\sigma+1)\sigma^{-\sigma} S^{k_1} \tag{4.43}$$

$$\psi = 1.4434\ \beta\ S^{k_1} \tag{4.44}$$

$f_{Ie,Te}(i_e,t_e)$ can be rewritten as

$$f_{Ie,Te}(i_e,t_e) = \phi\ \frac{t_e^{k_2}}{i_e^{k_1}}\ \exp\left[-\delta t_e - \psi\ i_e^{k_3}\ t_e^{k_2}\right] \tag{4.45}$$

Denoting i_{e1} and i_{e2} the lower and upper limits of integration when this operation is performed along i_e direction, one obtains:

$$\int_{i_{e1}}^{i_{e2}} f_{Ie,Te}(i_e,t_e)di_e = g(i_{e1},i_{e2},t_e) \tag{4.46}$$

with

$$g(i_{e1},i_{e2},t_e) = \frac{\phi\ \exp(-\delta t_e)}{\psi\ k_3}\left[\exp\left[-\psi\ i_{e1}^{k_3}\ t_e^{k_2}\right] - \exp\left[-\psi\ i_{e2}^{k_3}\ t_e^{k_2}\right]\right] \tag{4.47}$$

where $i_{e1} \leq i_{e2}$. Referring back to Figure 4.2, using the corresponding definition for each region and taking Equation (4.47) to (4.42), $F_{Q_m}(Q)$ can be computed as

$$F_{Q_m}(Q) = P[i_e = 0,\ t_e = 0] + \int_{(t_{e2})_1}^{t_{emax}} g[i_{e11}(t_e),\ i_{e212}(t_e), t_e]dt_e$$

$$+ \sum_{i=2}^{4} \left\{ \int_{(t_{e1})_i}^{(t_{e2})_i} g[i_{e1i}(t_e),\ i_{e2i1}(t_e), t_e]dt_e \right.$$

$$\left. + \int_{(t_{e2})_i}^{t_{emax}} g[i_{e1i}(t_e),\ i_{e2i2}(t_e),\ t_e]dt_e \right\} \qquad (4.48)$$

Some features have to be explained in Equation (4.48). The first integral following the null runoff probability represents Region 1, while the summation covers Regions 2 to 4. As except for Region 1, the computation covers two subregions within each region, two integrals appear within the brackets for the summation. Besides, within each region i_{e1} does not change from one subregion to the second, while i_{e2} does, then the former has been denoted i_{e1i} and the latter i_{e2ij}, with $i = 1,..,4$ and $j = 1,2$. Emphasis has been done on the fact that i_{e1i} and i_{e2ij} are functions of t_e. For each region, except for the first, there are three integration limits: $(t_{e1})_i$ the lower, $(t_{e2})_i$ the intermediate and t_{emax} is always the upper. Table 4.1 presents the equivalent notation for application of Equation (4.48).

Table 4.1. Equivalent notation for computation of $F_{Q_m}(Q)$.

Region i	i_{eli}	$(t_{el})_i$	$(t_{e2})_i$	Subregion j	i_{e2ij}
1	$t_e=t_s+t_c$	--	t_{el2}	1	--
				2	$Q_{m1}(i_e,t_e) = Q$
2	$t_e=t_c$	t_{e24}	t_{el2}	1	$Q_{m2}(i_e,t_e) = Q$
				2	$t_e = t_s + t_c$
3	zero	t_{emin}	t_{e43}	1	$Q_{m3}(i_e,t_e) = Q$
				2	$t_e = t_p - t''_s$
4	$t_e=t_p-t''_s$	t_{e43}	t_{e24}	1	$Q_{m4}(i_e,t_e) = Q$
				2	$t_e = t_c$

Additional emphasis is put on the fact that i_{eli} and i_{e2ij} as presented above express functional relationship between the effective duration t_e and the effective intensity i_e. In order to clarify this, the different functions referred in Table 4.1 are presented completely in the following:

1. $t_e = t_s + t_c$:

$$\left[\frac{L_c}{\alpha_c (2Wi_e)^{\beta c-1}}\right]^{1/\beta c} + \left[\frac{W\, i_e^{\,1-\beta p}}{\alpha_p}\right]^{1/\beta p} - t_e = 0 \qquad (4.49)$$

2. $t_e = t_c$:

$$\left[\frac{W\, i_e^{\,1-\beta p}}{\alpha_p}\right]^{1/\beta p} - t_e = 0 \qquad (4.50)$$

3. $t_e = t_p - t_s''$:

$$\left\{\frac{L_c}{\alpha_c\left[2\alpha_p(i_e\ t_e)^{\beta p}\right]^{\beta c-1}}\right\}^{1/\beta c} - \frac{W}{\alpha_p\beta p(i_e t_e)^{\beta p-1}} - \frac{t_e}{\beta p} = 0 \qquad (4.51)$$

4. $Q_{m1}(i_e, t_e) = Q$:

$$2L_c\ W\ i_e - Q = 0 \qquad (4.52)$$

5. $Q_{m2}(i_e, t_e) = Q$:

$$t^* = \left[\frac{L_c}{\alpha_c(2Wi_e)^{\beta c-1}}\right]^{1/\beta c} + \left[\frac{W\ i_e^{\,1-\beta p}}{\alpha_p}\right]^{1/\beta p} \qquad (4.53)$$

$$0.02\left[-129.697 + 49.878\left[\frac{100\ t_e}{t^*}\right]\right] L_c\ W\ i_e - Q = 0 \qquad (4.54)$$

6. $Q_{m3}(i_e, t_e) = Q$:

$$2L_c\ \alpha_p(i_e t_e)^{\beta p} - Q = 0 \qquad (4.55)$$

7. $Q_{m4}(i_e, t_e) = Q$

$$t_p = \frac{\beta p - 1}{\beta p}\ t_e + \frac{W}{\alpha_p\beta p(i_e t_e)^{\beta p-1}} \qquad (4.56)$$

$$t_s'' = \left\{\frac{L_c}{\alpha_c\left[2\alpha_p(i_e t_e)^{\beta p}\right]^{\beta c-1}}\right\}^{1/\beta c} \qquad (4.57)$$

$$0.02\left[-118.552 + 47.458\ \mathrm{Ln}\left(\frac{100\ t_p}{t_e+t''_s}\right)\right] L_c\alpha_p(i_e t_e)^{\beta p} - 1 = 0 \qquad (4.58)$$

For the computation of the coefficients α_p, βp, α_c, βc, and the definition of notation, the reader is addressed to Chapter 3, Section 3.2 and 3.10.

For Equations (4.49), (4.51), (4.53), (4.54), (4.56), (4.57) and (4.58) it is impossible to obtain i_e as an explicit function of t_e. For the other equations ((4.50), (4.52) and (4.55)) an explicit solution can be obtained. Besides, the computation of the intersection points detailed in Table 4.1 requires simultaneous solution of different system of equations, many of them not linear.

The aforementioned restrictions, added to the fact that a closed integration of Equation (4.47) is impossible, make necessary the implementation of a numerical algorithm to compute $F_{Q_m}(Q)$ using Equation (4.48).

The primary objective of such algorithm is to compute each of the integrals in Equation (4.48) within a certain tolerance. In other words, once the algorithm has performed two successive approximations to any integral, in any stage of the computation, the absolute value of their difference must be less or equal than the specified tolerance, in order to be accepted as the final approximation.

The requirement of a numerical algorithm to compute the cumulative pdf for the peak flow is the reason for which nothing has been mentioned, up to this point, about the integration limits, t_{emin} and t_{emax}, appearing in Equation (4.48). If this equation could be solved analytically, t_{emin} and t_{emax} would have to be replaced by zero and infinite respectively. Due to the structure of the functions

involved in the numerical algorithm, it is difficult to estimate a value for t_{emin} such that a specified tolerance can be attained in the integration. Hence the lower integration limit has to be defined by the user. For the present study, $t_{emin} = 0.05$ sec was used and good accuracy was obtained.

However, the value of t_{emax} can be estimated to achieve the desired tolerance. First, all boundary functional relationships, defined in Table 4.1 and through Equations (4.49) to (4.58), tend to zero when t_e tends to infinite. Therefore, one can compute

$$\lim_{t_e \to \infty} g(i_{e1}, i_{e2}, t_e) = \frac{\phi}{\phi k_3} \lim_{t_e \to \infty} [\exp(-\delta t_e)]$$

$$\left\{ \lim_{t_e \to \infty} \left[\exp\left(-\psi \; i_{e1}^{\,k_3} \; t_e^{\,k_2} \right) \right] - \lim_{t_e \to \infty} \left[\exp\left(-\psi \; i_{e2}^{\,k_3} t_e^{\,k_2} \right) \right] \right\}$$

$$= \frac{\phi}{\psi k_3} \times 0 \times (1 - 1) = 0 \qquad (4.59)$$

The value of t_{emax} can be chosen imposing the following condition,

$$\frac{\phi}{\psi k_3} \exp(-\delta t_{emax}) \leq tol \qquad (4.60)$$

The required limit is then computed as

$$t_{emax} = - \frac{f_s}{\delta} \operatorname{Ln}\left(\frac{\psi \; k_3 \; tol}{\phi} \right) \qquad (4.61)$$

where tol stands for the tolerance and f_s for a safety factor ($f_s \geq 1$). For the present study $f_s = 1.2$ was taken.

In addition to the approximation of the integrals involved in the computation of the cumulative pdf for the peak discharge, the numerical algorithm has to solve the equations defining intersection points and the equations defining a value of i_e for any given value of t_e.

4.4 Description of the Algorithm to Compute the Flood Frequency Distribution Curve

In the previous section, the problem of obtaining the flood frequency distribution curve has been formulated and its solution has been presented. In this section, the set of procedures and instructions required to compute the flood frequency distribution curve for a collection of peak flow values, for a given watershed, is outlined. The reader is addressed to Figure 4.2 and Table 4.1, where most of the notation is explained.

The algorithm is presented as a sequence of steps. In many steps decisions about the truthfulness or falseness of certain statements has to be done. This is accomplished through logical if statements. In order to identify the structure of combined statements and its related possibilities, a number between parenthesis has been assigned to each one. For instance, any if statement or related instruction preceded by (1) is in the first level. Others with (2) are in the second level and contained within another branching instruction in the first level.

- Step 1: Data input

  Rainfall parameters: β, δ, m_ν

  Infiltration parameters: K_s, S

  Plane parameters: W, n_p, S_p

  Stream parameters: L_c, n_c, S_c, a, b

  Discharge values: Q(k), k = 1,..,nq

  Integration controlling parameters: n, toli, t_{emin}

  n: maximum number of iterations approximating integrals

  toli: tolerance for approximating integrals

  Solution of Equations controlling parameters: nit, nbis, tole.

  nit: maximum number of iterations solving equations

  nbis: maximum number of iterations for initial approximation to the root of an equation

- Step 2: Computation of parameters

  Plane's discharge coefficients: α_p, βp

  Stream's discharge coefficients: α_c, βc

  Joint pdf for i_e and t_e coefficients: σ, $\Gamma(\sigma+1)$, ϕ, ψ

  Null runoff probability: $P[i_e=0, t_e=0]$

  Let cdf1 = $P[i_e=0, t_e=0]$

  Upper integration limit: t_{emax}

- Step 3: Flags indicating results in Regions 2 to 4 are set equal zero

  Let ir2 = 0

  Let ir3 = 0

  Let ir3 = 0

- Step 4: The flood frequency computation begins

  For k = 1,..,nq, do steps 5 to 45

Let $F_{Q_m}(k)$ = cdf1

- Step 5: Region 3

- Step 6: When ir3 = 1, the integral in this region has reached a constant value and the computation is not performed anymore

(1) if ir3 = 0 then

- Step 7: The intersection point, t_{e43}, between $t_e = t_p - t_s''$ and $Q_{m3}(i_e, t_e) = Q(k)$ is computed

- Step 8: t_{e43} is checked to be greater than t_{emax}

(2) if $te_{43} \geq t_{emax}$ then

- Step 9: Integrate from t_e axis to $Q_{m3}(i_e, t_e) = Q(k)$ for the interval $[t_{emin}, t_{emax}]$

- Step 10: t_{e43} is checked to be greater than t_{emin}

(2) else if $t_{e43} > t_{emin}$ then

- Step 11: Integrate from t_e axis to $Q_{m3}(i_e, t_e) = Q(k)$ for the interval $[t_{emin}, t_{e43}]$ and from t_e axis to $t_e = t_p - t_s''$ for $[t_{e43}, t_{emax}]$

(2) else

- Step 12: The integral in Region 3 reaches a constant value for the first time. Integrate from t_e axis to $t_e = t_p - t_s''$ for the interval $[t_{emin}, t_{emax}]$. Update ir3 = 1 and cdf1

(2) end if

- Step 13: Update $F_{Q_m}(k)$ adding the integral results

(1) end if

- Step 14: Region 4

- Step 15: When ir4 = 1, the integral in this region has reached a constant value and the computation is not performed anymore

(1) if ir4 = 0 then

- Step 16: The intersection point found in the previous region is checked to be greater than t_{emax}

(2) if $t_{e43} \geq t_{emax}$ then

- Step 17: The integral in Region 4 is zero

(2) else

- Step 18: The integral in Region 4 does exist. The intersection point t_{e24} between $t_e = t_c$ and $Q_{m4}(i_e, t_e) = Q(k)$ is computed

- Step 19: t_{e43} within the integration range is considered

(3) if ir3 = 0 then

- Step 20: t_{e24} is checked to be greater than t_{emax}

(4) if $t_{e24} \geq t_{emax}$ then

- Step 21: Integrate from $t_e = t_p - t_s''$ to $Q_{m4}(i_e, t_e) = Q(k)$

(4) else

- Step 22: Integrate from $t_e = t_p - t_s''$ to $t_e = t_c$ for the interval $[t_{e24}, t_{emax}]$ and from $t_e = t_p - t_s''$ to $Q_{m4}(i_e, t_e) = Q(k)$ for $[t_{e43}, t_{e24}]$

(3) else if $t_{e24} \geq t_{emax}$

- Step 23: Integrate from $t_e = t_p - t_s''$ to $Q_{m4}(i_e, t_e) = Q(k)$ for the interval $[t_{emin}, t_{emax}]$

(3) else if $t_{e24} \geq t_{emin}$

- Step 24: Integrate from $t_e = t_p - t_s''$ to $t_e = t_c$ for $[t_{e24}, t_{emax}]$ and from $t_e = t_p - t_s''$ to $Q_{m4}(i_e, t_e) = Q(k)$ for $[t_{emin}, t_{e24}]$

(3) else

- Step 25: The integral in Region 4 reaches a constant value for the first time. Integrate from $t_e = t_p - t_s''$ to $t_e = t_c$ for the interval $[t_{emin}, t_{emax}]$. Update ir4 = 1 and cdf1

(3) end if

(2) end if

- Step 26: Update $F_{Q_m}(k)$ adding the integral results

(1) end if

- Step 27: Region 2

- Step 28: When ir2 = 1, the integral in this region has reached a constant value and the computation is not performed anymore

(1) if ir2 = 0 then

- Step 29: The intersection point found in the previous region is checked to be greater than t_{emin}

(2) if $t_{e24} > t_{emin}$ then

- Step 30: A new value for t_{e24} is computed as the intersection point between $t_e = t_c$ and $Q_{m2}(i_e, t_e) = Q(k)$

(2) else

- Step 31: Let $t_{e24} = t_{emin}/2$

(2) end if

- Step 32: The intersection point t_{e24} is checked to be greater than t_{emax}

(2) if $t_{e24} \geq t_{emax}$ then

- Step 33: The integral in Region 2 is zero

(2) else

- Step 34: The integral in Region 2 does exist and the intersection point t_{e12} between $t_e = t_c + t_s$ and $Q_{m2}(i_e, t_e) = Q(k)$ is computed

- Step 35: t_{e24} within the range of integration is considered

(3) if ir4 = 0 then

- Step 36: t_{e12} is checked to be greater than t_{emax}

(4) if $t_{e12} \geq t_{emax}$ then

- Step 37: Integrate from $t_e = t_c$ to $Q_{m2}(i_e, t_e) = Q(k)$

(4) else

- Step 38: Integrate from $t_e = t_c$ to $t_e = t_c + t_s$ for $[t_{e12}, t_{emax}]$ and from $t_e = t_c$ to $Q_{m2}(i_e, t_e) = Q(k)$ for $[t_{e24}, t_{e12}]$

(3) else if $t_{e12} \geq t_{emax}$ then

- Step 39: Integrate from $t_e = t_c$ to $Q_{m2}(i_e, t_e) = Q(k)$ for the interval $[t_{emin}, t_{emax}]$

(3) else if $t_{e12} \geq t_{emin}$ then

- Step 40: Integrate from $t_e = t_c$ to $t_e = t_c + t_s$ for $[t_{e12}, t_{emax}]$ and from $t_e = t_c$ to $Q_{m2}(i_e, t_e) = Q(k)$ for $[t_{emin}, t_{e12}]$

(3) else

- Step 41: The integral in Region 2 reaches a constant value for the first time. Integrate from $t_e = t_c$ to $t_e = t_c + t_s$ for $[t_{emin}, t_{emax}]$. Update ir2 = 1 and cdf1.

(3) end if

(2) end if

- Step 42: Update $F_{Q_m}(k)$ adding the integral results

  (1) end if

- Step 43: Region 1

- Step 44: Integrate from $t_e = t_c + t_s$ to $Q_{m1}(i_e, t_e) = Q(k)$ for $[t_{e12}, t_{emax}]$

- Step 45: Repeat computation for next discharge

- Step 46: For k = 1,..,nq compute the return period $T_r(k)$

- Step 47: Output

  Same parameters as in step 1

  Cumulative distribution function $F_{Q_m}(k)$, k = 1,..,nq

  Flood frequency distribution curve $T_r(k)$, k = 1,..,nq

- Step 48: Stop

Within the general algorithm others have to be considered in order to solve equations and perform the required integrations. To solve equations, a combination of Bisection and False Position methods was used. The first one provides an interval containing the root for the equation, such that the function changes sign within that interval. The False Position method takes that interval and, approaching the derivative of the function by means of a secant line, iterates until the desired tolerance is attained or the maximum number of allowed iterations is overpassed. For more details about these algorithms, the interested reader is referred to Burden and Douglas (1985).

For the integration algorithm Romberg method was chosen (Burden and Douglas (1985)). It uses a composite trapezoidal rule to give preliminary approximations and then applies Richardson extrapolation

process to improve the initial approximations. In order to approach the definite integral between a and b for a given function f(x), the composite trapezoidal rule is applied for k = 1,..,n, where n is some positive integer, as

$$m_k = 2^{k-1} \tag{4.62}$$

$$h_k = (b - a)/m_k \tag{4.63}$$

$$R_{1,1} = \frac{h_1}{2} [f(a) + f(b)] \tag{4.64}$$

$$R_{k,1} = \frac{1}{2} \left\{ R_{k-1,1} + h_{k-1} \sum_{i=1}^{m_k/2} f\left[a + \left(i - \frac{1}{2}\right) h_{k-1}\right] \right\} \tag{4.65}$$

To improve the initial approximations Richardson extrapolation algorithm is applied by making for i = 2,..,n and j = 2,..,i

$$R_{i,j} = \left(4^{(j-1)} R_{i,j-1} - R_{i-1,j-1}\right) / \left(4^{(j-1)} - 1\right) \tag{4.66}$$

The term with the largest values for i and j, i.e., $R_{n,n}$ provides the best approximation to the integral. Hence, the larger the n the better the approximation.

The algorithm here described was translated into a FORTRAN computer code. Appendix B presents the user manual for such a program.

4.5 Computation of the Flood Frequency Distribution Curve for Hypothetical Configurations

The flood frequency distribution computation was applied to the five catchment configurations used in Chapter 3, Section 3.9 (Table 3.5). Other parameters were required in addition to those described in Table 3.5 and these were:

- Mean areal rainfall intensity: $1/\beta = 1.0$ in/hr
- Mean rainfall duration: $1/\delta = 4.0$ hr
- Hydraulic conductivity: $K_s = 0.4$ in/hr
- Sorptivity: $S = 0.5$ in/hr$^{1/2}$
- Mean number of independent events: $m_\nu = 10$

The flood frequency distribution curves for the five configurations are presented in Figures 4.8 through 4.12. They depict normal graphical results in the sense that the curves obtained are smooth. The results can be also classified as logical, since the slight upward concavity in the curves shows that a small increase in the return period will increase appreciably the flood discharge, as it shall be.

Configurations 1 and 4 (Table 3.5) exhibit the same geometry, but the plane and channel slope are different. The flood frequency distribution curves depicted in Figures 4.8 and 4.11 are practically the same, showing a low sensitivity of the method to the variation on these parameters. The same conclusion is yielded from Configurations 3 and 5 and Figures 4.10 and 4.12.

4.6 Sensitivity Analysis for the Flood Frequency Derivation

In order to infer the behavior of the flood frequency distribution curve when some parameters are changed, a sensitivity

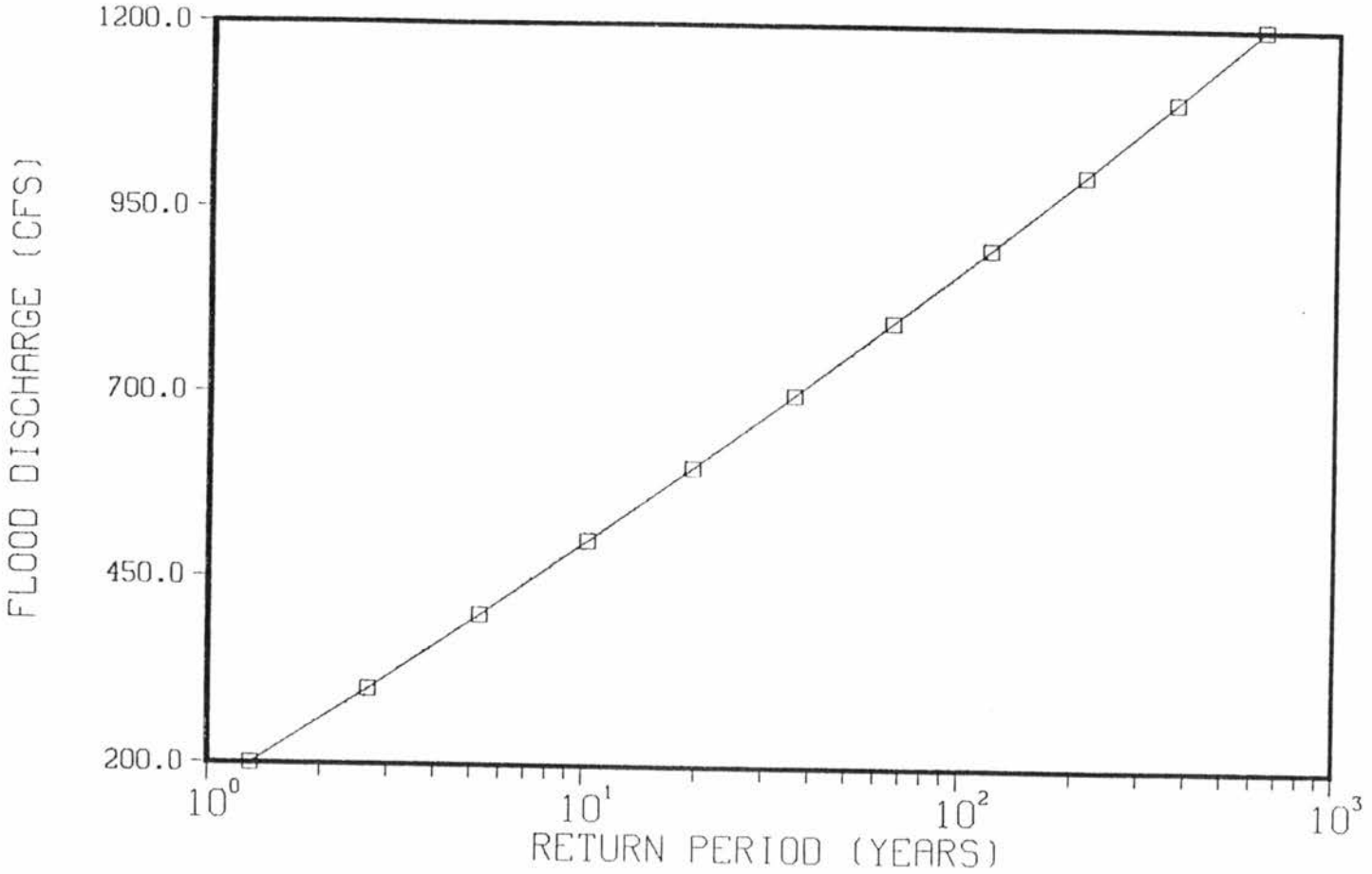

Figure 4.8. Flood frequency distribution curve for Configuration 1 (see Table 3.5 for configuration definition).

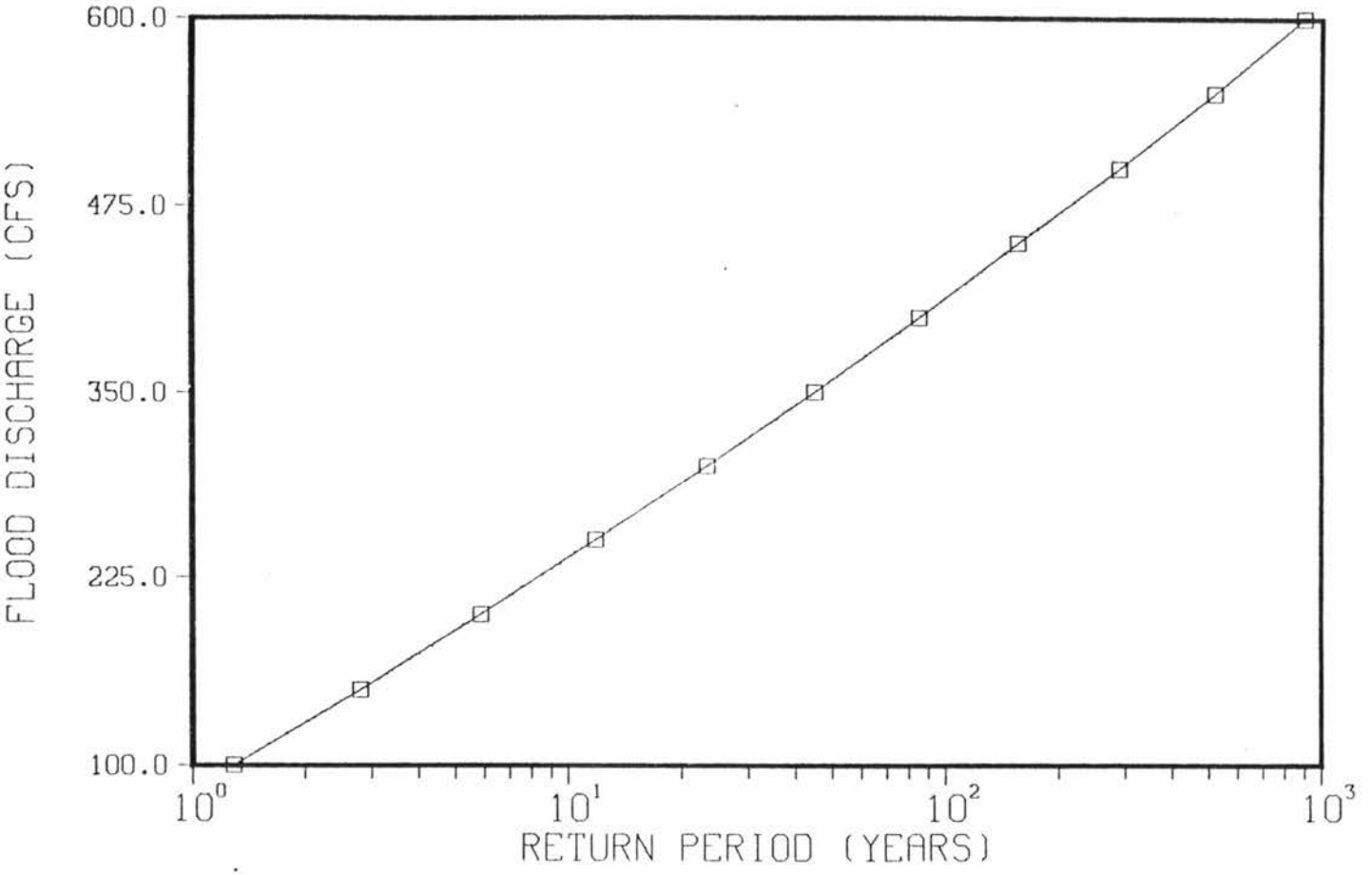

Figure 4.9. Flood frequency distribution curve for Configuration 2 (see Table 3.5 for configuration definition).

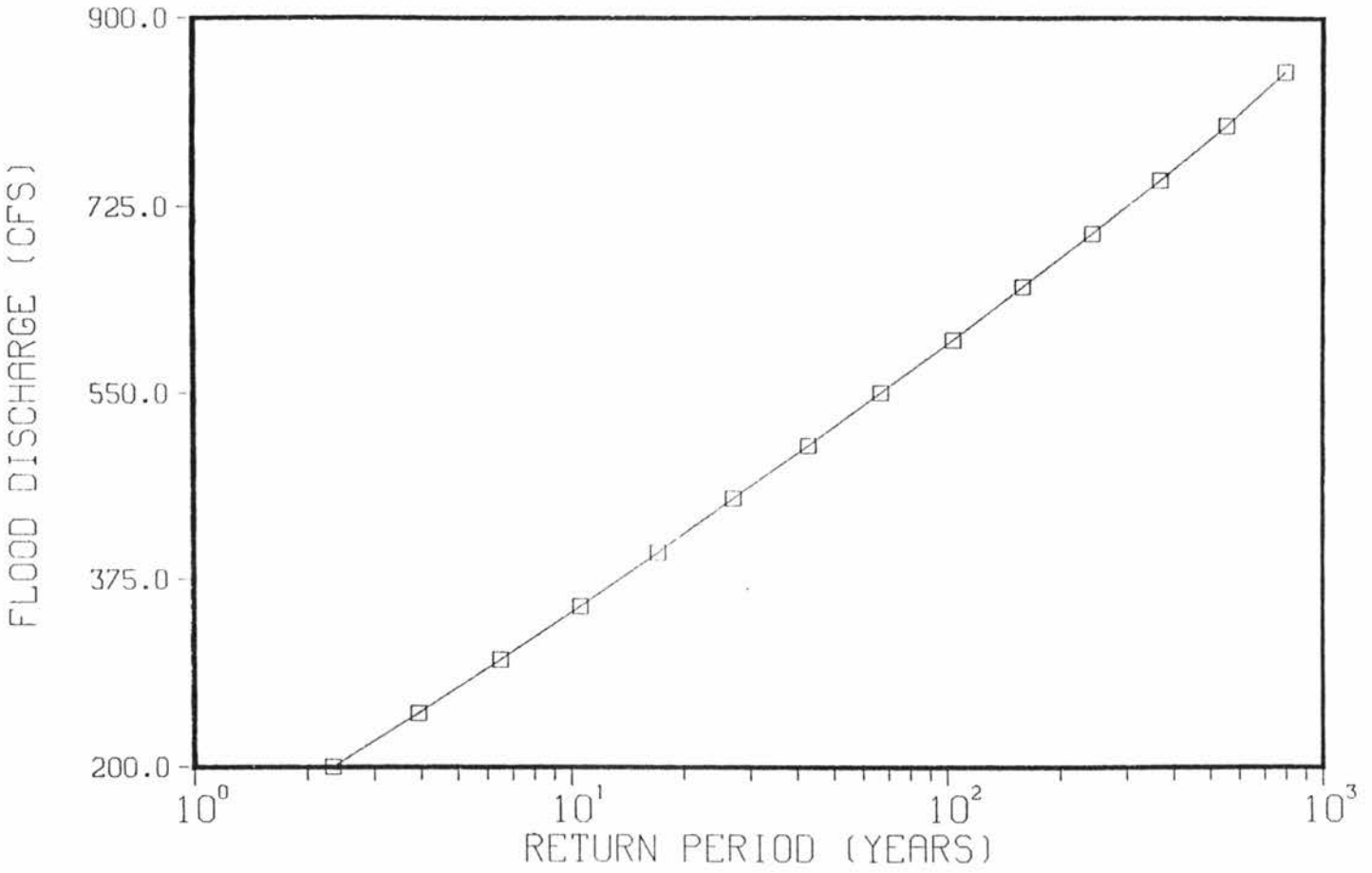

Figure 4.10. Flood frequency distribution curve for Configuration 3 (see Table 3.5 for configuration definition).

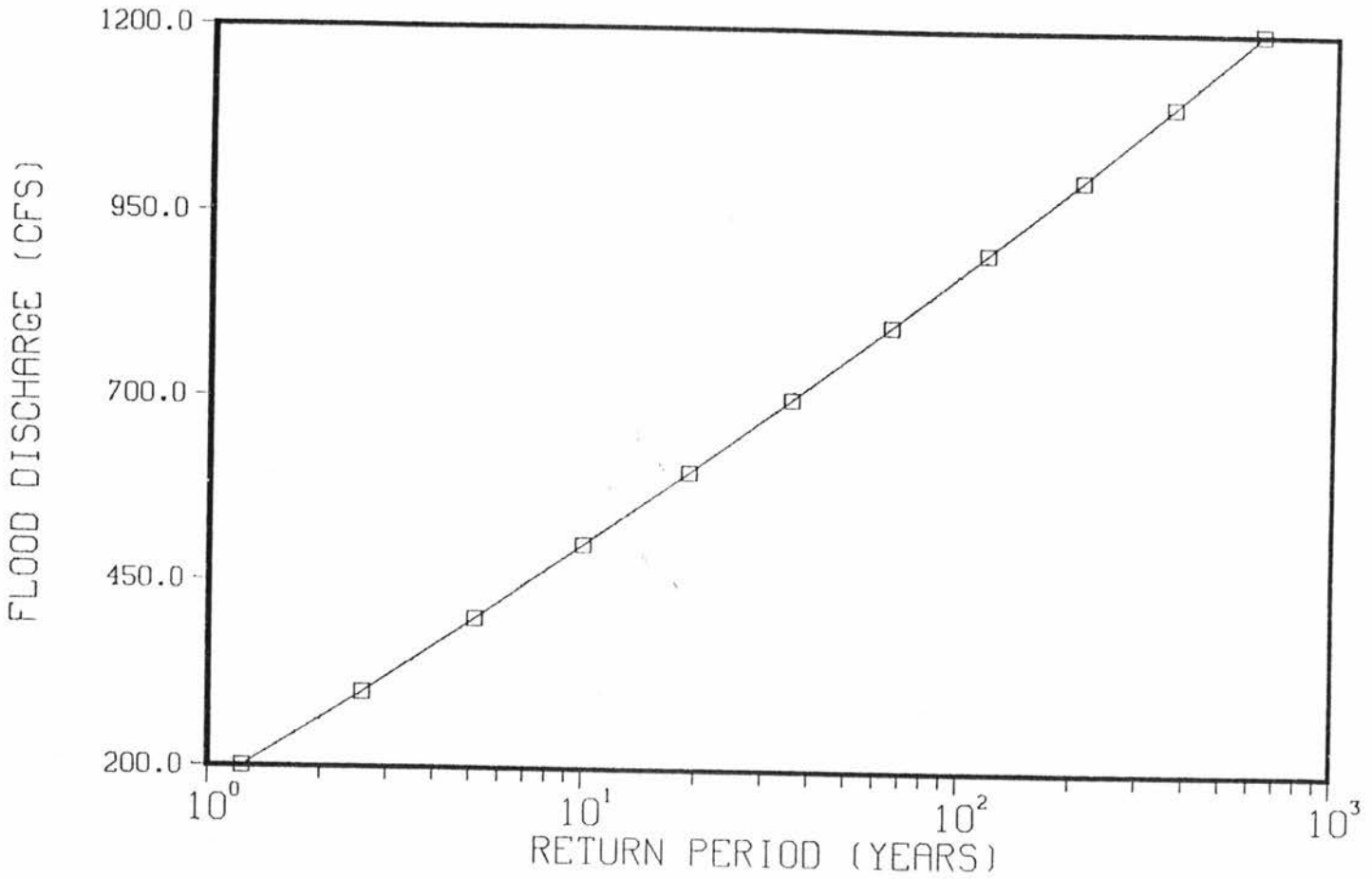

Figure 4.11. Flood frequency distribution curve for Configuration 4 (see Table 3.5 for configuration definition).

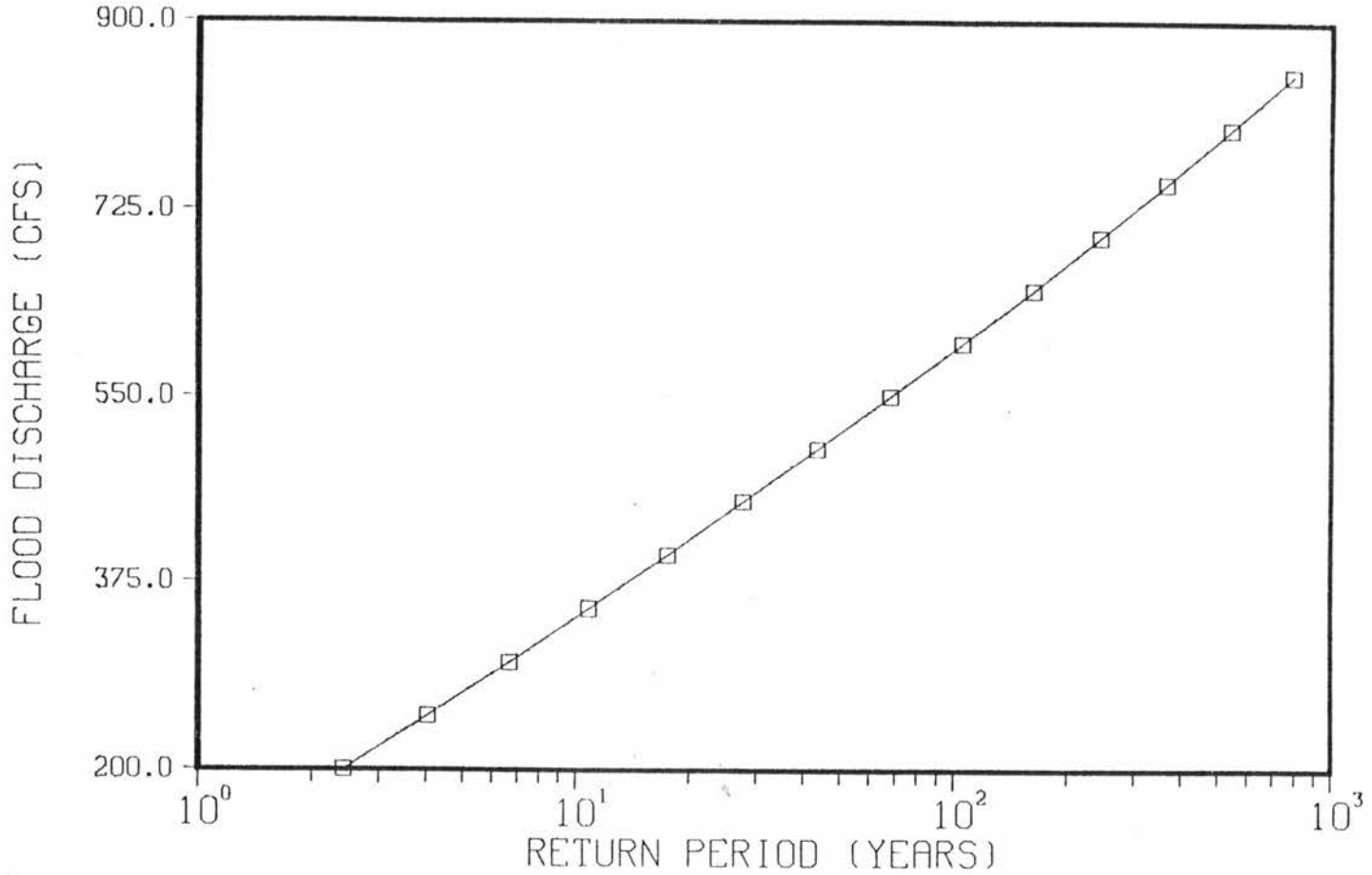

Figure 4.12. Flood frequency distribution curve for Configuration 5 (see Table 3.5 for configuration definition).

analysis was performed. The configuration for these case was chosen more realistic, corresponding to a catchment area of 4.0 square miles. The parameters describing catchment geometry and dynamics are:

Plane width: $W = 3520$ ft

Plane roughness: $n_p = 0.25$

Plane slope: $S_p = 0.268$

Channel length: $L_c = 15840$ ft

Channel roughness: $n_c = 0.03$

Channel slope: $S_c = 0.026$

The values selected, describing the rainfall infiltration model are listed below:

Mean areal rainfall intensity: $1/\beta = 1.0$ in/hr

Mean rainfall duration: $1/\delta = 4.0$ hr

Hydraulic conductivity: $K_s = 0.4$ in/hr

Sorptivity: $S = 0.5$ in/hr$^{1/2}$

Number of independent events: $m_\nu = 20$

The parameters selected to perform the sensitivity analysis were: W, S_p, L_c, S_c, $1/\beta$, $1/\delta$, K_s , and S. Each parameter was changed once, as described in the following:

$W = 1760$ ft, half the initial value

$S_p = 0.134$, half the initial value

$L_c = 7920$ ft, half the initial value

$S_c = 0.052$, two times the initial value

$1/\beta = 2.0$ in/hr, two times the initial value

$1/\delta = 8.0$ hr, two times the initial value

$K_s = 0.2$ in/hr, half times the initial value

$S = 1.0$ in/hr$^{1/2}$, two times the initial value.

Figure 4.13 to 4.20 present the graphical results, obtained when each one of the aforementioned parameters are changed.

The first result to be pointed out, already outlined in the previous section, is the low sensitivity of the flood frequency derivation technique to slope variations, as shown in Figures 4.14 and 4.16. However, the effective rainfall-runoff model is the component responsible for this behavior, since slopes are included as part of the discharge coefficients.

Between the analyzed parameters, there are two which quantify the ability of the soil to incorporate water. These are the hydraulic conductivity K_s and the sorptivity S. As shown in Figures 4.19 and 4.20, an increase in the value of these parameters yields an increase in the return period, when the discharge is held constant. This behavior sounds reasonable, since an increase in K_s or S means that more extraordinary rainfall events are required to produce the same discharge and, therefore, an increase in the return period is obtained.

The remaining parameters, W, L_c, $1/\beta$ and $1/\delta$, are classified as a measure of the watershed and climate ability to produce runoff. The greater those parameters, the more frequent high flood discharges and consequently the lesser the return period for the same discharge value. This is exactly the behavior shown by Figures 4.13, 4.15, 4.17 and 4.18.

Although, the observed behavior depends on the values assigned to the aforementioned parameters, there are some that tend to change the value of the null runoff probability, while the others change the relative position of the maximum for the joint pdf for i_e and t_e. In the first category $1/\delta$ and K_s can be included, since they induce a

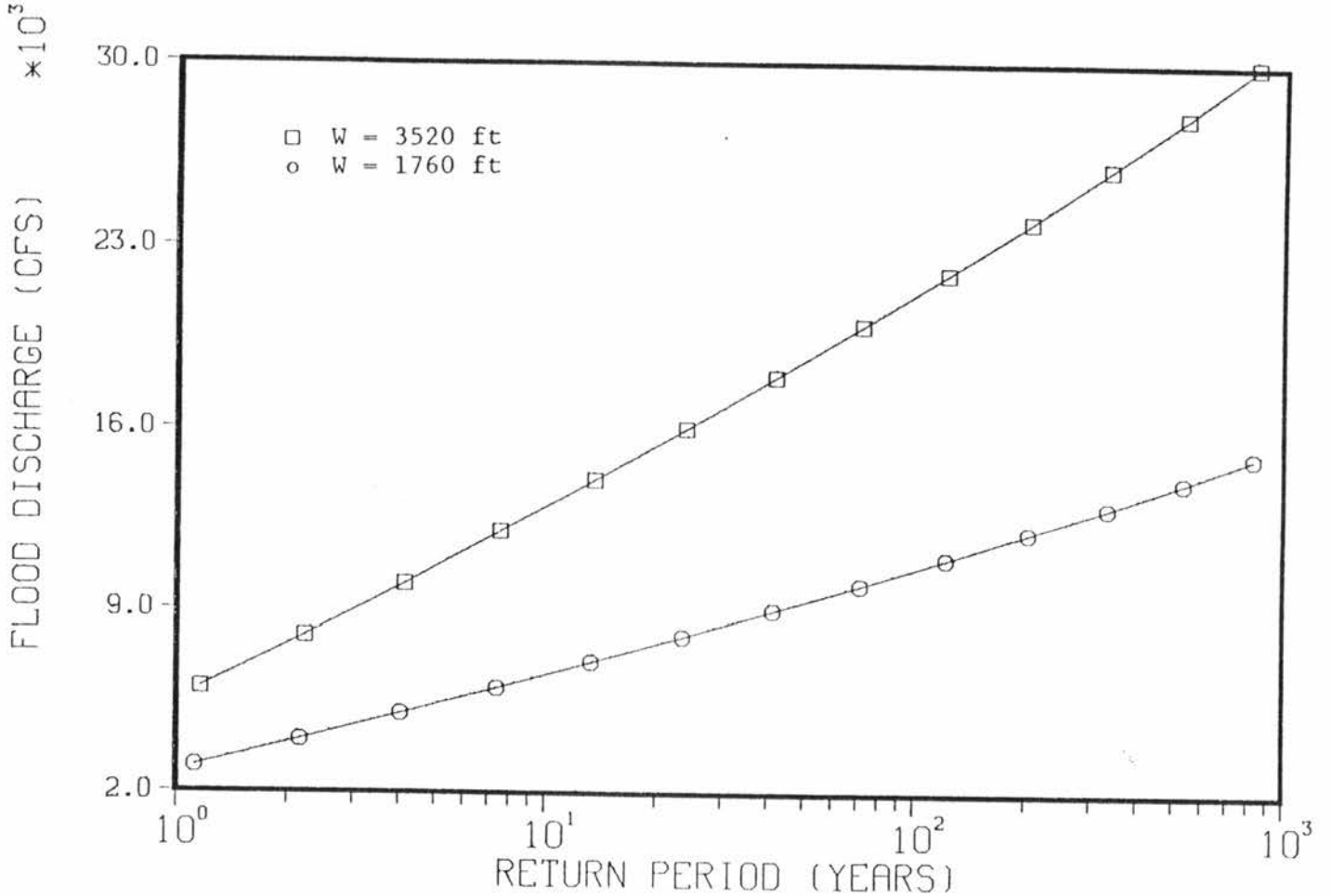

Figure 4.13. Sensitivity of the flood frequency distribution curve to changes in the plane width.

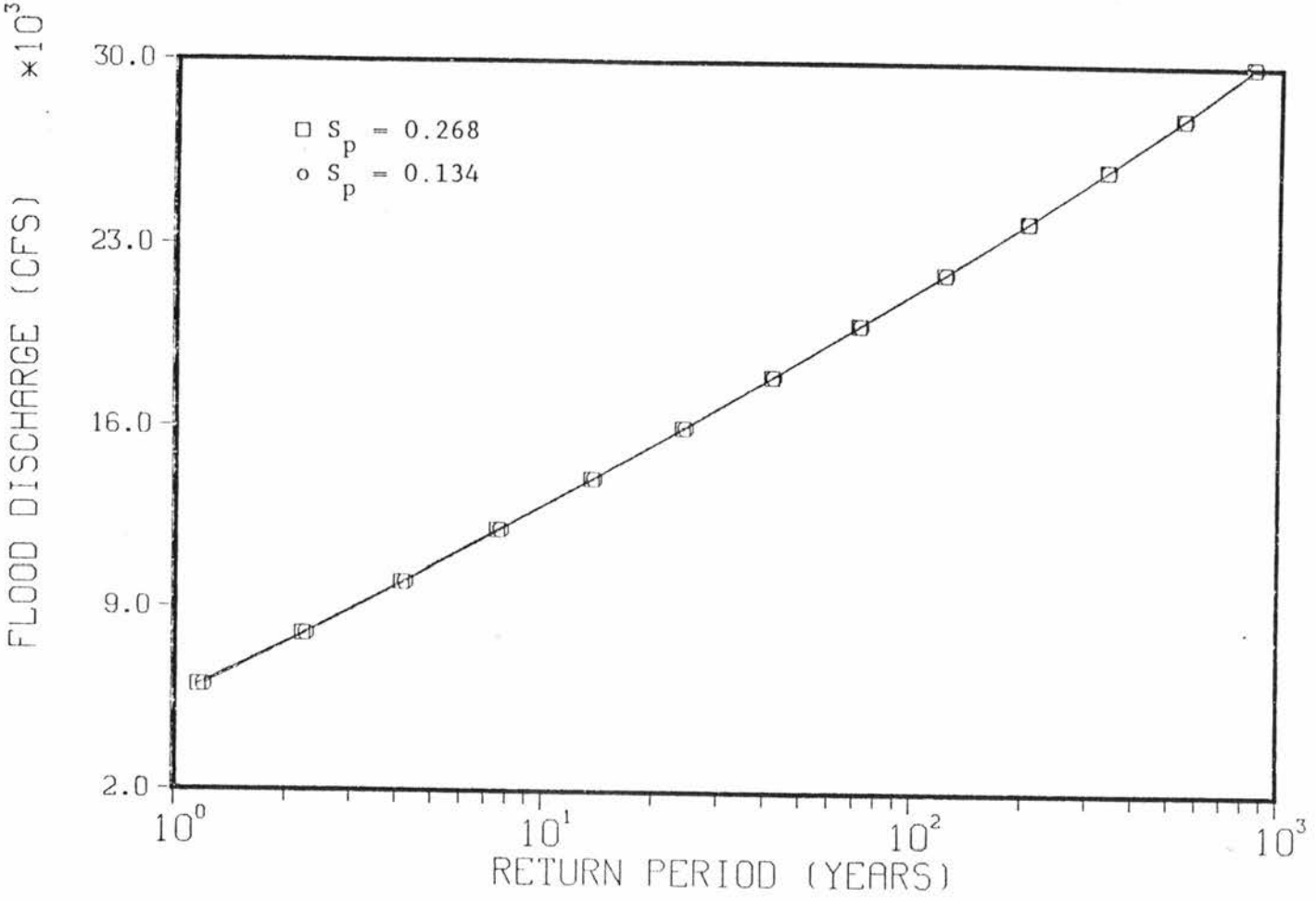

Figure 4.14. Sensitivity of the flood frequency distribution curve to changes in the plane slope.

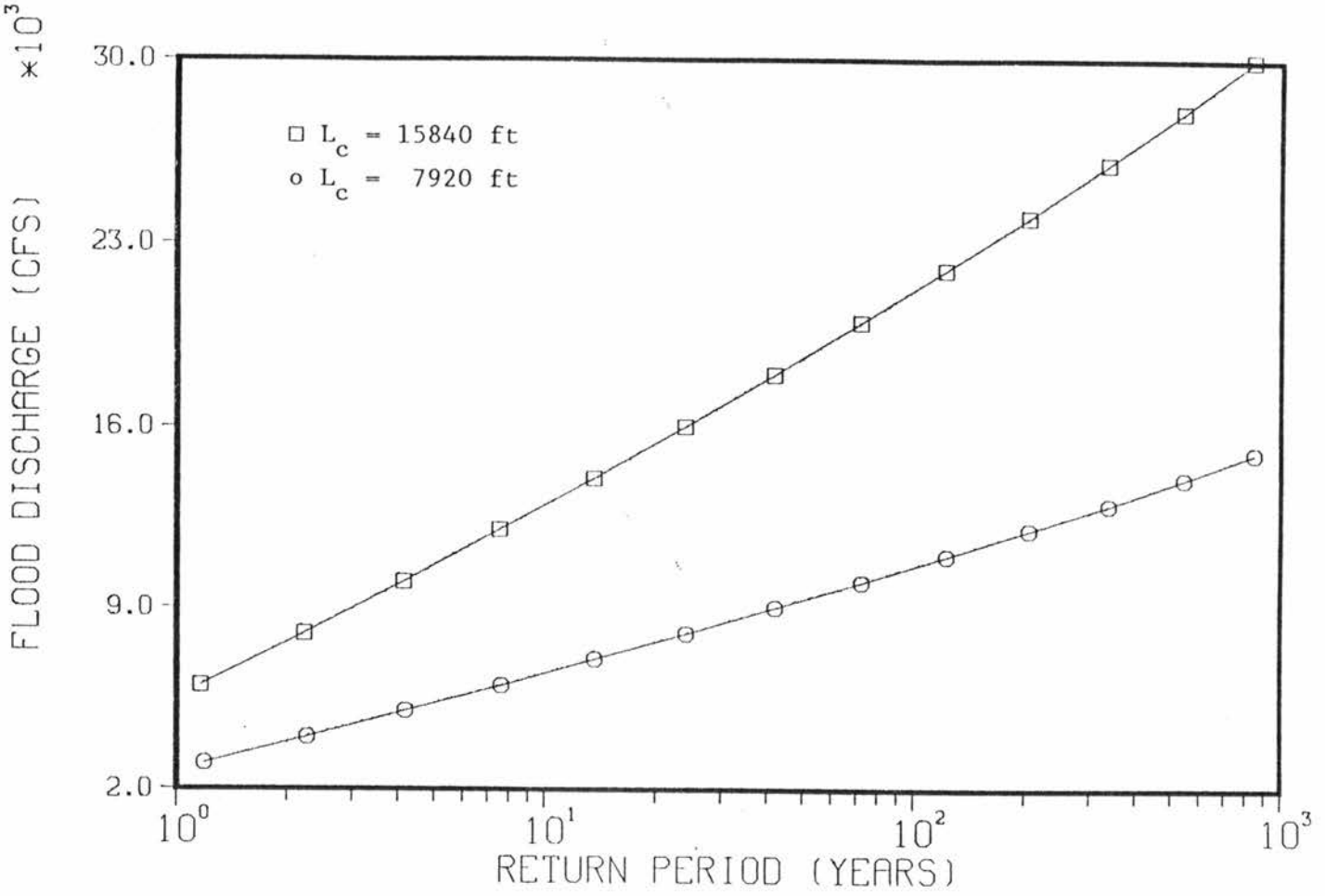

Figure 4.15. Sensitivity of the flood frequency distribution curve to changes in the channel length.

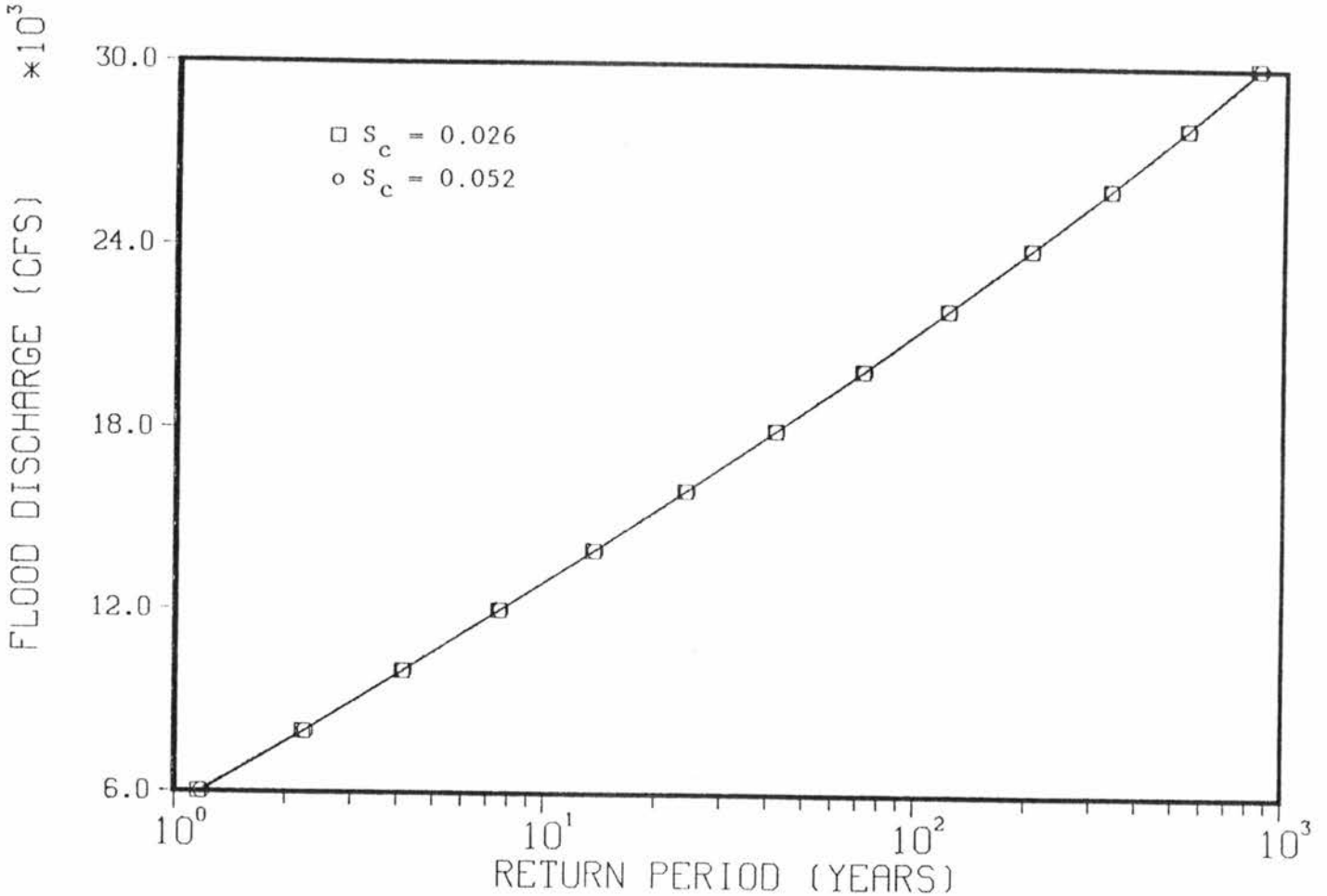

Figure 4.16. Sensitivity of the flood frequency distribution curve to changes in the channel slope.

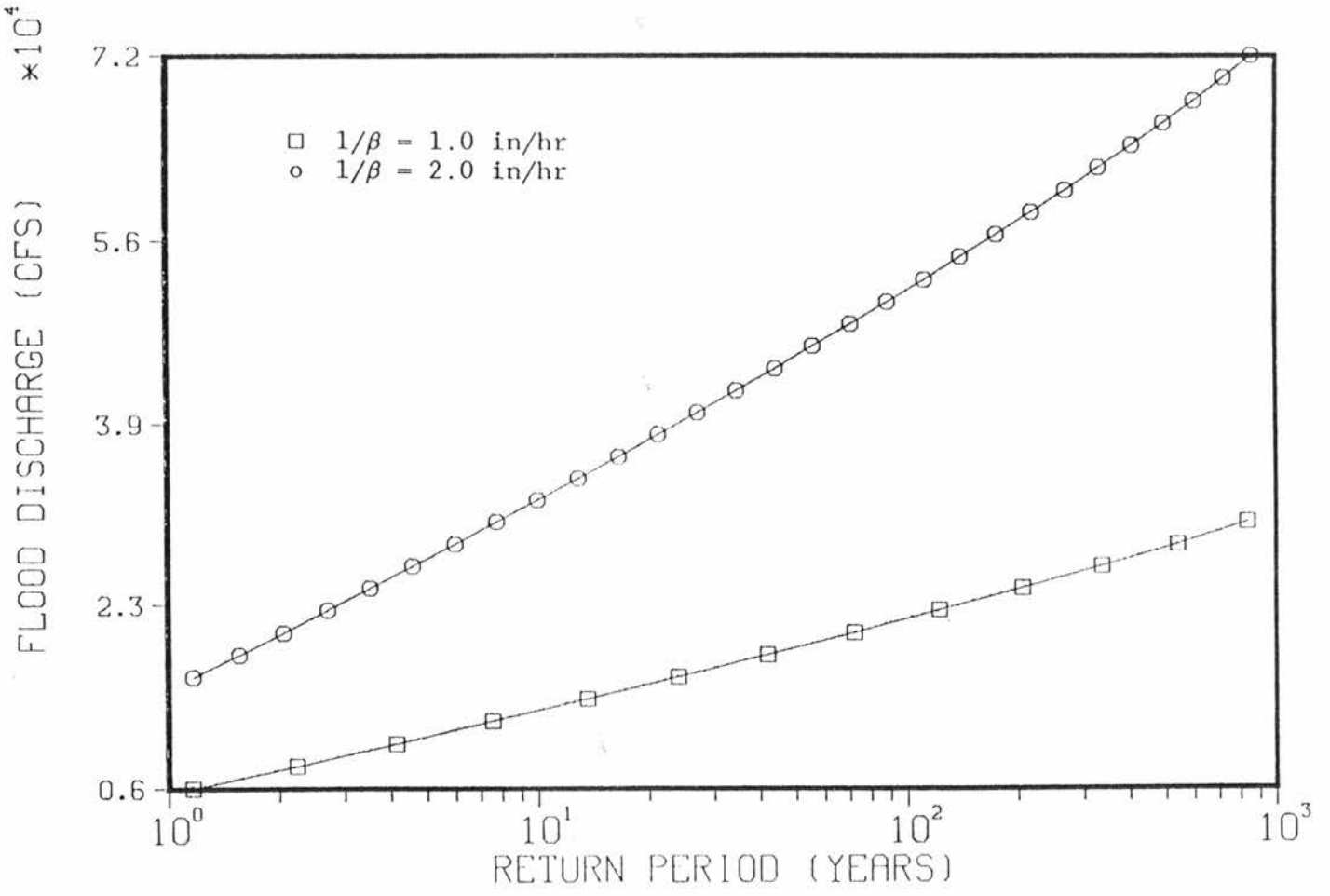

Figure 4.17. Sensitivity of the flood frequency distribution curve to changes in the mean rainfall intensity.

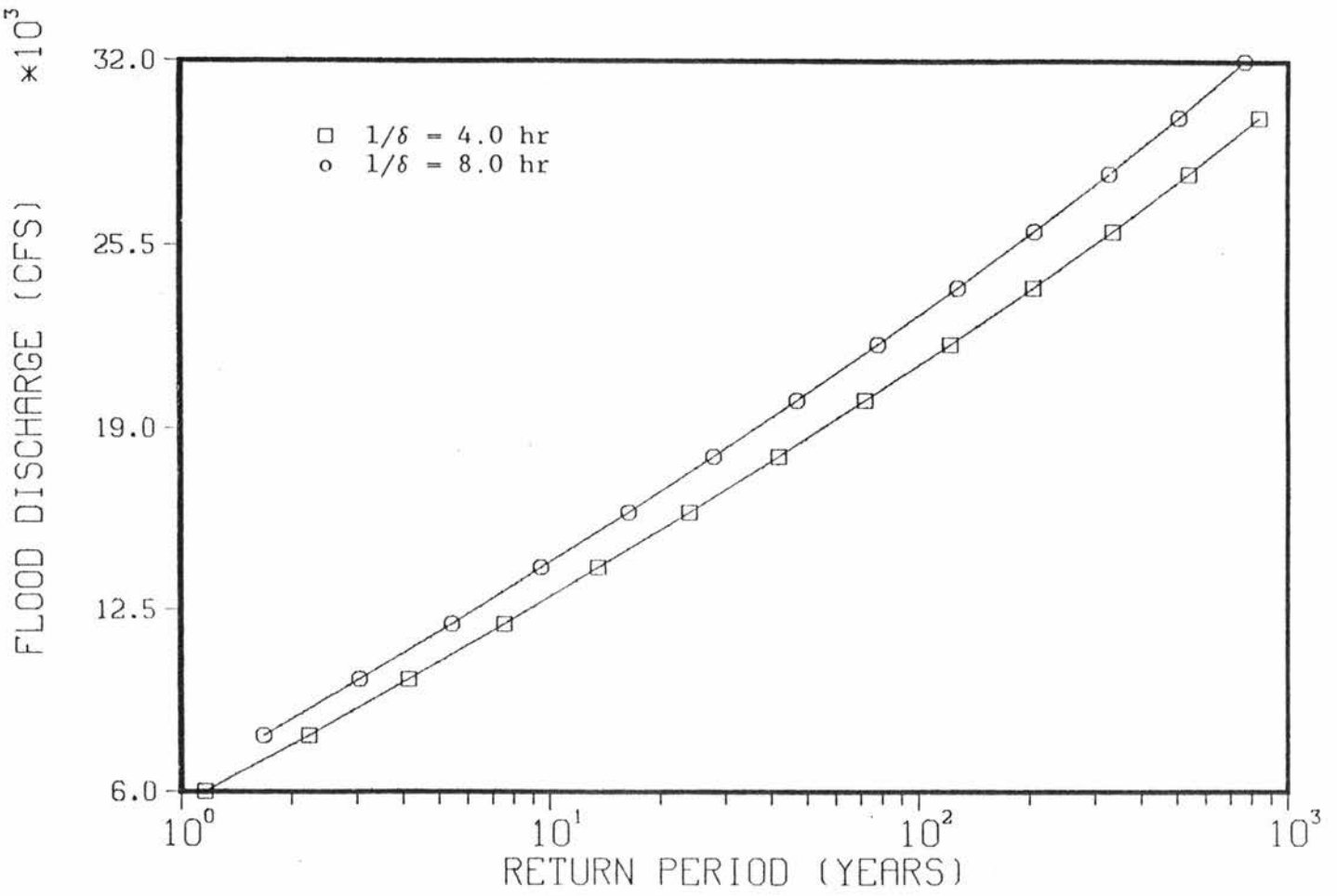

Figure 4.18. Sensitivity of the flood frequency distribution curve to changes in the mean rainfall duration.

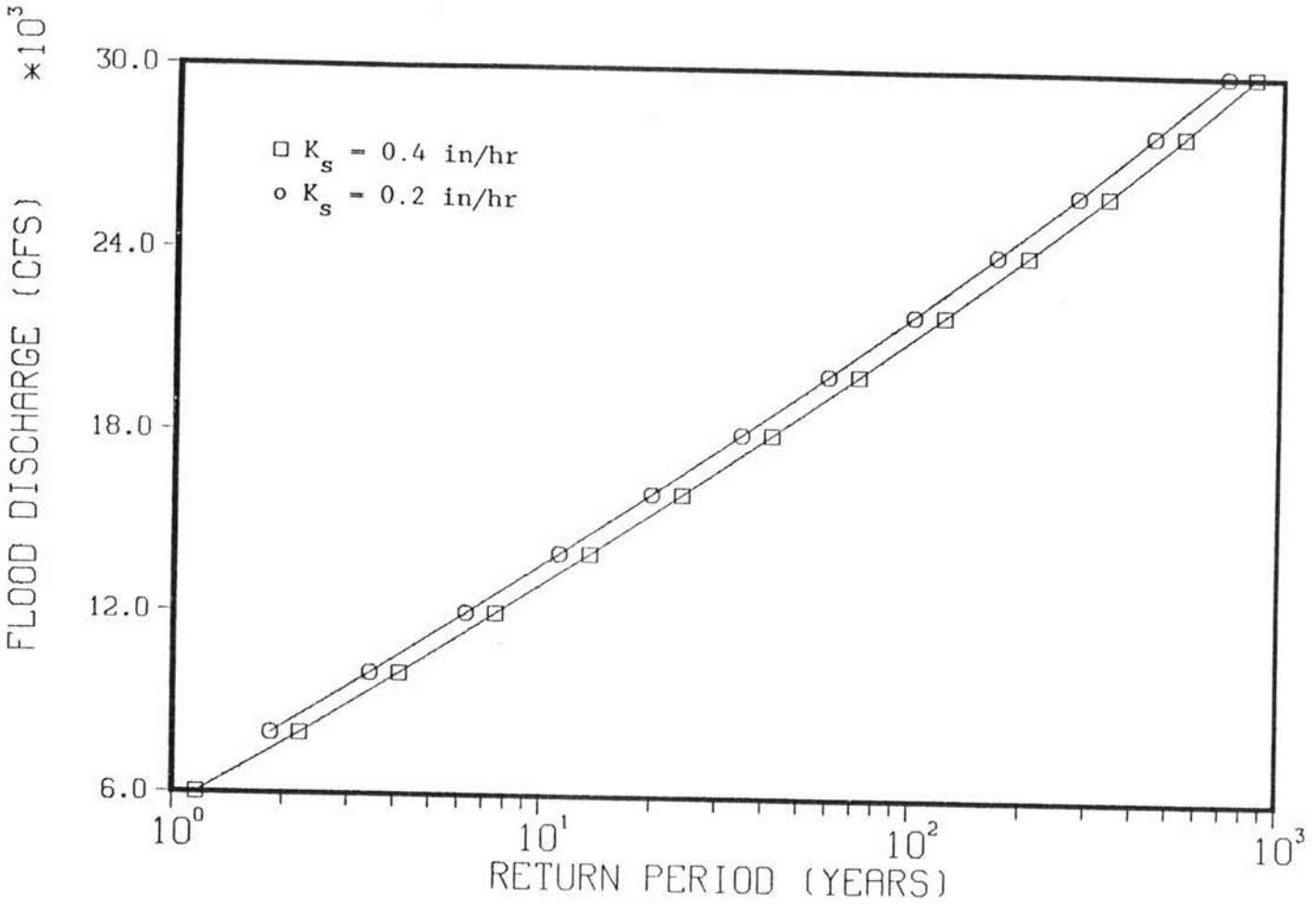

Figure 4.19. Sensitivity of the flood frequency distribution curve to changes in the hydraulic conductivity.

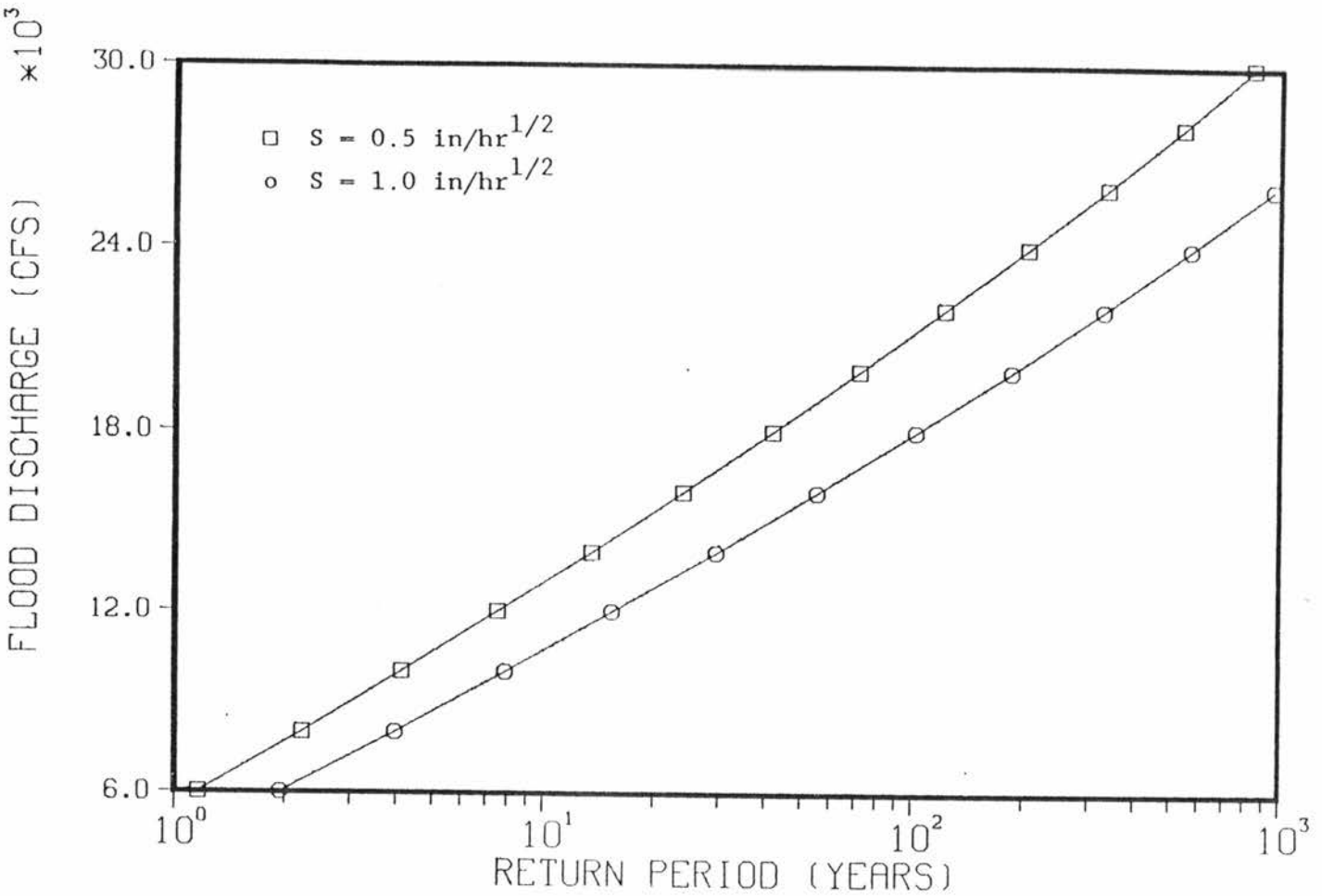

Figure 4.20. Sensitivity of the flood frequency distribution curve to changes in the sorptivity.

parallel displacement of the flood frequency curve. By the other hand, in the second type, W, L_c, $1/\beta$ and S are listed. Besides of producing a change in the initial probability, they generate a relative change in the position of the maximum for the original pdf, translated into a rotation of the flood frequency curve.

4.7 Application of the Flood Frequency Derivation Technique to Actual Watersheds

The application of the flood frequency derivation technique to two real world small watersheds intends the establishment of final judgments about the usefulness of the method for ungaged watersheds. In other words, this section deals with the ability of the flood frequency derivation technique to approach the historical annual flood series, using reasonable values for the parameters included in the model.

Before any application is intended, some considerations are presented regarding the parameters included in the methodology. First, the mean rainfall intensity $1/\beta$ and the mean rainfall duration $1/\delta$ have to be estimated from historical rainfall records. Such estimation procedure is usually time consuming since most of the data is comprised by a collection of cumulative rainfall depth versus time. When time is considered to be an important constraint, educated guesses can be obtained. For the present study, the first approximation for the parameters describing rainfall distributions were taken from Chow (1964), who presents maps for the continental United States giving total rainfall depth, associated to given durations and return periods. For the present application, rainfall depth values with a return period of two (2) years and two different

durations were selected, for each watershed. The value of two (2) years in the return period was considered the most adequate due to its direct relationship to mean values. Once the total depth and total duration are chosen, the intensity is computed as the quotient between the former and the latter. It is important to emphasize that this procedure does not yield the sample mean values for the parameters describing rainfall distribution, but given the lack of data and the constraints in its compilation, the method can provide a normal educated guess.

In regard to the parameters describing the infiltration process, they are not usually measured for actual watersheds, although some values for experimental watersheds or obtained under laboratory conditions may be found in the current literature. For example, Billica and Morel-Seytoux (1984) gives typical values for the hydraulic conductivity K_s and for the water content $\theta_s - \theta_i$, according to the type of soil. If a value of the suction head H_c is also obtained (Morel-Seytoux, (1981)), application of Equation (4.12) completes the guessing process for K_s and S. For practical applications, the predominant type of soil within the watershed shall be taken into account.

The first watershed to be analyzed is located in Iowa. In fact, the gaging station is situated within Iowa City urban perimeter, although the watershed has not been modified appreciably and there is no upstream regulation. The gaging station, classified according to the U.S.G.S as 5-4550, measures the discharge in Ralston Creek.

A sketch for Ralston Creek Watershed is shown in Figure 4.21. The values defining Ralston Creek configuration, conceived as a first order stream with two symmetrical overland flow planes, were measured

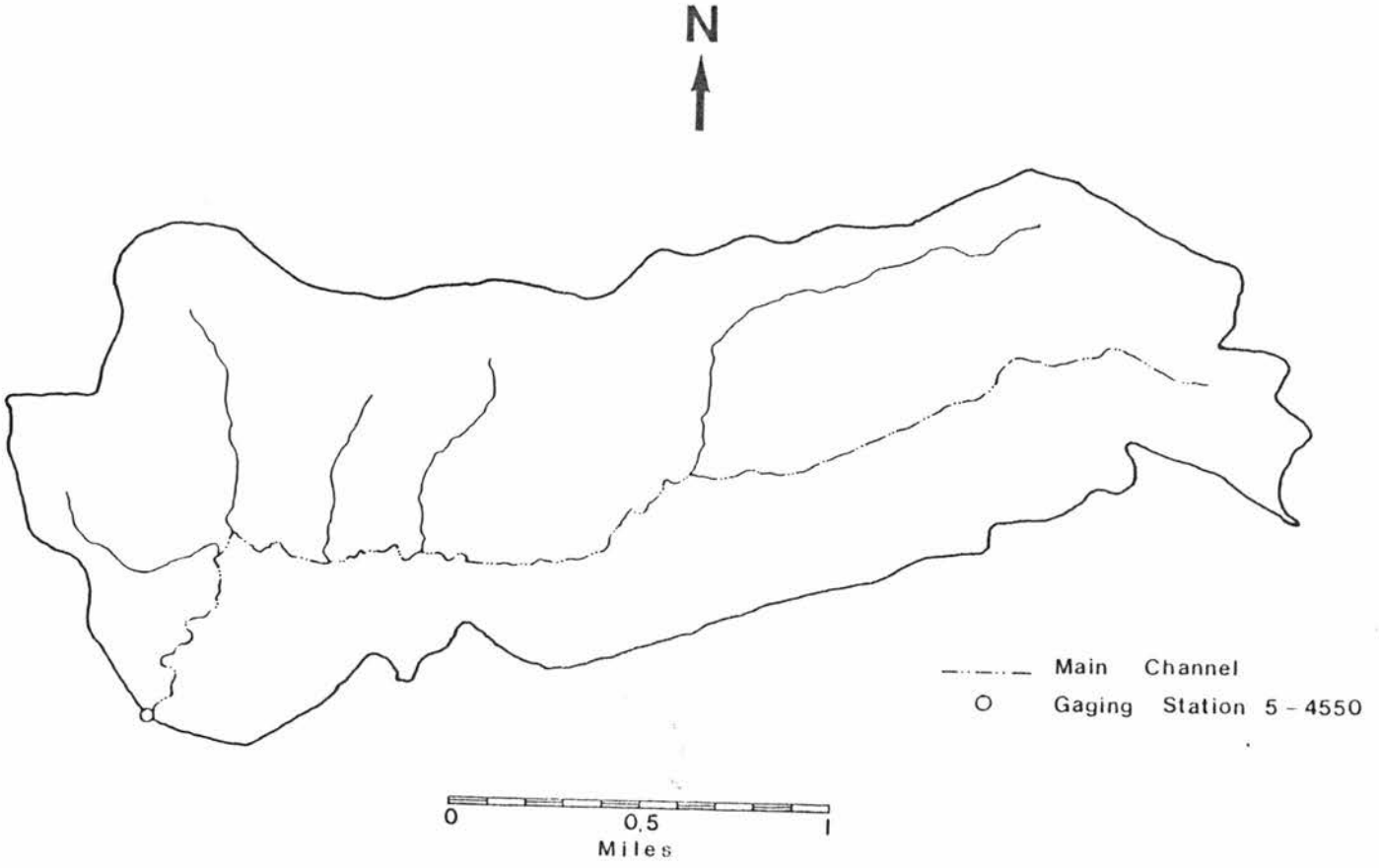

Figure 4.21. Ralston Creek Watershed near Iowa City, Iowa.

on topographical maps to 1:24000 scale, provided by the U.S.G.S.. These values, along with assumed roughness values are listed bellow:

Average plane width:	$W = 2579$ ft
Plane roughness:	$n_p = 0.30$
Average plane slope:	$S_p = 0.106$
Main channel length:	$L_c = 16266$ ft
Channel roughness:	$n_c = 0.04$
Average main channel slope:	$S_c = 0.005$

Average plane width and main channel length values presented correspond to an area of 3.01 square miles, as detailed by the U.S.G.S.. The main channel, for this case, was chosen as the longest identified on planes, but it also corresponds to the main flow collector.

In order to obtain a point of comparison, the historical annual flood series was obtained from data published by the U.S.G.S. (1965, 1971), conformed by 28 values, from 1938 to 1965. The return period was computed for each value using the Weibull plotting position formula (U.S. Water Resources Council, 1976). After discharge values are ranked in decreasing order, the return period for the nth value is given by:

$$T_r(n) = \frac{N + 1}{n} \qquad (4.67)$$

As an additional comparison point, a Log-Pearson III distribution was fitted to the historical records. For this purpose, the discharge associated to a return period T_r is computed via (U.S. Water Resources Council, 1976)

$$\text{Log } Q_r = (\text{Log } Q)_m + K(T_r , G) \times S_{Log} \qquad (4.68)$$

where Log Q_r is the logarithm (base 10) of the flood discharge, and $(\text{Log } Q)_m$, S_{Log} and G are the mean, standard deviation and the skewness coefficient, respectively, for the series obtained after logarithmic transformation on the original historical data. Besides, $K(T_r , G)$ stands for a coefficient, function of T_r and G, values for which are given in tabular form by the U.S. Water Resources Council (1976).

The aforementioned statistics for the historical sample, using moments estimators, are given as

$$(\text{Log } Q)_m = \left\{ \sum_{i=1}^{N} (\text{Log } Q_i) \right\} / N \qquad (4.69)$$

$$S_{Log} = \left\{ \sum_{i=1}^{N} \left[(\text{Log } Q_i) - (\text{Log } Q)_m \right]^2 / (N - 1) \right\}^{1/2} \qquad (4.70)$$

$$G = N \left\{ \sum_{i=1}^{N} \left[(\text{Log } Q_i) - (\text{Log } Q)_m \right]^3 / (N - 1) \right.$$

$$\left. / (N - 2) / (S_{Log})^3 \right] \qquad (4.71)$$

Applying Equations (4.69) through (4.71) the following values are obtained for the sample statistics at Ralston Creek:

$$(\text{Log } Q)_m = 2.5796$$

$$S_{Log} = 0.4292$$

$G = -0.4643$

The calibration of the derived flood frequency distribution curve for Ralston Creek is based on a trial and error process. The values describing the catchment area configuration, as listed above, were not changed during this calibration. The variation was given to the mean areal rainfall intensity $1/\beta$ and to the mean rainfall duration $1/\delta$ mainly, and secondly to the hydraulic conductivity K_s and sorptivity S. The initial values for $1/\beta$ and $1/\delta$ were obtained from Chow (1964), as described previously. The value for $1/\beta$ varies from 2.56 in/hr for $1/\delta = 0.5$ hr to 1.56 in/hr for $1/\delta = 1.0$ hr. The best calibration for Ralston Creek yielded the following values for the parameters describing rainfall and infiltration:

Aereal mean rainfall intensity:	$1/\beta = 0.60$ in/hr
Mean rainfall duration:	$1/\delta = 0.90$ hr
Hydraulic conductivity:	$K_s = 0.25$ in/hr
Sorptivity:	$S = 1.10$ in/hr$^{1/2}$
Number of independent events:	$m_\nu = 20$

Figure 4.22 depicts the flood frequency distributions obtained for Ralston Creek: these are historical, Log-Pearson III and derived distribution. Although, the Log-Pearson III distribution fits the historical distribution quite well, the derived distribution shows its ability to reproduce, at least in part, the historical sequence of events.

Some tentative explanations, for the difference between the historical values and the derived curve, for high and low values of the flood discharge, will be addressed later.

The second application watershed is depicted in Figure 4.23. The stream is located in California, near Sierra Madre. The watershed has

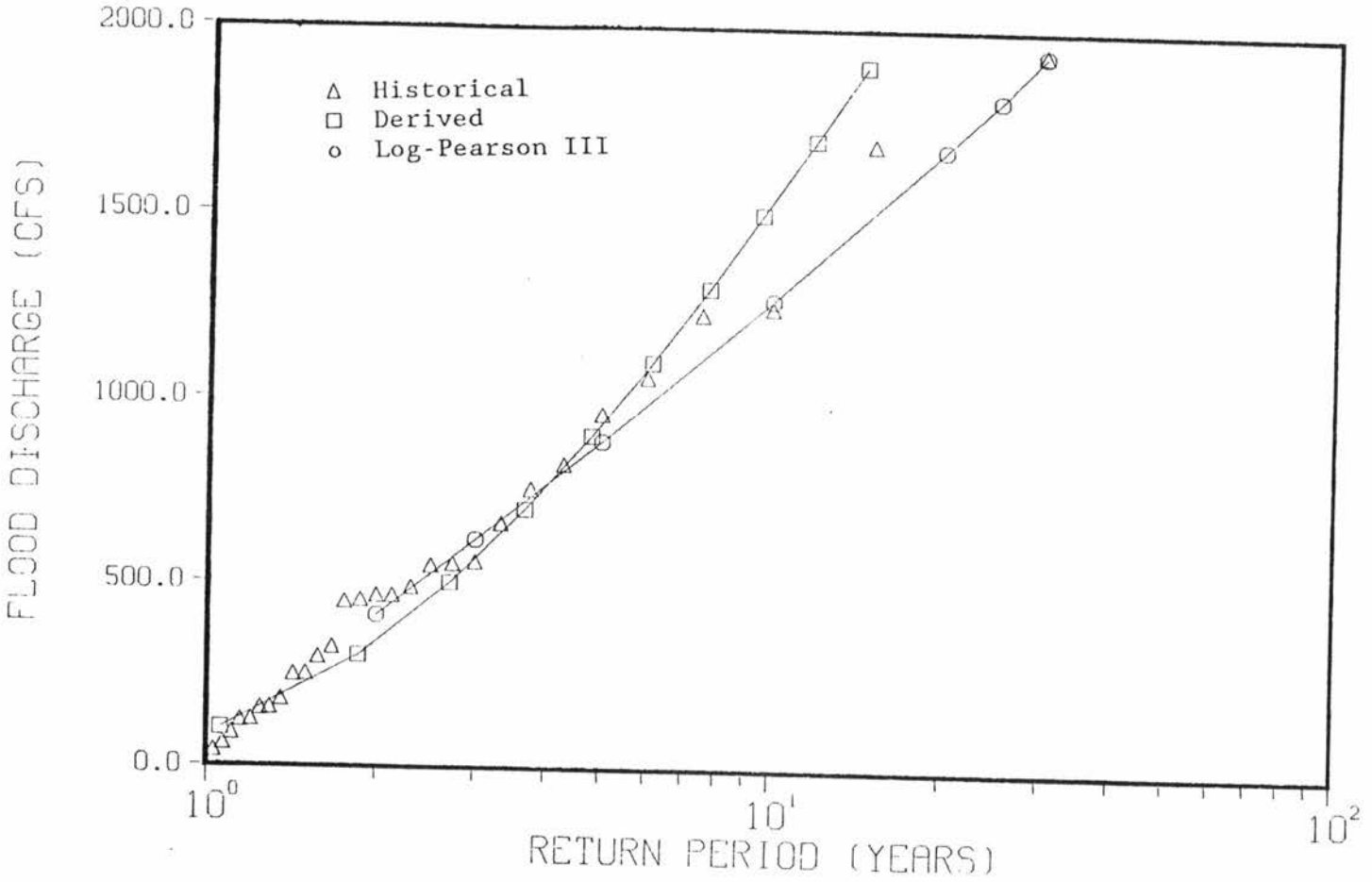

Figure 4.22. Flood frequency curves for Ralston Creek.

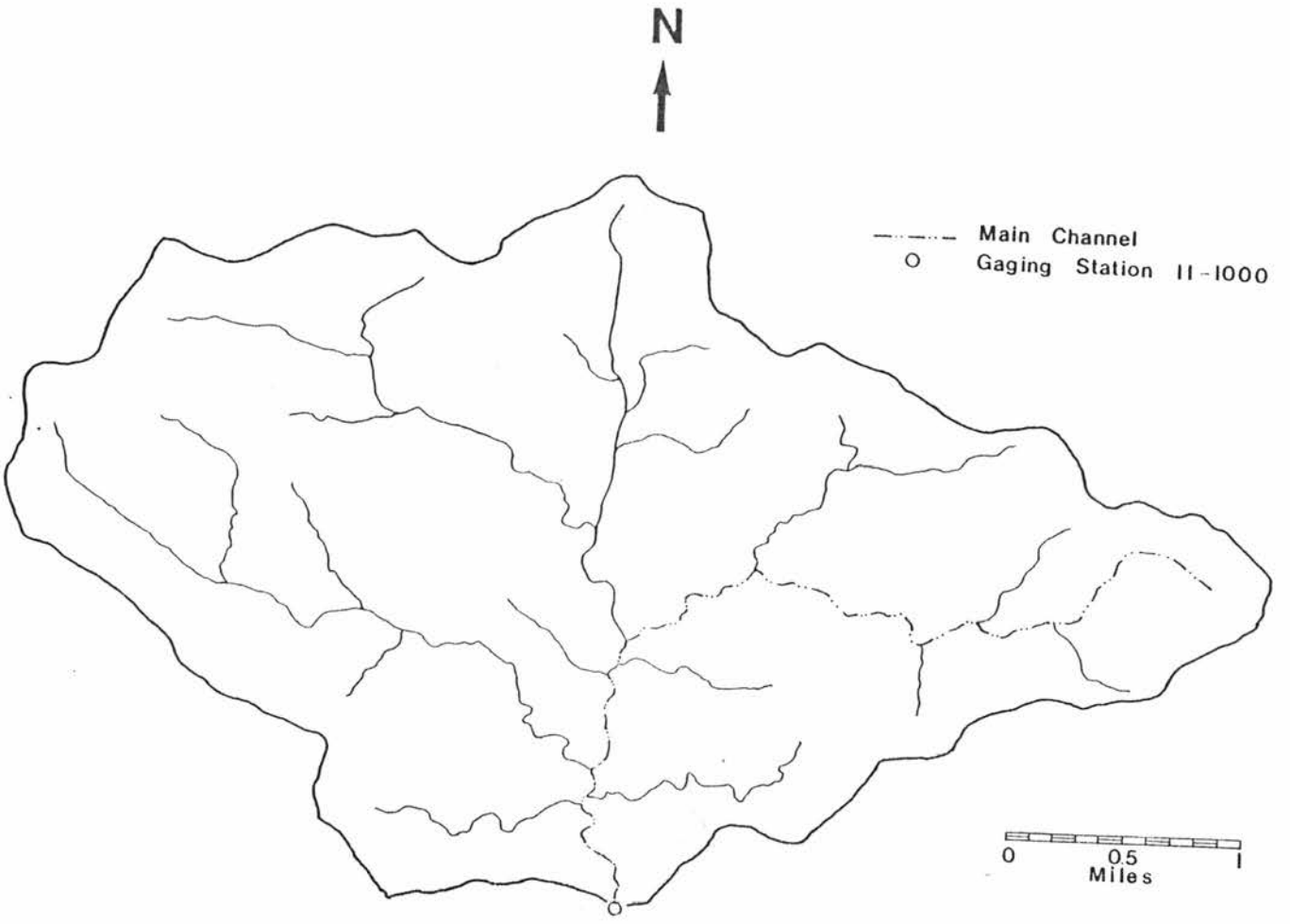

Figure 4.23. Santa Anita Creek Watershed near Sierra Madre, California.

not been modified appreciably and there is no upstream regulation. The gaging station, classified according to the U.S.G.S as 11-1000, measures the discharge in Santa Anita Creek.

As in the first watershed, the values defining Santa Anita Creek configuration, assuming a first order symmetrical Wooding geometry, were measured on topographical maps to 1:24000 scale, provided by the U.S.G.S.. These values, along with assumed roughness values are listed bellow:

Average plane width:	$W = 5688$ ft
Plane roughness:	$n_p = 0.30$
Average plane slope:	$S_p = 0.582$
Main channel length:	$L_c = 23795$ ft
Channel roughness:	$n_c = 0.04$
Average main channel slope:	$S_c = 0.172$

The watershed area, as given by the U.S.G.S, is 9.71 square miles. The main channel was selected as the longest identified on planes.

The historical annual flood series for Santa Anita Creek was obtained from data published by the U.S.G.S. (1965, 1970, 1976), conformed by 51 values, from 1917 to 1970 (three missing values). The recorded flood frequency distribution was computed by applying Equation (4.67).

Again, as a second point of comparison, the Log-Pearson III distribution was fitted to the historical values. The sample moments, computed using Equations (4.69) through (4.71) were:

$$(\text{Log } Q)_m = 2.4482$$

$$S_{Log} = 0.5910$$

$G = 0.0632$

Following the same procedure as for Ralston Creek the flood frequency curve was calibrated for Santa Anita Creek. The initial value for $1/\beta$, obtained from Chow (1964), ranges from 1.2 in/hr for $1/\delta = 0.5$ hr to 0.8 in/hr for $1/\delta = 1.0$ hr. After calibration was performed, the values obtained for the parameters were:

Aereal mean rainfall intensity:	$1/\beta = 0.94$ in/hr
Mean rainfall duration:	$1/\delta = 0.30$ hr
Hydraulic conductivity:	$K_s = 0.80$ in/hr
Sorptivity:	$S = 1.12$ in/hr$^{1/2}$
Number of independent events:	$m_\nu = 20$

Figure 4.24 presents the flood frequency curves for Santa Anita Creek, obtained by three methods outlined above. Similar comments as those presented for Ralston Creek are valid here.

4.8 Discussion Regarding the Flood Frequency Derivation Technique

In this chapter, an algorithm allowing the computation of flood frequency distribution curves for small watersheds has been developed. Besides, such technique has been applied to several hypothetical catchment configurations and to a couple of small watersheds.

Through the sensitivity analysis, the flood frequency derivation technique has proved its ability to account for the influence of parameters describing watershed geometry, watershed dynamics and rainfall-infiltration process, providing explanation on the physical process of flood discharges. Although, such conclusion is not new, it confirms an important feature already outlined in some previous similar works.

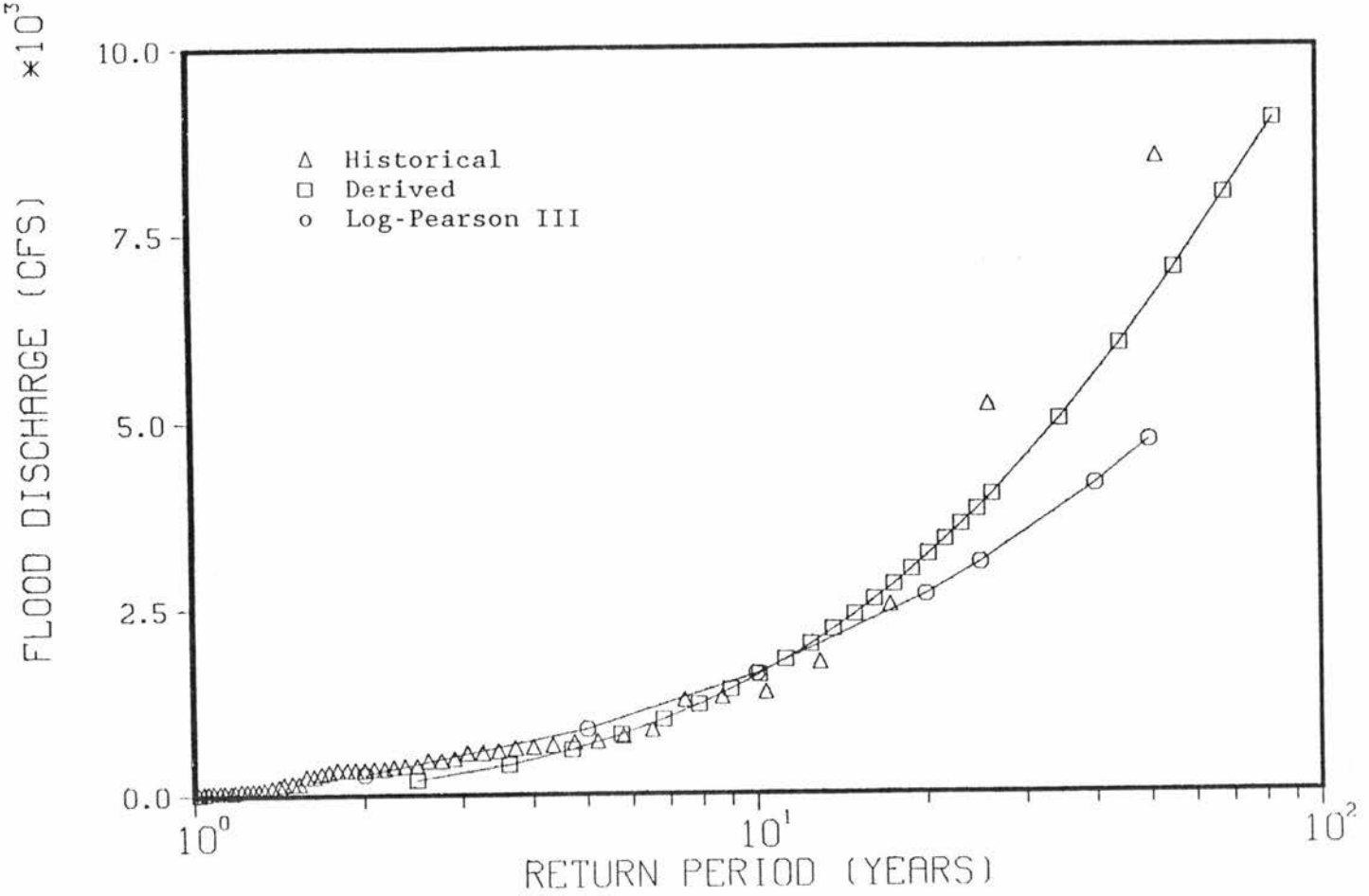

Figure 4.24. Flood frequency curves for Santa Anita Creek.

In Chapter 3, an effective rainfall-runoff model was developed. Despite of the inclusion of the well known Manning equation in the runoff model, no sensitivity was identified for the flood frequency derivation technique on slopes, for plane and channel. As these parameters are incorporated in the effective rainfall-runoff component, and they do not appear at any other point, such component is responsible for the observed behavior.

Besides, the effective rainfall-runoff model was developed with emphasis on its applicability to small watersheds, where overland flow phase is supposed to be an important component. However, once this model is added to the flood frequency derivation technique, nothing inhibits its application to small watersheds with a small contributing rainfall area. Although no statistical distribution was considered for the plane width, such an application can be obtained through a parametric variation in this quantity.

In regard to applicability of the flood frequency derivation technique to some real world watersheds and based on the values obtained during the calibration for the parameter set, it has also proved its ability to resemble, at least in part, the historical distribution.

The values obtained during the calibration for the parameters describing rainfall in both watersheds do not match at all the variation ranges obtained from Chow (1964). The values for Ralston Creek exhibit a good result for the mean rainfall duration $1/\delta$, while for the mean rainfall intensity $1/\beta$ the calibrated value departs considerably. An opposite behavior is observed for Santa Anita Creek, this is, a good agreement for $1/\beta$, but fairly poor for $1/\delta$. However, the values obtained during the calibration can be considered as

normal, in the sense that they are not low neither high, and they resemble values which could be obtained from historical precipitation records.

A possible explanation for the observed behavior can be put in the fact that kinematic wave based rainfall-runoff models tend to overestimate discharge, as pointed out by Eagleson (1972). Hence, the lower value for some of the two parameter can be visualized as a trend to solve the overestimation. Besides, the reader must bear in mind that the initial values obtained from Chow (1964) were taken as educated guesses and therefore they are approximations to historical values.

As stated previously, a detailed look at Figures 4.22 and 4.24, shows that for high flood values or low discharge events, there is an appreciable deviation between the derived and the historical distribution. For the high values, this can be explained, in part, by the uncertainity inherent to the estimation of high return periods from historical records. For low values, as well as for high values, there is an additional uncertainty, given by the possibility that parameter values controlling the dynamics of flood formation are different for low and high return periods.

A second reason for the observed behavior may be stated in the fact that the derived flood frequency distribution technique yields a population result, in the sense that it covers all possible realizations of the process, while the historical result conforms just a sample from the population.

As a last point, additional emphasis is put in the fact that the historical results were yielded along time, with quite different parameters describing rainfall, infiltration and catchment geometry

and dynamics, perhaps reflecting climatic, physiographic or geomorfological changes within the watershed. When the flood frequency derivation technique is used, several average values are included, which no necessary resemble the history of the watershed.

The two real world watersheds herein considered to test the applicability of the flood frequency derivation technique are quite different. Santa Anita Creek is much steeper and larger than Ralston Creek. Due to their location, their climatic behavior should be also different and so should be the runoff process. Despite this appreciable difference, the results yielded for both streams are qualitatively similar, in the sense that the historical record is reproduced more or less within the same accuracy range.

The previous analysis yields the conclusion that the flood frequency derivation technique can be applied to small ungaged watersheds. Care must be exercised in the selection of the parameters. As long as possible, rainfall parameters shall be obtained from records, specially the mean rainfall intensity, one of the most important values conditioning results. Several authors recommend values for the parameters describing the infiltration process, according to the equation here used (Morel-Seytoux, 1981). In any case it is wise to compare the ungaged watershed with other similar, where some records are available.

Chapter 5

SUMMARY, CONCLUSIONS AND RECOMMENDATIONS

5.1 Summary

Since 1972, there has appeared in the hydrological literature a set of works referred to as flood frequency derivation. Three components are common to all these works: a rainfall-infiltration component, an effective rainfall-runoff model and a probabilistic component. Depending on the basis of the effective rainfall-runoff model, the technique can be classified as physical or geomorphological.

The present study considers the derivation of a physically based flood frequency technique, applicable to small ungaged watersheds, where the overland flow phase is an important timing component.

In the last decade, the Geomorphological Instantaneous Unit Hydrograph (GIUH) has been an important tool used in discharge forecasting and flood frequency derivation. Considering the aforementioned scope, a review of the GIUH is performed on its own basis, that is, comparing it with the Instantaneous Unit Hydrograph obtained via detailed kinematic simulation, in order to establish the applicability of the GIUH to small watersheds, where the overland flow phase is an important component.

Due to the fact that the GIUH lacks the required feature, a model, based on kinematic wave assumption, is developed and calibrated. The new effective rainfall-runoff model covers all

possible responses and solves the plane timing problem in a small watershed, conformed by two planes and a first order stream. In order to achieve this goal, an approximate kinematic routing model is used as an intermediate tool.

Based on the developed model and previous results published by other authors, the flood frequency distribution technique is assembled, formulated as a numerical algorithm and translated into a computer program. The technique is tested for several hypothetical catchment configurations. Also, a sensitivity analysis is performed in order to establish the capability of the whole technique to account for parameters variation. As last point, the particular derived methodology is tested with real world small watersheds, these conceived as first order streams with two symmetrical planes.

5.2 Conclusions

The conclusions obtained throughout the present study, following the order in which it was developed, are summarized in the following points:

1. The GIUH is appears to be inadequate to describe watershed response when the overland flow is considered to be an important timing component.

2. Another concern is the ability of the geomorphological ratios to describe the watershed shape and arrangement. In small watersheds, sample variations on those parameters are larger than in medium or large watersheds, and such variations are not included in the GIUH.

3. The effective-rainfall runoff model developed follows closely Eagleson's work (1972) in the determination of characteristic times for the catchment area. However, in Eagleson's work the following features were not included: first, the runoff cases considered depend on his decision tree, which was reduced upon the basis of particular values for rainfall intensity and discharge coefficients, and second, the development does not cover all possible effective-rainfall runoff events.

4. In the study reported herein the shortcomings found in Eagleson's work are solved. The calibration of the model, performed on dimensionless variables, as well as the obtained expressions, account for all variables representing the process under consideration.

5. A shortcoming of the effective rainfall-runoff model results since regression analysis was employed. However, this makes the model more flexible, since the same technique may be applied to other configurations, actual or hypothetical.

6. The use of the model for forecasting peak discharge and time to peak is recommended. Also, the employment of kinematic approximate routing is recommended for small watersheds, where the plane holding time dominates within the watershed, when the hydrograph shape is a important. The above recommendations are based on the agreement found via detailed

kinematic simulation. The physical basis given to the derivation supports this recommendation.

7. The effective rainfall-runoff model was developed with emphasis on its applicability to small watersheds, where overland flow phase is supposed to be an important component. However, nothing inhibits its application to small watersheds with a small contributing rainfall area, since a parametric variation can be given to the catchment width, even when considered jointly with the flood frequency derivation technique, although no statistical distribution was considered for the plane width.

8. Through sensitivity analysis, the general flood frequency derivation technique has proved its ability to account for the influence of parameters describing watershed geometry, watershed dynamics and rainfall-infiltration process, providing explanation on the physical process of flood discharges.

9. In regard to applicability of the flood frequency derivation technique to some particular problems, it encompasses, due to the algorithm design, the inclusion of other joint pdf for the effective rainfall intensity and duration.

10. The following shortcomings are inherent to the proposed methodology: symmetrical planes, first order stream, limitations in the kinematic wave approach, low sensitivity

to slope variations and average parameters describing the infiltration process. The modeler must be aware of these shortcomings for actual applications of the methodology.

11. The application of the flood frequency derivation technique to ungaged watersheds is recommended, followed by a careful analysis of the required and available data (from the same watershed or from others with similar hydrological behavior). As much as possible, a comparison with a catchment area with available records is encouraged.

12. The fitting of the derived distribution to the historical one can be made by considering different values of the parameters according to the discharge stage. This shows that flood events are not governed by the same type of rainfall distribution.

5.3 Recommendations for Future Investigations

Many could be the investigation guidelines arising from this study. Those considered as most important are listed bellow.

1. In regard to the GIUH, the inclusion of an extra state, given by the holding time in the planes as suggested by Gupta et al. (1980), could make this approach applicable to overland flow component.

2. Further analytical investigation is necessary in regard to the watershed dynamics as well as in understanding the physics of the process.

3. A wider calibration of effective rainfall-runoff model could open the possibility of a better fitting of the derived distribution to historical data.

4. Consideration, within the framework of the flood frequency derivation technique, of more realistic rainfall distributions and other ponding time infiltration models.

5. Analysis of flood frequency curves coming from different or similar populations, with different parameters.

BIBLIOGRAPHY

Billica, J. A. and H. J. Morel-Seytoux, "User's Manual for SOILWAT," Colorado State University, Engineering Report CER83-84HJM- JAB36, 1984.

Burden, R. L. and J. D. Faires, "Numerical Analysis," Third Edition, PWS Publishers, 1985.

Chow, V. T., "Handbook of Applied Hydrology," Mc-Graw Hill, 1964.

Diaz-Granados, M. A., J. B. Valdes and R. L. Bras, "A Derived Flood Frequency Distribution Based on the Geomorphoclimatic IUH and Density Function for Rainfall Excess," Ralph M. Parsons Laboratory, Hydrology and Water Resources Systems, Report N. 292, Massachusetts Institute of Technology, Massachusetts, 1983.

Eagleson, P. S., "Dynamic Hydrology," Mc-Graw Hill, 1970.

Eagleson, P. S., "Dynamics of Flood Frequency," Water Resources Research, V. 8, N. 4, 1972.

Eagleson, P. S., "Climate, Soil and Vegetation. 5. A Derived Distribution of Storm Surface Runoff," Water Resources Research, V. 14, N. 5, 1978.

Freeman, H., "Introduction to Statistical Inference," Addison-Wesley Publishing Company, 1963.

Garbrecht, J., "The Physical Basis of Stream Flow Hydrology with Emphasis on Drainage Morphology," Dissertation, Colorado State University, Fort Collins, Colorado, 1984.

Gupta, V. K., E. Waymire and C. T. Wang, "A Representation of an Instantaneous Unit Hydrograph from Geomorphology," Water Resources Research, V. 16, N. 5, 1980.

Hebson, C. and E. F. Wood, "A Derived Flood Frequency Distribution Using Horton Ratios," Water Resources Research, V. 18, N. 5, 1982.

Henderson, F. M., "Some Properties of the Unit Hydrograph," Water Resources Research, V. 68, N. 16, 1963.

Koch, G. J., "Flood Peak Forecasting for Small Watersheds," Thesis, Colorado State University, Fort Collins, Colorado, 1985.

Koch, R. W., "A Stochastic Streamflow Model Based on Physical Principles," Water Resources Research, V. 21, N. 4, 1985.

Morel-Seytoux, H. J., "Application of Infiltration Theory for the Determination of Excess Rainfall Hyetograph," Water Resources Bulletin, American Water Resources Association, V. 17, N. 6, 1981.

Rodriguez-Iturbe, I. and J. B. Valdes, "The Geomorphologic Structure of the Hydrologic Response," Water Resources Research, V. 15, N. 6, 1979.

Simons, D. B., R. M. Li and K. G. Eggert, "Storm Water and Sediment Runoff Simulation for Upland Watersheds Using Analytical Routing Technique, Volume I - Water Routing and Yield," Colorado State University, Engineering Report CER77-78DBS-RML-KGE16, 1976.

Spronk, B. E., "Simulation of Rainfall Runoff from a System of Multiple Watersheds," Thesis, Colorado State University, Fort Collins, Colorado, 1978.

United States Geological Survey, "Flood Peak Runoff and Associated Precipitation in Selected Drainage Basins in the United States," Water Supply Paper, N. 1813, 1965.

United States Geological Survey, "Surface Water Supply of the United States 1961-65. Part 11 Pacific Slope Basins in California," Water Supply Paper, N. 1928, 1970.

United States Geological Survey, "Surface Water Supply of the United States 1961-65. Part 5 Hudson Bay and Upper Mississippi River Basins," Water Supply Paper, N. 1914, 1971.

United States Water Resources Council, "Guidelines for Determining Flood Flow Frequency," Bulletin N. 17, 1976.

Valdes, J. B., Y. Fiallo and I. Rodriguez-Iturbe, "A Rainfall-Runoff Analysis of the Geomorphologic IUH," Water Resources Research, V. 15, N. 6, 1979.

United States Geological Survey, "Surface Water Supply of the United States 1966-70. Part 11 Pacific Slope Basins in California," Water Supply Paper, N. 2128, 1976.

Viessman, W., J. W. Knapp, G. L. Lewis and T. E. Harbaugh, "Introduction to Hydrology," Second Edition, Harper and Row, 1977.

Appendix A

HYDRAULIC ROUTING MODEL

A.1 Introduction

This appendix presents a description of the hydraulic model used for the simulation of the rainfall-direct runoff process in a given watershed.

The model is traced back to Simons, Li and Eggert (1976). Spronk (1978) enhanced it substantially and it was modified later by Garbrecht (1984). Furthermore, Koch (1985) did some fine-tuning as did the author of the present study.

In order to achieve that objective, a general description of the model is given, followed by its analytical basis, i.e., the kinematic wave approach. At that point, the main hypothesis, assumptions and limitations of the model are pointed out.

As one of the shortcomings of the model is the large amount of data required, even for small watersheds, the reader is addressed to Garbrecht (1984), where a complete procedure for obtaining a simplified representation of the watershed is given.

For the sake of simplicity, not all analytical derivations are presented. An excellent guide for this purpose can be found in Garbrecht (1984). Also, Eagleson (1970) presents a complete study of cases where physical interpretations of analytical solutions are available.

Any person ineterested in the User Manual for the corresponding computer program can get it from the Hydrology and Water Resouces Program, Colorado State University.

A.2 General Description of the Model

The purpose of the hydraulic routing model is the simulation of the rainfall-direct runoff process for a given watershed. The simulation is performed under the basis of a kinematic wave approach.

The first step in the simulation process is the representation of the watershed and its respective channel network as a set of modular units. Each unit is composed by a channel link and two adjacent planes. This kind of geometry is known in the literature as Wooding planes or open book representation.

Upon the basis of the type of intermediate result obtained, there are two kinds of modular units: the first type corresponds to all planes drainaging directly into first order streams, and, since there are no upstream tributaries to the link, an analytical solution to the kinematic wave equations can be obtained. The second type of modular units is given by those links with order greater or equal than two, composed of two upstream tributaries, two lateral planes and one channel link. The presence of upstream tributaries forces the use of a numerical scheme for the solution in the second type of modular units. Figure A.1 depicts the map and model representation for a given watershed. It must be noted that since the planes do not present upstream boundary condition, the overland plane hydrograph is obtained by means of the analytical solution.

Once the model representation for the watershed has been obtained, the planes are described by their width, slope and

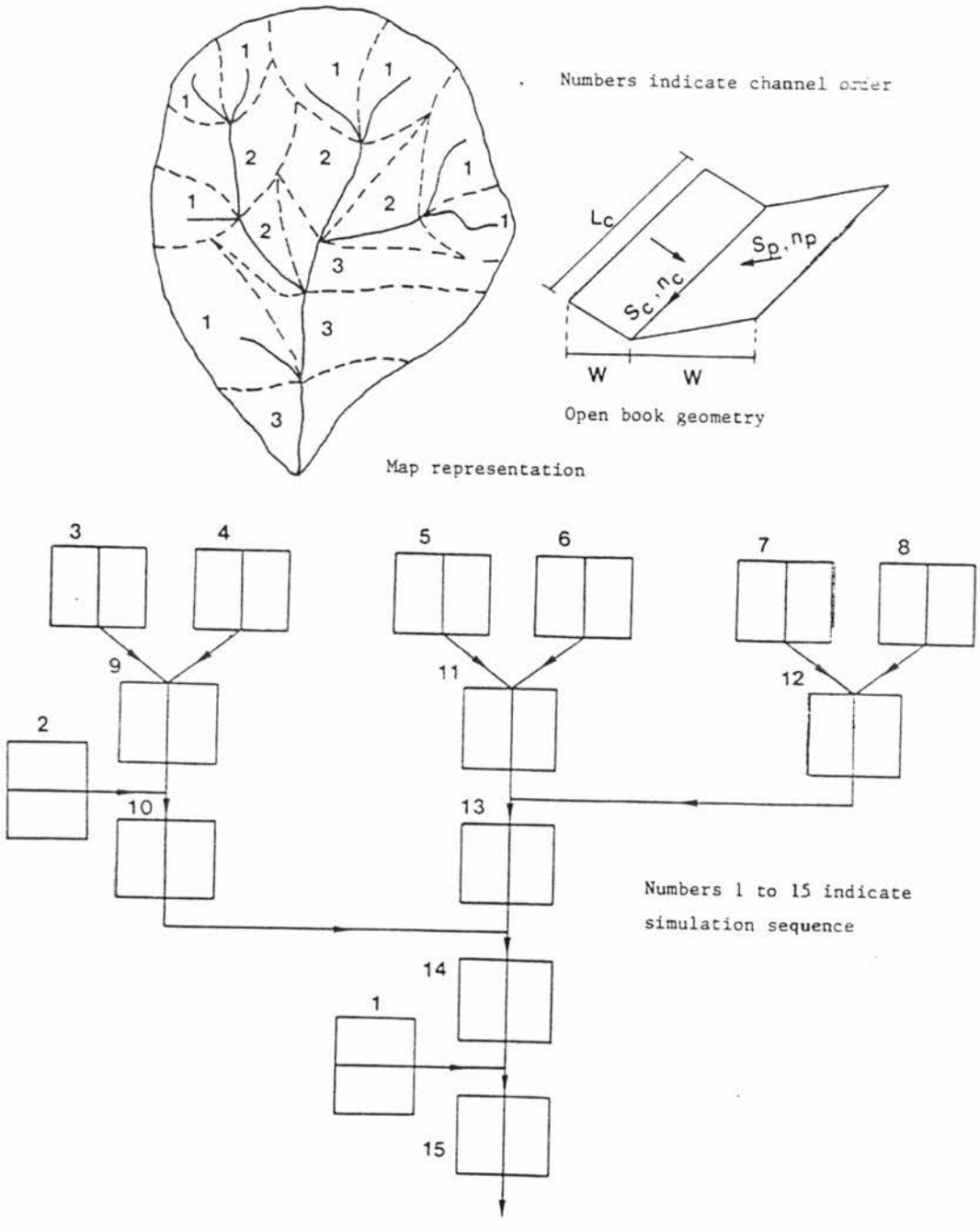

Figure A.1. Map and model representation for a given watershed.

roughness, and the channels by their length, slope, roughness and an empirical or analytical relationship between the flow area and the hydraulic radius. This description has two inherent hypotheses: 1) the flow in the planes is considered to be turbulent and to take place in a wide rectangular channel, 2) the flow in the channels are considered to be turbulent.

The operation of the model proceeds in the same way as the paths followed by the water to get the catchment outlet. Beginning with the first order streams in the upper paths, a rainfall intensity pattern is imposed to the plane. This pattern is uniform across the plane, but can be changed from plane to plane.

At this point, depending on the problem requirements, one of three possibilities for infiltration purposes must be specified: 1) describe the infiltration as an exponential decay law using Horton's equation, 2) consider constant infiltration along time, and 3) define no infiltration, i.e., the original rainfall intensity pattern is in fact effective rainfall. The two first choices imply that an instantaneous ponding takes place in the whole watershed, and, as a characteristic inherent to the model, the infiltration continues after the rainfall ends. The third choice enables the user to make an external to the model treatment of the infiltration, considering for example ponding type infiltration formulas, like Philip's equation or Green-Ampt equation (Morel-Seytoux, 1981). Similar to the rainfall intensity, the infiltration parameters are considered constant across a given plane, but can change from plane to plane. As the last feature, the user can specify for each plane the percentage of the area where infiltration takes place.

The definition of infiltration along time allows the computation of the effective rainfall intensity pattern for a given plane. This intensity pattern is routed, using the analytical solution, to the plane outlet. The basic result at this stage of the simulation is given by the overland plane hydrograph, whose dimensions correspond to discharge per unit width.

Once the overland plane hydrographs for two adjacent planes draining into the same first order channel have been computed, they are added and the resultant hydrograph is translated into a histogram of discharge per unit width. The translation from hydrograph to histogram is performed in such a way that quantity and distribution of water along time are preserved, and it is required in order to obtain the analytical solution for the first order streams. Notice that at this point the solution for the first order streams is identical to the solution for the planes, since in both cases there is a uniform distributed input along length, either plane width or channel length and no upstream boundary condition. It is important to mention that no infiltration is considered along channels.

When two first order streams joining and forming a second order stream have been completely solved, the next step is given by the solution of the latter. The two lateral planes are solved as explained above and the result is given by the discharge per unit width histogram uniformly distributed along the channel length. The hydrographs for the two upstream tributaries are then added and translated into a histogram giving the upstream boundary condition. The two inputs, upstream and lateral histograms, are collected and routed along the second order channel using a numerical scheme for the solution of the kinematic wave equations. The result is given by the

discharge hydrograph at the downstream end of the second order channel.

The simulation continues with the same procedure, taking into account that the solution for any channel link must be preceded by the solution of all links and planes located upstream of the new link.

The final result is given by the discharge hydrograph for the whole watershed at the catchment outlet.

The numbers in the model representation in Figure A.1 describe the sequence or order of simulation.

As can be concluded from the general description of the model, this has three main parts: the hydrologic component, the geomorphic component and the hydraulic component. These are described in the following paragraphs.

A.3 The Hydrologic Component

The hydrologic component of the model comprises the total rainfall, the infiltration and the effective rainfall. It is basically operated as a water mass balance. Although no explicit treatment of other abstractions, like evaporation, interception or depression storage are considered within the model, they can be included, when considered important enough, as part of the infiltration.

The rainfall duration, intensity, and pattern, are boundary conditions and are assigned arbitrary values.

Infiltration is the flow of water into the soil through the ground surface. The rate at which it occurs is influenced by such factors as the type and extent of vegetative cover, the condition of the ground, rainfall intensity, and physical properties of the soil.

The infiltration process was studied by Horton in the early 1930s, and an outgrowth of his work was the following exponential relationship determining infiltration capacity

$$f = f_c + (f_o - f_c)\, e^{-kt} \qquad (A.1)$$

where f is the infiltration capacity at some time t, k is the recession constant for infiltration, f_c is the final or equilibrium capacity, and f_o is the initial infiltration rate. Equation (A.1) indicates that if rainfall supply exceeds infiltration capacity, infiltration tends to decrease in a exponential manner. For short duration and high intensity storms, one can generally expect the rainfall intensity to exceed the infiltration capacity and Equation (A.1) applies.

After the storm ends, there is still surface runoff on the ground and the infiltration process continues as long as surface runoff exists. Since, for post rainfall conditions, rainfall water rapidly concentrates into many small rills, an additional parameter, defining the percent area over which the post rainfall infiltration is effective, is incorporated into the runoff analysis.

By accounting for the abstractions, the total rainfall intensity and duration is reduced to an effective rainfall intensity and its duration.

A.4 The Geomorphic Component

The drainage basin receives the rainfall, collects it in a system of catchments and channels, and transforms it into a flow hydrograph as the water flows through the channel network. This section defines

channel network, channel network composition and channel ordering scheme.

Catchment areas, which receive effective rainfall, produce overland flow which in turn is collected by the channel network. The different runoff characteristics and the sequential coupling of overland flow and channel flow suggest two separte entities, the overland flow and the channel flow phase. The overland flow phase corresponds to the catchment areas of the drainage basin. A catchment area is defined as an area receiving effective rainfall and draining it into a specific channel reach defined as a link. The dashed lines in Figure A.1 define the boundaries of catchment areas, and the bordering channel links receive all overland flow from these catchments. Because the geometry of the catchments depends on the spatial arrangement of the channel network, the determination of the catchment geometry is addressed after the channel network description which follows.

The channel network is an arrangement of channel links and connecting points. If the channels are displayed as single lines the resulting diagram is the channel network.

Referring to Figure A.1, sources are the points farthest upstream in a channel network, and the outlet is the point farthest downstream. The point at which two channels combine to form one is called a junction. It is assumed that multiple junctions do not occur. An exterior link is a segment of channel network between a source and the first junction downstream; an interior link is a segment of stream network between two successive junctions or between the outlet and the first junction upstream. A channel network with n sources has n exterior links, n-1 interior links, and n-1 junctions (Smart, 1972).

With these definitions, a channel network ordering scheme, which quantitatively defines channel lengths, slopes, number and spatial arrangement, can be defined. This channel ordering scheme must reproduce hydrologically significant basin features.

Strahler's channel ordering scheme is selected (Strahler, 1957) because it is simple, meets the proposed requirements and leads to concise channel network composition laws. Strahler's (1957) ordering scheme can be summarized as follows (Figure A.1): channels that originate at a source are called first order channels; when two channels of order ω join, a channel or order $\omega+1$ is created, and when two channels of different orders join, the channel immediately downstream of the junction retains the higher of the orders of the two joining channels. The highest channel order (Ω) in a channel network is also the network order.

To complete the description of the channel network, channel cross section must be defined. Since the model is not limited to a specific set data for a given channel, a power relation between hydraulic radius and flow area is selected to define the cross-sectional shape

$$R = a\, A^{b} \tag{A.2}$$

where R is hydraulic radius, A is flow area perpendicular to the flow direction, and a and b are empirically defined coefficients. Three stable channel design methods were used by Garbrecht (1984) to determine values of the coefficients a and b, ranging from 0.23 to 0.30 and 0.35 to 0.50 respectively. The hydraulic radius is thus approximately proportional to the square root of the flow area.

Nevertheless, whenever possible, field data for the specific region under consideration should be used to determine cross-sectional relationships.

In view of the numerical simulation of the rainfall runoff process, the catchment shape is approximated by a rectangle. The length of the rectangle corresponds to the length of the adjacent channel link into which the catchments drains, and the width of the catchment is obtained by dividing the catchment area by its length. As for the definition of catchment slope, Horton's (Horton, 1947) relation between catchment slope S_p and channel gradient S_c is used.

$$\text{slope ratio} = \frac{S_c}{S_p} \tag{A.3}$$

Steep catchment slopes thus correspond to steep channel gradients and vice versa. Strahler (1950) confirmed this relationship by arguing that high sediment yield from steep catchment slopes demand a steep channel gradient for continuity of sediment transport. Strahler's quantitative relation for nine maturely dissected regions is

$$S_p = 4\, S_c^{0.8} \tag{A.4}$$

where S_p and S_c are in degrees.

A.5 The Hydraulic Component

The differential equations of motion for one-dimensional, incompressible, free surface flow in a moderately wide channel can be written as:

$$\frac{\partial A}{\partial t} + \frac{\partial Q}{\partial x} = q \tag{A.5}$$

$$\frac{\partial Q}{\partial t} + \frac{\partial}{\partial x}\left(\frac{Q^2}{A}\right) + gA\frac{\partial y}{\partial x} = gA\,(S_o - S_f) \tag{A.6}$$

where Q represents the discharge through the cross-sectional area A in a given time t, q represents the lateral inflow per unit length in x direction, y is the average depth of flow in the section, S_o stands for the channel slope, S_f for the friction slope and g denotes the gravity constant. The above equations represent a gradually varied unsteady flow and other assumptions inherent to them are: uniform distribution of velocities through the section, hydrostatic pressure distribution along the vertical, small channel slope and no momentum exchange due to lateral inflow. The solution for these two equations must yield the flow properties Q and A as a function of position x and time t.

The kinematic wave approximation considers the inertia and pressure terms in the equations of motion negligible compared to the gravity and friction terms, so that the following set of equations is obtained

$$\frac{\partial A}{\partial t} + \frac{\partial Q}{\partial x} = q \tag{A.7}$$

$$S_o = S_f \tag{A.8}$$

Equation (A.8) can be expressed as a uniform flow resistance formula. For the model, Manning's equation according to the English system of units is selected, and was given by:

$$Q = \frac{1.486}{n} AR^{2/3} S_f^{1/2} \tag{A.9}$$

where n is Manning's roughness coefficient and R is the hydraulic radius. By definition, $R = A/P$, in which P stands for the wetted perimeter and can be expressed as a function of the area. Thus, the cross-sectional shape is described by means of Equation (A.2).

Plugging Equation (A.2) into Equation (A.9) yields the following result

$$Q = \alpha A^{\beta} \tag{A.10}$$

$$\alpha = \frac{1.486}{n} a^{2/3} S_f^{1/2} \tag{A.11}$$

$$\beta = 1 + \frac{2b}{3} \tag{A.12}$$

Notice that Equation (A.10) enables the consideration of other flow resistance formulas different from Manning's equation.

The kinematic wave equation is obtained by multiplying Equation (A.7) by $\partial Q/\partial A$, yielding

$$\frac{\partial Q}{\partial t} + \frac{\partial Q}{\partial A} \left(\frac{\partial Q}{\partial x} - q\right) = 0 \tag{A.13}$$

The term $\partial Q/\partial A$ is known as kinematic wave celerity (also referred to as the Kleitz-Seddon celerity) and represents the local travel velocity for the incremental unit width discharge $\partial Q/\partial x - q$:

$$\frac{\partial Q}{\partial A} = \alpha\beta A^{\beta-1} = \beta\frac{Q}{A} = \beta V \qquad (A.14)$$

where V stands for the mean velocity of flow.

The equations of motion considering kinematic wave approximation for the overland flow are obtained by analogy with Equations (A.7) and (A.8), taking into account that such a flow is similar to that in a wide channel. Therefore, the flow properties are expressed per unit width:

$$\frac{\partial y}{\partial t} + \frac{\partial q}{\partial x} = i-f \qquad (A.15)$$

$$q = \alpha y^{\beta} \qquad (A.16)$$

where y represents the flow depth, q the discharge per unit width, i the total precipitation intensity and f the instantaneous rate of infiltration.

A.6 Solution to Kinematic Flow Equations for Overland Flow by the Method of Characteristics

In the following paragraphs, Equations (A.15) and (A.16) are solved by the method of characteristics. The resulting solution is applied to the case of overland flow with temporally variable rainfall and infiltration rates.

The essence of the method of characteristics, when applied to the equations of motion, is to find a space-time locus ($x = x(t)$) along which a discontinuity of the partial derivatives of the flow properties, unit width discharge and depth flow, exists. This locus defines the path of wave propagation along which an observer moving with it can describe the process in terms of an ordinary differential equation.

Considering the definition of a total differential, the following two equations can be written

$$\frac{\partial q}{\partial x} dx + \frac{\partial q}{\partial t} dt = dq \tag{A.17}$$

$$\frac{\partial y}{\partial x} dx + \frac{\partial y}{\partial t} dt = dy \tag{A.18}$$

Equations (A.15) to (A.18) comprise a system of equations where the partial derivatives are considered as unknowns. If this system is expressed in matrix notation, the discontinuity is given, first, by vanishing the determinant of the coefficient matrix, and secondly, by applying the same condition to four determinants, obtained replacing the columns in the matrix coefficient by the independent term vector. The first condition, after some term manipulations, gives rise to the equation

$$\frac{dx}{dt} = \alpha\beta y^{\beta-1} \tag{A.19}$$

The second condition implies the equations

$$\frac{dq}{dx} = i-f \tag{A.20}$$

$$\frac{dy}{dt} = i-f \tag{A.21}$$

$$\frac{dq}{dt} = (i-f)\ \alpha\beta y^{\beta-1} \tag{A.22}$$

Equation (A.19) defines the characteristics lines in space time coordinates and it simply states that the discontinuity or perturbation travels along those lines with a velocity equal to the previous defined celerity.

Equations (A.20) through (A.22) are only valid along the characteristic lines. An important physical observation obtained from those equations is that the discharge, the depth, the mean flow velocity and the celerity remain constant along the characteristic lines, under the absence of effective rainfall intensity.

Calling W the width of the plane and i_e the effective rainfall intensity, in the more general case varying with time, and posing the following initial and boundary conditions, respectively,

$$y = 0, \text{ for } 0 \leq x \leq W, \ t = 0 \tag{A.23}$$

$$y = 0, \text{ for } x = 0, \ t \geq 0. \tag{A.24}$$

integration of Equation (A.20) gives the time variation of the depth along a characteristic line crossing through the point (t_o, x_o):

$$y = \int_{t_o}^{t} i_e(t)\ dt + y_o \tag{A.25}$$

Now, plugging this equation into (A.19) and integrating again, the characteristic lines are described by:

$$x - x_o = \alpha\beta \int_{t_o}^{t} \left\{ \int_{t_o}^{t^1} i_e(\tau)d\tau + y_o \right\}^{\beta} dt^1 \qquad (A.26)$$

where τ represents a dummy variable of integration and y_o stands for the depth at location x_o at time t_o.

Expression (A.26) is only integrable in a closed equation under very particular conditions.

At this point it is important to point out that the initial and upstream boundary condition have the inherent assumption of dryness of the plane at the beginning of the rainfall.

However, one question remains unanswered. Why does the integration of Equations (A.25) and (A.26) enable the solution of the problem herein considered?

The main magnitude in which the engineer is interested in is given by the discharge hydrograph at the plane outlet. This means that once a time t_w at the plane outlet has been specified, the discharge should be computed straightforwardly. Now, it is assumed that the starting point for the characteristic generating this discharge is such that $t_o \neq 0$, $x_o = 0$ and $y_o \neq 0$, where t_o is unknown and y_o is known. Besides x=W and if Equation (A.26) is integrated, just one unknown remains: t_o. Once t_o has been found, the integrability of Equation (A.25) between t_o and t_w allows the computation of the depth at the plane outlet. Finally Equation (A.16) gives the desired discharge.

The notation chosen enables a differentiation between the starting and arrival times t_o and t_w for a given characteristic line. They are measured in the same scale with the same origin, but their physical meanings are different.

When in the Equation (A.26), describing the characteristic lines, $i_e(\tau)$ is given as a histogram, a piecewise integration must be performed.

Following the notation shown in Figure A.2, from any point (x_i, t_i) on characteristic C, the value of x_{i+1} for time t_{i+1} may be calculated as

$$x_{i+1} = x_i + \alpha\beta \int_{t_i}^{t_{i+1}} \left\{ i_{ei+1}(t^1-t_i) + y_i \right\}^{\beta-1} dt^1 \qquad (A.27)$$

Besides, for the same interval

$$y_{i+1} = y_i + i_{ei+1} (t_{i+1} - t_i) \qquad (A.28)$$

and integration of Equation (A.27) yields

$$x_{i+1} = x_i + \frac{\alpha}{i_{ei+1}} \left\{ [i_{ei+1} (t_{i+1} - t_i) + y_i]^{\beta} - y_i^{\beta} \right\} \qquad (A.29)$$

For a given plane of width W, values of x_{i+1} are calculated until $x_{i+1}>W$. If (x_j, t_j) represents the last point for which $x_j<W$, the arrival time of characteristic C at the downstream boundary may be obtained from Equation (A.29) as

$$t_w = t_j + \frac{1}{i_{ej+1}} \left\{ \left[\frac{i_{ej+1}}{\alpha} (W-x_j) + y_j^{\beta} \right]^{1/\beta} - y_j \right\} \qquad (A.30)$$

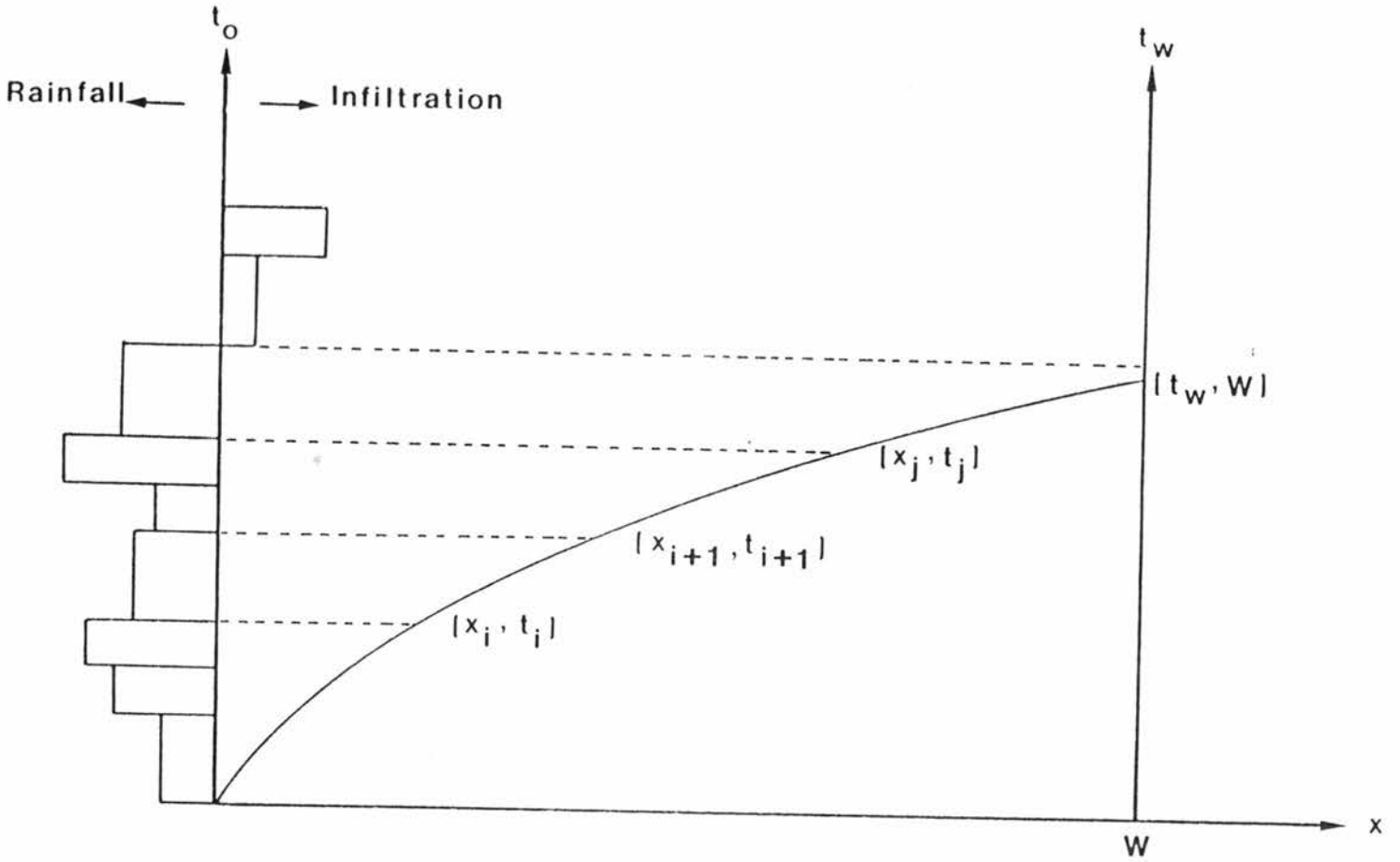

Figure A.2. Piecewise integration of characteristic lines arising in the x axis.

Hence, the discharge at the plane outlet is computed via

$$\left.\begin{aligned} q_w(t_w) &= \alpha[y(t_w)]^{\beta} \\ y(t_w) &= y_j + i_{ej+1}(t_w - t_j) \\ y_i &= \sum_{j=1}^{i} i_{ej}\,(t_j - t_{j-1}) \end{aligned}\right\} \qquad (A.31)$$

The foregoing procedure is also valid for any characteristic arising from the x axis. Due to the fact that for this characteristic lines $y_o=0$ for $t_o = 0$, the solution is straight forward. However, as shown in Figure A.3, the solution becomes more difficult when characteristic lines arise from the t (or t_o) axis. Making $x=W$ and $x_o=0$, Equation (A.26) becomes

$$\frac{W}{\alpha\beta} = \int_{t_o}^{t_w} \left\{ \int_{t_o}^{t^1} i_e(\tau)d\tau \right\}^{\beta-1} dt^1 \qquad (A.32)$$

In Figure A.3 the interval $[t_k,t_{k+1}]$ is defined as that containing the time of arrival t_w of the characteristic C to the plane outlet, while $[t_j,t_{j+1}]$ contains the starting time t_o. With this notation in mind, the piecewise integration of (A.19) may be written as:

$$\frac{W}{\alpha\beta} = \int_{t_k}^{t_w} \left\{ \int_{t_o}^{t^1} i_e(\tau)d\tau \right\}^{\beta-1} dt^1 + \int_{t_{j+1}}^{t_k} \left\{ \int_{t_o}^{t^1} i_e(\tau)d\tau \right\}^{\beta-1} dt^1$$

$$+ \int_{t_o}^{t_{j+1}} \left\{ \int_{t_o}^{t^1} i_e(\tau)d\tau \right\}^{\beta-1} dt^1 \qquad (A.33)$$

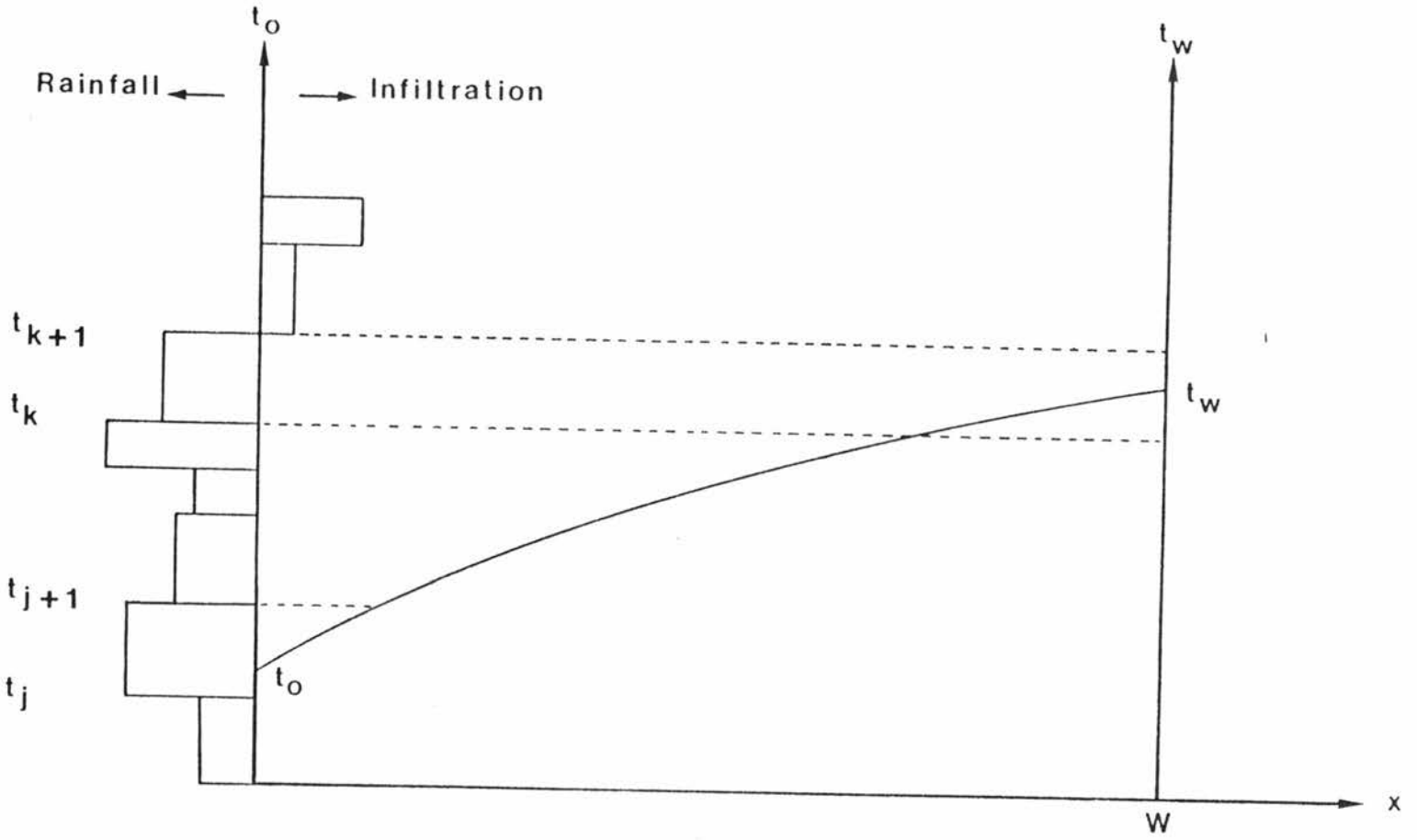

Figure A.3. Piecewise integration of chacracteristic lines arising in the t (or t_o) axis.

The inner integral in the last equation can be expressed as

$$\int_{t_o}^{t^1} i_e(\tau)d\tau = y(t^1)-y_o \tag{A.34}$$

where $y(t^1)$ stands for depth accreation evaluated between zero and t^1. With this result, Equation (A.33) becomes

$$\frac{W}{\alpha\beta} = \int_{t_k}^{t_L}\left\{ i_{ek+1}\ (t^1-t_k)+y(t_k)-y(t_j)-i_{ej+1}(t_o-t_j)\right\}^{\beta-1}dt^1$$

$$+ \sum_{i=j+2}^{k} \int_{t_{i-1}}^{t_i} \left\{i_{ei}(t^1-t_{i-1})+y(t_{i-1})-y(t_j)-i_{ej+1}(t_o-t_j)\right\}^{\beta-1}dt^1$$

$$+ \int_{t_o}^{t_{j+1}}\left\{i_{ej+1}(t^1-t_o)\right\}^{\beta-1}\ dt^1 \tag{A.35}$$

When some operations are performed and calling

$$C_i = -\ i_{ei}\ t_{i-1} + y(t_{i-1}) - y(t_j)+i_{ej+1}\ t_j \tag{A.36}$$

Equation (A.35) becomes:

$$\frac{W}{\alpha\beta} = \int_{t_k}^{t_L}\left\{ i_{ek+1}\ t^1 + C_{k+1} - i_{ej+1}\ t_o\right\}^{\beta-1}dt^1$$

$$+ \sum_{i=j+2}^{k} \int_{t_{i-1}}^{t_i} \left\{ i_{ei}t^1 + C_i - i_{ej+1}\ t_o\right\}^{\beta-1}dt^1$$

$$+ \int_{t_o}^{t_{j+1}}\left\{ i_{ej+1}t^1 - i_{ej+1}t_o\right\}^{\beta-1}dt^1 \tag{A.37}$$

Performing the integrations, the following equation is obtained

$$\frac{1}{\beta\ i_{ek+1}}\left\{(i_{ek+1}t_w + C_{k+1} - i_{ej+1}+t_o)^{\beta} - (i_{ek+1}t_k + C_{k+1} - i_{ej+1}t_o)^{\beta}\right\}$$

$$+ \sum_{i=j+2}^{k} \frac{1}{\beta\ i_{ei}}\left\{(i_{ei}t_i + C_i - i_{ej+1}t_o)^{\beta} - (i_{ei}\ t_{i-1} + C_i - i_{ej+1}\ t_o)^{\beta}\right\}$$

$$+ \frac{1}{\beta\ i_{ej+1}}(i_{ej+1}\ t_{j+1} - i_{ej+1}\ t_o)^{\beta}\Big\} - \frac{W}{\alpha\beta} = 0 \qquad \text{(A.38)}$$

If t_w is specified in the above equation, only one unknown remains, t_o. The solution of Equation (A.38) can be accomplished by using some numerical scheme. In particular, for the model a second order Newton-Raphson method is used.

Once t_o has been obtained numerically, the discharge at the plane outlet is computed using the following equations:

$$\left.\begin{aligned} y(t_w) &= i_{ej+1}(t_{j+1} - t_o) + \sum_{i=j+2}^{k} i_{ei}(t_i - t_{i-1}) + i_{ek+1}\ (t_w - t_k) \\ q_w(t_w) &= \alpha[y(t_w)]^{\beta} \end{aligned}\right\} \qquad \text{(A.39)}$$

A.7 Solution of the Kinematic Flow Equations for Channel Flow with no Upstream Tributaries (First Order Streams)

The equations governing the flow routing in the channel are

$$\frac{\partial A}{\partial t} + \frac{\partial Q}{\partial x} = q \qquad \text{(A.40)}$$

$$Q = \alpha A^{\beta} \qquad \text{(A.41)}$$

where q represents the total lateral inflow entering the channel from both planes.

If a first order stream, i.e., no upstream tributaries, is now considered, the initial and boundary conditions are given as:

$$A = 0, \text{ for } 0 \leq x \leq L \text{ and } t = 0 \tag{A.42}$$

$$A = 0, \text{ for } x = 0 \text{ and } t \geq 0 \tag{A.43}$$

The value of q is obtained by following the procedure described in Section A.6. This means that for both planes, left and right, q_l and q_r are obtained and added point by point. The hydrograph q is then formed by a collection of ordered pairs of time and discharge. If, following some procedures, q is translated into a histogram of discharge, the methodology presented for the plane can also be applied for the first order channel. The accuracy of the treatment given to the channel stands on the translation of a continuous function to a discrete function. Therefore, the more accurate the results the more similar the histogram and the hydrograph are in terms of shape and volume.

A.8 Solution of the Flow Equations for Channel Flow with Upstream Tributaries (Second or Higher Order Channels)

For channels with order higher than one, the presence of an upstream boundary condition, given by the entering hydrograph, makes impossible the solution by procedures similar to those presented in Sections A.6 and A.7. Therefore, a finite difference scheme is used,

applied to the equations governing the flow in the channel, but not to the characteristic equations.

Equations (A.40) and (A.41) represent the system to be solved, with Q and A the unknown variables. In order to obtain a finite difference scheme the network presented in Figure A.4 is used. The finite difference form of Equation (A.40) using the values of Q and A at the four points shown in Figure A.4 is

$$\left[\frac{Q_{i+1}^{n+1}-Q_i^{n+1}}{\Delta x}(1-\delta)+\frac{Q_{i+1}^{n}-Q_i^{n}}{\Delta x}\delta\right]+\left[\frac{A_{i+1}^{n+1}-A_{i+1}^{n}}{\Delta t}(1-\Phi)+\frac{A_i^{n+1}-A_i^{n}}{\Delta t}\Phi\right]=$$

$$(1-\Phi)\,q^{n}+\Phi\,q^{n+1} \qquad (A.44)$$

where δ stands for the weighting factor in time direction and Φ does in x direction. For the present case q does not change along the x direction.

At this point, a selection about the dependent variable must be made. Equation (A.44) presents two unknowns, A_{i+1}^{n+1} and Q_{i+1}^{n+1}, since these quantities are supposed to be known at the other three points of the grid. Besides, Equation (A.41) relates area and discharge, and also their relative errors as:

$$\frac{dQ}{Q}=\beta\,\frac{dA}{A} \qquad (A.45)$$

Assuming that this relationship stands for the numerical scheme, if one computes the discharge incorrectly, and since $\beta>1$, the relative error in the flow area would be smaller than the relative error in the discharge. On the other hand, the error in the discharge is magnified

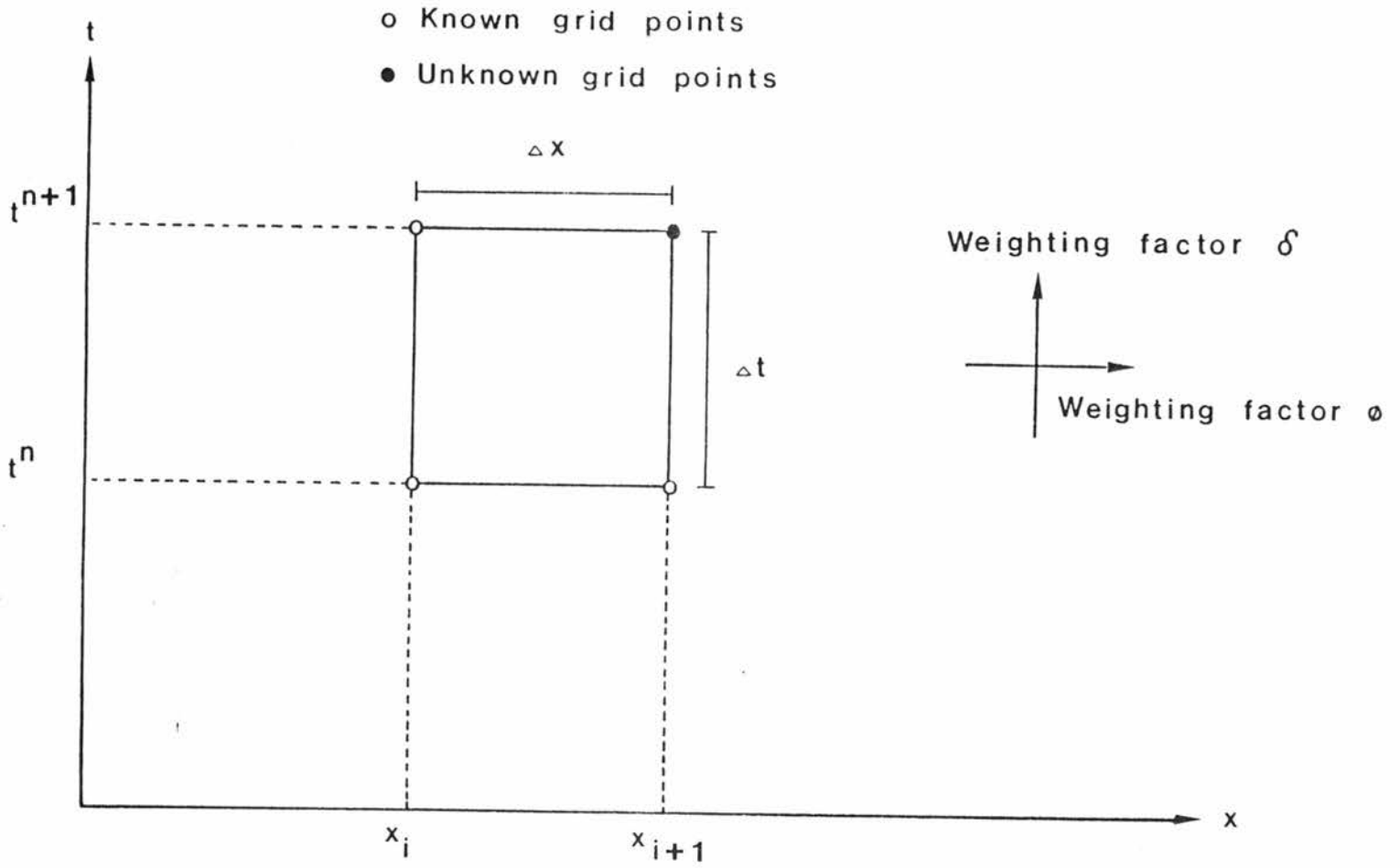

Figure A.4. Rectangular network in the x-t plane.

if the numerical computations are performed on the flow area. Therefore, the discharge is the better selection for the unknown in the numerical computations. Performing the following transformations:

$$\beta' = 1/\beta \quad , \quad \alpha' = (1/\alpha)^{\beta'} \tag{A.46}$$

the discharge-area of flow relationship becomes

$$A = \alpha' A^{\beta'} \tag{A.47}$$

and for any point in the network

$$A_i^n = \alpha' (Q_i^n)^{\beta'} \tag{A.48}$$

Taking this last relationship to the finite difference scheme and performing some operations, the following result is obtained

$$\frac{\Delta t}{\Delta x}(1-\delta)\, Q_{i+1}^{n+1} + \alpha'(1-\Phi)(Q_{i+1}^{n+1})^{\beta'} = \frac{\Delta t}{\Delta x}[(1-\delta)\, Q_i^{n+1} - \delta(Q_{i+1}^n - Q_i^n)]$$

$$+\alpha'(1-\Phi)(Q_{i+1}^n)^{\beta'} - \Phi[\alpha'(Q_i^{n+1})^{\beta'} - \alpha'(Q_i^n)^{\beta'}] + \Delta t[(1-\Phi)q^n + \Phi q^{n+1}] \tag{A.49}$$

The right hand side in Equation (A.49) is a known quantity and will be represented by Ω. Besides, making $\theta = \Delta t/\Delta x$ and $r = Q_{i+1}^{n+1}$ Equation (A.49) is written as:

$$\theta(1-\delta)r + \alpha'(1-\Phi)r^{\beta'} = \Omega \tag{A.50}$$

As this equation is not linear on r, it is necessary to apply an iterative technique. Again, the second order Newton-Raphson algorithm is proposed.

The initial guess, r_o, is the key to obtain a fast convergence to the numerical solution of Equation (A.50). The best way to determine r_o is to use a linear scheme. In Equation (A.40), the following replacement is performed:

$$\frac{\partial A}{\partial t} = \frac{\partial A}{\partial Q} \frac{\partial Q}{\partial t} \tag{A.51}$$

But, from Equation (A.47)

$$\frac{\partial A}{\partial Q} = \alpha' \beta' \, Q^{\beta'-1} \tag{A.52}$$

Then, Equation (A.40) becomes:

$$\alpha' \beta' Q^{\beta'-1} \frac{\partial Q}{\partial t} + \frac{\partial Q}{\partial x} = q \tag{A.53}$$

The linear finite difference scheme is obtained from equation (A.53), but not including the unknown in the coefficient of the partial time derivative:

$$\alpha' \beta \left[\frac{Q_i^{n+1} + Q_{i+1}^n}{2} \right]^{\beta-1} \left[\frac{Q_{i+1}^{n+1} - Q_{i+1}^n}{\Delta t} (1-\Phi) + \frac{Q_i^{n+1} - Q_i^n}{\Delta t} \Phi \right] +$$

$$\left[\frac{Q_{i+1}^{n+1} - Q_i^n}{\Delta x} (1-\delta) + \frac{Q_{i+1}^n - Q_i^n}{\Delta x} \delta \right] = (1-\Phi) q^n + \Phi \, q^{n+1} \tag{A.54}$$

and solving for Q_{i+1}^{n+1}

$$(Q_{i+1}^{n+1})_o = \left\{ \frac{1-\delta}{\Delta x} + \alpha'\beta' \frac{(1-\Phi)}{\Delta t} \left[\frac{Q_i^{n+1} + Q_{i+1}^n}{2} \right]^{\beta'-1} \right\}^{-1} \left\{ \frac{(1-\delta)}{\Delta x} Q_i^{n+1} \right.$$

$$- \delta \frac{Q_{i+1}^n - Q_i^n}{\Delta x} - \alpha'\beta' \left[\frac{Q_i^{n+1} + Q_{i+1}^n}{2} \right]^{\beta'-1} \left[- \frac{(1-\Phi)}{\Delta t} Q_{i+1}^n + \Phi \frac{Q_i^{n+1} - Q_i^n}{\Delta t} \right]$$

$$\left. + (1-\Phi)\, q^n + \Phi\, q^{n+1} \right\} \qquad \text{(A.55)}$$

The above equation provides the best initial estimate r_o or $(Q_{i+1}^{n+1})_o$ for solving Equation (A.50). However, Equation (A.55) is not applicable when $Q_i^{n+1} = Q_{i+1}^n = 0$ and in this case Equation (A.50) can be used with $\beta'=1$:

$$r_o = \frac{\Omega}{\theta(1-\delta) + \alpha'(1-\Phi)} \qquad \text{(A.56)}$$

Although this topic will not be developed here, the stability conditions for the numerical scheme are:

$$a \leq 1/2, \quad a \leq \frac{\theta}{\theta + \alpha'\beta' (Q_i^{n+1})^{\beta'-1}}, \quad b \leq 1/2 \qquad \text{(A.57)}$$

For a more detailed description of this topic see Garbrecht (1984).

A.9 Summary of Assumptions and Limitations for the Model

In the following, a list of the more important assumptions and limitations encountered in the development of the model is presented.

1. The type of flow considered in the model, in planes and channels is one-dimensional, incompressible and turbulent. Besides it are treated as free surface flow in a wide channel, with uniform

distribution of velocities in the depth for planes and across the section for channels. The intertia and pressure forces are considered negligibles and the kinematic wave model allows the propagation of perturbations in the downstream direction, without attenuation of the peak discharge.

2. The Manning's equation is considered acceptable for describing the force balance in the flow.
3. Within a given plane, its properties, slope and roughness are considered constant.
4. For a given channel, its properties, slope, roughness and cross-sectional shape are considered constant.
5. The rainfall intensity is considered constant for a given plane, but may change from plane to plane. No simulation can be performed with gaps in the rainfall intensity histogram.
6. The infiltration is considered uniform within a given plane, but can change from plane to plane. No ponding type equations for infiltration are considered in the model. In the best of the cases, the infiltration behaves like a exponential decay law by means of Horton equation.
7. No infiltration takes place in the channels.
8. The simulation begins with a dry watershed: this means no moisture nor flow in planes or channels prior to the beginning of rainfall, as neither subsurface or groundwater flows along simulation horizon.

Appendix B

FLOOD FREQUENCY DERIVATION
USER MANUAL FOR THE COMPUTER PROGRAM

B.1 Introduction

This appendix contains the User Manual for the computer program used to calculate the flood frequency curve for a given watershed.

For a complete understanding of the algorithm translated into the program and its theoretical basis, the reader is addressed to Chapters 3 and 4 of this thesis.

B.2 Input Data File Description

In the following, a complete description of the records contained in the input file, required to perform any program run, is presented. Special care is recommended for the units, as specified for each variable.

LINE	COLUMN	FORTRAN NAME	FORMAT	DESCRIPTION
1	1	P(13)	F10.0	Mean areal rainfall intensity, (in/hr).
1	11	P(14)	F10.0	Mean rainfall duration (hr).
2	1	AMV	F10.0	Mean number of independent rainfall events within the year (dimensionless).
3	1	P(20)	F10.0	Minimum rainfall intensity to be considered in the integrations (in/hr).

LINE	COLUMN	FORTRAN NAME	FORMAT	DESCRIPTION
4	1	P(15)	F10.0	Hydraulic conductivity at natural saturation (in/hr).
4	11	P(16)	F10.0	Soil sorptivity ($in/hr^{1/2}$)
5	1	P(5)	F10.0	Plane width (ft).
5	11	ANP	F10.0	Plane roughness (dimensionless).
5	21	SP	F10.0	Plane slope (dimensionless).
6	1	P(6)	F10.0	Channel length (ft).
6	11	ANC	F10.0	Channel roughness (dimensionless).
6	21	SC	F10.0	Channel slope (dimensionless).
6	31	AC	F10.0	Coefficient in the area hydraulic radius relationship.
6	41	BC	F10.0	Exponent in the area hydraulic radius relationship.
7	1	QP(1)	F10.0	Initial discharge for the flood frequency computation (cfs).
7	11	DQP	F10.0	Increment for the discharge in the flood frequency computation (cfs).
7	21	QPMAX	F10.0	Maximum discharge for the flood frequency computation (cfs).
8	1	N	I5	Maximum number of iterations allowed for integration.
8	6	P(25)	E14.7	Integration tolerance.
9	1	NIT	I5	Maximum number of iterations allowed for solving equations.
9	6	NBIS	I5	Maximum number of iterations allowed for initial approximations to equation roots
9	6	P(26)	E14.7	Tolerance for solving equations.

B.3 Program Capacity

The program for computing the flood frequency distribution curve was designed to run in the CYBER205. Due to the extent and requirement of the computations, it could be expensive to run it in another type of machine.

In regard to memory requirements, the maximum number of discharge values to be considered within a run shall not exceed 100. For larger requirements it is necessary to modify the program.

B.4 Output Description

Once the program has been run, the user gets three different printouts. The first gives a trace of the particular execution, informing the user about the regions and subregions covered, intersection points, partial integration results and limits. The second, considered a formal listing, prints the catchment geometry and dynamic description and rainfall-infiltration parameters. It also provides a table, in which, for each considered discharge, the values for cumulative pdf and return period are given. The last printout gives a list of return period and discharge, as sequence of ordered pairs, designed as input file to plotting facilities.

B.5 Program Source Code

```
      PROGRAM FLOOD(OUTPUT,TAPE1,TAPE2=OUTPUT,TAPE3)
C
C
C     THIS PROGRAM PERFORMS THE INTEGRATION OF THE JOINT PROBABILITY
C     DISTRIBUTION FUNCTION FOR EFFECTIVE RAINFALL INTENSITY AND DURA-
C     TION, OVER REGIONS DEFINED BY SEVERAL EXPRESSIONS USED TO COMPU-
C     TE THE PEAK DISCHARGE, GIVEN A RAINFALL EVENT.  THE EQUATIONS
C     USED TO COMPUTE THE PEAK DISCHARGE ARE THOSE OBTAINED BY LUIS
C     CADAVID.
C
C     INPUT UNIT:  TAPE1
C     OUTPUT UNIT: TAPE2
C     PLOTING:     TAPE3
C
C     AUTHOR: LUIS CADAVID
C
C     COLORADO STATE UNIVERSITY, FORT COLLINS, COLORADO.
C     NOVEMBER, 1986
C
C
      DIMENSION CDF(100),QP(100),P(30),TRET(100)
      EXTERNAL FNUL,FBR43,FBR24,FBR12,FQ3,FQ4,FQ2,FQ1,FINT4,FINT2,FIN
C
C-----------------------------------------------------------------------
C
C               DATA INPUT AND CONVERSION
C
C-----------------------------------------------------------------------
C
C
C     THE RAINFALL PARAMETERS ARE READ
C
      READ(1,100)P(13),P(14)
  100 FORMAT(8F10.0)
      READ(1,100)AMV
      P(13)=12.*3600./P(13)
      P(14)=1./3600./P(14)
      READ(1,100)P(20)
      P(20)=P(20)/3600./12.
C
C     THE INFILTRATION PARAMETERS ARE READ
C
      READ(1,100)P(15),P(16)
      P(15)=P(15)/3600./12.
      P(16)=P(16)/60./12.
C
C     THE PLANE PARAMETERS ARE READ
C
      READ(1,100)P(5),ANP,SP
C
C     THE STREAM PARAMETERS ARE READ
C
      READ(1,100)P(6),ANC,SC,AC,BC
C
C     THE FLOOD PARAMETERS ARE READ
C
```

```
      READ(1,100)QP(1),DQP,QPMAX
C
C     THE INTEGRATION PARAMETERS ARE READ
C
      READ(1,200)N,P(25)
  200 FORMAT(I5,E14.7)
      READ(1,100)TEMIN
C
C     PARAMETERS CONTROLLING THE SOLUTION OF EQUATION ARE READ
C
      READ(1,300)NIT,NBIS,P(26)
  300 FORMAT(2I5,E14.7)
C
C-----------------------------------------------------------------------
C
C              GENERAL PARAMETERS COMPUTATION
C
C-----------------------------------------------------------------------
C
      P(1)=1.486*SQRT(SP)/ANP
      P(2)=5./3.
      P(3)=1.486*(AC**(2./3.))*SQRT(SC)/ANC
      P(4)=1.+2.*BC/3.
      P(7)=-129.697
      P(8)=49.878
      P(9)=-118.552
      P(10)=47.458
      P(11)=P(14)*(P(13)*P(16)/2./SQRT(2.)/P(14))**(2./3.)
      P(12)=GAMMA(P(11)+1.)
      CDF1=1.-EXP(-P(13)*P(15)-2.*P(11))*P(12)*(P(11)**(-P(11)))
      PIN=CDF1
      P(22)=1.2185*P(13)*P(14)*EXP(-P(13)*P(15)-2.*P(11))*P(12)
     1      *(P(11)**(-P(11)))*(P(16)**0.1558)
      P(23)=1.4434*P(13)*(P(16)**0.1558)
      P(27)=FLOAT(NIT)
      R=20./3600./12.
      TEMAX=-1.2*ALOG(0.8442*P(23)*P(25)/P(22))/P(14)
      P(17)=TEMIN
      P(18)=TEMAX
      WRITE(2,500)
  500 FORMAT(1H1,///,T5,'GENERAL PARAMETER SET',/,T5,'I',
     1       T20,'VALUE',/)
      WRITE(2,550)(I,P(I),I=1,18)
  550 FORMAT(T3,I3,T20,G12.6)
      WRITE(2,600)P(20)
  600 FORMAT(T4,'20',T20,G12.6)
      WRITE(2,550)(I,P(I),I=22,23)
      WRITE(2,550)(I,P(I),I=25,27)
      IR2=0
      IR3=0
      IR4=0
C
C     THE COUNTER DEFINING THE NUMBER OF FLOOD VALUES IS COMPUTED AND
C     COMPARED WITH THE MAXIMUN.  THE VALUE OF THE MAXIMUN FLOOD IN
C     THE INTEGRATION IS REDEFINED
C
```

```
      NQ=INT((QPMAX-QP(1))/DQP)+1
      IF(NQ.GT.100)THEN
        WRITE(2,1000)NQ
 1000   FORMAT(1H1,///,T5,'THE NUMBER OF FLOOD VALUES ',I5,
     1          'EXCEEDS THE ALLOWED MAXIMUN: 100')
        STOP
      END IF
      QPMAX=FLOAT(NQ)*DQP
C
C-----------------------------------------------------------------------
C
C              FLOOD FREQUENCY CURVE COMPUTATION
C
C-----------------------------------------------------------------------
C
C
C     THE INTEGRATION BEGINS
C
      DO 10 I=1,NQ
        QP(I)=QP(1)+FLOAT(I-1)*DQP
        WRITE(2,1005)I,QP(I)
 1005   FORMAT(2X,'I= ',I5,2X,'QP(I)= ',F8.1)
        P(19)=QP(I)
        P(24)=P(19)/2./P(6)/P(5)
C
C       THE CDF FOR THE ACTUAL VALUE OF QP IS INITIALIZED
C
        CDF(I)=CDF1
C
C-----------------------------------------------------------------------
C       REGION E3
C-----------------------------------------------------------------------
C
C
C       FOR THE ACTUAL VALUE OF QP, THE FIRST THIRD OF INTEGRATION (E3)
IS
C       DEFINED, AS THE INTERSECTION OF R3 AND Q3.
C
        WRITE(2,1010)
 1010   FORMAT(T2,'**** REGION E3 ****')
C
C       WHEN IR3=1 THE INTEGRAL IN THIS REGION HAS REACHED A CONSTANT
C       VALUE AND IS NOT PERFORMED ANYMORE
C
        IF(IR3.EQ.0)THEN
C
C         THE INTERSECTION POINT OF FBR43 AND FQ3 IS TESTED TO BE
C         GREATER THAN TEMIN
C
          RE3=FQ3(P,TEMIN)
          RE43=FBR43(P,TEMIN)
          IF(RE3.LT.RE43)THEN
C
C         THE INTERSECTION POINT IS COMPUTED
C
            D=(P(19)/2./P(6)/P(1))**(1./P(2))
```

```
            TE43=P(5)/P(1)/(D**(P(2)-1.))-P(2)*(P(6)/P(3)/((2.*P(1)*
     1           (D**P(2)))**(P(4)-1.)))**(1./P(4))
            IF(TE43.LE.0.0)TE43=TEMIN/2.
C
C         TE43 IS LESS THAN TEMIN
C
          ELSE
            TE43=TEMIN/2.
          END IF
          WRITE(2,1015)TE43
 1015     FORMAT(T2,'INT. POINT: ',G14.7)
C
C         THE INTERSECTION POINT TE43 IS CHECKED TO BE GREATER THAN THE
C         MAXIMUN
C
          IF(TE43.GE.TEMAX)THEN
C
C           E3 :TE AXIS TO FQ3 FOR [ TEMIN,TEMAX ]
C
            WRITE(2,1020)
 1020       FORMAT(T2,'E3 :TE AXIS TO FQ4 FOR [ TEMIN,TEMAX ]')
            CALL ROMB(N,TEMIN,TEMAX,P(25),P,IR,AC1,FIN,FQ3,FNUL)
            IF(IR.EQ.1)THEN
              WRITE(2,1025)I,QP(I),N
 1025         FORMAT(/,T5,'ROMBERG ALGORITHM DOES ',
     1               'NOT CONVERGE.',/,T10,'I= ',I5,/,T10,
     2               'QP(I)= ',G12.6,/,T10,'NUMBER OF ITERATIONS:'
     3               ,' ',I5)
              STOP
            END IF
            AC2=0.0
C
C         THE INTERSECTION POINT TE43 IS CHECKED TO BE WITHIN THE RANGE
C         OF INTEGRATION
C
          ELSE IF(TE43.GT.TEMIN)THEN
C
C           E3 :TE AXIS TO FQ3 FOR [ TEMIN,TE43 ]
C               TE AXIS TO FBR43 FOR [ TE43,TEMAX ]
C
            WRITE(2,1030)
 1030       FORMAT(T2,'E3 :TE AXIS TO FQ3 FOR [ TEMIN,TE43 ]',
     1           /,T7,'TE AXIS TO FBR43 FOR [ TE43,TEMAX ]')
            CALL ROMB(N,TE43,TEMAX,P(25),P,IR,AC1,FIN,
     1                FBR43,FNUL)
            IF(IR.EQ.1)THEN
              WRITE(2,1025)I,QP(I),N
              STOP
            END IF
            CALL ROMB(N,TEMIN,TE43,P(25),P,IR,AC2,FIN,FQ3,FNUL)
            IF(IR.EQ.1)THEN
              WRITE(2,1025)I,QP(I),N
              STOP
            END IF
          ELSE
```

```
C
C           E3 :TE AXIS TO FBR43 FOR [ TEMIN,TEMAX ]
C
            WRITE(2,1035)
 1035       FORMAT(T2,'E3 :TE AXIS TO FBR43 FOR [ TEMIN,TEMAX ]')
            CALL ROMB(N,TEMIN,TEMAX,P(25),P,IR,AC1,FIN,
     1                FBR43,FNUL)
            IF(IR.EQ.1)THEN
              WRITE(2,1025)I,QP(I),N
              STOP
            END IF
            AC2=0.0
            IR3=1
            CDF1=CDF1+AC1
          END IF
C
C           THE TOTAL INTEGRAL IS UPDATED
C
           CDF(I)=CDF(I)+AC1+AC2
           WRITE(2,1040)AC1,AC2,CDF(I)
 1040      FORMAT(T2,'RESULTS FOR E3:',/,T5,'AC1= ',G14.7,/,T5,
     1           'AC2= ',G14.7,/,T5,'CDF(I)= ',G14.7,//)
       END IF
C
C-----------------------------------------------------------------------
C       REGION E4
C-----------------------------------------------------------------------
C
C
C       FOR THE ACTUAL VALUE OF QP, THE FOURTH REGION OF INTEGRATION C
   (E4) IS DEFINED AS THE INTERSECTION OF R4 AND Q4
C
        WRITE(2,1045)
 1045   FORMAT(T2,'**** REGION E4 ****')
C
C       WHEN IR4=1 THE INTEGRAL IN THIS REGION HAS REACHED A CONSTANT
C       VALUE AND IS NOT PERFORMED ANYMORE
C
        IF(IR4.EQ.0)THEN
C
C         THE INTERSECTION POINT FOUND IN THE PREVIOUS REGION IS CHECKED
C         TO BE INSIDE THE RANGE OF INTEGRATION.  WHEN IT IS GREATER
C         THAN TEMAX REGION E4 DOES NOT EXIST.
C
          IF(TE43.GE.TEMAX)THEN
C
C           E4 DOES NOT EXIST
C
            WRITE(2,1050)
 1050       FORMAT(T2,'E4 DOES NOT EXIST')
            AC1=0.0
            AC2=0.0
          ELSE
```

```
C
C           E4 DOES EXIST AND THE INTERSECTION POINT BETWEEN BR24 AND Q4
C           IS TESTED TO BE GREATER THAN TEMIN
C
            RE4=FQ4(P,TEMIN)
            RE24=FBR24(P,TEMIN)
            IF(RE4.LT.RE24)THEN
C
C             THE INTERSECTION POINT IS COMPUTED
C
              TE1=TE43
              TE2=(P(5)*(P(24)**(1.-P(2)))/P(1))**(1./P(2))
              DO 15 J=1,NBIS
                TE3=(TE1+TE2)/2.
                IF(FINT4(P,TE1)*FINT4(P,TE3).LE.0.0)THEN
                  TE2=TE3
                ELSE
                  TE1=TE3
                END IF
   15         CONTINUE
              CALL FALSI(NIT,TE1,TE2,P(26),P,IT,IR,TE24,FINT4)
C
C             THE FLAG INDICATING THE TYPE OF RESULT IS ANALYZED
C
              IF(IR.EQ.1)THEN
C
C               THE SOLUTION DOES NOT CONVERGE FOR THE GIVEN NUMBER OF
C               ITERATIONS
C
                WRITE(2,1055)I,QP(I),NIT
 1055           FORMAT(/,T5,'FALSE POSITION ALGORITHM DOES ',
     1                 'NOT CONVERGE FOR REGION E4.',/,T10,'I= ',I5,/,
     2                 T10,'QP(I)= ',G12.6,/,T10,'MAXIMUN NUMBER OF'
     3                 ,' ITERATIONS: ',I5)
                STOP
              ELSE
C
C               THE INTERSECTION POINT HAS BEEN FOUND SUCCESSFULLY
C
                IF(TE24.LE.0.0)TE24=TEMIN/2.
              END IF
            ELSE
              TE24=TEMIN/2.
            END IF
            WRITE(2,1015)TE24
C
C           TE43 BEING WITHIN THE RANGE OF INTEGRATION IS CONSIDRED
C
            IF(IR3.EQ.0)THEN
C
C             TE24 IS CHECKED TO BE GREATER THAN TEMAX
C
              IF(TE24.GE.TEMAX)THEN
C
C               E4 :FBR43 TO FQ4 FOR [ TE43,TEMAX ]
C
```

```
                WRITE(2,1060)
 1060           FORMAT(T2,'E4 :FBR43 TO FQ4 FOR [ TE43,TEMAX ]')
                CALL ROMB(N,TE43,TEMAX,P(25),P,IR,AC1,FIN,
     1                  FQ4,FBR43)
                IF(IR.EQ.1)THEN
                  WRITE(2,1025)I,QP(I),N
                  STOP
                END IF
                AC2=0.0
              ELSE
C
C               E4: FBR43 TO FBR24 FOR [ TE24,TEMAX ]
C                   FBR43 TO FQ4 FOR [ TE43,TE24 ]
C
                WRITE(2,1065)
 1065           FORMAT(T2,'E4: FBR43 TO FBR24 FOR [ TE24,TEMAX ]',
     1                 /,T5,'FBR43 TO FQ4 FOR [ TE43,TE24 ]')
                CALL ROMB(N,TE24,TEMAX,P(25),P,IR,AC1,FIN,
     1                  FBR24,FBR43)
                IF(IR.EQ.1)THEN
                  WRITE(2,1025)I,QP(I),N
                  STOP
                END IF
                CALL ROMB(N,TE43,TE24,P(25),P,IR,AC2,FIN,
     1                  FQ4,FBR43)
                IF(IR.EQ.1)THEN
                  WRITE(2,1025)I,QP(I),N
                  STOP
                END IF
              END IF
            ELSE IF(TE24.GE.TEMAX)THEN
C
C             E4 :FBR43 TO FQ4 FOR [ TEMIN,TEMAX ]
C
              WRITE(2,1070)
 1070         FORMAT(T2,'E4 :FBR43 TO FQ4 FOR [ TEMIN,TEMAX ]')
              CALL ROMB(N,TE43,TE24,P(25),P,IR,AC1,FIN,
     1                FQ4,FBR43)
              IF(IR.EQ.1)THEN
                WRITE(2,1025)I,QP(I),N
                STOP
              END IF
              AC2=0.0
            ELSE IF(TE24.GE.TEMIN)THEN
C
C             E4 :FBR43 TO FBR24 FOR [ TE24,TEMAX ]
C                 FBR43 TO FQ4 FOR [ TEMIN,TE24 ]
C
              WRITE(2,1075)
 1075         FORMAT(T2,'E4 :FBR43 TO FBR24 FOR [ TE24,TEMAX ]',
     1                 /,T7,'FBR43 TO FQ4 FOR [ TEMIN,TE24 ]')
              CALL ROMB(N,TE24,TEMAX,P(25),P,IR,AC1,FIN,
     1                FBR24,FBR43)
              IF(IR.EQ.1)THEN
                WRITE(2,1025)I,QP(I),N
                STOP
```

```
                END IF
                CALL ROMB(N,TEMIN,TE24,P(25),P,IR,AC2,FIN,
     1                    FQ4,FBR43)
                IF(IR.EQ.1)THEN
                  WRITE(2,1025)I,QP(I),N
                  STOP
                END IF
              ELSE
C
C               E4 :FBR43 TO FBR24 FOR [ TEMIN,TEMAX ]
C
                WRITE(2,1080)
 1080           FORMAT(T2,'E4 :FBR43 TO FBR24 FOR [ TEMIN,TEMAX ]')
                CALL ROMB(N,TEMIN,TEMAX,P(25),P,IR,AC1,FIN,
     1                    FBR24,FBR43)
                IF(IR.EQ.1)THEN
                  WRITE(2,1025)I,QP(I),N
                  STOP
                END IF
                AC2=0.0
                CDF1=CDF1+AC1
                IR4=1
              END IF
            END IF
C
C       THE TOTAL INTEGRAL IS UPDATED
C
        CDF(I)=CDF(I)+AC1+AC2
        WRITE(2,1085)AC1,AC2,CDF(I)
 1085   FORMAT(T2,'RESULTS FOR E4:',/,T5,'AC1= ',G14.7,/,T5,
     1          'AC2= ',G14.7,/,T5,'CDF(I)= ',G14.7,//)
      END IF
C
C-----------------------------------------------------------------------
C       REGION E2
C-----------------------------------------------------------------------
C
C
C       FOR THE ACTUAL VALUE OF QP, THE SECOND REGION OF INTEGRATION C
   (E2) IS DEFINED AS THE INTERSECTION OF R2 AND Q2
C
        WRITE(2,1090)
 1090   FORMAT(T2,'**** REGION E2 ****')
C
C       WHEN IR2=1 THE INTEGRAL IN THIS REGION HAS REACHED A CONSTANT
C       VALUE AND IS NOT PERFORMED ANYMORE
C
        IF(IR2.EQ.0)THEN
C
C         THE INTERSECTION POINT BETWEEN BR24 AND Q2 IS TESTED TO
C         BE GREATER THAN TEMIN
C
          IF(TE24.GT.TEMIN)THEN
C
C           THE INTERSECTION POINT IS COMPUTED
C
```

```
            TE1=0.95*TE24
            TE2=(P(5)*(P(24)**(1.-P(2)))/P(1))**(1./P(2))
            DO 25 J=1,NBIS
              TE3=(TE1+TE2)/2.
              IF(FINT2(P,TE1)*FINT2(P,TE3).LE.0.0)THEN
                TE2=TE3
              ELSE
                TE1=TE3
              END IF
   25       CONTINUE
            CALL FALSI(NIT,TE1,TE2,P(26),P,IT,IR,TE24,FINT2)
C
C           THE FLAG INDICATING THE TYPE OF RESULT IS ANALYZED
C
            IF(IR.EQ.1)THEN
C
C             THE SOLUTION DOES NOT CONVERGE FOR THE GIVEN NUMBER OF
C             ITERATIONS
C
              WRITE(2,1095)I,QP(I),NIT
 1095         FORMAT(/,T5,'FALSE POSITION ALGORITHM DOES ',
     1               'NOT CONVERGE FOR REGION E2.',/,T10,'I= ',I5,/,
     2               T10,'QP(I)= ',G12.6,/,T10,'MAXIMUN NUMBER OF'
     3               ,' ITERATIONS: ',I5)
              STOP
            ELSE
C
C             THE INTERSECTION POINT HAS BEEN FOUND SUCCESSFULLY
C
             IF(TE24.LE.0.0)TE24=TEMIN/2.
            END IF
          END IF
          WRITE(2,1015)TE24
C
C         THE INTERSECTION POINT FOUND IS CHECKED TO BE INSIDE THE
C         RANGE OF INTEGRATION.  WHEN IT IS GREATER THAN TEMAX,
C         REGION E2 DOES NOT EXIST.
C
          IF(TE24.GE.TEMAX)THEN
C
C           E2 DOES NOT EXIST
C
            WRITE(2,1100)
 1100       FORMAT(T2,'E2 DOES NOT EXIST')
            AC1=0.0
            AC2=0.0
          ELSE
C
C           E2 DOES EXIST AND THE INTERSECTION POINT BETWEEN BR12 AND Q2
C           IS COMPUTED.
C
            RI=P(24)
            TE12=(P(5)*(RI**(1.-P(2)))/P(1))**(1./P(2))+(P(6)/(P(3)*
     1           ((2.*P(5)*RI)**(P(4)-1.))))**(1./P(4))
            WRITE(2,1015)TE12
```

```
C
C           TE24 BEING WITHIN THE RANGE OF INTEGRATION IS CONSIDRED
C
            IF(IR4.EQ.0)THEN
C
C               TE12 IS CHECKED TO BE GREATER THAN TEMAX
C
                IF(TE12.GE.TEMAX)THEN
C
C                 E2 :FBR24 TO FQ2 FOR [ TE24,TEMAX ]
C
                  WRITE(2,1105)
 1105             FORMAT(T2,'E2 :FBR24 TO FQ2 FOR [ TE24,TEMAX ]')
                  CALL ROMB(N,TE24,TEMAX,P(25),P,IR,AC1,FIN,
     1                    FQ2,FBR24)
                  IF(IR.EQ.1)THEN
                    WRITE(2,1025)I,QP(I),N
                    STOP
                  END IF
                  AC2=0.0
                ELSE
C
C                 E2 :FBR24 TO FBR12 FOR [ TE12,TEMAX ]
C                     FBR24 TO FQ2 FOR [ TE24,TE12 ]
C
                  WRITE(2,1110)
 1110             FORMAT(T2,'E2 :FBR24 TO FBR12 FOR [ TE12,TEMAX ]',
     1                 /,T5,'FBR24 TO FQ2 FOR [ TE24,TE12 ]')
                  CALL ROMB(N,TE12,TEMAX,P(25),P,IR,AC1,FIN,
     1                    FBR12,FBR24)
                  IF(IR.EQ.1)THEN
                    WRITE(2,1025)I,QP(I),N
                    STOP
                  END IF
                  CALL ROMB(N,TE24,TE12,P(25),P,IR,AC2,FIN,
     1                   FQ2,FBR24)
                  IF(IR.EQ.1)THEN
                    WRITE(2,1025)I,QP(I),N
                    STOP
                  END IF
                END IF
               ELSE IF(TE12.GE.TEMAX)THEN
C
C                 E2 :FBR24 TO FQ2 FOR [ TEMIN,TEMAX ]
C
                  WRITE(2,1115)
 1115             FORMAT(T2,'E2 :FBR24 TO FQ2 FOR [ TEMIN,TEMAX ]')
                  CALL ROMB(N,TEMIN,TEMAX,P(25),P,IR,AC1,FIN,
     1                    FQ2,FBR24)
                  IF(IR.EQ.1)THEN
                    WRITE(2,1025)I,QP(I),N
                    STOP
                  END IF
                  AC2=0.0
               ELSE IF(TE12.GE.TEMIN)THEN
```

```
C
C               E2 :FBR24 TO FBR12 FOR [ TE12,TEMAX ]
C                   FBR24 TO FQ2 FOR [ TEMIN,TE12 ]
C
                WRITE(2,1120)
 1120           FORMAT(T2,'E2 :FBR24 TO FBR12 FOR [ TE12,TEMAX ]',
     1                 /,T7,'FBR24 TO FQ2 FOR [ TEMIN,TE12 ]')
                CALL ROMB(N,TE12,TEMAX,P(25),P,IR,AC1,FIN,
     1                    FBR12,FBR24)
                IF(IR.EQ.1)THEN
                  WRITE(2,1025)I,QP(I),N
                  STOP
                END IF
                CALL ROMB(N,TEMIN,TE12,P(25),P,IR,AC2,FIN,
     1                    FQ2,FBR24)
                IF(IR.EQ.1)THEN
                  WRITE(2,1025)I,QP(I),N
                  STOP
                END IF
              ELSE
C
C               E2 :FBR24 TO FBR12 FOR [ TEMIN,TEMAX ]
C
                WRITE(2,1125)
 1125           FORMAT(T2,'E2 :FBR24 TO FBR12 FOR [ TEMIN,TEMAX ]')
                CALL ROMB(N,TEMIN,TEMAX,P(25),P,IR,AC1,FIN,
     1                    FBR12,FBR24)
                IF(IR.EQ.1)THEN
                  WRITE(2,1025)I,QP(I),N
                  STOP
                END IF
                AC2=0.0
                CDF1=CDF1+AC1
                IR2=1
              END IF
            END IF
C
C       THE TOTAL INTEGRAL IS UPDATED
C
        CDF(I)=CDF(I)+AC1+AC2
        WRITE(2,1130)AC1,AC2,CDF(I)
 1130   FORMAT(T2,'RESULTS FOR E2:',/,T5,'AC1= ',G14.7,/,T5,
     1          'AC2= ',G14.7,/,T5,'CDF(I)= ',G14.7,//)
      END IF
C
C-----------------------------------------------------------------------
C       REGION E1
C-----------------------------------------------------------------------
C
        WRITE(2,1135)
 1135   FORMAT(T2,'**** REGION E1 ****')
C
C       FOR THE ACTUAL VALUE OF QP, THE FIRSTH REGION OF INTEGRATION
C       (E1) IS DEFINED AS THE INTERSECTION OF R1 AND Q1
C
```

```
C
C       E1 :FBR12 TO FQ1 FOR [ TE12,TEMAX ]
C
        WRITE(2,1140)
 1140   FORMAT(T2,'E1 :FBR12 TO FQ1 FOR [ TE12,TEMAX ]')
        CALL ROMB(N,TE12,TEMAX,P(25),P,IR,AC1,FIN,FQ1,FBR12)
        IF(IR.EQ.1)THEN
          WRITE(2,1025)I,QP(I),N
          STOP
        END IF
C
C       THE TOTAL INTEGRAL IS UPDATED
C
        CDF(I)=CDF(I)+AC1
        WRITE(2,1145)AC1,CDF(I)
 1145   FORMAT(T2,'RESULTS FOR E1:',/,T5,'AC1= ',G14.7,/,T5,
     1         'CDF(I)= ',G14.7,//)
C
C       A NEW FLOOD VALUE IS OBTAINED
C
        WRITE(2,1150)CDF(I)
 1150   FORMAT(2X,'CDF(I)= ',G14.7)
   10 CONTINUE
C
C     THE RETURN PERIOD IS COMPUTED FOR EACH DISCHARGE
C
      DO 35 I=1,NQ
        TRET(I)=1./AMV/(1-CDF(I))
   35 CONTINUE
C
C-----------------------------------------------------------------------
C
C       PRINTOUT OF RESULTS
C
C-----------------------------------------------------------------------
C
C
C     THE HEADING IS PRINTED
C
      WRITE(2,1300)
 1300 FORMAT(1H1,///,T5,'FLOOD FREQUENCY DISTRIBUTION',///)
C
C     THE WATERSHED PARAMETERS ARE PRINTED
C
      WRITE(2,1500)P(5),ANP,SP,P(6),ANC,SC,AC,BC
 1500 FORMAT(//,T10,'WATERSHED PARAMETERS',/,
     1       T20,'PLANE WIDTH: ',T50,F8.0,T65,'FT',/,
     2       T20,'PLANE ROUGHNESS: ',T50,F8.5,T65,'-',/,
     3       T20,'PLANE SLOPE: ',T50,F8.5,T65,'-',/,
     4       T20,'STREAM LENGTH: ',T50,F8.0,T65,'FT',/,
     6       T20,'STREAM ROUGHNESS: ',T50,F8.5,T65,'-',/,
     7       T20,'STREAM SLOPE: ',T50,F8.5,T65,'-',/,
     8       T20,'CROSS-SECTIONAL AREA PARAMETERS: ',/,T30,'AC: ',
     9       T50,F8.5,/,T30,'BC: ',T50,F8.5,/)
```

```
C
C     THE INFILTRATION PARAMETERS ARE PRINTED
C
      WRITE(2,1700)P(15),P(16)
 1700 FORMAT(//,T10,'INFILTRATION PARAMETERS',/,
     1       T20,'HYDRAULIC CONDUCTIVITY: ',T50,F9.7,T65,'FT/SEC',/,
     2       T20,'SORPTIVITY: ',T50,F8.5,T65,'FT/(SEC**.5)',/)
C
C     THE RAINFALL PARAMETERS ARE PRINTED
C
      P(13)=1./P(13)
      P(14)=1./P(14)
      MV=INT(AMV)
      WRITE(2,1800)P(13),P(14),TEMIN,TEMAX,MV
 1800 FORMAT(//,T10,'RAINFALL PARAMETERS',/,
     1       T20,'MEAN INTENSITY: ',T50,F9.7,T65,'FT/SEC',/,
     2       T20,'MEAN DURATION: ',T50,F9.2,T65,'SEC',/,
     3       T20,'MINIMUN DURATION: ',T50,F9.2,T65,'SEC',/,
     4       T20,'MAXIMUN DURATION: ',T50,F9.2,T65,'SEC',/,
     5       T20,'NUMBER OF INDEPENDENT EVENTS: ',T50,I5,/)
C
C     THE FLOOD FREQUENCY DISTRIBUTION CURVE IS PRINTED
C
      WRITE(2,2000)NQ,PIN
 2000 FORMAT(1H1,///,T5,'VALUES OF THE CUMULATIVE DISTRIBUTION ',
     1       'FUNCTION',/,T10,'NUMBER OF POINTS: ',I5,//,T20,
     2       'P[IE=0.0 AND T=0.0]= ',F7.5,//,T20,
     3       'DISCHARGE',T50,'PROBABILITY',T70,'RETURN PERIOD',/,
     4       T20,'(CFS)',T55,'(-)',T70,'(YEARS)',/)
      DO 20 I=1,NQ
        WRITE(2,2100)QP(I),CDF(I),TRET(I)
 2100   FORMAT(T20,F9.2,T50,F7.5,T70,F7.2)
   20 CONTINUE
C
C     THE VALUES OF THE CUMULATIVE DISTRIBUTION FUNCTION ARE SAVED ON
C     TAPE3 IN ORDER TO BE USED (PLOTTED) LATER
C
      DO 30 I=1,NQ
        WRITE(3,2200)TRET(I),QP(I)
 2200   FORMAT(2X,F9.2,4X,F9.2)
   30 CONTINUE
      STOP
      END
```

```
      SUBROUTINE ROMB(N,A,B,TOL,P,IR,APP,FRO,FSUP,FINF)
C
C
C*****************************************************************
C
C     SUBROUTINE ROMB
C
C     PURPOSE
C
C     APPROXIMATE A GIVEN DEFINITE INTEGRAL USING ROMBERG ALGORITHM.
C     THE STOPPING CRITERIA USED IS GIVEN BY THE COMPARISON OF THE
C     ABSOLUTE ERRORS FOR TWO CONSECUTIVE ROWS WITH THE TOLERANCE.
C
C     REFERENCE: DOCUMENTATION ABOUT THE ALGORITHM HERE IMPLEMENTED
C     CAN BE FOUND IN "NUMERICAL ANALYSIS" BY R. L. BURDEN AND
C     J. D. FAIRES, 3RD EDITION.
C
C     AUTHOR: LUIS CADAVID, COLORADO STATE UNIVERSITY, SUMMER 1986.
C
C     COURSE: NUMERICAL ANALYSIS I, M 350.
C
C     INPUT VARIABLES:
C
C           N: MAXIMUN NUMBER OF ITERATIONS ALLOWED IN THE PROCESS.
C           A: LEFT END POINT OR LOWER INTEGRATION LIMIT.
C           B: RIGHT END POINT OR UPPER INTEGRATION LIMIT.
C           P: SET OF PARAMETERS USED TO EVALUATE THE FUNCTION FRO.
C           TOL: TOLERANCE.
C
C     OUTPUT VARIABLES:
C
C           I: ACTUAL NUMBER FO PERFORMED ITERATIONS.
C           IR: FLAG INDICATING THE TYPE OF RESULT.
C               IR=0: THE PROCESS CONVERGES BEFORE OR AT N ITERATIONS.
C               IR=1: THE PROCESS DOES NOT CONVERGE WITHIN N ITERATIONS.
C           R: ARRAY OF SIZE I TIMES I. IT CONTAINS THE APPROXIMATION
C              TABLE. PARTICULARLY, R(I,I) CONTAINS THE BEST
C              APPROXIMATION
C              FOR THE DEFINITE INTEGRAL
C
C     LOCAL VARIABLES:
C
C           H: INTERVAL LENGTH.
C           LI: UPPER SUMMATION LIMIT FOR THE EXTENDED TRAPEZOIDAL
C               APPROXIMATION.
C           X: ANY VALUE OF THE INDEPENDENT VARIABLE.
C           EXJ: EXPONENT USED IN THE EXTRAPOLATING FORMULAE.
C
C     SUBROUTINES NEEDED:
C           FRO: FUNCTION PROGRAM WRITTEN BY THE USER. IT EVALUATES THE
C                FUNCTION TO BE INTEGRATED AT ANY POINT.
C
C*****************************************************************
C
      DIMENSION R(100,100),P(30)
      EXTERNAL FSUP,FINF
```

```
C
C     THE FLAG INDICATING THE TYPE OF RESULT IS INITIALIZED.
C
      IR=0
C
C     THE LENGTH FOR THE ENTIRE INTERVAL AND THE FIRST APPROXIMATION
C     ARE CALCULATED.
C
      H=B-A
      CALL FRO(P,A,FSUP,FINF,RES1)
      CALL FRO(P,B,FSUP,FINF,RES2)
      R(1,1)=(RES1+RES2)*H/2.
C
C     BEGINING WITH THE SECOND, A NEW ROW IS CALCULATED UNTIL THE
C     THE PROCESS CONVERGES OR FAILS.
C
      DO 10 I=2,N
C
C       THE FIRST ELEMENT FOR THE ITH ROW IS CALCULATED.
C
        IF(I.EQ.2)THEN
          LI=1
        ELSE
          LI=2**(I-2)
        END IF
        R(I,1)=0.0
        DO 20 J=1,LI
          X=A+(FLOAT(J)-0.5)*H
          RES1=0.0
          CALL FRO(P,X,FSUP,FINF,RES1)
          R(I,1)=R(I,1)+RES1
   20   CONTINUE
        R(I,1)=(R(I-1,1)+R(I,1)*H)/2.
C
C       THE EXTRAPOLATION IS PERFORMED.
C
        DO 30 J=2,I
          EXJ=FLOAT(J-1)
          R(I,J)=((4.**EXJ)*R(I,J-1)-R(I-1,J-1))/((4.**EXJ)-1.)
   30   CONTINUE
        IF(I.EQ.2)GO TO 35
C
C       WHEN MORE THAN TWO ROWS HAVE BEEN COMPUTED THE STOPPING CRITERIA
C       IS APLIED.
C
        IF(ABS(R(I,I)-R(I,I-1)).LT.TOL)THEN
          IF(ABS(R(I-1,I-1)-R(I-1,I-2)).LT.TOL)THEN
            APP=R(I,I)
            RETURN
          END IF
        END IF
C
C       A NEW ITERATION IS PERFORMED.
C
   35   H=H/2.
   10 CONTINUE
```

```
C
C     THE PROCEDURE FAILS AFTER N ITERATIONS. THE FLAG INDICATING THE
C     RESULT IS UPDATED
C
      IR=1
      RETURN
      END
```

```
      SUBROUTINE FALSI(NIT,Y0,Y1,TOL,P,I,IR,Y,FFAL)
C
C
C*********************************************************************
C
C
C     THIS SUBROUTINE FINDS AN APPROXIMATION FOR THE ZERO Y OF A
C     FUNCTION F(X)=0.0.  TO PERFORM THIS TASK THE FALSE POSITION
C     ALGORITMH IS USED.  THE STOPPING CRITERIA IS GIVEN BY THE
C     ABSOLUTE ERROR BETWEEN TWO CONSECUTIVE APPROXIMATIONS.
C
C     AUTHOR: LUIS CADAVID, COLORADO STATE UNIVERSITY, NOVEMBER 1986.
C
C     SUBROUTINES NEEDED:
C       FFAL: FUNCTION PROGRAM WRITTEN BY THE USER.  IT EVALUATES THE
C             FUNCTION TO BE SOLVED AT ANY POINT.
C
C     INFORMATION ABOUT THE ALGORITHM HERE IMPLEMENTED CAN BE FOUND
C     IN "NUMERICAL ANALYSIS" BY R. L. BURDEN AND J. D. FAIRES, 3RD
C     EDITION.
C
C*********************************************************************
C
C
      DIMENSION P(30)
C
C     THE FLAG INDICATING THE FINAL RESULT, IR, IS INITIALIZED.
C
      IR=0
C
C     THE POSSIBILITY OF THE SOLUTION BEING AT THE INITIAL END POINTS
C     IS INVESTIGATED.
C
      IF(FFAL(P,Y0).EQ.0.0)THEN
        Y=Y0
        RETURN
      ELSE IF(FFAL(P,Y1).EQ.0.0)THEN
        Y=Y1
        RETURN
      END IF
C
C     THE FALSE POSITION METHOD IS APPLIED.
C
      DO 10 I=1,NIT
C
C       A NEW ITERATE IS CALCULATED.
C
        Y=Y0-FFAL(P,Y0)*(Y1-Y0)/(FFAL(P,Y1)-FFAL(P,Y0))
C
C       IF THE ABSOLUTE ERROR FOR THE LAST TWO BOUNDARY POINTS IS LESS
C       THAN THE TOLERANCE, TOL, THE PROCEDURE IS CONSIDERED SUCCESSFUL.
C
        IF(ABS(Y-Y1).LT.TOL)RETURN
C
C       NEW ENDING POINTS FOR THE INTERVAL CONTAINING Y ARE DETERMINED.
C
```

```
          IF(FFAL(P,Y)*FFAL(P,Y1).LT.0.0)THEN
            Y0=Y1
            Y1=Y
          ELSE
            Y1=Y
          END IF
       10 CONTINUE
C
C       THE ITERATIVE PROCESS FAILS AFTER N ITERATIONS.  THE CORRES-
C       PONDING FLAG IS UPDATED.
C
          IR=1
          RETURN
          END
```

```
      SUBROUTINE FIN(P,TE,FSUP,FINF,RES)
      DIMENSION P(30)
      R1=FINF(P,TE)
      R2=FSUP(P,TE)
      RES=P(22)*(EXP(-P(23)*(R1**0.8442)*(TE**(-0.0779)))
     1     -EXP(-P(23)*(R2**0.8442)*(TE**(-0.0779))))*
     2     EXP(-P(14)*TE)/P(23)/0.8442
      RETURN
      END
C
C
      FUNCTION FNUL(P,TE)
      DIMENSION P(30)
      FNUL=0.0
      RETURN
      END
C
C
      FUNCTION FBR43(P,TE)
      DIMENSION P(30)
      EXTERNAL FUNC43
      P(21)=TE
      NIT=INT(P(27))
      R1=P(20)
      IF(ABS(FUNC43(P,R1)).LE.P(26))THEN
        FBR43=R1
        RETURN
      END IF
      IF(FUNC43(P,R1).GT.0.0)THEN
        DO 10 I=1,NIT
          R2=2.*R1
          IF(FUNC43(P,R1)*FUNC43(P,R2).LT.0.0)GO TO 30
          R1=R2
   10   CONTINUE
      ELSE
        DO 20 I=1,NIT
          R2=R1/2.
          IF(FUNC43(P,R1)*FUNC43(P,R2).LT.0.0)GO TO 30
          R1=R2
   20   CONTINUE
      END IF
      WRITE(2,500)
  500 FORMAT(/,T5,'NO INITIAL APPROXIMATION ATTAINED FOR FBR43')
      STOP
   30 CALL FALSI(NIT,R1,R2,P(26),P,IT,IR,RES,FUNC43)
      IF(IR.EQ.1)THEN
        WRITE(2,1000)
 1000   FORMAT(/,T5,'FALSE POSITION ALGORITHM DOES ',
     1          'NOT CONVERGE FOR REGION FBR43')
        STOP
      END IF
      FBR43=RES
      RETURN
      END
```

```
      FUNCTION FBR24(P,TE)
      DIMENSION P(30)
      FBR24=(P(1)*(TE**P(2))/P(5))**(1./(1.-P(2)))
      RETURN
      END
C
C
      FUNCTION FBR12(P,TE)
      DIMENSION P(30)
      EXTERNAL FUNC12
      P(21)=TE
      NIT=INT(P(27))
      R1=P(20)
      IF(ABS(FUNC12(P,R1)).LE.P(26))THEN
        FBR12=R1
        RETURN
      END IF
      IF(FUNC12(P,R1).GT.0.0)THEN
        DO 10 I=1,NIT
          R2=2.*R1
          IF(FUNC12(P,R1)*FUNC12(P,R2).LT.0.0)GO TO 30
          R1=R2
   10   CONTINUE
      ELSE
        DO 20 I=1,NIT
          R2=R1/2.
          IF(FUNC12(P,R1)*FUNC12(P,R2).LT.0.0)GO TO 30
          R1=R2
   20   CONTINUE
      END IF
      WRITE(2,500)
  500 FORMAT(/,T5,'NO INITIAL APPROXIMATION ATTAINED FOR FBR12')
      STOP
   30 CALL FALSI(NIT,R1,R2,P(26),P,IT,IR,RES,FUNC12)
      IF(IR.EQ.1)THEN
        WRITE(2,1000)
 1000   FORMAT(1H1,///,T5,'FALSE POSITION ALGORITHM DOES ',
     1         'NOT CONVERGE FOR FBR12')
        STOP
      END IF
      FBR12=RES
      RETURN
      END
C
C
      FUNCTION FQ3(P,TE)
      DIMENSION P(30)
      FQ3=((P(19)/2./P(6)/P(1))**(1./P(2)))/TE
      RETURN
      END
C
C
      FUNCTION FQ4(P,TE)
      DIMENSION P(30)
      EXTERNAL FUNC4
      P(21)=TE
```

```
      NIT=INT(P(27))
      R1=P(20)
      IF(ABS(FUNC4(P,R1)).LE.P(26))THEN
        FQ4=R1
        RETURN
      END IF
      IF(FUNC4(P,R1).LT.0.0)THEN
        DO 10 I=1,NIT
          R2=2.*R1
          IF(FUNC4(P,R1)*FUNC4(P,R2).LT.0.0)GO TO 30
          R1=R2
   10   CONTINUE
      ELSE
        DO 20 I=1,NIT
          R2=R1/2.
          IF(FUNC4(P,R1)*FUNC4(P,R2).LT.0.0)GO TO 30
          R1=R2
   20   CONTINUE
      END IF
      WRITE(2,500)
  500 FORMAT(/,T5,'NO INITIAL APPROXIMATION ATTAINED FOR FQ4')
      STOP
   30 CALL FALSI(NIT,R1,R2,P(26),P,IT,IR,RES,FUNC4)
      IF(IR.EQ.1)THEN
        WRITE(2,1000)
 1000   FORMAT(/,T5,'FALSE POSITION ALGORITHM DOES ',
     1          'NOT CONVERGE FOR FQ4')
        STOP
      END IF
      FQ4=RES
      RETURN
      END
C
C
      FUNCTION FQ2(P,TE)
      DIMENSION P(30)
      EXTERNAL FUNC2
      P(21)=TE
      NIT=INT(P(27))
      R1=P(20)
      IF(ABS(FUNC2(P,R1)).LE.P(26))THEN
        FQ2=R1
        RETURN
      END IF
      IF(FUNC2(P,R1).LT.0.0)THEN
        DO 10 I=1,NIT
          R2=2.*R1
          IF(FUNC2(P,R1)*FUNC2(P,R2).LT.0.0)GO TO 30
          R1=R2
   10   CONTINUE
      ELSE
        DO 20 I=1,NIT
          R2=R1/2.
          IF(FUNC2(P,R1)*FUNC2(P,R2).LT.0.0)GO TO 30
          R1=R2
   20   CONTINUE
```

```
      END IF
      WRITE(2,500)
  500 FORMAT(/,T5,'NO INITIAL APPROXIMATION ATTAINED FOR FQ2')
      STOP
   30 CALL FALSI(NIT,R1,R2,P(26),P,IT,IR,RES,FUNC2)
      IF(IR.EQ.1)THEN
        WRITE(2,1000)
 1000   FORMAT(1H1,///,T5,'FALSE POSITION ALGORITHM DOES ',
     1          'NOT CONVERGE FOR FQ2')
        STOP
      END IF
      FQ2=RES
      RETURN
      END
C
C
      FUNCTION FQ1(P,TE)
      DIMENSION P(30)
      FQ1=P(24)
      RETURN
      END
C
C
      FUNCTION FINT4(P,TE)
      DIMENSION P(30)
      RI=(P(1)*(TE**P(2))/P(5))**(1./(1.-P(2)))
      TP=(P(2)-1.)*TE/P(2)+P(5)/P(1)/P(2)*((RI*TE)**(1.-P(2)))
      TS=(P(6)/P(3)*((2.*P(1)*((RI*TE)**P(2)))**(1.-P(4))))**(1./P(4))
      FINT4=0.02*(P(9)+P(10)*ALOG(100.*TP/(TE+TS)))*P(6)*P(1)*((RI*TE)
     1      **P(2))-P(19)
      RETURN
      END
C
C
      FUNCTION FINT2(P,TE)
      DIMENSION P(30)
      RI=(P(1)*(TE**P(2))/P(5))**(1./(1.-P(2)))
      TS=(P(6)/(P(3)*((2.*P(5)*RI)**(P(4)-1.))))**(1./P(4))
      FINT2=0.02*(P(7)+P(8)*ALOG(100.*TE/(TE+TS)))*P(6)*P(5)*RI
     1     -P(19)
      RETURN
      END
C
C
      FUNCTION FUNC43(P,R)
      DIMENSION P(30)
      FUNC43=P(5)/(P(1)*P(2)*((R*P(21))**(P(2)-1.)))-P(21)/P(2)-(P(6)
     1       /P(3)/((2.*P(1)*((R*P(21))**P(2)))**(P(4)-1.)))
     2       **(1./P(4))
      RETURN
      END
C
C
      FUNCTION FUNC4(P,R)
      DIMENSION P(30)
      TP=(P(2)-1.)*P(21)/P(2)+P(5)/P(1)/P(2)*((R*P(21))**(1.-P(2)))
```

```
      TS=(P(6)/P(3)*((2.*P(1)*((R*P(21))**P(2)))**(1.-P(4))))**(1./P(4))
      FUNC4=0.02*(P(9)+P(10)*ALOG(100.*TP/(P(21)+TS)))*P(6)*P(1)*
     1      ((R*P(21))**P(2))-P(19)
      RETURN
      END
C
C
      FUNCTION FUNC2(P,R)
      DIMENSION P(30)
      TC=(P(5)*(R**(1.-P(2)))/P(1))**(1./P(2))+(P(6)/P(3)/((2.*P(5)*R)
     1   **(P(4)-1.)))**(1./P(4))
      FUNC2=0.02*(P(7)+P(8)*ALOG(100.*P(21)/TC))*P(6)*P(5)*R-P(19)
      RETURN
      END
C
C
      FUNCTION FUNC12(P,R)
      DIMENSION P(30)
      FUNC12=(P(5)*(R**(1.-P(2)))/P(1))**(1./P(2))+(P(6)/P(3)/
     1       ((2.*P(5)*R)**(P(4)-1.)))**(1./P(4))-P(21)
      RETURN
      END
```